U.S. DEPARTMENT OF COMMERCE
DANIEL C. ROPER, Secretary
BUREAU OF STANDARDS
LYMAN J. BRIGGS, Director

BUREAU OF STANDARDS JOURNAL OF RESEARCH

November 1933
Vol. 11, No. 5

UNITED STATES
GOVERNMENT PRINTING OFFICE
WASHINGTON : 1933

For sale by the Superintendent of Documents, Washington, D.C. - - Price 25 cents; $2.50 per year on subscription

DEPOSITED BY THE
UNITED STATES OF AMERICA

DEC 29 '33

U.S. DEPARTMENT OF COMMERCE, BUREAU OF STANDARDS

RESEARCH PAPER RP609

Part of Bureau of Standards Journal of Research, Vol. 11, November 1933

TESTS ON A REINFORCED-CONCRETE ARCH OF THE ARLINGTON MEMORIAL BRIDGE

By Cyrus C. Fishburn and John L. Nagle

ABSTRACT

Tests were made on one of the arches of the Arlington Memorial Bridge to determine, during its construction and after its completion, changes in the temperature of the concrete, deflections, and deformations with changes in temperature and in load. The effect of the restraint of the superstructure on the deflection caused by changes of temperature was determined by comparing the vertical deflections of the arch before and after the construction of the superstructure. The effects of removing the centering from a portion of the arch barrel, the addition of the superstructure loads, shrinkage, and time-yield on the vertical deflections of the arch were shown and discussed. A transverse deflection of the arch was produced by differences in physical properties between the concrete barrel and the granite voussoir facing arches. The coefficient of thermal expansion of the arch was determined.

CONTENTS

	Page
I. Introduction	568
II. Description of arch span no. 7	569
III. Testing equipment and its location	573
IV. Testing procedure	575
V. Method of reduction and estimated precision of the observations	576
1. Temperature measurements	576
(*a*) Temperature measurements on radial observation sections	576
(*b*) Calculation of the average temperature and the temperature gradient	576
(*c*) Precision of the temperature measurements	577
2. Clinometer observations	578
3. Strain-gage and telemeter observations	579
VI. Results of the tests	580
1. Temperatures and temperature changes of the arch	580
(*a*) Initial temperature rise of the arch barrel blocks during hardening of the concrete	580
(*b*) Variation of the arch temperature with seasonal temperature changes	580
2. Coefficient of thermal expansion of the arch barrel	583
3. Vertical deflections of the arch barrel	584
(*a*) Deflection resulting from decentering the downstream inner strip	584
(*b*) Deflection produced by the addition of the superstructure walls and deck	584
(*c*) Effect of superstructure restraint on deflection produced by temperature changes	787
(*d*) Deflection occurring with time	589
(*e*) Vertical deflections in transverse sections	592
4. Strains at the principal sections due to thrust and bending	593
5. Pier movements	595
6. Movements of the expansion joints	596
VII. Summary	597
VIII. Acknowledgments	598

I. INTRODUCTION

The Bureau of Standards cooperated with the Arlington Memorial Bridge Commission in an investigation of the structural behavior of one of the reinforced-concrete arch spans of the Arlington Memorial Bridge. Information was obtained on the temperature changes of

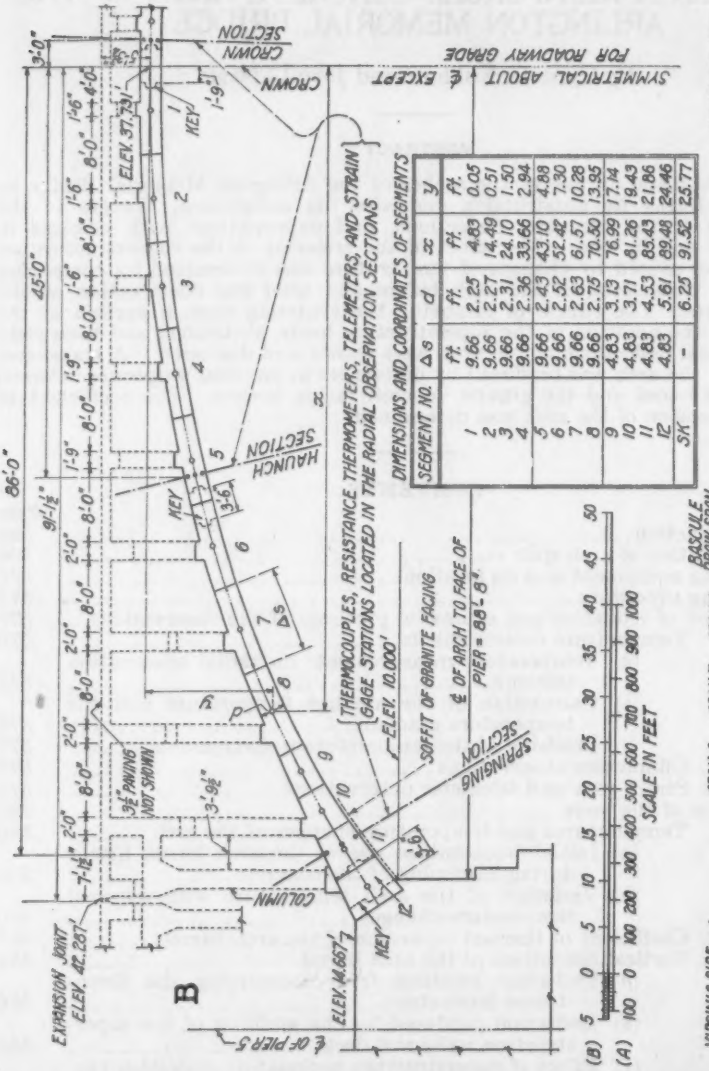
CROWN SECTION
CROWN
KEY
ELEV. 37.731'
45'-0"
86'-0"
HAUNCH SECTION
KEY
Δs
SPRINGING SECTION
SOFFIT OF GRANITE FACING
℄ OF ARCH TO FACE OF PIER = 88' 8"
ELEV. 10.000'
THERMOCOUPLES, RESISTANCE THERMOMETERS, TELEMETERS, AND STRAIN GAGE STATIONS LOCATED IN THE RADIAL OBSERVATION SECTIONS
SYMMETRICAL ABOUT ℄ EXCEPT FOR ROADWAY GRADE
DIMENSIONS AND COORDINATES OF SEGMENTS
SEGMENT NO. | Δs | d | x | y
1 2 3 4 | 9.66 | 2.25 | 4.83 | 0.05
1 2 3 4 | 9.66 | 2.27 | 14.49 | 0.51
1 2 3 4 | 9.66 | 2.31 | 24.10 | 1.50
1 2 3 4 | 9.66 | 2.36 | 33.66 | 2.94
5 6 7 8 | 9.66 | 2.43 | 43.10 | 4.88
5 6 7 8 | 9.66 | 2.52 | 52.42 | 7.30
5 6 7 8 | 9.66 | 2.63 | 61.57 | 10.28
5 6 7 8 | 9.66 | 2.75 | 70.50 | 13.95
9 10 11 12 | 4.83 | 3.13 | 76.99 | 17.14
9 10 11 12 | 4.83 | 3.71 | 81.26 | 19.43
9 10 11 12 | 4.83 | 4.53 | 85.43 | 21.86
9 10 11 12 | 4.83 | 5.61 | 89.48 | 24.46
SK | - | 6.25 | 91.52 | 25.77
EXPANSION JOINT ELEV. 42.237'
COLUMN
KEY
ELEV. 14.667'
℄ OF PIER 5
B
A
SCALE IN FEET
(B) 5 0 5 10 15 20 25 30 35 40 45 50
(A) 100 0 100 200 300 400 500 600 700 800 900 1000
VIRGINIA SIDE
ARCH 8
ARCH 7
ARCH 6
BASCULE DRAW SPAN
WASHINGTON SIDE
ROCK
PIER 5
PIER 4
ABUTMENT 3
MEAN LOW WATER ELEV. 0.000'

FIGURE 1.—*A, Elevation of the Arlington Memorial Bridge, looking upstream, B, elevation of half span, arch no. 7.*

the concrete, the coefficient of thermal expansion of the arch, the deflections and deformations of the arch, and movements of the piers and expansion joints due to changes in temperature and the addition of the superstructure.

The Arlington Memorial Bridge [1] extends over the Potomac River from the Lincoln Memorial in Washington, D.C., to Columbia Island,

[1] For a further description of the Arlington Memorial Bridge see Nagle, John L., The Arlington Memorial Bridge, Military Engineer (Society of American Military Engineers), vol. 20, p. 154, 1928.

near the Virginia shore. The structure consists of two small approach spans, eight reinforced-concrete arches, and a bascule draw span in the center of the bridge. The concrete arches diminish gradually and symmetrically in rise and span from the bascule bridge toward the shore abutments. All exposed portions of the concrete except the interior of the arch soffits are faced with white granite ashlar. The facing on the up and down-stream edges of the arch barrels consists of heavy granite voussoir blocks dovetailed into the concrete of the barrel. The piers supporting the arches are of mass concrete.

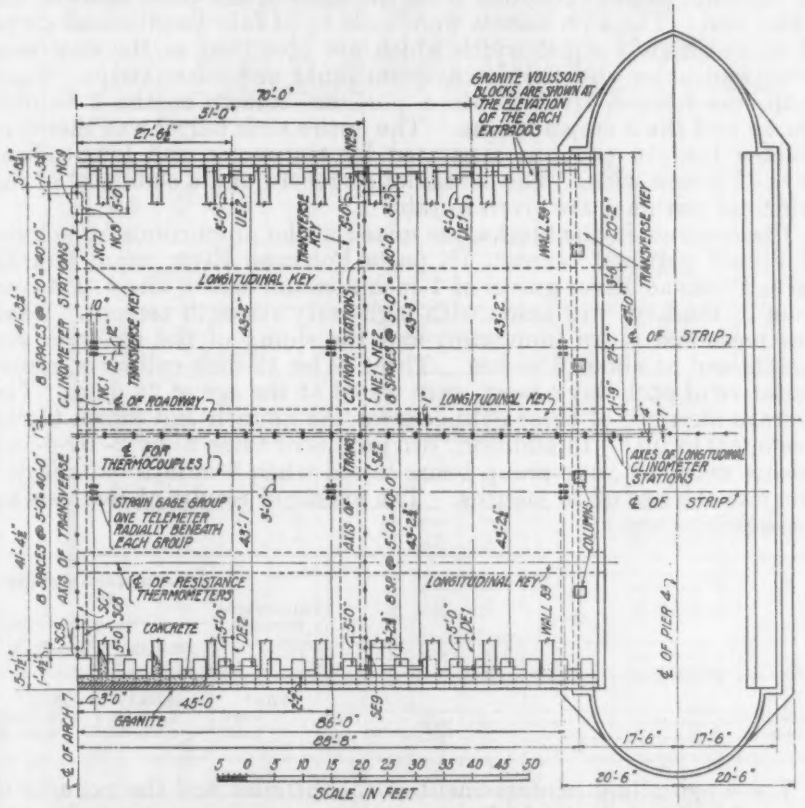

FIGURE 2.—*Plan of half span, arch no. 7, showing location of testing equipment.*
The granite voussoir blocks are cut on radial lines and extend upwards above the extrados of the barrel.

The over-all length of the bridge (including the abutments and the small abutment bypass arches) is 2,163 feet. The 60-foot roadway is flanked by two 15-foot sidewalks and heavy granite balustrades. The distance between the granite faces of the spandrel walls is 94 feet. A small scale elevation of the bridge is shown in figure 1 (A).

II. DESCRIPTION OF ARCH SPAN NO. 7

The design and assembly of testing apparatus and equipment was completed about the time the construction of the arch span designated as no. 7 was started, and this arch was, therefore, selected for

testing. The structural details of this arch are shown in figures 1 and 2.

Pier no. 4 at the east end of arch no. 7 is 41 feet wide and 130 feet long. The average rock elevation at the bottom is −36.6 feet (see figure 1 (A). Pier no. 5 at the west end of the span is 39 feet wide and 129 feet long. The elevation of rock under this pier is −33.3 feet.

The centering support for the arch barrels consisted of steel trusses connected with a hinge beneath the crown of the arch and supported on concrete ledges extending from the sides of the piers beneath the water line. The arch barrels were built up of four longitudinal strips of approximately equal width which are identified as the upstream inner and outer and the downstream inner and outer strips. Each strip was further divided into 4 portions, known as the 2 haunch blocks and the 2 crown blocks. The entire arch barrel was therefore divided into 16 portions separated by transverse and longitudinal keys 42 inches wide. The construction record and a summary of the principal test data are given in table 1.

The concrete in the blocks was mixed in the proportions by volume of 1 part portland cement, 1¾ parts Potomac River sand, and 3½ parts Potomac River gravel of 1-inch nominal size. The 1:2:4 concrete in the keys was made with high early strength cement. Sand was measured in an inundator, and the slump of the concrete was maintained at about 6 inches. Three 6- by 12-inch cylinders, representative of each day's pour, were tested at the age of 28 days. The average strength of these cylinders for the haunch and crown blocks was 3,900 lb./in.² In addition, two groups of three 2- by 2- by 4-foot prisms were cast, one group being tested when 1 month old and the other at the age of 25 months. The averaged results of the tests on these prisms are:

Age	Compressive strength	Secant modulus of elasticity at—	
		200 lb./in.²	2,000 lb./in.²
	lb./in.²	*lb./in.²*	*lb./in.²*
1 month	3,000	3,700,000	2,700,000
25 months	5,400	4,200,000	4,200,000

The longitudinal reinforcement at the intrados and the extrados of the arch consisted of 1-inch square bars 8 inches apart, resulting in slightly less than 1 percent of longitudinal reinforcement at the crown of the arch. The distance from the surface of the concrete to the face of the bars was 2 inches. The transverse reinforcement consisted of ½-inch square bars wired to the inside of the longitudinal bars on 30-inch centers. Shear reinforcement consisted of ¼-inch round bars running normal to the plane of the intrados and bent around the longitudinal bars at alternate intersections of the transverse and longitudinal reinforcement.

TABLE 1.—*Summary of construction data for arches 6, 7, and 8 with principal test data for arch 7*

[The sign of t is (+) when the intrados temperature is higher than the extrados temperature]

Date	Arch no.	Test no.	Relative crown elevation	Average temperature—T				Temperature gradient—t				Deck temperature	Remarks
				Springing	Haunch	Crown	Average	Springing	Haunch	Crown	Average		
			Inch	° *F.*	° *F.*	° *F.*	° *F.*	° *F./ft.*	° *F./ft.*	° *F./ft.*	° *F./ft.*	° *F.*	
July 17, 1928	8												Decentered i.u.s.[1]
Sept. 28, 1928	6												Do.
Oct. 6, 1928	7												Poured haunch blocks i.u.s.
Oct. 8, 1928	7												Poured crown blocks i.u.s.
Oct. 11, 1928	7												Poured cross keys i.u.s.
Oct. 17, 1928	7												Decentered i.u.s.
Oct. 19, 1928	6												Decentered i.d.s.[2]
Oct. 19, 1928	7												Poured haunch blocks i.d.s.
Oct. 20, 1928	7												Poured crown blocks i.d.s.
Oct. 23, 1928	7												Poured cross keys i.d.s.
Nov. 1, 1928	7	1	0	52.2	44.9	44.6	46.7	+1.5	+0.7	0	+0.7		Before decentering i.d.s.
Nov. 2, 1928	7												Decentered i.d.s.
Nov. 5, 1928	7	2	−.525	53.2	51.6	51.3	51.9	−.1	+.2	+.5	+.2		After decentering i.d.s.
Nov. 6, 1928	7	3	−.577	54.0	50.1	50.7	51.2	+.4	+1.6	+1.3	+1.2		Do.
Nov. 10, 1928	8												Decentered i.d.s.
Nov. 21, 1928	7	4	−.913	54.2	50.5	49.9	51.3	+.3	+2.3	+2.1	+1.8		Construction loads on i.d.s.
Nov. 22, 1928	7												Poured haunch blocks o.u.s.[3]
Nov. 23, 1928	6												Decentered o.u.s.
Dec. 3, 1928	7												Poured crown blocks o.u.s.
Dec. 10, 1928	7												Poured cross keys o.u.s.
Dec. 29, 1928	7												Poured center longitudinal key.
Jan. 2, 1929	7												Decentered o.u.s.
Jan. 3, 1929	7												Poured center longitudinal key blocks.
Jan. 18, 1929	8												Decentered o.u.s.
Feb. 5, 1929	7	5	−1.740	25.3	23.4	24.1	24.0	+.1	+1.3	+.4	+.8		No loads on two center strips.
Feb. 16, 1929	7	6	−1.465	32.0	30.9	31.5	31.2	−.1	+.5	+.1	+.3		No change in load.
Mar. 2, 1929	7	7	−1.220	38.6	40.1	40.0	39.7	0	+.2	+.5	+.2		Do.
Mar. 9, 1929	7	8	−1.368	37.4	34.7	34.6	35.3	0	+.7	−.7	+.2		Do.
Mar. 21, 1929	7	10	−.899	50.5	51.5	51.9	51.3	−.4	−.7	−.1	−.5		Do.
Mar. 27, 1929	7												Poured upstream longitudinal key.
Apr. 12, 1929	6												Decentered o.d.s.[4]
Apr. 17, 1929	7												Poured haunch blocks o.d.s.
Apr. 23, 1929	6												Started pouring cross walls.

Footnotes at end of table.

TABLE 1.—*Summary of construction data for arches 6, 7, and 8 with principal test data for arch 7*—Continued

[The sign of t is (+) when the intrados temperature is higher than the extrados temperature]

Date	Arch no.	Test no.	Relative crown elevation	Average temperature—T				Temperature gradient—t				Deck temperature	Remarks
				Springing	Haunch	Crown	Average	Springing	Haunch	Crown	Average		
			Inch	° *F.*	° *F.*	° *F.*	° *F.*	° *F./ft.*	° *F./ft.*	° *F./ft.*	° *F./ft.*	° *F.*	
Apr. 24, 1929	7												Poured crown blocks o.d.s.
Apr. 30, 1929	7												Poured cross keys o.d.s.
May 2, 1929	6												Deck slab concreted.
May 6, 1929	8												Decentered o.d.s.
May 8, 1929	7												Do.
May 11, 1929	7												Poured downstream longitudinal key.
May 22, 1929	7	11	−0.821	60.2	56.6	55.1	57.1	+0.3	+0.6	+1.2	+0.7		Wall forms and reinforcing steel in place.
May 22, 1929	7												Started concreting cross walls.
May 24, 1929	7	12	−.767	61.3	58.4	60.1	59.55	0	+1.4	+.5	+.8		Some of the cross walls concreted.
May 26, 1929	7	13	−.560	64.2	64.8	66.4	65.05	−.1	+.2	−.4	0		Additional cross walls concreted.
May 29, 1929	7												All cross walls concreted.
June 1, 1929	7	14	−.149	72.6	73.8	75.1	73.8	+.2	+.7	+.3	+.5		Resistance thermometers used.
June 3, 1929	7												Deck slab concreted.
June 5, 1929	7	15	−.715	64.9	60.4	61.0	61.7	+.8	+1.0	+.2	+.8		
June 6, 1929	7												Started construction of spandrel walls.
June 6, 1929	8												Started pouring cross walls.
June 20, 1929	8												Deck slab concreted.
June 22, 1929	7	16	−.339	76.1	78.1	77.3	77.4	+.3	−.7	+.3	−.2		Deck and wall forms partially wrecked.
Aug. 15, 1929	7												Spandrel walls completed.
Sept. 4, 1929	7												All debris removed from the arch.
Sept. 6, 1929	7	17	−.426	74.7	75.8	75.7	75.5	−.4	−1.2	−1.2	−1.0		Superstructure loads only.
Nov. 5, 1929	7	18	−.990	56.1	56.4	56.3	56.3	−1.4	−3.4	−4.2	−3.1		No change in load.
Jan. 7, 1930	7	19	−1.445	38.6	38.3	38.3	38.4	0	0	0	0	36.5	Do.
Jan. 25, 1930	7	20	−1.698	30.7	27.1	26.2	27.8	−1.5	−2.0	−2.2	−1.9	21.5	Do.
Feb. 8, 1930	7	21	−1.585	32.2	31.9	32.1	32.0	−.3	−.9	−1.2	−.8	30.7	Do.
Feb. 28, 1930	7	22	−1.260	44.5	46.9	47.8	46.5	−1.0	−4.0	−4.7	−3.4	43.6	Do.
Mar. 25, 1930	7	23	−1.261	46.2	47.5	48.0	47.3	+1.0	+1.6	+2.2	+1.6	54.5	Do.
Apr. 15, 1930	7	24	−.996	54.4	59.0	60.7	58.3	+1.1	−.7	−1.3	−.4	63.9	Do.
Apr. 19, 1930	7	25	−1.082	53.7	55.4	55.6	55.0	+.7	+.7	+1.4	+.9	60.3	Do.
May 5, 1930	7	26	−.733	68.0	69.8	69.4	69.25	−.9	−3.3	−3.0	−2.6	66.0	Do.
June 12, 1930	7	27	−.681	70.3	71.3	71.4	71.1	−1.0	−3.4	−3.7	−2.9	72.6	Do.
July 23, 1930	7	28	−.382	81.7	84.2	85.1	83.8	−.7	−3.8	−4.0	−3.1	82.1	Do.
Aug. 8, 1930	7	29	−.353	84.1	85.5	86.0	85.3	−1.0	−3.4	−3.8	−2.9	85.9	Do.
Oct. 10, 1930	7	30	−.993	65.7	63.8	63.7	64.25	−1.1	−2.0	−1.9	−1.8	63.6	Do.
Jan. 6, 1931	7	31	−1.737	34.4	35.1	35.5	35.0	+.9	+1.6	+1.6	+1.4	37.6	Do.

[1] I.u.s.: Abbreviated from inner upstream strip.
[2] I.d.s.: Abbreviated from inner downstream strip.
[3] O.u.s.: Abbreviated from outer upstream strip.
[4] O.d.s.: Abbreviated from outer downstream strip.

III. TESTING EQUIPMENT [2] AND ITS LOCATION

The temperature-measuring devices consisted of mercury in glass thermometers, thermocouples, and resistance thermometers. Strains were measured with telemeters and hand strain gages, and the deflection of the arch was observed by means of clinometers.

The thermocouples were of the single-junction copper-constantan type, connected to a 16-point potentiometer recorder. The recorder and samples of the thermocouple wire were calibrated at this Bureau.

The copper-coil resistance thermometers, including those within the telemeter cartridges, had a resistance of approximately 500 ohms. The resistance measurements were made with a portable wheatstone bridge which was connected directly to the leads of the thermometers at the extrados of the arch. Changes in resistance of about 0.5 ohm corresponding to changes in temperature as small as 0.5° F. were considered significant.

The clinometer,[3] figure 4, assembled at the navy yard, Washington, D.C., consisted of a tubular steel frame on which was mounted a spirit level and a micrometer-caliper head. The longitudinal spirit level was of such a sensitivity that a rotation of about 0.000015 radian caused the bubble to move one division (2 mm). The size of the bubble could be controlled by the use of an auxiliary reservoir, and the bubble came to rest quickly at all temperatures. The micrometer head could be read to the nearest 0.0001 inch by means of a vernier, corresponding to a rotation of 0.0000017 radian.

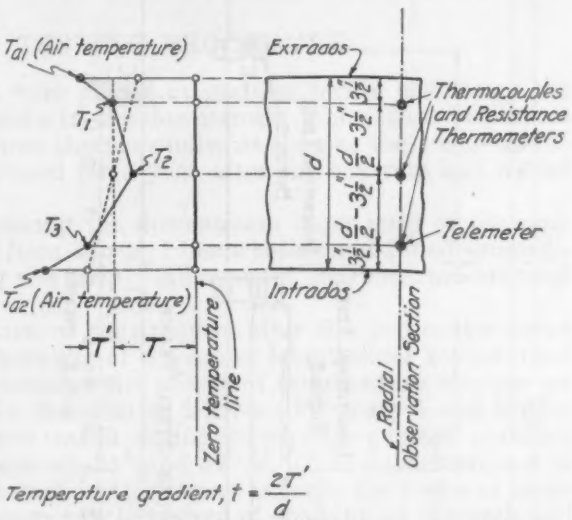

FIGURE 3.—*Detail of a radial observation section.*

The clinometer supports at the ends of each clinometer station consisted of steel and bronze bars set vertically in the concrete. They were alternately drilled and slotted to provide for small changes in length of the instruments or of the clinometer stations.

The 10 telemeters were of the single-resistor cartridge type.[4] During the construction of the superstructure water was ponded at the

[2] For a partial description of the testing equipment and the earlier tests see: Fishburn, C. C., Test measurements on the Arlington Memorial Bridge, at Washington, D.C., First International Congress for Concrete and Reinforced Concrete, Liége, Belgium (La Technique des Travaux—196 Rue Gretry, Liége), 1930.

[3] A clinometer was previously used in an investigation by the Special Committee on Concrete and Reinforced Concrete Arches of the American Society of Civil Engineers. See Bull. No. 174, Engineering Experiment Station, University of Illinois, Urbana, Ill.

[4] For a description of the telemeter see: McCullom, B., and Peters, O. S., A New Electric Telemeter, B.S.Tech. Paper No. 247, 1924, and Report on Arch Dam Investigation, Proc. Am. Soc. of Civil Eng., part 4, May 1928.

crown between the cross walls and evidently penetrated through the leads of the two telemeters at the crown, rendering them useless.

The deformations of the extrados of the arch were measured with 10-inch Whittemore strain gages.[5] The strain-gage stations were

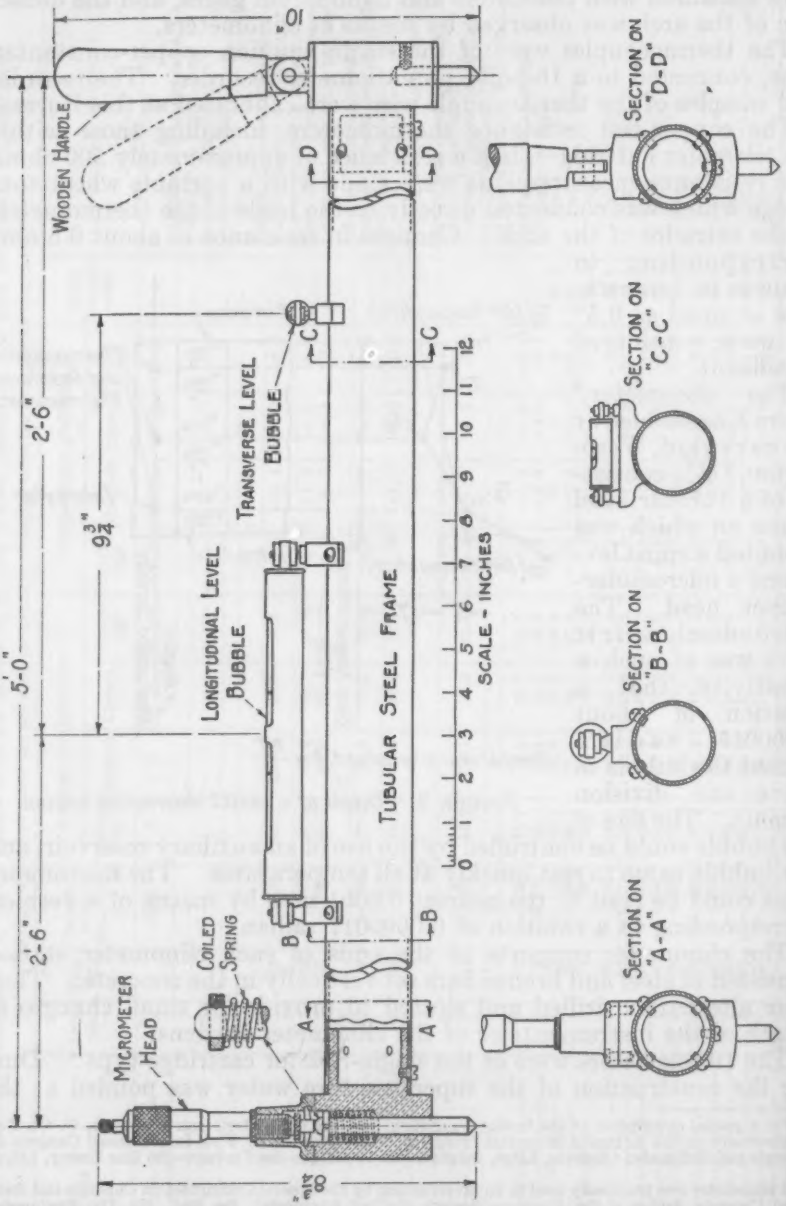

FIGURE 4.—*The clinometer.*

divided into 10 groups of 3 gage lines each, located as shown in figure 2, in a direction tangential to the curve of the extrados. Each gage

[5] For a description of a similar gage used on the Engineering Foundation Arch Dam Investigation, see Report of Arch Dam Investigation, Proc. Am. Soc. Civil Eng., May 1928.

length was marked by two bronze plugs flush with the surface of the concrete.

The location of the observation stations and of that part of the testing equipment which was fixed in position is shown in figures 1, 2, and 3. The thermocouples, resistance thermometers, telemeters, and the strain-gage stations were embedded in the concrete at five radial observation sections defined as the springing, haunch, and crown sections, according to their location as shown in figure 1. The two haunch sections and the two springing sections were symmetrically located about the crown. There were 9 thermocouples (not shown in the figures) located in the deck slab over the crown of the arch in 3 groups—1 group at the center of the roadway, 1 near the curb, and 1 midway between. The distance between the surfaces of the roadway slab and the upper and lower thermocouples in each group was 1½ inches.

IV. TESTING PROCEDURE

The thermocouples were placed in position before concreting the haunch and crown blocks in the downstream inner strip. Observations were made on these thermocouples as soon as the concrete was placed and were continued for a year after the concrete had cooled to air temperature.

The effect of decentering the downstream inner strip of the arch barrel was determined from 3 tests, 1 made before and 2 made immediately after decentering this strip. All types of instruments were used on these tests.

A temporary cessation of construction after the two center strips were joined by the concreting of the center longitudinal key afforded an opportunity to determine the effects of temperature changes on the unloaded arch. In the interval between February 5 and March 21, 1929, six tests were made during which the average concrete temperature varied between 24° and 51° F. The data from one of these (no. 9) were not used in this report because the test was made during the daylight hours and the effect of sunlight on the arch and clinometers affected the readings. Ninety percent of all observations were made during the late night or early morning hours when the fluctuations in air temperature usually were small.

Six tests to determine the effects of loads were made during the construction of the superstructure. Since the form work and timber bracing for the walls and deck interfered with the making of observations and the rapid addition and shifting of materials made it difficult to estimate loads, the study was confined to a comparison of the condition of the arch immediately before and after the construction of the superstructure, all debris having been removed from the span.

Fifteen tests were made on the completed structure. They included, in addition to the observations relating to the temperatures and deformations of the arch barrel, measurements of the deck temperatures, the widths of the expansion joints, and the difference in elevation between the ends of the transverse clinometer stations.

V. METHOD OF REDUCTION AND ESTIMATED PRECISION OF THE OBSERVATIONS

1. TEMPERATURE MEASUREMENTS

(a) TEMPERATURE MEASUREMENTS ON RADIAL OBSERVATION SECTIONS

The temperature of the arch barrel was determined from measurements made upon the radial observation sections shown in figures 1 and 3. Since, in radial sections located symmetrically about the crown the difference between the temperatures was small, the temperatures at such stations were averaged.

During tests 1 to 13, thermocouples were used to measure the temperatures T_1, T_2, and T_3 (fig. 3). The temperature T_3 was also measured with resistance thermometers located within each telemeter cartridge. Both the temperatures of the concrete extrados (T_{a1}) and the intrados (T_{a2}) were assumed equal to the air temperature measured at the base of the clinometer support. In the determinations of temperature with the thermocouples the average of a number of readings from each thermocouple was used. Because of slight maladjustment of the potentiometer recorder and a temperature gradient at the lead terminals, the readings from the group of thermocouples at each radial section contained constant errors which were not eliminated by averaging the readings. Since temperatures were measured more precisely with resistance thermometers and a portable bridge than with thermocouples and recorder, the temperature at a couple was considered to be that indicated by the couple plus the difference between the average temperature of the two resistance thermometers in the same radial plane and that of couple T_3 in the same group.

After test 13 the 15 resistance thermometers located in the downstream longitudinal key (fig. 2) were used for the determination of the temperatures T_1, T_2, and T_3, and thermocouples were used only for measuring the temperature of the deck slab. Enclosing the air space above the extrados by the completion of the superstructure resulted in differences in the temperature of the air at the intrados and at the extrados so that the temperature T_{a1} was determined as stated in the preceding paragraph and the temperature T_{a2} was assumed equal to the observed air temperature either on shore or above the roadway deck.

(b) CALCULATION OF THE AVERAGE TEMPERATURE AND THE TEMPERATURE GRADIENT

The equivalent linear temperature distribution which would have caused the arch to assume the same shape as that produced by the observed temperatures T_{a1}, T_1, T_2, T_3, and T_{a2}, is shown on the left half of figure 3. This equivalent temperature distribution was expressed for convenience by two components, the average temperature T and the radial increment of temperature T'. The component temperatures were computed from the observed temperatures under the assumption that the temperature gradient was constant between any two adjacent stations in a group T_{a1}, T_1, T_2, T_3, and T_{a2}.

The value of T may be written:

$$T=\frac{7(T_{a1}+T_1+T_3+T_{a2})+(d-7)\ (T_1+2T_2+T_3)}{4d},$$

where d is measured in inches.

The radial increment of temperature T' is equal to

$$T' = \frac{6S}{d^2},$$

in which S is the statical moment (about the gravity axis of the section) of the area between the broken line $T_{a1}T_1T_2T_3T_{a2}$ and the zero temperature line. The effect of differences in the temperature of the longitudinal reinforcement on the value of T' was included. The temperature gradient t given in table 1 is used in the text instead of the value T'. This temperature gradient is equal to:

$$t = \frac{2T'}{d},$$

and is taken as positive when the temperature of the intrados is higher than that of the extrados.

In the deflection calculations the temperatures of the segments (fig. 1) between radial observation sections were computed on the assumption that the increments in temperature of the segments varied as the increments of their radial thickness. If the temperatures and lengths of these segments be represented respectively by T and Δs then the average arch temperature $\frac{\Sigma T \Delta s}{\Sigma \Delta s}$ was found to be closely approximated by:

$$T_{Av} = 0.25T_s + 0.5T_h + 0.25T_c,$$

in which T_s, T_h, and T_c represent respectively the average temperature at the springing, haunch, and crown.

The changes in the values of T and t, denoted by ΔT and Δt may be obtained from the data in table 1.

(c) PRECISION OF THE TEMPERATURE MEASUREMENTS

A study was made of the temperature data from eight tests taken at random to determine the precision of the measurements of the average temperatures and temperature changes. In the study it was assumed that points within the arch barrel, symmetrically located relative to the crown and midplane of the barrel, were at the same temperatures during the tests. The standard deviations[6] of the temperature measurements T_s, T_h, and T_c on radial observation sections were computed from the standard deviations of observations made with the several types of instruments as indicated in table 2, cases I, II, and III. Each of the radial observation sections contained three resistance thermometers at the location T_3 (fig. 3), so that for both the springing and the haunch there were six like observations of temperature. The mean and the deviation from the mean of the temperature measurements made on these groups of six stations during a test were calculated, and the standard deviation of a resistance-thermometer observation for m measurements on n stations was taken as

$$\sigma = \frac{1}{m}\left[\sqrt{\frac{\Sigma V_a^2}{nc_1^2}} + \sqrt{\frac{\Sigma V_b^2}{nc_1^2}} + \cdots \sqrt{\frac{\Sigma V_m^2}{nc_1^2}}\right]$$

[6] See Mellor, J. W., "Higher Mathematics" (Longmans, Green and Company), p. 530 (1909 edition.

in which v is the deviation from the mean of n observations and c_1 is the coefficient given by Shewhart.[7]

TABLE 2.—*Precision of temperature measurements*

Case description	Standard deviation of the average temperature—T				Standard deviation of the changes in average temperature—ΔT			
	Springing	Haunch	Crown	Average [1]	Springing	Haunch	Crown	Average [1]
	°F.	°F.	°F.	°F.	°F.	°F.	°F.	°F.
I. Thermocouples only. Early hardening period	0.8	0.8	0.8	0.5	1.1	1.1	1.1	0.7
II. Tests nos. 1 to 13. Thermocouples corrected by reference to telemeter temperature	.4	.4	.4	.2	.6	.6	.6	.3
III. Tests nos. 14 to 31. Resistance thermometers and telemeters	.15	.15	.22	.10	.2	.2	.3	.1

[1] The average for the arch.

The standard deviations of measurements made with thermocouples (table 2, cases I and II) were calculated similarly by comparing the thermocouple temperature with the average temperature of those resistance thermometers in like locations. The deviation was taken as the difference between the thermocouple and the corresponding resistance-thermometer temperature for each of 15 thermocouples during a test. The temperature observations made with resistance thermometers were assumed to be correct, and the standard deviation of the resistance-thermometer observations was neglected except for the measurement at T_3 in case II.

The standard deviation of all observations made with mercury in glass thermometers (stations T_{a1} and T_{a2}) was taken as 0.7° F. It can be seen that for those tests in which the 15 resistance thermometers and the 10 telemeters were used, the standard deviation for the average temperature changes occurring between tests was 0.3° F. for the crown section and 0.2° F. for the springing and haunch sections. The temperature gradients, observed before both the construction of the superstructure and the use of the resistance thermometers in the downstream longitudinal key, were too small compared with their standard deviations to be considered significant.

2. CLINOMETER OBSERVATIONS

The original clinometer data consisted (for each test) of two (or more) readings on each station. The second of these readings was made with the instrument reversed on the supports so that errors due to misalignment of the longitudinal level bubble with the frame were eliminated. A check on the accuracy of the observations and the seating of the instrument on the supports was made by adding the two readings on each station. This sum should be constant at all stations if the observations were correctly made.

The difference in elevation between the two ends of a station during the tests was equal to one half the difference between the readings on the station with clinometer reversed. Corrections were made for the effect of temperature on the length of the supports.

[7] Shewart, W. A., Basis for analysis of test results of die casting alloy investigation, Proc.A.S.T.M. vol. 29, part I, p. 200, 1929.

The crown deflections of the arch were calculated by adding algebraically the changes in the differences of elevations between the ends of the longitudinal stations between the center lines of the piers and the crown. Since the summation, if made from both piers, usually resulted in a small apparent change in the elevation of one pier relative to the other, the observed crown deflection was corrected by an amount equal to one half the change in relative pier elevation.

Changes in curvature of the arch barrel occurring between tests were determined by applying to the clinometer observations a correction for the slope of the arch. The change in curvature, λ, at a clinometer support is given by:

$$\lambda = (\beta_1 - \beta_2)\frac{1}{m},$$

in which β_1 and β_2 are the changes in the slope of two adjacent stations and m is the average chord length of the arch axis at these stations. For a horizontal station (crown) m was 60 inches. The strain at the extrados due to change in curvature is equal to $\frac{\lambda d}{2}$, in which d is the radial depth of the arch.

The precision of the clinometer observations was calculated from the data obtained during a special test. A total of 120 observations was made with 2 clinometers on 3 longitudinal clinometer stations. The standard deviation of a measurement representing the actual difference in elevation between the two ends of a station was found to be 0.00018 inch, and the resulting standard deviation for a measurement of a change in the difference in elevation between the two ends of a station was 0.00025 inch.

Using these values, the standard deviation of the measurement of a crown deflection would be 0.0012 inch, and the standard deviation of the change in the relative elevation of the piers would be 0.0016 inch. This special test was free from errors due to the rotation of the supports and changes in length of the instrument, as well as possible errors in the temperature correction for the length of the clinometer supports. It is reasonable, however, to suppose that indicated changes in relative pier elevation greater than 0.01 inch are due to the settlement of one pier relative to the other rather than to errors in observation.

3. STRAIN-GAGE AND TELEMETER OBSERVATIONS

The original strain-gage data consisted of two or more readings at each of the gage lines. Additional readings were made whenever the difference between the first two observations on a gage line exceeded 0.00001 inch per inch. Two readings were made on each telemeter during a test, one at the start and one near the finish of the test. The average value of the observations was used in the determination of strain and temperature.

A study was made of the standard deviation of the strain gage and the telemeter readings. For this purpose the observed deformations occurring consecutively between tests 17 to 31 were used. Assuming that the deformations at stations located symmetrically about the crown were equal, it was found that the standard deviation of observations made from 12 gage lines was roughly 3 times the standard

deviation of similar observations made from 4 telemeters. The standard deviations calculated from the telemeter observations did not include the effects of possible changes in calibration of these instruments.

The standard deviations for strain-gage and telemeter observations are as follows:

	Strain × 10^6
For single strain-gage station	35
For average of 12 strain-gage stations	10
For single telemeter station	7
For average of 4 telemeter stations	3

VI. RESULTS OF THE TESTS

1. TEMPERATURES AND TEMPERATURE CHANGES OF THE ARCH

(a) INITIAL TEMPERATURE RISE OF THE ARCH BARREL BLOCKS DURING HARDENING OF THE CONCRETE

The temperature of the concrete at the west springing in the downstream inner strip after placing and until air temperature had been attained is shown in figure 5. The initial temperature of the concrete when pouring was begun (about 8 a.m.) was approximately 75° F. A maximum temperature of 143° F. was observed about 25 hours after placing. The evolution of heat accompanying the hardening of the concrete continued for some time after the maximum temperature was reached, and it was nearly 15 days before the slowly dropping temperature of the concrete approximated the temperature of the air. Unless the construction of transverse keys in arches of this type be delayed more than a few days, there will be little advantage in pouring the keys separately from the main body of the arch.

The thermal insulating effect of the bottom forms and the wetting down of the concrete extrados caused a positive temperature gradient between the intrados and the extrados that lasted until thermal equilibrium with the air was established. The existence of a positive temperature gradient near the piers was of advantage in compensating for the strains caused by cooling of the arch concrete after the keys were placed.

The maximum observed temperature attained in the thinner portions of the arch barrel blocks varied between 90° and 100° F. As in the thicker portions of the arch, the maximum temperature was attained within 25 hours after placing the concrete. Positive temperature gradients were found to exist for about 8 days after pouring when thermal equilibrium with the air was reached.

(b) VARIATION OF THE ARCH TEMPERATURE WITH SEASONAL TEMPERATURE CHANGES

The maximum, minimum, and average air temperatures for 5-day periods between October 1928 and February 1931 are shown in figure 6. The temperatures of the arch barrel during the tests are also shown by numbered points and may be seen to approximate closely the mean air temperature for corresponding 5-day periods.

The minimum observed average temperature of the arch barrel, 24° F., was measured on February 5, 1929. After the completion of the superstructure the minimum observed average temperature was 28° F. on January 25, 1930. At this time the temperature of the

enclosed air beneath the deck was 27° F. and that of the outside air was 19° F.

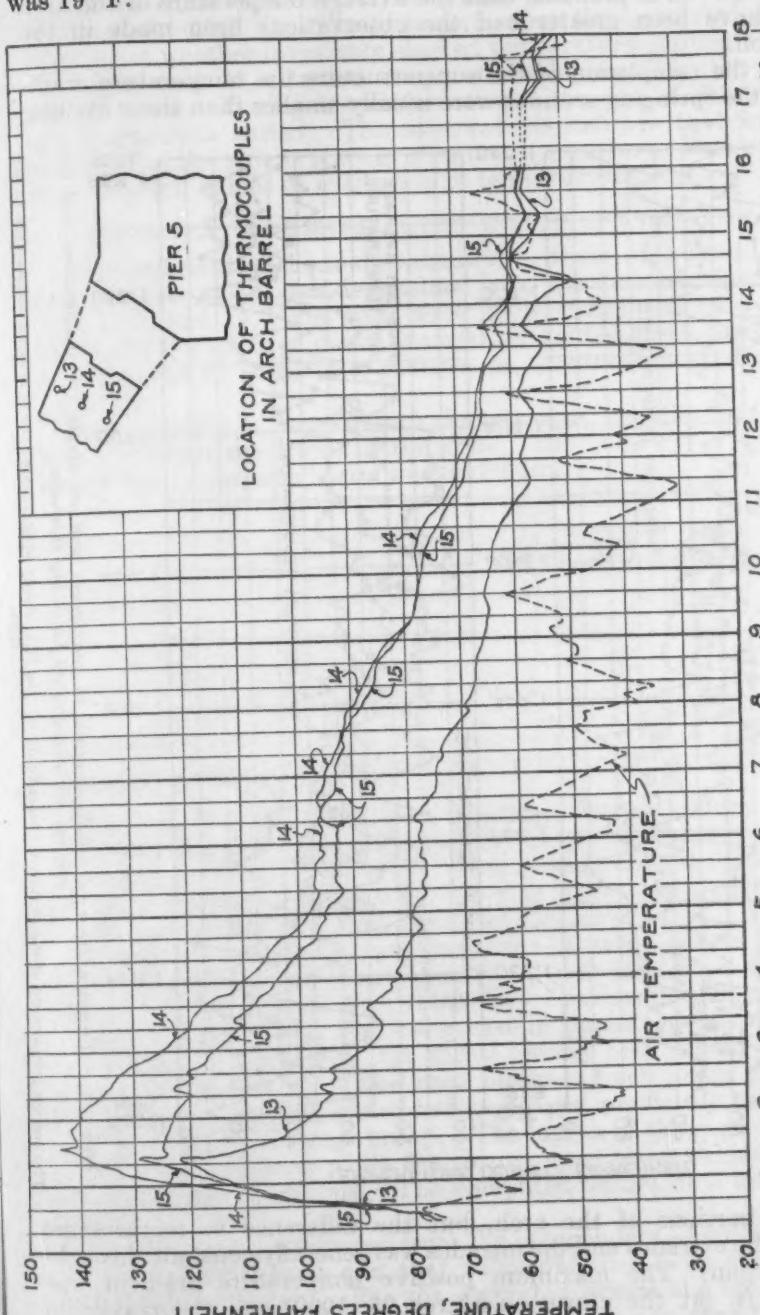

FIGURE 5.—*Initial temperature rise in the haunch block near pier 5.*

The thermal insulation of the bottom forms is responsible for the relatively high temperature indicated by thermocouple no. 15, as compared with that indicated by thermocouple no. 13.

The maximum observed temperature of the arch barrel was 85° F. at 6 a.m. on August 8, 1930 (test 29). The temperature of the

enclosed air beneath the deck was 89° F. and that of the outside air was 75° F. It is probable that the average temperature of the arch would have been greater had the observations been made in the afternoon.

After the completion of the superstructure the temperature gradients at the springing sections were usually smaller than those existing

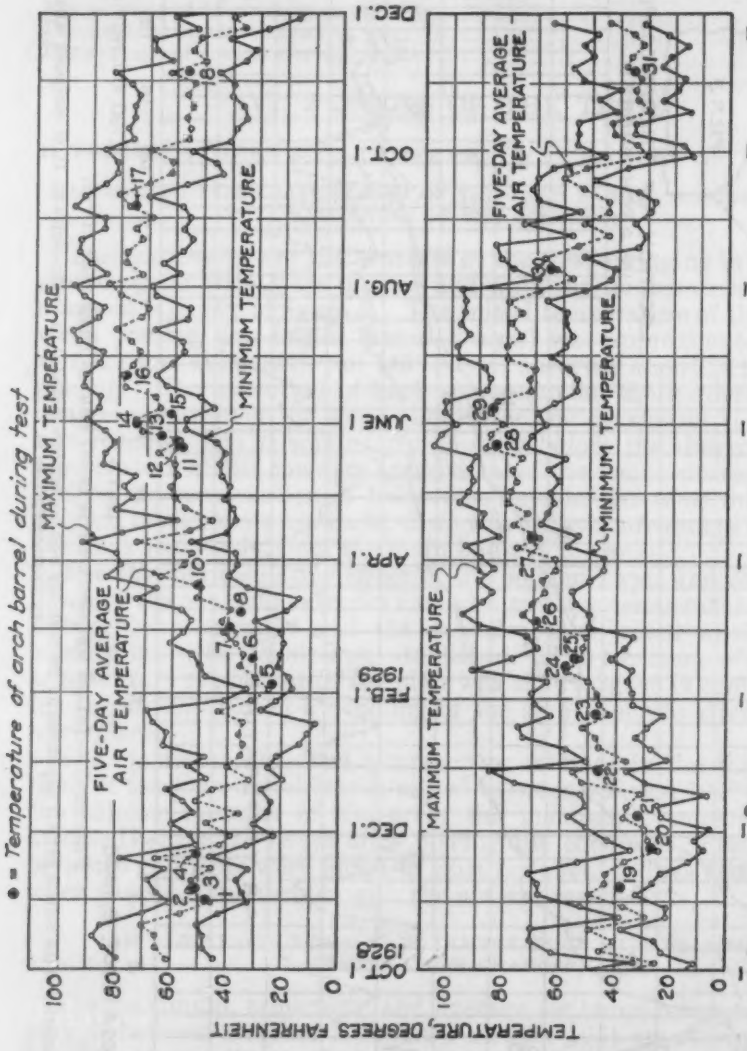

FIGURE 6.—*Temperature record—Fluctuation in maximum and minimum air temperature and the average air temperature for 5-day intervals.*

The average temperature of the arch-barrel concrete during the tests closely approximated the average air temperature for the previous 5 days.

at other portions of the arch, but the difference in temperature between the extrados and the intrados was generally constant throughout the span. The maximum positive temperature gradient was +2.2° F./ft. (at the crown on March 25, 1930) and the maximum negative temperature gradient was −4.7° F./ft. (at the crown on February 28, 1930). The temperature gradients at the springing rarely exceeded 1° F./ft.

During test 29 the difference between the temperature of the enclosed air space and that of the outside air caused a temperature gradient of −3° F./ft. The tests made upon the completed structure during hot weather invariably showed temperature gradients of negative sign, that is, extrados temperatures higher than the intrados temperatures. During the colder months the sign of these temperature gradients varied. The observations indicate that for arches of this type the temperature gradients are negative at both extremely low and high values of average arch temperature.

2. COEFFICIENT OF THERMAL EXPANSION OF THE ARCH BARREL

The coefficient of thermal expansion, α, of the arch barrel, without superstructure loads was determined from the data obtained in tests 5, 6, 7, 8, and 10. The tests were made during the early morning hours and the effect of direct sunlight on the temperature of the arch extrados was so small that changes in temperature gradients were neglected.

In calculating α, temperature changes were considered to be symmetrical about the crown of the arch. The values of α for the two inner strips of the arch barrel were as follows:

Test no.	Change in average arch temperature	Crown deflection	Coefficient of linear thermal expansion, α
	°F.	*Inch*	*Millionths per °F.*
5–6	+7.8	0.275	7.5
6–7	+8.4	0.245	6.3
7–8	−4.4	• −0.148	7.0
8–10	+16.0	0.469	6.3
Average (weighted)			6.7

• Downward deflection.

The standard deviation of α calculated from weighted values of each test, depending upon the amount of the change in average temperature, was about 1.5×10^{-6}. It is possible that the difference between separate determinations of α may have been partially caused by changes in the moisture content of the concrete.

A study of volume changes was made on seven prisms of concrete which were cut from the extrados of the arch after the completion of test 31. These prisms were about 5 by 5 inches in cross section and 20 inches long. They had been cast in paraffined metal U-shaped forms open at both ends, the forms having been placed in position before the concreting of the arch blocks. Each prism contained a single strain-gage line, which had been used previously as the center gage line of a strain-gage group. The length of the gage lines in the prisms was measured while the prisms were being subjected to different storage conditions. The computed values of α are shown in table 3.

The value of α computed from the independent observations made on the air-dry prisms and that value obtained from the arch tests checked very closely. For the saturated prisms the coefficient was found to be slightly less. In all calculations applying to the arch, the coefficient of thermal expansion of the arch barrel was taken as 65×10^{-7} per ° F.

TABLE 3.—*Prism tests*

Test no.	Storage conditions	Temperature			Change in length per unit of length		α Coefficient of linear thermal expansion
		Duration	Average	Change between consecutive tests	Change between consecutive tests	Cumulative change	
		Days	° *F.*	° *F.*	*Millionths*	*Millionths*	*Millionths per* ° *F.*
1	Air dry, uncontrolled humidity	0	69.0			0	
				+59.4	+370		
2	do	24	128.4			+370	6.2
				−59.4	−410		
3	do	50	69.0			−40	6.9
				+0.2	+380		
4	Immersed in water	82	69.2			+340	
				+43.5	[1] +345		
5	do	52	112.7			+685	[1] 7.9
				−44.0	−260		
6	do	46	68.7			+425	5.8
				+40.5	+250		
7	do	44	109.2			+675	6.2
				−40.9	−235		
8	do	30	68.3			+440	5.8
				+2.0	−320		
9	Air dry, uncontrolled humidity	388	70.3			+120	

[1] This comparatively large expansion was measured the first time the prisms were immersed in hot water, and was not used in the determination of the average of α.

3. VERTICAL DEFLECTIONS OF THE ARCH BARREL

(a) DEFLECTION RESULTING FROM DECENTERING THE DOWNSTREAM INNER STRIP

A vertical settlement of pier no. 4 relative to pier no. 5 was found to have occurred after decentering the arch strip. Since the clinometer data do not indicate an appreciable rotation of either pier, the horizontal displacement of the top of pier no. 4 was neglected. The possible effects of the differences in temperature gradients were not determined because the accuracy of these temperature measurements was relatively poor.

The theoretical deflection of the arch due to changes in average temperature and to the settlement of pier no. 4 as well as the deflection due to decentering are shown in figure 7. The deflection (effect of decentering) is equal to the difference between the observed deflection and the theoretical deflection.

(b) DEFLECTION PRODUCED BY THE ADDITION OF THE SUPERSTRUCTURE WALLS AND DECK

Tests 10 and 17 were compared to determine the deflection produced by the addition of the superstructure walls and deck. Test 10 was made before work on the superstructure was started and test 17 was made after this work was completed. The results of this study are illustrated in figure 8, which shows the observed deflection of the arch (curve *A*), the deflection produced by movements of Pier No. 4 together with that theoretically due to temperature changes (curve *B*), the load deflection (curve *C*), and, on the assumption of a modulus of elasticity of 4,000,000 lb./in.^{2}, the theoretical load deflection produced by the superstructure loads (curve *D*). Throughout the paper the effects of superstructure restraint on theoretical deflections have been neglected unless otherwise stated.

The longitudinal clinometer data indicated that the top of Pier No. 4 had rotated through an angle of about 30 millionths of a radian

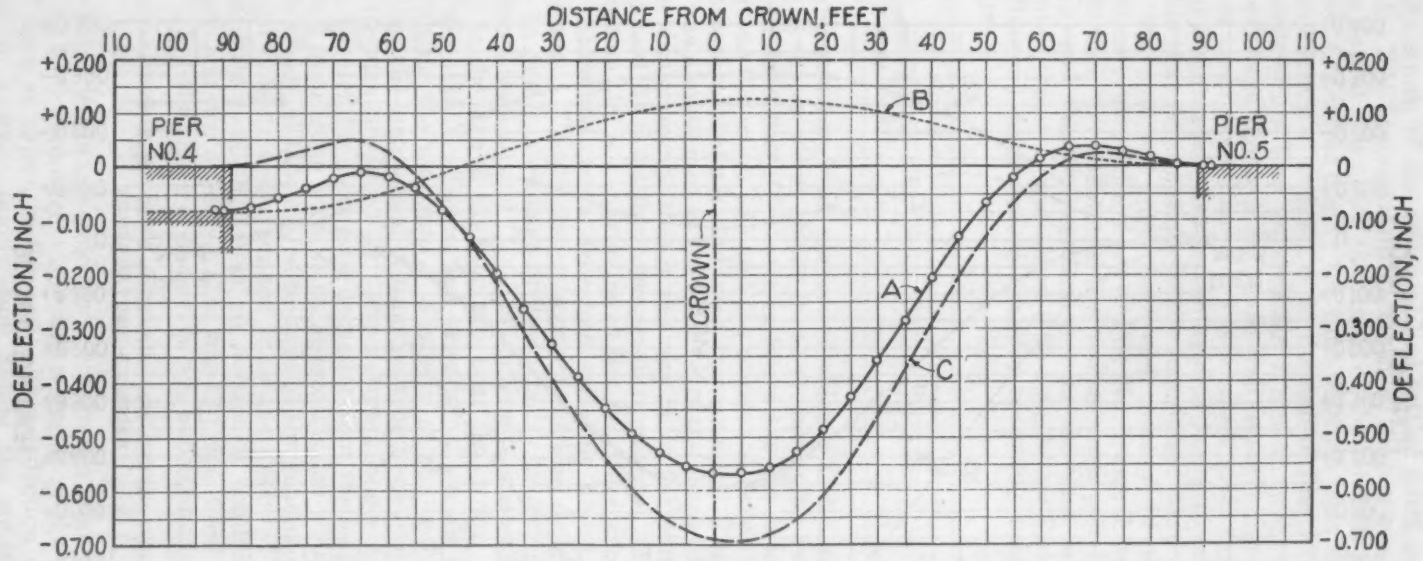

FIGURE 7.—*Deflection produced by decentering the downstream inner strip of the arch barrel.*

A, the observed deflection occurring between tests 1 and 2; *B*, the theoretical deflection produced by temperature changes and the vertical settlement of pier no. 4; *C*, the deflection caused by decentering.

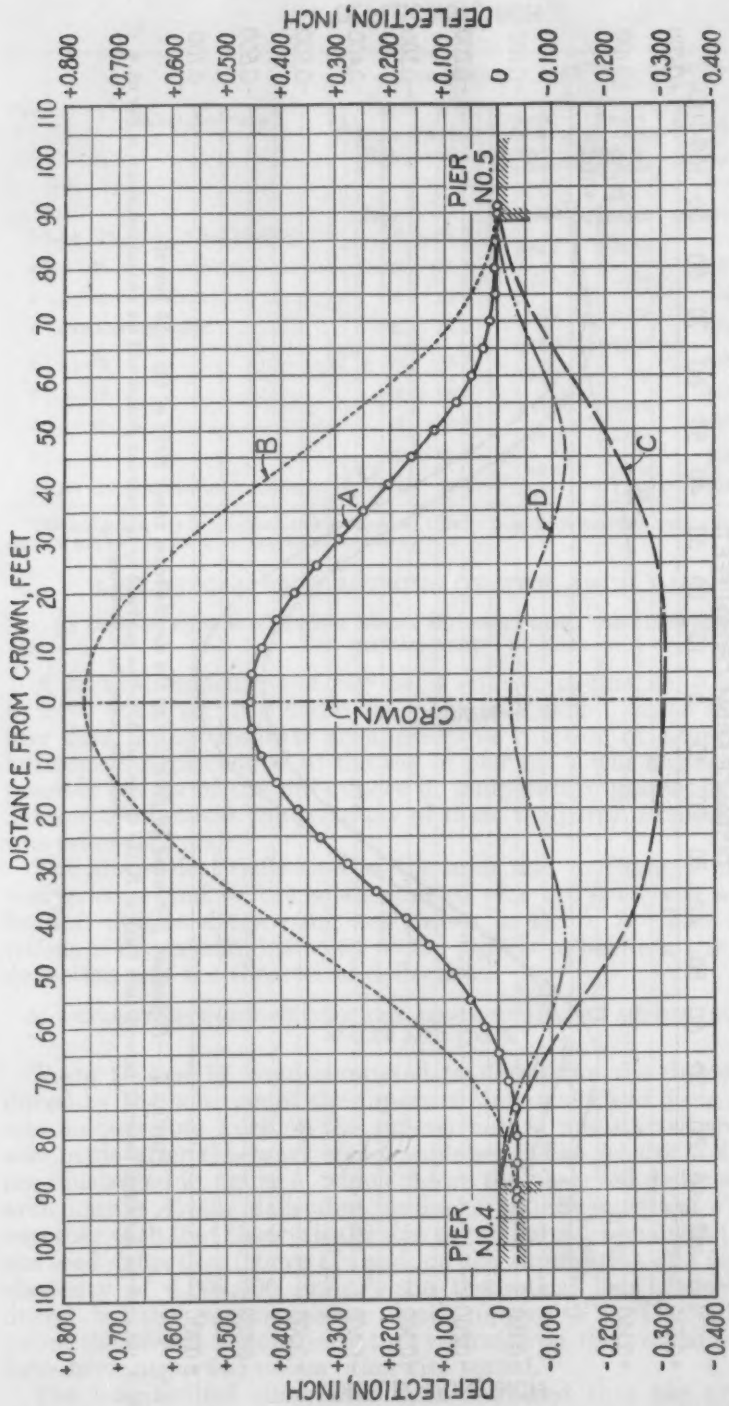

FIGURE 8.—*Deflection produced by the addition of the superstructure walls and deck.*

A, the observed deflection occurring between tests 10 and 17.
B, the theoretical deflection produced by temperature changes and pier movements.
C, the load deflection. (The difference between curves *A* and *B*.)
D, the theoretical load deflection for $E_c = 4{,}000{,}000$ lb./in.^{2}

toward the crown of the arch and had settled 0.022 inch relative to Pier No. 5. The horizontal displacement of the pier was not measured. From the data it was noted that most of the rotation and settlement of Pier No. 4 occurred during the time between tests 10 and 11 when the superstructure of arch no. 6, to the east of Pier No. 4, was built. The superstructure load on arch no. 7 during test 11 included the major portions of the deck and cross-wall forms. Since the observed rotation of the top of Pier No. 4 was much greater than could be caused by deformation due to the applied forces from arch no. 6, it is probable that deformations in the foundation were responsible for most of the observed settlement and rotation of the pier. The horizontal movement of the top of Pier No. 4 was, therefore, assumed to be 0.02 inch (30 millionths of a radian times pier height) toward the crown, and the total settlement near the west side of the pier, at the end of the arch, was about 0.03 inch, below Pier No. 5.

The observed temperature changes occurring between tests 10 and 17 are:

Change in	Springing	Haunch	Crown	Average
Average temperature ΔT, °F	+24.2	+24.3	+23.8	+24.2
Temperature gradient Δt, °F./ft.	0	−.5	−1.1	−.5

The superstructure loads per foot of width of arch barrel varied from 2,500 lb. at the crown to 10,500 lb. at the springing line.

The load deflection (*C*) shown in figure 8 is the difference between the measured deflection (*A*) and the calculated deflection (*B*) caused by temperature changes and pier movements. This load deflection (*C*) was a maximum at the crown and the shape of the deflection curve was similar, except that it was very much flatter near the crown, to one caused by a uniform temperature change. The theoretical load deflection (*D*) is a maximum 45 feet on either side of the crown, and the theoretical crown deflection was only about 20 percent of this maximum. The difference between the load deflections (*D*) and (*C*) may be due to shrinkage or flow which occurred during the 170 days between tests 10 and 17. This difference was sufficient to cause a reversal in the sign of the moments near the crown.

The study of the load deflection was originally made for the purpose of determining the modulus of elasticity of the arch barrel. It is evident that the long period of time between tests 10 and 17, and the large deflections produced by temperature changes and pier movements so affected the measured deflection that the load deflection, as determined from these tests, is an approximation which includes the indefinite effects of flow and shrinkage of the concrete.

The load deflection determined from the observed deflections on the assumption that there was no horizontal displacement of Pier No. 4, gave a crown deflection that was 13 percent less than shown in curve (*C*), but the shape of the curve was substantially the same.

(c) EFFECT OF SUPERSTRUCTURE RESTRAINT ON DEFLECTION PRODUCED BY TEMPERATURE CHANGES

The vertical deflections produced by a change in average arch temperature (p. 577) were affected by the restraint of the superstructure wall and deck as shown in figure 9. The deflection produced by a 1° change in average temperature before the superstructure was built (curve *A*) was plotted from data obtained on tests 5, 6, 7, 8,

and 10 and closely approximates the theoretical temperature deflection for the coefficient of expansion 65×10^{-7} per °F. The curve (B) was plotted from data obtained in tests 17 to 31, which were made after the superstructure was completed, except that the comparison between test 22 and test 23 was not included because the changes in average temperature occurring between these tests were much less relative to the changes in temperature gradients than between other tests. The effects of changes in temperature gradients were neglected because theoretically the deflection produced by these changes is much less than that caused by changes in average tempera-

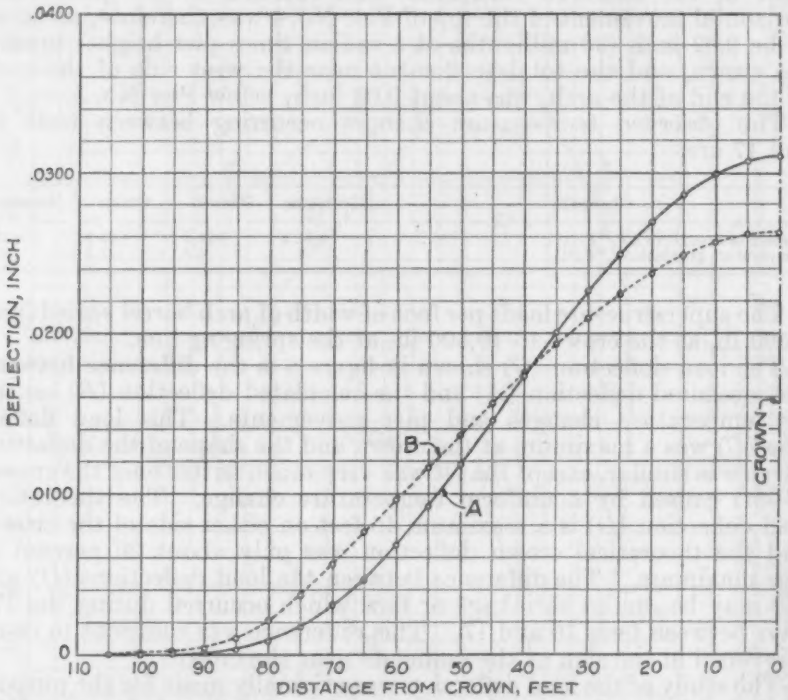

FIGURE 9.—*Observed deflection produced by a change in average arch temperature.*
A, before the construction of the superstructure; *B*, after the construction of the superstructure.

ture. From figure 9 it is evident that the superstructure restraint reduced the crown deflection and the curvature near the crown of the arch and increased the deflections near the piers.

The effect of changes in temperature gradients, Δt, and in average temperature, ΔT, on the crown deflection after the construction of the superstructure was determined also. The method of least squares was applied to data representing the crown deflection and temperature changes occurring between 15 consecutive tests (17 to 31). Since the crown deflections were small compared to the dimensions of the arch, they could be expressed linearly, thus:

Crown deflection (inch) $= +0.027\,\Delta T - 0.015\,\Delta t_s + 0.033\,\Delta t_h - 0.020\,\Delta t_c$

in which ΔT is the change in average arch temperature (°F.), and Δt_s, Δt_h, and Δt_c represent respectively the changes in the temperature gradients (°F./ft.) at the springing, haunch, and crown

sections. The standard deviations of the coefficients of ΔT, Δt_s, Δt_h, and Δt_c are respectively 4, 190, 145, and 155 percent of the coefficients.

For a change in the temperature gradient throughout the arch such that the extrados temperature dropped 1° lower than the intrados temperature (positive change), the crown deflection computed from the equation is +0.001 inch. Theoretically (assuming no superstructure restraint) the crown deflection produced by such a change in gradient is −0.002 inch. The deflections caused by changes in the temperature gradients were so small in comparison with those caused by change in average temperature that the data do not furnish a reliable measure of the effects of temperature gradients. The value of the coefficient +0.027 (inch per °F.) which gives the crown deflection caused by a change of 1° F. in average temperature of the arch, compares favorably with the value of 0.0262 shown on curve (*B*) in figure 9.

(d) DEFLECTION OCCURRING WITH TIME

The deflections due to shrinkage and flow are computed for periods of approximately 1 and 2 years.

The deflection for the 2-year period, shown in figure 10, was obtained by comparing test 2 (when the age of the inner strips was about 18 days) with test 30. In this figure the observed deflection is shown in curve *A*; the theoretical deflection produced by temperature changes, superstructure loads, and movements of the piers is shown in curve *B*; and the time-deflection (difference between *A* and *B*) is shown in curve *C*. The change in average temperature was about +12° F. and the vertical settlement of Pier No. 4 relative to Pier No. 5 was 0.07 inch. The theoretical load deflection (included in the ordinate of curve *B*) is shown in figure 8 (D). The deflections due to the slight horizontal and angular pier displacements and to changes in temperature gradients were negligible compared to the other relatively large deflections. The time-deflection (curve *C*) closely approximates at all points the deflection computed for a temperature drop of about 27° F.

The deflection for the 1-year period between test 19 and 31 (starting when the age of the two inner strips of the arch barrel was about 15 months) was determined from the data obtained in those tests and is shown in figure 11 (*A*). The theoretical deflection produced by the temperature changes is shown by curve *B*, and the deflection shown by curve *C* (the difference between *A* and *B*) represents the cumulative effect of all other changes during the period. The temperature changes which occurred at the radial observation sections and in the deck slab are.

	Temperature change at—				
	Springing	Haunch	Crown	Average	Deck
Average temperature ΔT, °F	−4.2	−3.2	−2.8	−3.4	+0.9
Temperature gradient Δt, °F./ft	+.9	+1.6	+1.6	+1.4	----------

There was no change in dead load on the arch, and the pier displacements were negligible.

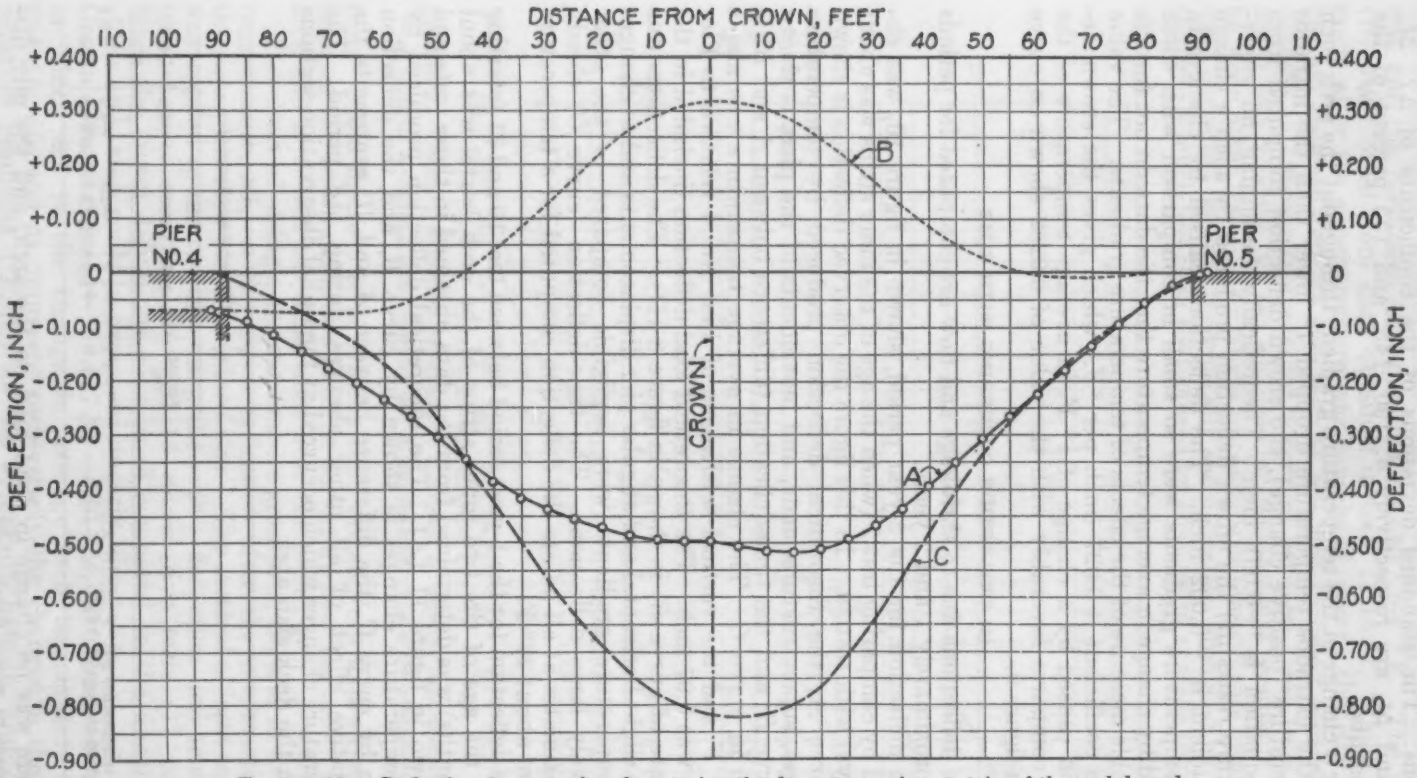

FIGURE 10.—*Deflection 2 years after decentering the downstream inner strip of the arch barrel.*

A, the observed deflection occurring between tests 2 and 30; *B*, the theoretical deflection produced by temperature changes, pier displacement, and the addition of the superstructure walls and deck; *C*, the deflection occurring with time.

superstructure walls and deck; *C*, the deflection occurring with time.

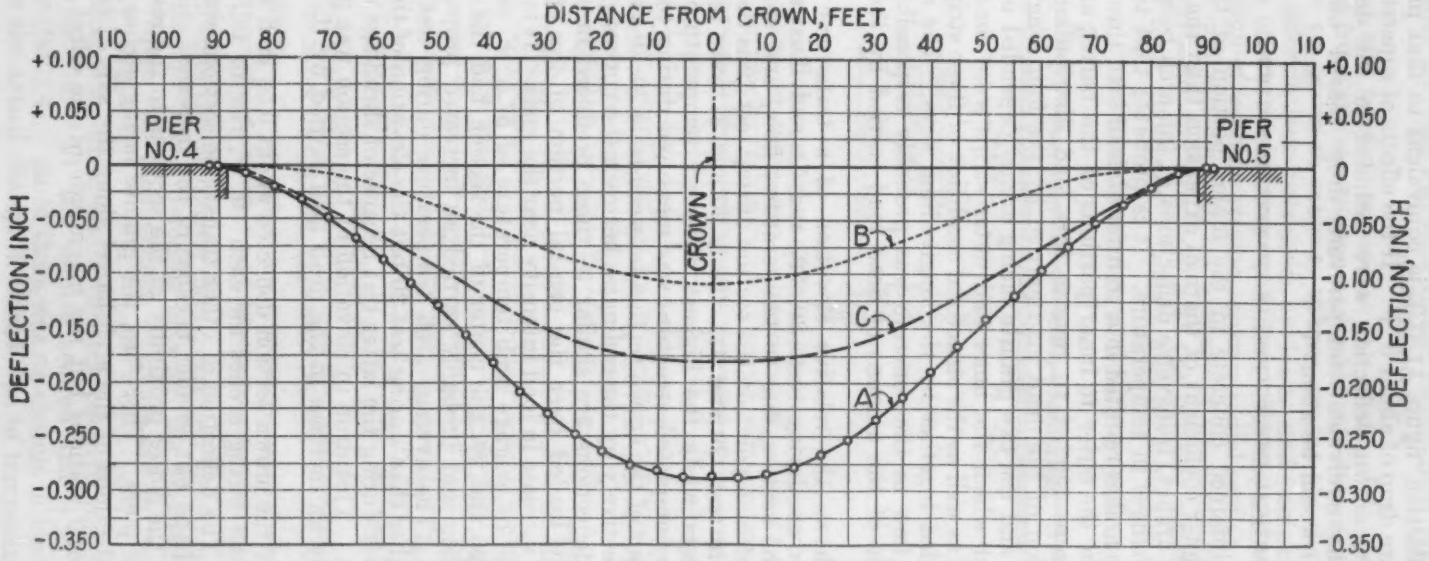

FIGURE 11.—*The deflection between January 7, 1930, and January 6, 1931.*

A, the observed deflection between tests 19 and 31; *B*, the theoretical deflection produced by temperature changes (no superstructure restraint); *C*, the deflection caused by flow and shrinkage of the concrete.

The time-deflection, figure 11 (*C*), is equivalent to that produced by a temperature drop of about 6° F. If the effects of superstructure restraint on the crown deflection were included in the deflection calculations, the equivalent temperature drop (based on crown deflection only) would be about 7° F.

(e) VERTICAL DEFLECTIONS IN TRANSVERSE SECTIONS

Since the reinforced concrete in the major portion of the arch barrel has a higher coefficient of thermal expansion than the granite voussoir facing arches, transverse deflections of the arch barrel were produced by changes in temperature. It is probable that temperature rises in the arches resulted in a transfer of dead load through the cross walls from the outer to inner portions of the barrel, and that temperature drops tended to reverse this load distribution. The actual proportion of the dead load carried by the four longitudinal concrete strips and the two granite facing arches depended upon the temperatures at which the inner and outer strips were constructed and decentered as well as the structural condition of these strips when they were bonded together by the longitudinal keys. The effect of shrinkage and flow in the concrete was probably responsible for a gradual increase of the amount of dead load carried by the facing arches.

Figure 12 shows the relative elevation of a transverse section through the crown during tests 20, 29, and 31 and illustrates the deflection of the section due to temperature, flow, and shrinkage. The elevation of each point on the section during test 29 is the datum for that point in tests 20 and 31. Tests 20 and 31 were both low-temperature tests while the highest observed temperature of the concrete in the completed structure was measured during test 29.

The deflections of the crown section between tests 20–29 and 29–31 are shown respectively by the ordinates between the curves *A*–*B* and *A*–*C*. These deflections are similar to those produced in a simple beam uniformly loaded over the central portion of the span and having a slight increase in load intensity near the ends. It is evident that with a rise in average arch temperature of 57.5° F. occurring between tests 20 and 29, the center of the section had the greatest upward deflection and probably carried an increased proportion of the dead load. The average arch temperature during test 31 was about 7° F. higher than during test 20 but the elevation of the crown section was lower during the latter test because of shrinkage and flow in the concrete. This drop in elevation of the section was probably accompanied by an increase in the dead load carried by the granite facing arches.

The center of the crown section deflected about 0.03 inch above or below the granite facing arches for each 10° F. rise or fall in arch temperature. The deflection of other transverse sections was of the same general shape but smaller because of the increased stiffness of the bridge and the closer proximity of the sections to the restraining influence of the piers. Therefore, the granite facing arches affected the vertical deflections of the arch barrel along the axis of the longitudinal clinometer stations but the magnitude of the effect was not determined.

4. STRAINS AT THE PRINCIPAL SECTIONS DUE TO THRUST AND BENDING

Thrust and bending strains at the principal observation stations obtained from the strain-gage and telemeter data corrected for temperature are given in table 4. These strains are the strains due to elastic deformations produced by loads and temperature changes plus the effects of shrinkage and flow. On the assumption that the distribution of bending strains across a radial section was linear, the thrust strain was equal to the average of the strains on the extreme fibers (extrados and intrados) and the bending strain was equal to one half their difference. Table 4 also includes the bending strains

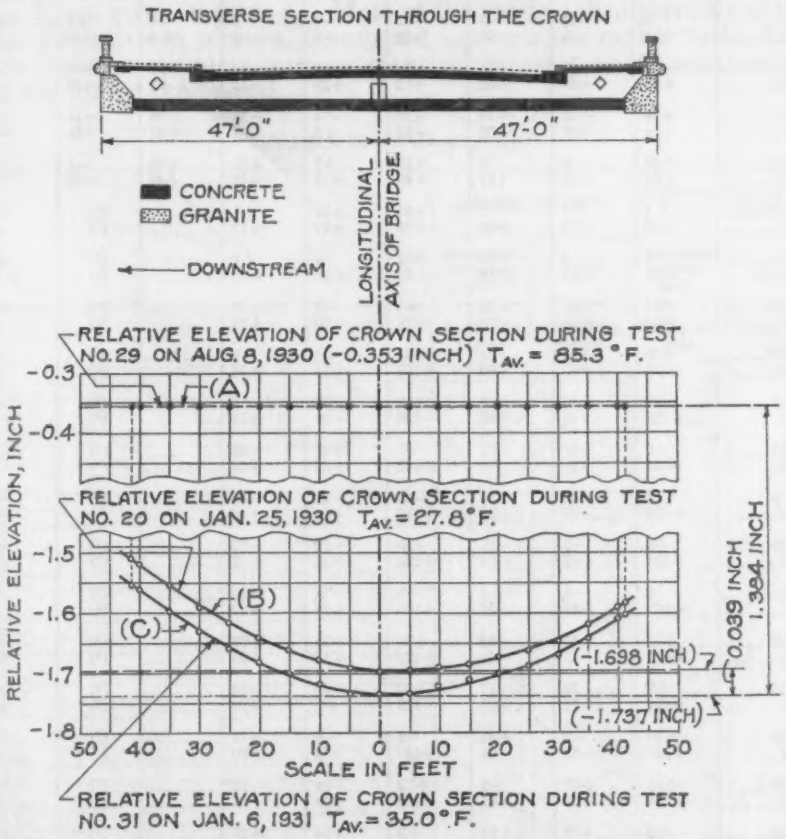

FIGURE 12.—*Vertical deflection of a transverse section through the crown.*

A, datum for crown section (test 29); *B* and *C*, deflection from datum, tests 20 and 31, respectively.

calculated from the clinometer data, corrected for changes in temperature gradients. The differences between the bending strains calculated by these two independent methods are in most cases comparatively small.

The changes in thrust strain between tests 19 and 31 were respectively $+67\times10^{-6}$ at the haunch section and $+66\times10^{-6}$ at the springing (table 4). Since there was no change in loads on the arch, and since the actual change in thrust due to temperature differences

TABLE 4.—*Extrados thrust and bending strains, corrected for temperature, at the radial observation sections*

NOTE.—Sign + = compressive strain, sign − = tensile strain.

Test no.	Springing (average)			Haunch (average)			Crown		
	Strain gage and telemeter		Clinometer bending	Strain gage and telemeter		Clinometer bending	Strain gage and telemeter		Clinometer bending
	Thrust	Bending		Thrust	Bending		Thrust	Bending	
	Millionths	*Millionths*	*Millionths*	*Millionths*	*Millionths*	*Millionths*	*Millionths*	*Millionths*	*Millionths*
5-6	+17	+23	+22	−2	+12	+7	+5	+11	−5
6-7	−8	0	+12	+1	−2	+4	−5	−21	−24
5-7	+9	+23	+34	−1	+10	+11	0	−10	−29
7-8	0	−10	−8	−11	−7	−8	−4	+4	+23
5-8	+9	+13	+26	−12	+3	+3	−4	−6	−6
8-10	+16	+35	+26	+24	+20	+14	+9	−14	−44
5-10	+25	+48	+52	+12	+23	+17	+5	−20	−50
10-11	+20	+21	+18	+20	−18	−18	+26	−14	+13
5-11	+54	+69	+70	+32	+5	−1	+31	−34	−37
11-12	+12	−4	−3	+17	+7	+13	+18	−4	−12
5-12	+66	+65	+67	+49	+12	+12	+49	−38	−49
12-13	+4	−5	−7	+10	+20	+7	----------	(1)	−20
5-13	+70	+60	+60	+59	+32	+19	----------	(1)	−69
13-14	−3	−16	−11	+14	+4	+7	----------	(1)	−49
5-14	+67	+44	+49	+73	+36	+26	----------	(1)	−118
14-15	+16	−26	−32	+5	−7	−11	----------	(1)	+49
5-15	+83	+18	+17	+78	+29	+15	----------	(1)	−69
15-16	+20	+44	+43	+41	+5	+9	----------	(1)	−20
5-16	+103	+62	+60	+119	+34	+24	----------	(1)	−89
16-17	+18	−16	−5	+19	−9	+5	----------	(1)	+10
5-17	+121	+46	+55	+138	+25	+29	----------	(1)	−79
57-18	0	−67	−62	+4	+17	+29	----------	(1)	+50
-18	+121	−21	−7	+142	+42	+58	----------	(1)	−29
18-19	−11	−58	−75	−26	−26	−18	----------	(1)	−15
5-19	+110	−79	−82	+116	+16	+40	----------	(1)	−44
19-20	−3	−3	−11	−10	+22	+22	----------	(1)	+27
5-20	+107	−82	−93	+106	+38	+62	----------	(1)	−17
20-21	0	−1	−4	−3	−18	−10	----------	(1)	−15
5-21	+107	−83	−97	+103	+20	+52	----------	(1)	−32
21-22	+12	+40	+56	+20	+24	+17	----------	(1)	+19
5-22	+119	−43	−41	+123	+44	+69	----------	(1)	−13
22-23	+2	−28	−17	+10	−42	−42	----------	(1)	−60
5-23	+121	−71	−58	+133	+2	+27	----------	(1)	−73
23-24	−19	−2	+32	−3	−5	+13	----------	(1)	+16
5-24	+102	−73	−26	+130	−3	+40	----------	(1)	−57
24-25	+42	+37	−5	+32	+26	−12	----------	(1)	−15
5-25	+144	−36	−31	+162	+23	+28	----------	(1)	−73
25-26	+2	+56	+56	+2	+14	+28	----------	(1)	+13
5-26	+146	+20	+25	+164	+37	+56	----------	(1)	−62
26-27	+9	+10	+13	0	−4	−1	----------	(1)	+4
5-27	+155	+30	+38	+164	+33	+55	----------	(1)	−58
27-28	+14	+22	+32	+26	−12	−1	----------	(1)	−10
5-28	+160	+52	+70	+190	+21	+54	----------	(1)	−68
28-29	−6	−4	+10	+4	−8	0	----------	(1)	−5
5-29	+163	+48	+80	+194	+13	+54	----------	(1)	−73
29-30	+34	−80	−77	+18	−7	−2	----------	(1)	+8
5-30	+197	−32	+3	+212	+6	+52	----------	(1)	−65
30-31	−23	−93	−133	−29	−20	−17	----------	(1)	+2
5-31	+174	−125	−130	+183	−14	+35	----------	(1)	−63

[1] Crown telemeters out of adjustment

was negligible (3 lb. per sq. in. at the crown), the above thrust strains may be attributed to shrinkage and flow, and are equivalent to a temperature drop of about 10° F. The equivalent temperature drop as determined from the crown deflection between these tests was about 7° F.

5. PIER MOVEMENTS

The pier movements, calculated from the longitudinal clinometer data, were usually so small that it was often difficult to determine whether they were significant or were the result of errors in observation. The rotation of the top surface of pier no. 4, and the vertical movements of the center of the area relative to the center of pier no. 5, are given in table 5. Most of the vertical displacement of pier no. 4 relative to pier no. 5 occurred between the earlier tests, when the loads on the piers were constantly increasing as the construction of the bridge progressed.

TABLE 5.—*Pier movement*

Test no.	Rotation [1] of pier 4		Deflection [2] of pier 4 relative to pier 5	
	Increment between tests	Total	Increment between tests	Total
	Millionths radian	*Millionths radian*	*Thousandths inch*	*Thousandths inch*
1-2			−83	−83
2-3			−6	−89
3-4			−53	−142
4-5			+34	−108
5-6			+6	−102
6-7			−2	−104
7-8			−2	−106
8-10			−3	−109
10-11	−43	−43	−16	−125
11-12	+10	−33	+1	−124
12-13	−1	−34	+3	−121
13-14	−19	−53	−5	−126
14-15	+17	−36	+1	−125
15-16	−1	−37	−5	−130
16-17	+8	−29	−1	−131
17-18	+29	0	+12	−119
18-19	+23	+23	−33	−152
19-20	0	+23	0	−152
20-21	+1	+24	−6	−158
21-22	−7	+17	+4	−154
22-23	−11	+6	+3	−151
23-24	−5	+1	+2	−149
24-25	−6	−5	+5	−144
25-26	−6	−11	−9	−153
26-27	−4	−15	+2	−151
27-28	−3	−18	−12	−163
28-29	−9	−27	+1	−162
29-30	+17	−10	+9	−153
30-31	+41	+31	+12	−141

[1] Sign: Positive rotation is away from the crown of arch 7.
[2] Sign: Positive deflection indicates a rise in pier 4 relative to pier 5.

The rotation of the clinometer stations on one side of the longitudinal axis of the pier surface was often greater than the rotation of the stations on the other side of this axis, indicating a warping of the

pier surface in addition to the rotation of the pier as a whole. This warping was concave for temperature rises and was probably caused by relative changes in temperature between the inner and outer portions of the pier.

The average rotation of the clinometer stations on pier no. 4 was toward the crown of arch no. 7 for rise in the temperature of the arch barrel. After the construction of the superstructure, and for temperature changes exceeding 10° or 15° F., the rotation of pier no. 4 was approximately proportional to the temperature change in the arch and equal to about 12×10^{-6} radian for a change of 10° F. The draw span abutment east of arch no. 7 was 50 percent wider than pier no. 4 and its bottom elevation was 3.5 feet below that of pier no. 4. The direction of rotation of the pier appeared to be influenced by changes in the temperature thrust from this abutment.

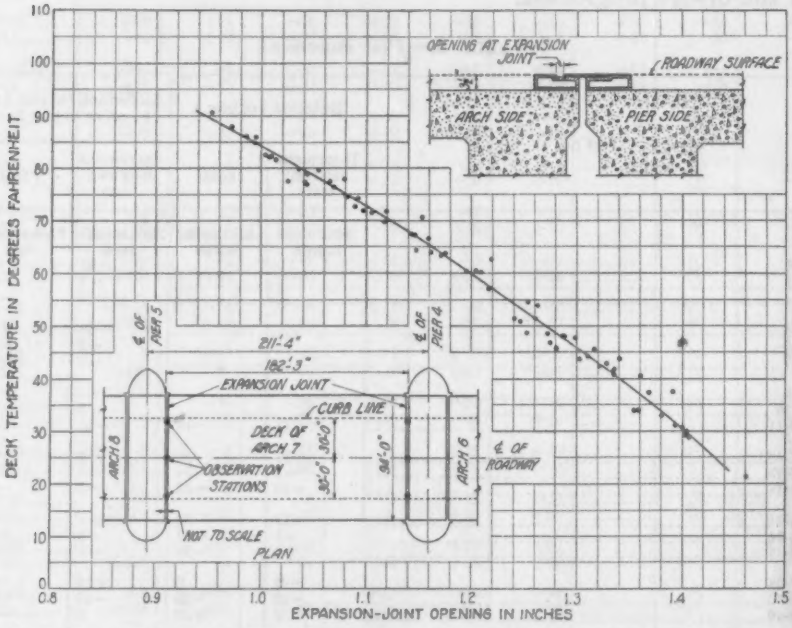

FIGURE 13.—*Changes in width of expansion joints; each point represents the average of 1 observation on each of the 6 stations.*

Location and essential details of the joints and observation stations are also shown.

6. MOVEMENTS OF THE EXPANSION JOINTS

Observations on the width of the expansion joints and the temperature of the deck slab were started in January 1930 and continued until January 1931. Figure 13 shows the results of the measurements, all of which were made in the early morning hours. The observed temperature of the deck slab varied between 20° and 90° F. and the coefficient of thermal expansion of the deck computed from the joint movement was 66×10^{-7} per ° F. This value agrees closely with that previously determined for the arch-barrel concrete, showing that the joints had functioned. The rate of movement of the joints showed a slight increase with increase in deck temperature.

VII. SUMMARY

1. A maximum temperature of approximately 143° F. (62° C.) was attained in the thicker portions of the arch barrel about 25 hours after the concrete was placed in the forms. The temperature of the air during the same period was about 73° F. (23° C.).

2. The temperature of the concrete of the crown section of the arch barrel (2.25 ft. thick) reached air temperature about 8 days, and that of the springing section (4.83 ft. thick) reached air temperature about 15 days after being placed.

3. After the concrete had cooled, the average temperature of the arch barrel closely approximated the average of the air temperature of the previous 5 days.

4. During a period of 27 months after the concrete had cooled, the maximum observed average temperature of the arch barrel was 85° F. (29° C.), and the minimum was 24° F. (−4° C.). The maximum and minimum air temperatures during the same period were 106° F. (41° C.) and 7° F. (−14° C.), respectively.

5. The linear coefficient of thermal expansion of the arch barrel, without superstructure restraint, as determined from the crown deflection and from the arch-barrel concrete cast in prisms was about 65×10^{-7} per ° F. (117×10^{-7} per ° C.), and that of the deck slab, calculated from measurements of the expansion joint movement, was approximately the same.

6. The restraint of the superstructure caused a reduction of about 13 percent in the crown deflection which would have been caused by changes in the average concrete temperature. For unit change in average temperature the deflection of and the bending moment in the arch barrel near the piers increased after the construction of the superstructure.

7. Unequal vertical deflections in transverse sections of the arch barrel occurred with changes in temperature because of differences in physical properties of the granite facing arches and the concrete arch barrel. On the completed structure the center of a transverse section through the crown deflected upward about 0.03 inch above the granite facing arches for a temperature rise of 10° F.

8. The vertical deflections of the arch barrel, produced by the addition of the superstructure walls and deck, were much greater than the theoretical (elastic) deflections. The shapes of the theoretical and observed load deflection curves were dissimilar and the theoretical and observed bending moments at the crown were different in sign. These differences in the deflections were probably caused by the shrinkage and flow in the concrete during the 170 days required for construction of the superstructure.

9. The effect of shrinkage and flow on the deflection of the arch during the period from the eighteenth day to the twenty-fourth month after the construction of the two inner arch-barrel strips was equivalent to a drop of 27° F. in the average arch temperature. The effect of shrinkage and flow after the superstructure was completed and during the period from the fifteenth to the twenty-seventh month was equivalent to a temperature drop of about 7° F.

13317—33——3

VIII. ACKNOWLEDGMENTS

Several members of the Bureau staff, especially A. U. Theuer and C. W. Ross; as well as J. C. Spotts, Joseph Hamilton, C. C. Costello, P. E. Kraemer, and others of the Arlington Memorial Bridge Commission, ably assisted the authors in the collection and interpretation of data.

WASHINGTON, July 29, 1933.

U.S. Department of Commerce, Bureau of Standards

RESEARCH PAPER RP610

Part of Bureau of Standards Journal of Research, Vol. 11, November 1933

SPECTRAL DIFFERENTIATION OF PURE HYDROCARBONS: A NEAR INFRARED ABSORPTION STUDY[1] [2]

By Urner Liddel[3] and Charles Kasper[4]

ABSTRACT

The spectra of 36 hydrocarbons have been recorded in the near infrared from 5,500 to 9,000 cm^{-1} (2μ to 1μ), using an automatic recording infrared glass spectrograph. Specific absorptive indices have been calculated from the results and plotted against wave numbers (wave lengths per centimeter). Correlations of the spectra of the various compounds have been made in regions associated with three energy transitions in the molecules. Characteristic differentiation of the compounds according to structural types has been indicated.

CONTENTS

	Page
I. Introduction	599
II. Experimental procedure	600
III. Results	602
1. Absorption from 7,900 to 9,000 cm^{-1}	603
(*a*) Aromatic hydrocarbons	603
(*b*) Naphthenes	603
(*c*) Normal aliphatic hydrocarbons	604
(*d*) Isomeric aliphatic hydrocarbons	608
2. Absorption from 6,400 to 7,400 cm^{-1}	609
(*a*) Aromatic hydrocarbons	609
(*b*) Naphthenes	610
(*c*) Normal aliphatic hydrocarbons	610
(*d*) Isomeric aliphatic hydrocarbons	610
3. Absorption from 5,400 to 6,400 cm^{-1}	610
(*a*) Aromatic hydrocarbons	610
(*b*) Naphthenes	612
(*c*) Normal aliphatic hydrocarbons	612
(*d*) Isomeric aliphatic hydrocarbons	614
IV. Discussion of results	614
V. Bibliography	618

I. INTRODUCTION

It was early (1881 to 1905) recognized (1, 2, 3)[5] that certain regions of the infrared absorption spectra of organic compounds might be associated with the presence of various atomic linkages in the mole-

[1] Financial assistance has been received from the research fund of the American Petroleum Institute. This work is part of project no. 6: The Separation, Identification, and Determination of the Constituents of Petroleum.

[2] This paper was presented before the Petroleum Division of the American Chemical Society at Washington, D.C., Mar. 29, 1933.

[3] Bureau of Chemistry and Soils, U.S. Department of Agriculture.

[4] Research associate representing the American Petroleum Institute.

[5] The arabic numbers in parentheses here and throughout the text refer to the bibliography at the end of the paper.

cules. Later work (4 to 27) (1923 to 1933) has added evidence in favor of this premise, and recent investigation (25) has shown that it may be possible to indicate the general type of the group; e.g., primary, secondary, or tertiary carbon atom combined with a hydrogen atom. If these premises prove applicable, an easy method would be provided for determining the structure of organic molecules, and would be of assistance where chemical methods are very difficult or fail. Careful investigations of the characteristics of these absorptions might lead to quantitative estimations of the amounts of various compounds present in a mixture. With these points in consideration, the generous cooperation of the American Petroleum Institute made possible this study to ascertain the possibility of the usefulness of this method in a study of the constituents of petroleum.

II. EXPERIMENTAL PROCEDURE

The spectrograph, of the Littrow form, is shown in figure 1. The source of continuous radiation is a tungsten ribbon-filament lamp which is enclosed in a water-jacketed cell. The light is collimated through a large brass tube 1 m long, and focused by a concave mirror on the slit of the spectograph. The absorption cell containing the solution or compound under investigation is fixed in the light path between the collimating tube and the slit. The light then goes to a large concave mirror from which parallel rays are reflected through two 60° glass prisms, then reflected by the plane Littrow mirror over the same path, giving four-prism dispersion, and finally focused on a sensitive vacuum thermocouple. Wave length variation is accomplished by rotation of the Littrow mirror which is coupled with the motion of a recording photographic plate by means of a lever system. As the incident energy on the thermocouple actuates the galvanometer, a beam of light reflected from the galvanometer mirror moves across the photographic plate, so that one has recorded a graph of galvanometer deflections with wave lengths, or a plot in arbitrary units of the intensity of transmitted light against frequency. As a check on the constancy of the intensity of emission of the tungsten filament, the cell was withdrawn from the light path by means of a solenoid arrangement moving the cell-holder along a dove-tail slide, thus producing on the recorded photographic plate segments of the curve of the emission of the source not modified by the absorption cell. Likewise, to determine the zero drift of the galvanometer, a shutter was thrown in front of the slit at certain times giving segments of the base line of the curve. The motion of these two auxiliary units was controlled by a breaker circuit operated by a synchronous motor; the motion of the photographic plate was controlled also by a synchronous motor, hence these segments of curves always appeared at the same frequency on the recorded plate, and it was thereby possible to compare the intensity of emission of the source during the recording of one plate with that of another. Thus by recording the transmission of the cell filled with carbon tetrachloride, then the cell containing the solution, it was possible to calculate the transmittancy from which the absorptive indices were derived.

Calibration of the instrument was effected with mercury arc spectra and water-vapor bands, using the wave numbers recorded by McAlister (33) and by Plyler (34). The thermocouple used was a modi-

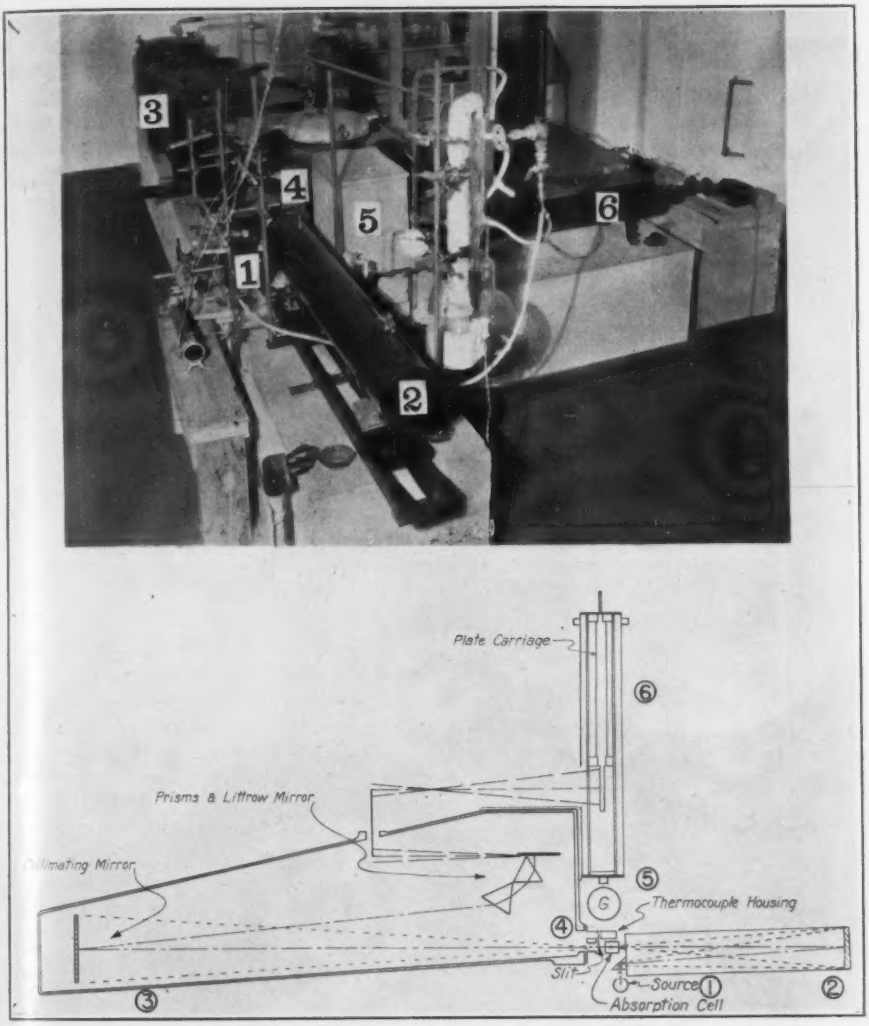

FIGURE 1.—*Photograph and diagrammatic sketch of the recording infrared vacuum spectograph.*

1, Cell containing source lamp; 2, external collimator; 3, spectograph proper; 4, thermocouple housing; 5, galvanometer shield; 6, recording mechanism.

fication of the type of single-junction vacuum thermocouple described by Brackett and McAlister (28). The electrical supply for the source lamp came from a battery of 6 large cells of 1,200 ampere-hour capacity in multiple connection, which held the voltage on the filament constant to within 0.01 volt during the time required for a run. The filament used about 18 amperes of current at 5.75 volts. Since absorption by water vapor is very strong in one of the regions under study, the water was removed by first evacuating the spectrograph casting, and then flushing and filling it to atmospheric pressure with carefully dried nitrogen. The collimating tube was treated in the same manner. Thus, only a very slight amount of water vapor absorption appears on the records and this allows, for the first time, accurate determinations of absorption indices of hydrocarbons in the region of 7,100 cm^{-1}.

Solutions of hydrocarbons were generally used, to enable accurate determination of the concentration of molecules absorbing in the light path. Since pure carbon tetrachloride does not absorb in this region, it was used as a solvent.[6] In stated instances when scarcity or value of the sample required its preservation in the pure state, 1- and 4-mm cells filled with the pure samples were used. The solutions were studied in a 5-cm absorption cell, and approximately 0.5 molar solutions were employed for the regions 6,400 to 7,400 cm^{-1} and 7,900 to 8,900 cm^{-1}, and 0.1 molar for the region 5,400 to 6,400 cm^{-1}.

TABLE 1

	Region 7900–8900	Region 6400–7400	Region 5400–6400	State studied	Purity, percent	Sources[1]	References[2]
	Figure numbers						
AROMATIC HYDROCARBONS							
Benzene	2	11	16	Solution		2	a
Toluene	2	11	17	do		2	a
Ethylbenzene	2	11	17	do		2	a
o-Xylene	3	11	18	do	99.0	1	b
m-Xylene	3	11	18	do	99.9	1	b
p-Xylene	3	11	18	do	99.9	1	b
Hemimellitene	4	11	18	do	99.9	1	c
Pseudocumene	4	11	18	do	99.9	1	c
Mesitylene	4	11	18	do	99.9	1	c
NAPHTHENES							
Cyclohexane	5	11	19	Solution	99.9	2	a
Methylcyclohexane	5	11	19	do	99.9	1	d
Methylcyclopentane	5	11	19	do	98.9	1	e
1, 2-Dimethylcyclopentane	5	11	19	Pure		4	f
1, 2-Dimethylcyclopentane	5	11	19	do		4	f
NORMAL ALIPHATIC HYDROCARBONS							
Pentane	6	12	20	Solution		1 a	g
Hexane	6	12	20	do	98.3	1	h
Heptane	6	12	21	do	99.8	1	d
Octane	6	12	21	do	99.1	1	i
Nonane	6	12	22	do	99.2	1	j
Decane	6	12	22	do	99.9	1	k
Undecane	6	12	22	do		1 a	g
Dodecane	6	12	22	do		1 a	g

See references at end of table.

[6] Commercial C.P. carbon tetrachloride was found to contain small amounts of chloroform which was removed by distillation in the 30-plate still of the Bureau, and fractionated to constant refractive index.

TABLE 1—Continued

ISOMERIC ALIPHATIC HYDROCARBONS

	Region 7900–8900	Region 6400–7400	Region 5400–6400	State studied	Purity, percent	Sources[1]	References[2]
	Figure numbers						
Isopentane	7	13	23	Solution		2	
2-Methylpentane	7	13	23	Pure	95	1	l
3-Methylpentane	8	14	24	Solution	95	1	l
2, 3-Dimethylbutane	8	14	24	do	95	1	l
2, 3-Dimethylpentane	9	15	25	Pure		3	m
2, 4-Dimethylpentane	9	15	25	do		3	m
3, 3-Dimethylpentane	9	15	25	do		3	m
2, 2-Dimethylpentane	9			do		3	m
2, 2, 3-Trimethylbutane	9	15	25	do		3	m
3-Ethylpentane	9	15	25	do		3	m
3-Methylhexane	9	15	25	do		3	m
2-Methylhexane	9	15	25	Solution	99.9	1	n
2, 2, 4-Trimethylpentane	10	15	25	do	99.8	1	o

[1] Sources: 1, American Petroleum Institute; 2, Bureau des Étalons Physico-Chimiques in Brussels; 3 Ethyl Gas Corporation; 4, Professor G. Chavanne.

[2] References:

a. J. Timmermanns et F. Martin, J.chim.phys., vol. 23, p. 747, 1926.
b. J. D. White and F. W. Rose, Jr., Bur. Standards J. Research, vol. 9, p. 711, 1932.
c. B. J. Mair and S. T. Schicktanz, ibid. In press.
d. M. M. Hicks-Bruun and J. H. Bruun, ibid, vol. 8, p. 525, 1932.
e. ibid, vol. 7, p. 799, 1931.
f. G. Chavanne, Extrait des Comptes rendus Congres National des Sciences-Bruxelles, 29 juin-2 juillet, 1930.
g. B. J. Mair, Bur. Standards J. Research, vol. 9, p. 457, 1932.
h. J. H. Bruun and M. M. Hicks-Bruun, ibid, vol. 6, p. 869, 1931.
i. R. T. Leslie and S. T. Schicktanz, ibid, vol. 6, p. 381, 1931.
j. J. D. White and F. W. Rose, Jr., ibid, vol. 7, p. 907, 1931.
k. J. H. Bruun and M. M. Hicks-Bruun, ibid, vol. 8, p. 583, 1932.
l. J. H. Bruun and M. M. Hicks-Bruun, ibid, vol. 5, p. 933, 1930.
m. G. Edgar et al., J.Am.Chem.Soc., vol. 51, p. 1493, 1929.
n. J. H. Bruun and M. M. Hicks-Bruun, Bur. Standards J. Research, vol. 10, p. 465, 1933.
o. J. H. Bruun and M. M. Hicks-Bruun, ibid, vol. 9, p. 269, 1932.

Most of the hydrocarbons were obtained from the Bureau of Standards, American Petroleum Institute research project no. 6, where they had been isolated from petroleum and carefully purified. The isomers of heptane were lent to us through the courtesy of Dr. G. Calingaert and Dr. Graham Edgar of the Ethyl Gas Corporation and the isomers of 1, 2-dimethylcyclopentane by Prof. G. Chavanne of the University of Brussels.

III. RESULTS

In order to make the results most generally useful, specific absorptive indices (molecular extinction coefficients) have been calculated, permitting direct comparisons between the spectra of any compounds by giving data independent of cell depth and, within certain ranges, of concentration. This last statement of course involves the validity of Lambert's and Beer's laws which has been questioned in previous investigations (23, 24). In the region from 1μ to 2μ, using cells greater than 1 mm in thickness, no deviation from Lambert's law was found, nor any definite deviations from Beer's law in the concentration range studied, roughly 0.03 to 0.8 molar. The slight deviations have always been well within experimental error.

The specific absorptive index is, by definition (31), $\frac{-\log_{10} I/I_0}{cd}$, I/I_0 being the fraction of transmitted light, c, concentration of the

solute in moles per liter of the solution, and d, the cell depth in centimeters.

While the following graphs are continuous curves, enough points have been calculated and critical visual comparisons made with the original records so that presentation of them in this manner seems justified. The accuracy in the wave number (which is proportional to the true frequency) is ± 10 cm^{-1}. The absolute accuracy of the specific absorptive index is ± 0.05 in the region 5,400 to 6,400 cm^{-1}, ± 0.02 in the region 6,400 to 7,400 cm^{-1}, and ± 0.01 from 7,900 to 9,000 cm^{-1}, although the relative accuracy within a given graph is much greater.

Absorption in the regions 5,900 and 8,500 cm^{-1} has generally been interpreted as the first and second overtones of a fundamental frequence around 3,000 cm^{-1}, which has been considered the vibration of the H atom along the valence bond with respect to the carbon atom. Absorption around 7,000 cm^{-1} has been interpreted as a combination frequency of the first overtone (5,900 cm^{-1}) plus another fundamental frequency associated with a "swinging" oscillation. The absorption of the hydrocarbons in each region will be considered separately.

1. ABSORPTION FROM 7,900 TO 9,000 CM^{-1}

(a) AROMATIC HYDROCARBONS

It is seen (fig. 2) that benzene has a strong absorption between 8,700 and 8,800 cm^{-1}. The corresponding absorption by toluene is shifted to slightly lower frequencies, decreased in intensity, and there appears near 8,400 cm^{-1} a band not quite half as intense. The strong component has nearly the same intensity in ethylbenzene but the component of lower frequency has increased approximately two thirds.

The two bands approach equality in the xylenes (fig. 3), intensities and separations of the maxima varying in the three isomers amongst themselves.

In the trimethylbenzenes (fig. 4), the component of higher frequency decreases slightly in intensity and the lower one is appreciably greater than in the xylenes. Separations and intensities of the maxima vary again as in the xylenes, and the lower frequency region is composed of three apparent maxima, as distinguished from the one or two of the xylenes. The high frequency component of mesitylene is considerably sharper than in any of the other methyl derivatives, suggesting that the position of the methyl groups therein places a considerable restraining force on the possible motions of the nuclear hydrogen.

(b) NAPHTHENES

Only a few of this group have been available for study at the present time. Cyclohexane (fig. 5) has a much more complex spectrum than benzene. It and methylcyclohexane exhibit by far the most complex bands observed. The methyl derivative might appear at first to be different in type from cyclohexane, yet if one adds the absorption of a methyl group around 8,350 cm^{-1} to cyclohexane, similarity is obvious. Cyclopentane has not yet been available for study, hence little can be said concerning the methyl compound except that the spectrum is much simpler in character than that of the six-membered ring. The two isomers of 1, 2-di-

methylcyclopentane were studied in the pure state. Little difference is exhibited between the two, as would be expected, yet scrutiny reveals that the low frequency satellite bands are somewhat more apparent in the high boiling compound.

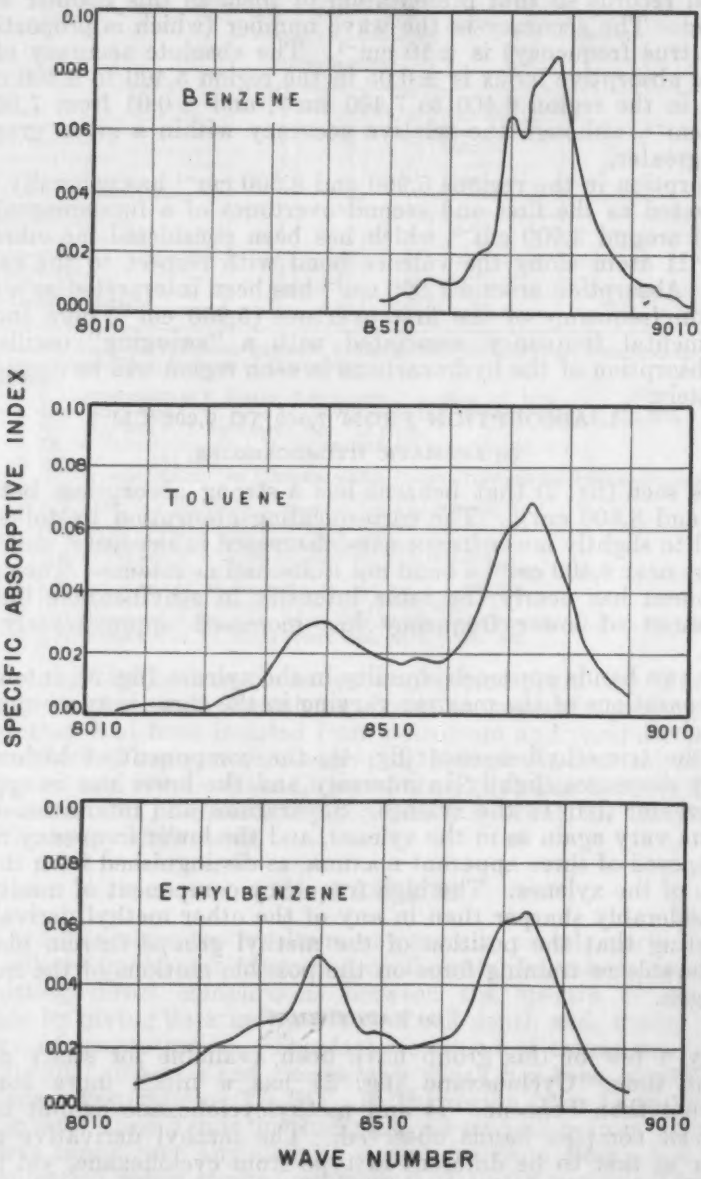

FIGURE 2.

(c) NORMAL ALIPHATIC HYDROCARBONS

The series from pentane to dodecane has been observed (fig. 6). This adds further evidence to Brackett's theory (25) that the absorption at 8,400 cm^{-1} arises from the methyl group, that around 8,250

cm^{-1} from the methylene group, and that the low frequency component shows a shift of the median of absorption to lower frequencies with increasing length of chain.

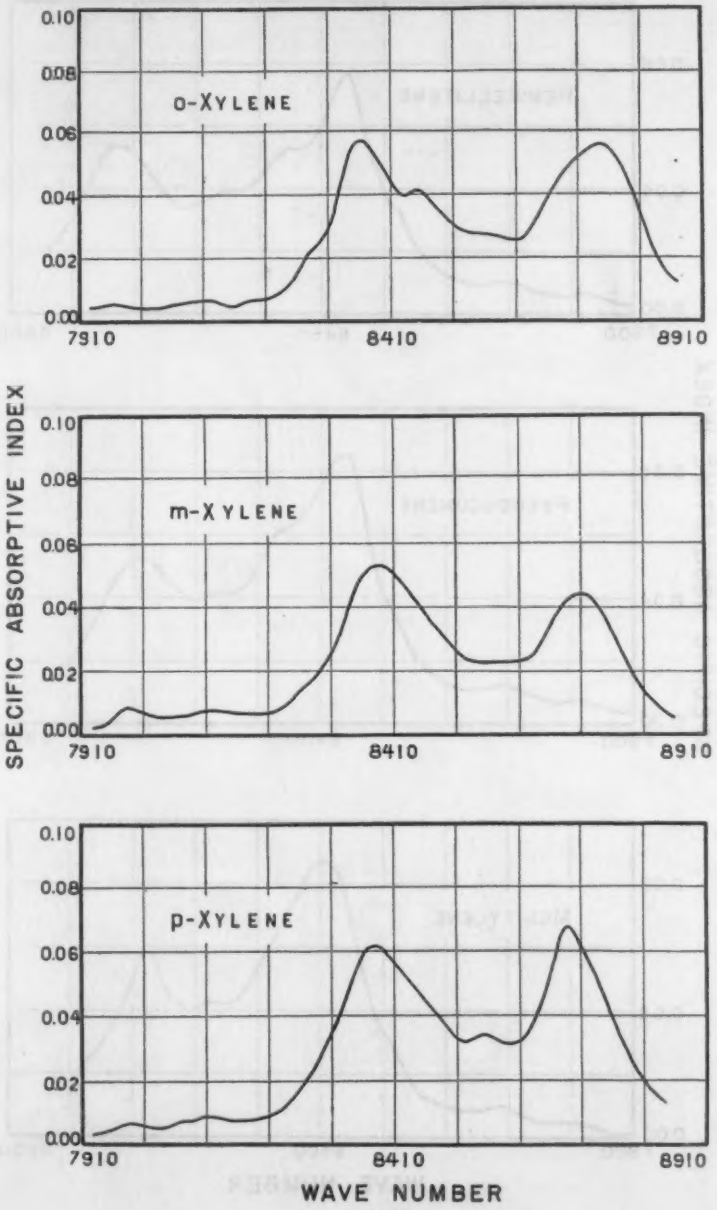

FIGURE 3.

These results, giving intensities of absorption, indicate that the absorption of each CH_2 group is not strictly additive, but nearly so, i.e., the 10 CH_2 groups in dodecane do not absorb as much per unit

as the 4 in hexane. The accuracy of the work does not permit determination of the relation. It may appear to those unfamiliar with this type of absorption that the band which is ascribed to the

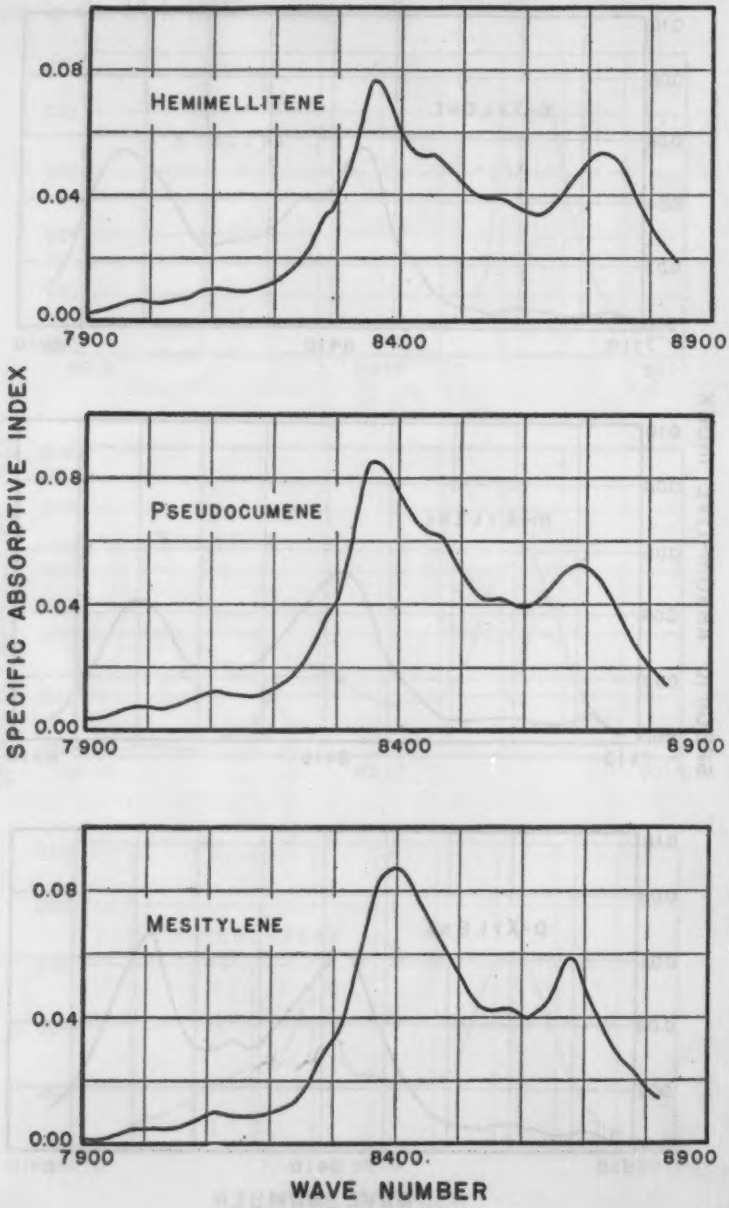

FIGURE 4.

methyl group is increasing in intensity in the longer chains, which is not true. It must be realized that these are integrated curves and that the separation of the maxima is insufficient to determine the

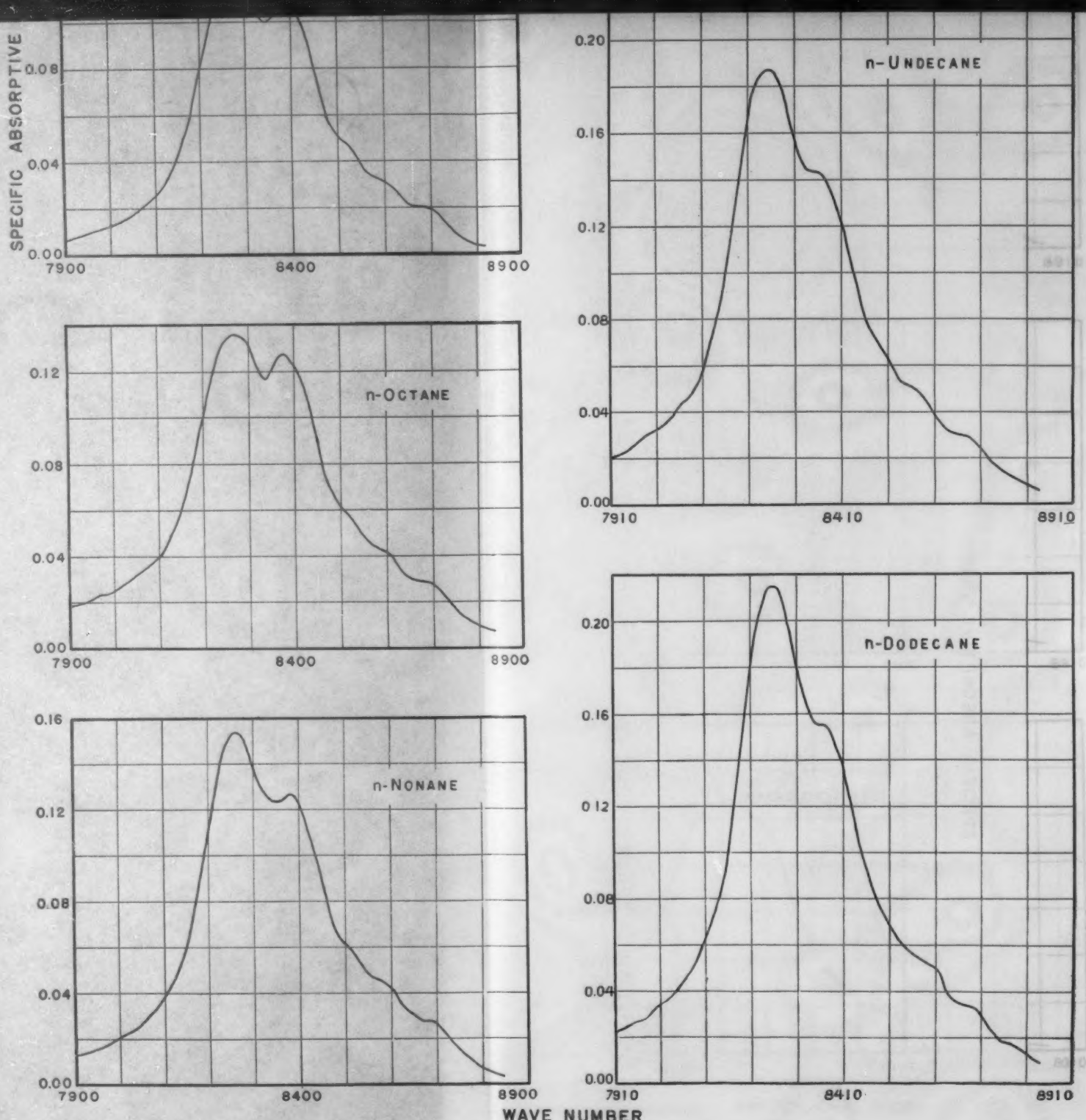

13317—33 (Face p. 607.) No. 2.

FIGURE 6

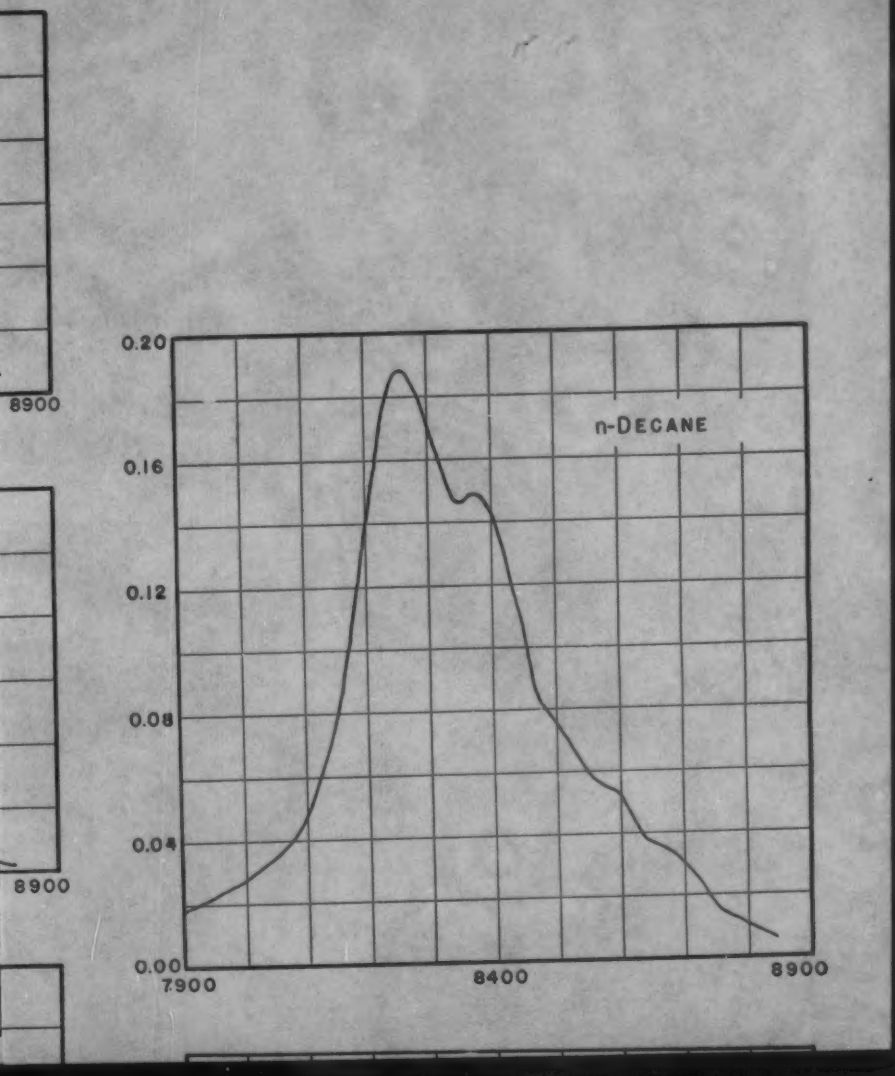
0.20
0.16
0.12
0.08
0.04
0.00
n-DECANE
7900
8400
8900

n-PENTANE
n-HEXANE
n-HEPTANE
7900
8400
8900
0.00
0.04
0.08
0.12
DEX

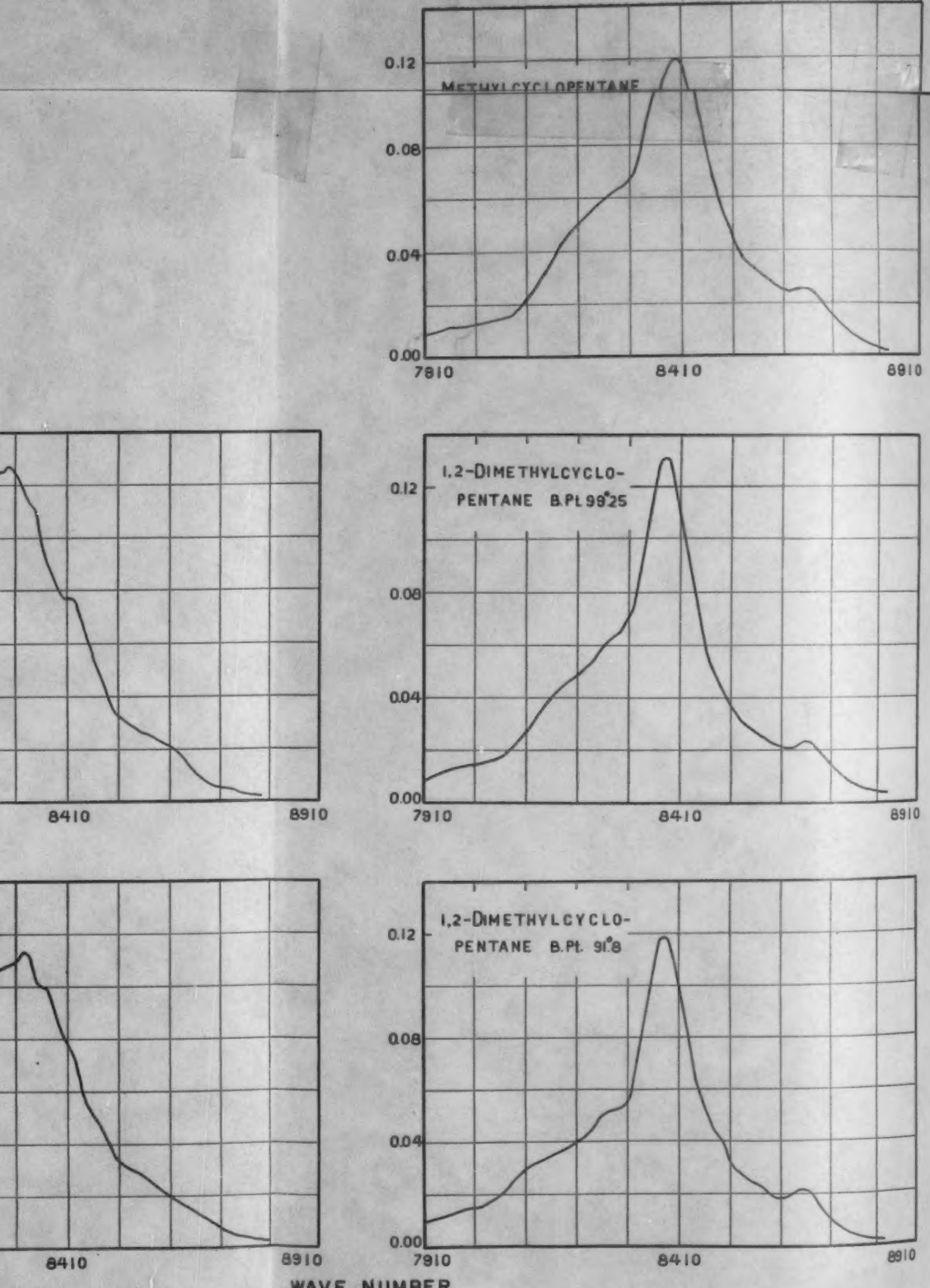
METHYLCYCLOPENTANE
1,2-DIMETHYLCYCLO-
PENTANE B.PT 99°25
1,2-DIMETHYLCYCLO-
PENTANE B.Pt. 91°8
0.12
0.08
0.04
0.00
7810
7910
8410
8910
WAVE NUMBER

FIGURE 5

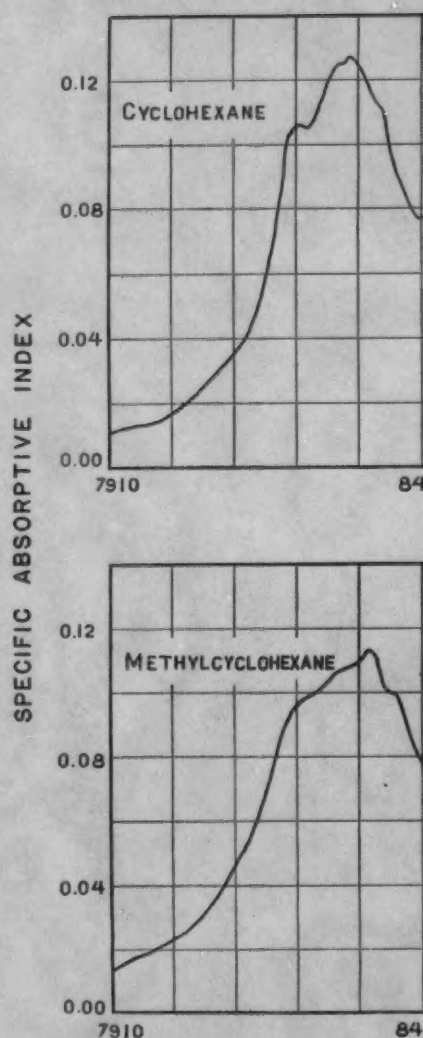

13317—33 (Face p. 607.) No. 1.

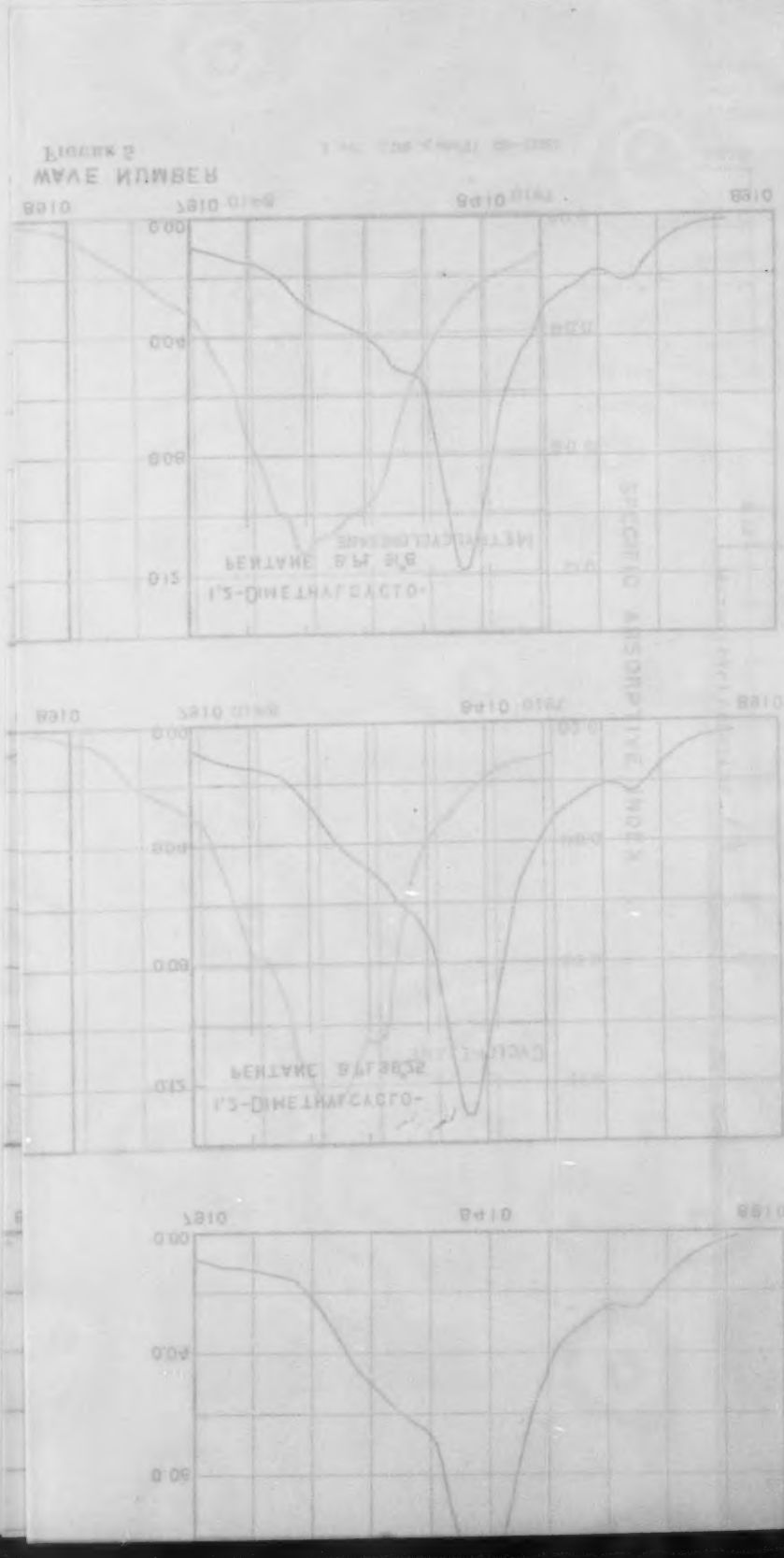
WAVE NUMBER

true intensity of each component, so that as the CH_2 absorption becomes more and more intense, the CH_3 maximum is carried up on the side of the curve. Possibly, it should be emphasized here that this is a true overlapping of bands. The lack of further resolution is not due to the apparatus used, but is an inherent characteristic of these large molecules which possess such large moments of inertia

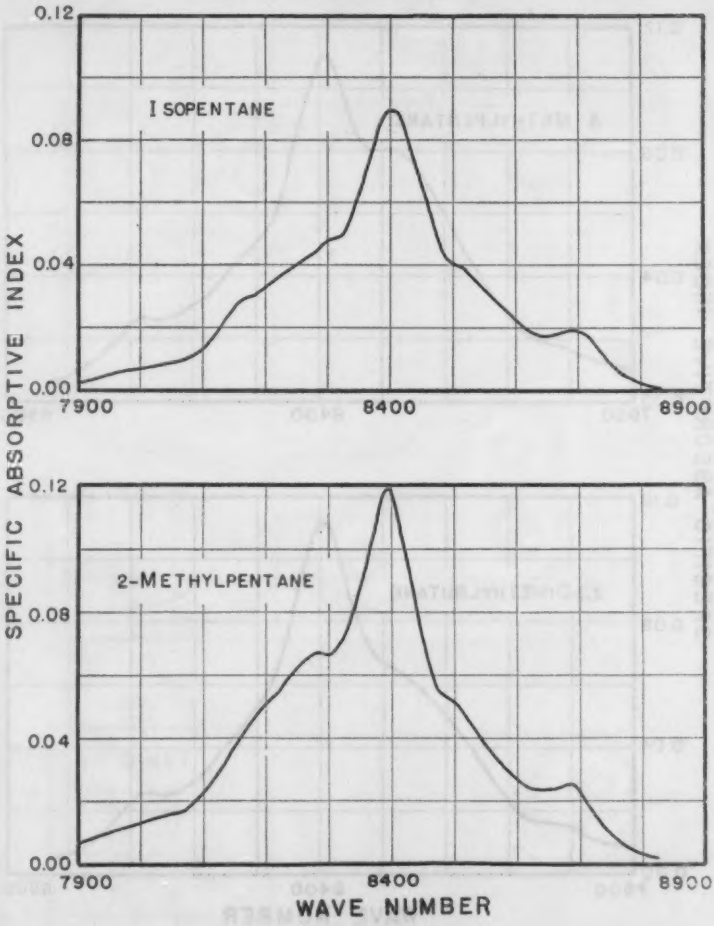

FIGURE 7.

that the separation of the rotation lines is far too small to be observed experimentally by any apparatus known.

An interesting observation is that the frequency of the maximum attributed to the methyl groups varies slightly between the odd- and even-numbered carbon atom chains, the variation decreasing with length of chain and becoming indistinguishable after decane. The other maximum shifts very slightly. This may be correlated with other known alternations in the properties of these compounds.

(d) ISOMERIC ALIPHATIC HYDROCARBONS

Perhaps the most valuable part of the work lies in the observation of the spectra of various isomers. In isopentane (Fig. 7) the secondary absorption has dropped very appreciably from that found in *n*-pentane and tertiary absorption appeared near 8,150 cm^{-1}. It was very interesting to note whether substitution of a methyl group in

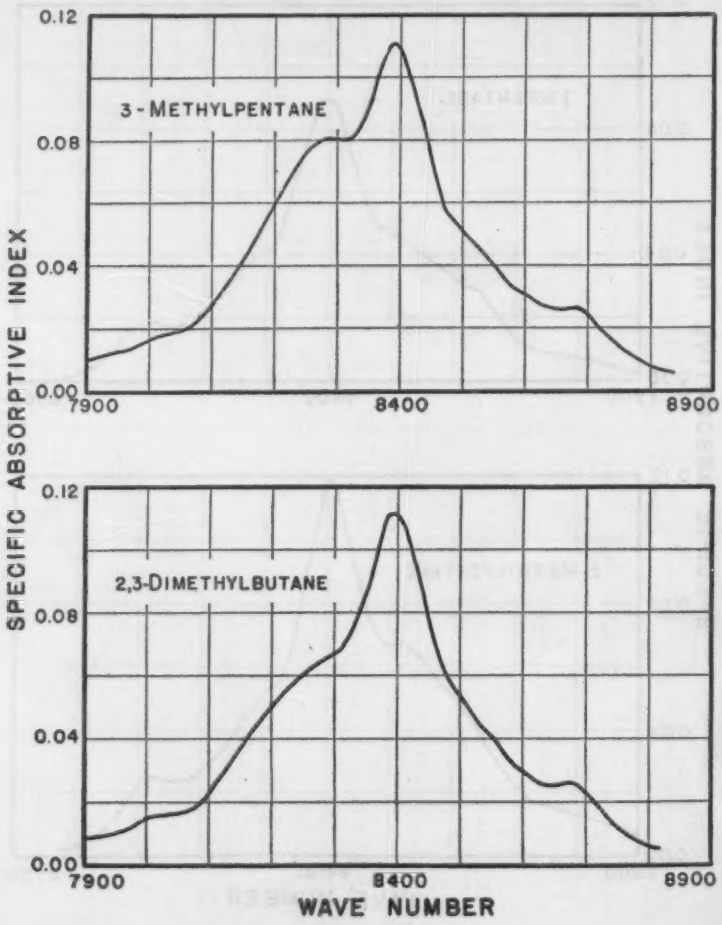

FIGURE 8.

various positions along the chain produced any differences in the absorption. 2-Methylpentane and 3-methylpentane (fig. 8) offer a good example of this. Minute differences cannot be stressed, since 2-methylpentane was observed in the pure state and the values are not so dependable. However, it appears that the maximum of the 2-isomer is sharper than that of the 3-isomer and certainly the ratio of primary to secondary absorption is greater in the 2-form than the 3-form. 2, 3-Dimethylbutane consists of 4 primary groups and 2 tertiary groups, and no secondary absorption appears in the spectrum. It must be pointed out that, while the general slope of the

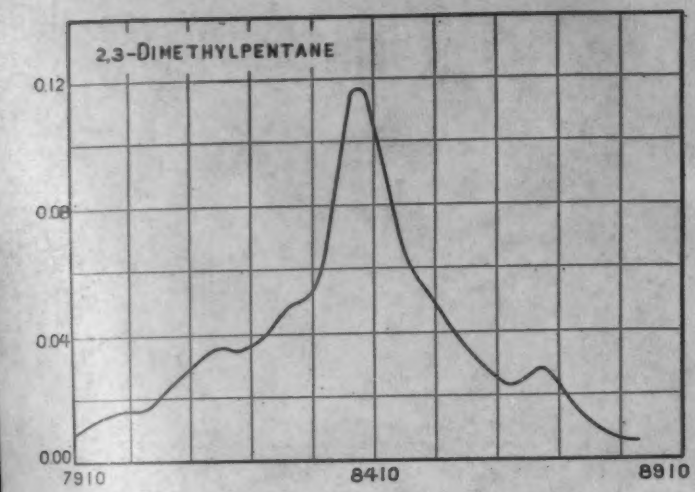

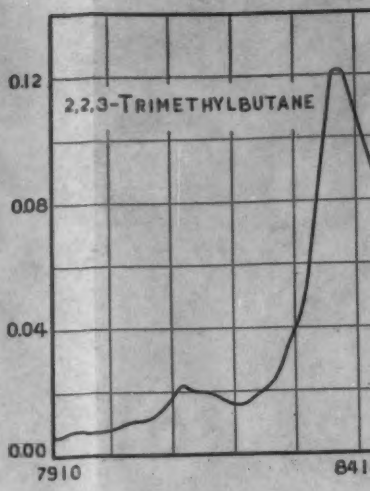

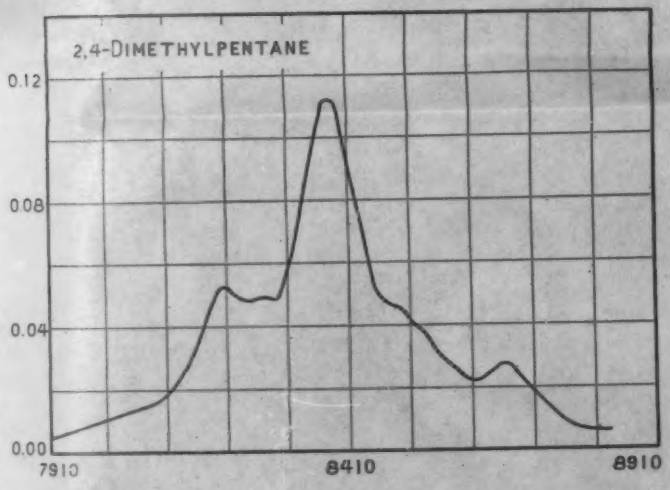

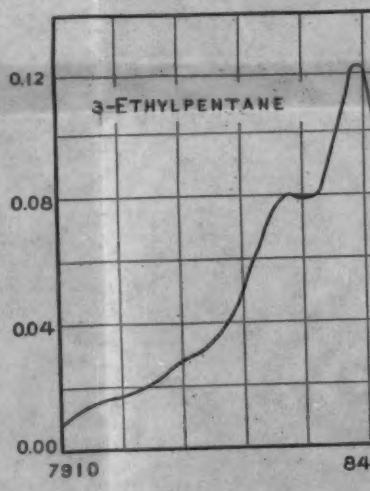

SPECIFIC ABSORPTIVE INDEX

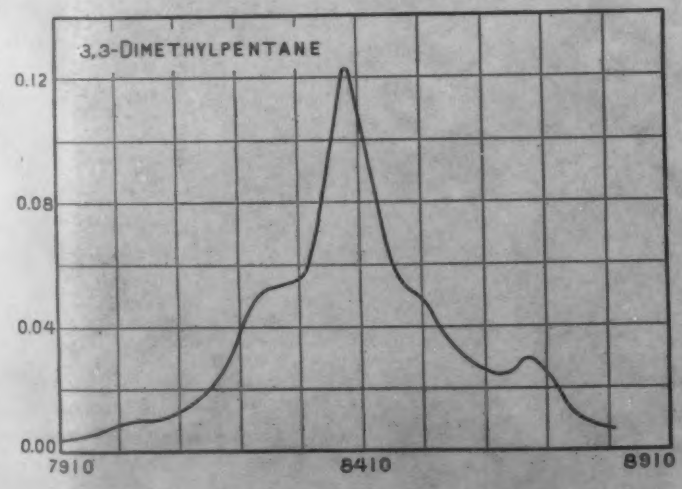

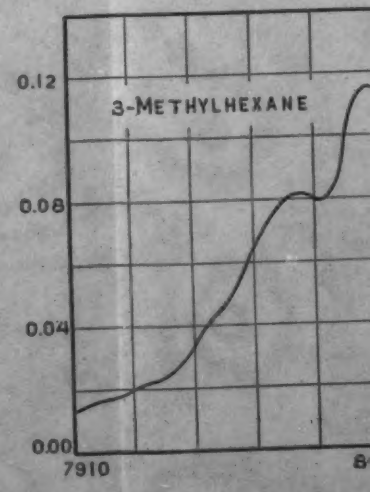

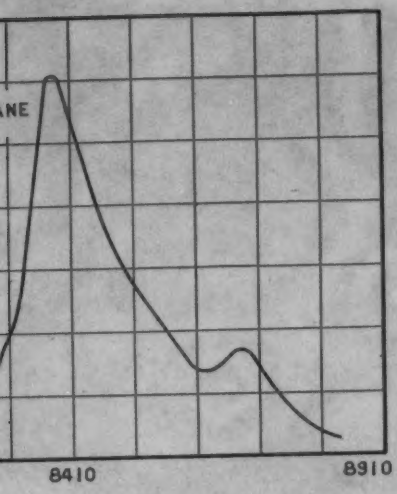
ANE
8410
8910

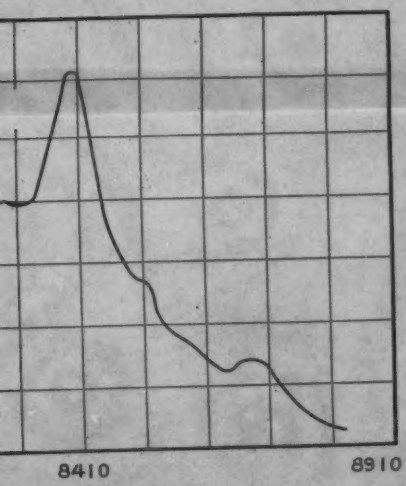
8410
8910

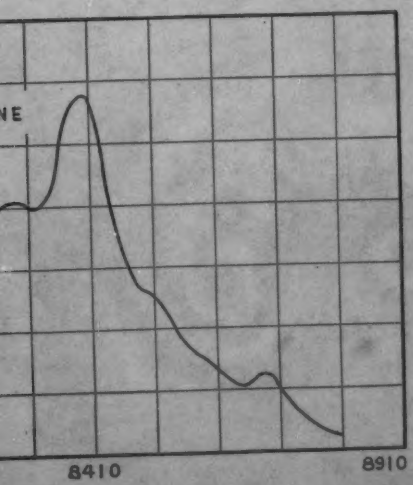
NE
8410
8910

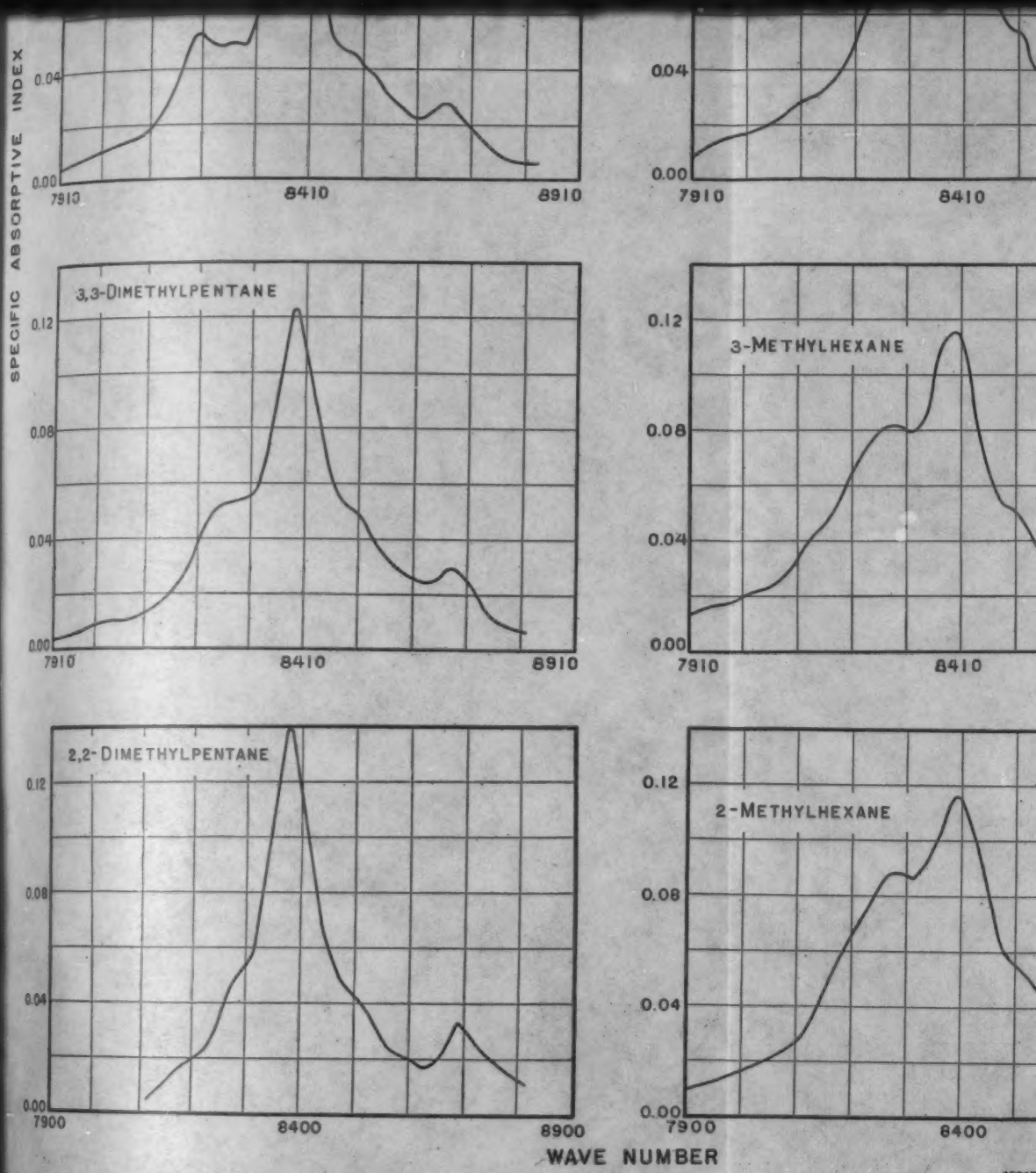

FIGURE 9.

15317

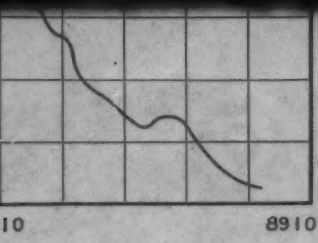

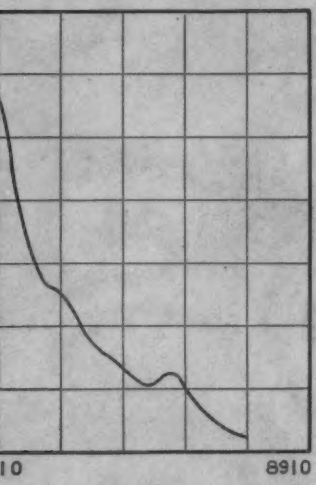

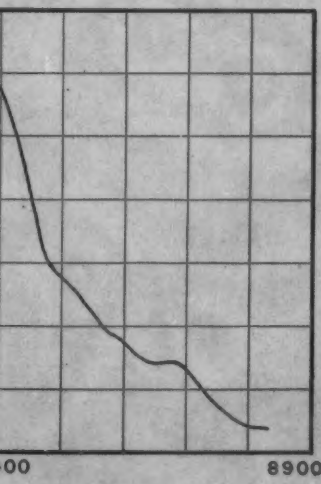

13317—23. (Face p. 608.)

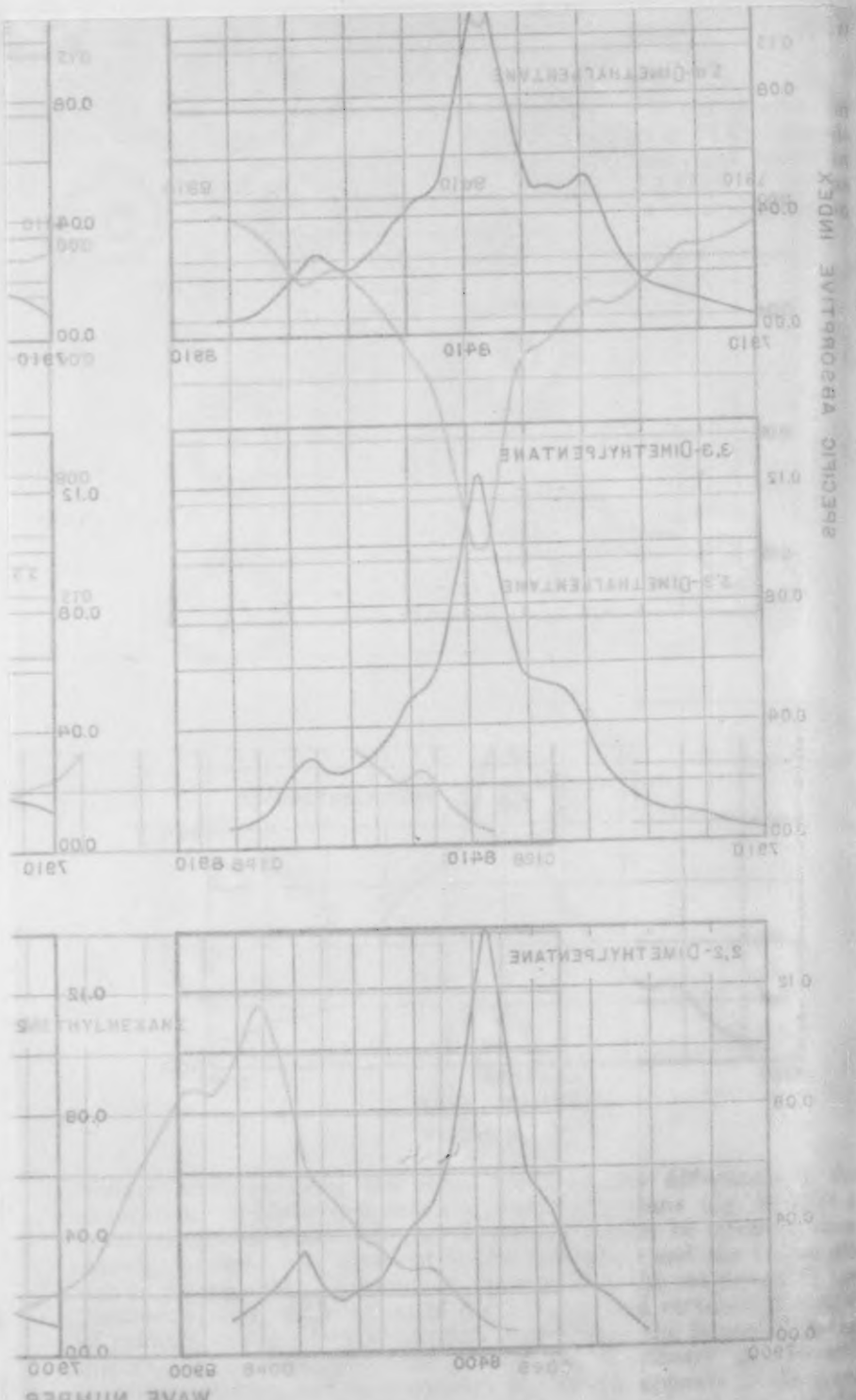
2,2-DIMETHYLPENTANE
3,3-DIMETHYLPENTANE
2,3-DIMETHYLPENTANE
8410
0.12
0.08
0.04
0.00
SPECIFIC ABSORPTIVE INDEX
WAVE NUMBER

curve might lead one to suspect the presence of secondary groups, the maximum, if completely resolved, would be of a nearly symmetrical character. Possibly adjacency of the methyl groups plays some part in the 2, 3-isomer. An unexpected difference appears in the spectra of 2, 3-, and 2, 4-dimethylpentane; unexpected since both molecules are composed of the same number of each type of carbon groups. In these curves the absorption of primary, secondary, and tertiary hydrocarbon linkages is clearly evidenced. 3, 3-, and 2, 2-Dimethylpentane are another interesting pair, and it is indeed unfortunate that no reliability can be placed on the results of the 2, 2-isomer since it was only available before accurate measurements could be made. It is included merely for comparison of frequencies and for rough ratios of intensities.

2-Methyl- and 3-methylhexane show the least difference of any two compounds that were studied in this region. Again, it was not

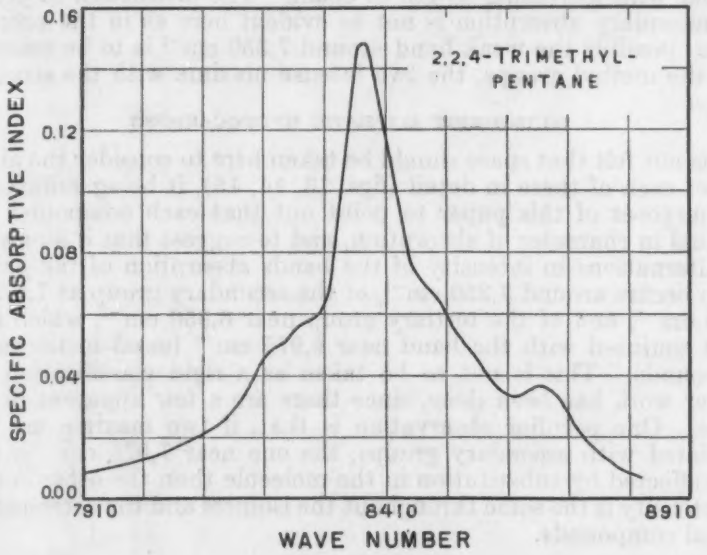

FIGURE 10.

possible to study them both in the same state, which may make a difference. 2, 2, 3-Trimethylbutane, being composed of 5 primary and 1 tertiary groups, has the distinct type of bands to be expected, as does 3-ethylpentane with 3 primary, 3 secondary, and 1 tertiary groups.

2. ABSORPTION FROM 6,400 TO 7,400 CM^{-1}

(a) AROMATIC HYDROCARBONS

The absorption by benzene (fig. 11) in this region is characterized by its weak intensity and multiplicity of structure. The addition of a methyl group to the nucleus considerably increases the intensity of absorption through the whole region and wipes out part of the apparent structure, as does the addition of an ethyl group. The absorption increases again in the xylenes, certain differentiating characteristics between the three isomers appearing. Similar remarks apply to the three trimethylbenzenes. A characteristic of the absorption

in this region seems to be that the aromatic linkages absorb much less than the aliphatic, i.e., per C-H bond; the reverse of this is true in the other two regions.

(b) NAPHTHENES

These curves show the presence of two relatively strong maxima with many satellite bands on the low frequency side. A more obvious similarity of these curves to bands around 5,700 cm^{-1} is apparent in the case of naphthenes than in the case of the preceding aromatic hydrocarbons.

(c) NORMAL ALIPHATIC HYDROCARBONS

The normal aliphatic hydrocarbons (fig. 12) show less apparent structure here than the naphthenes, although the relation of these two groups is more easily seen in this region than in the foregoing. Two strong maxima appear, increasing in intensity in a regular manner with increasing length of chain. The distinction of primary and secondary absorption is not as evident here as in the preceding region; possibly the weak band around 7,350 cm^{-1} is to be associated with the methyl groups, the two intense maxima with the secondary groups.

(d) ISOMERIC ALIPHATIC HYDROCARBONS

It is not felt that space should be taken here to consider the absorption of each of these in detail (figs. 13, 14, 15), it being sufficient for the purposes of this paper to point out that each compound is individual in character of absorption, and to suggest that it seems from the alternations in intensity of the bands absorption of the primary group occurs around 7,350 cm^{-1}, of the secondary group at 7,075 and 7,175 cm^{-1}, and of the tertiary group near 6,950 cm^{-1}, which is not to be confused with the band near 6,975 cm^{-1} found in the normal compounds. This is not to be taken as a rigid classification until further work has been done, since there are a few apparent discrepancies. One peculiar observation is that, if two maxima are to be associated with secondary groups, the one near 7,075 cm^{-1} is much more affected by substitution in the molecule than the other in which the intensity is the same throughout the isomers and the corresponding normal compounds.

3. ABSORPTION FROM 5,400 TO 6,400 CM^{-1}

(a) AROMATIC HYDROCARBONS

Benzene (fig. 16) exhibits two sharp, intense maxima with many satellite bands. Physical analysis shows that some of these bands are combinations of the main absorption with known low-frequency bands of benzene such as those found by Kettering and Sleator (32). Substitution by a methyl group, as in toluene (fig. 17), greatly decreases the intensity and slightly decreases the frequency of the main peak, and introduces three bands around 5,700 cm^{-1}. The absorption curve of ethylbenzene exhibits even more structure.

The frequencies of the main maxima decrease still further in the xylenes (fig. 18), each isomer varying in intensity of absorption and exhibiting characteristic bands. The three bands seen first in toluene around 5,700 cm^{-1} are present here with considerably greater intensity, which is even greater in the trimethyl substituted compounds, hence may be associated with the presence of side chains in the

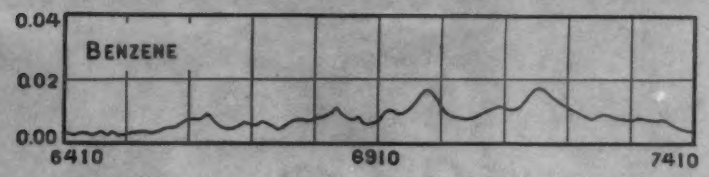

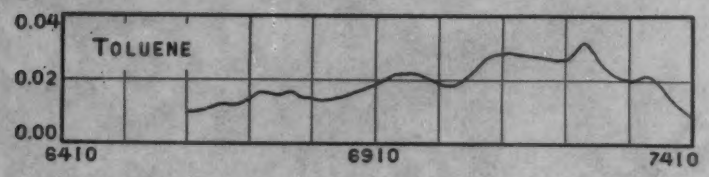

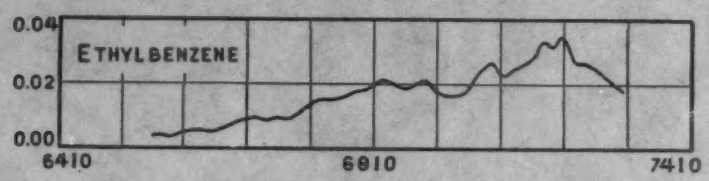

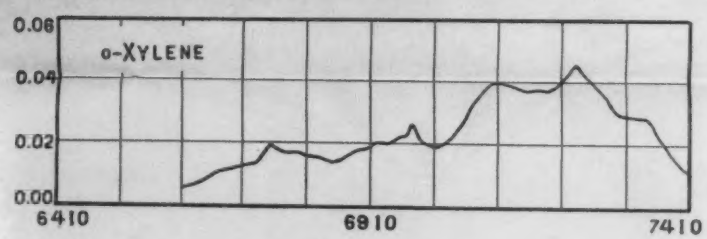

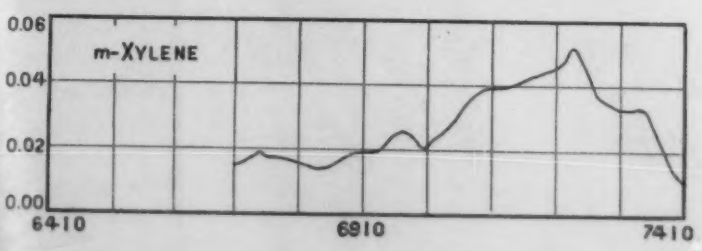

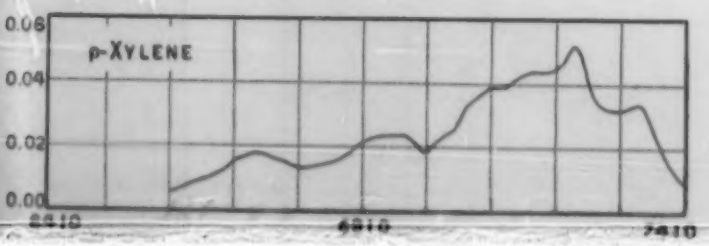

SPECIFIC ABSORPTIVE INDEX.

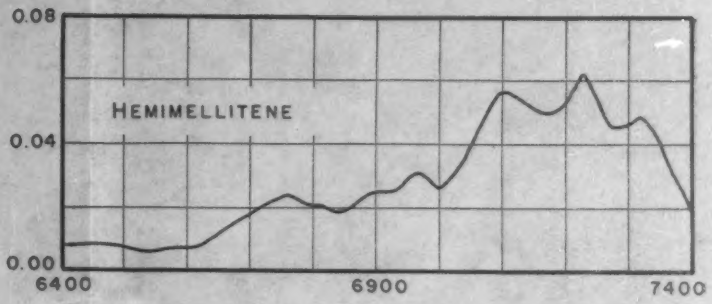

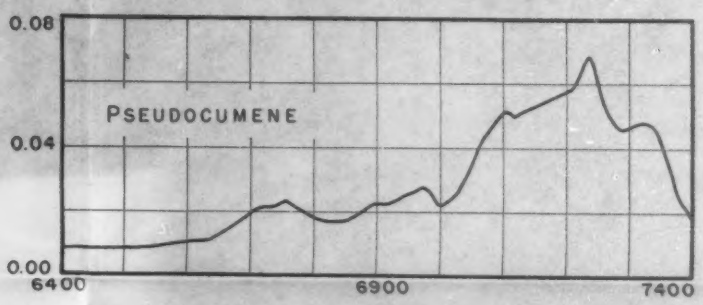

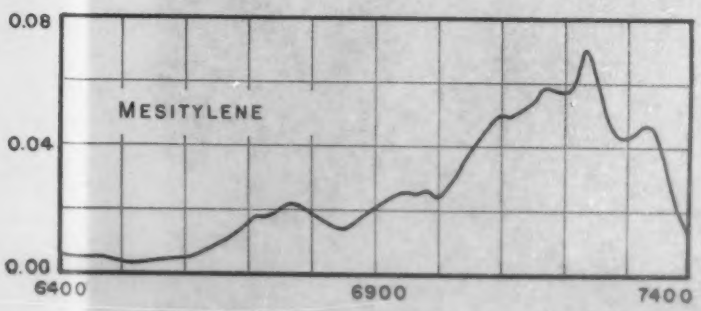

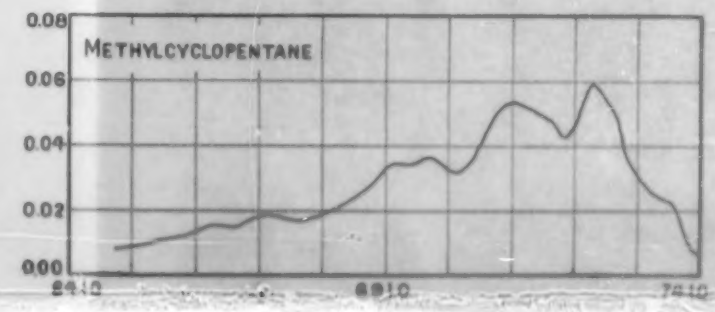

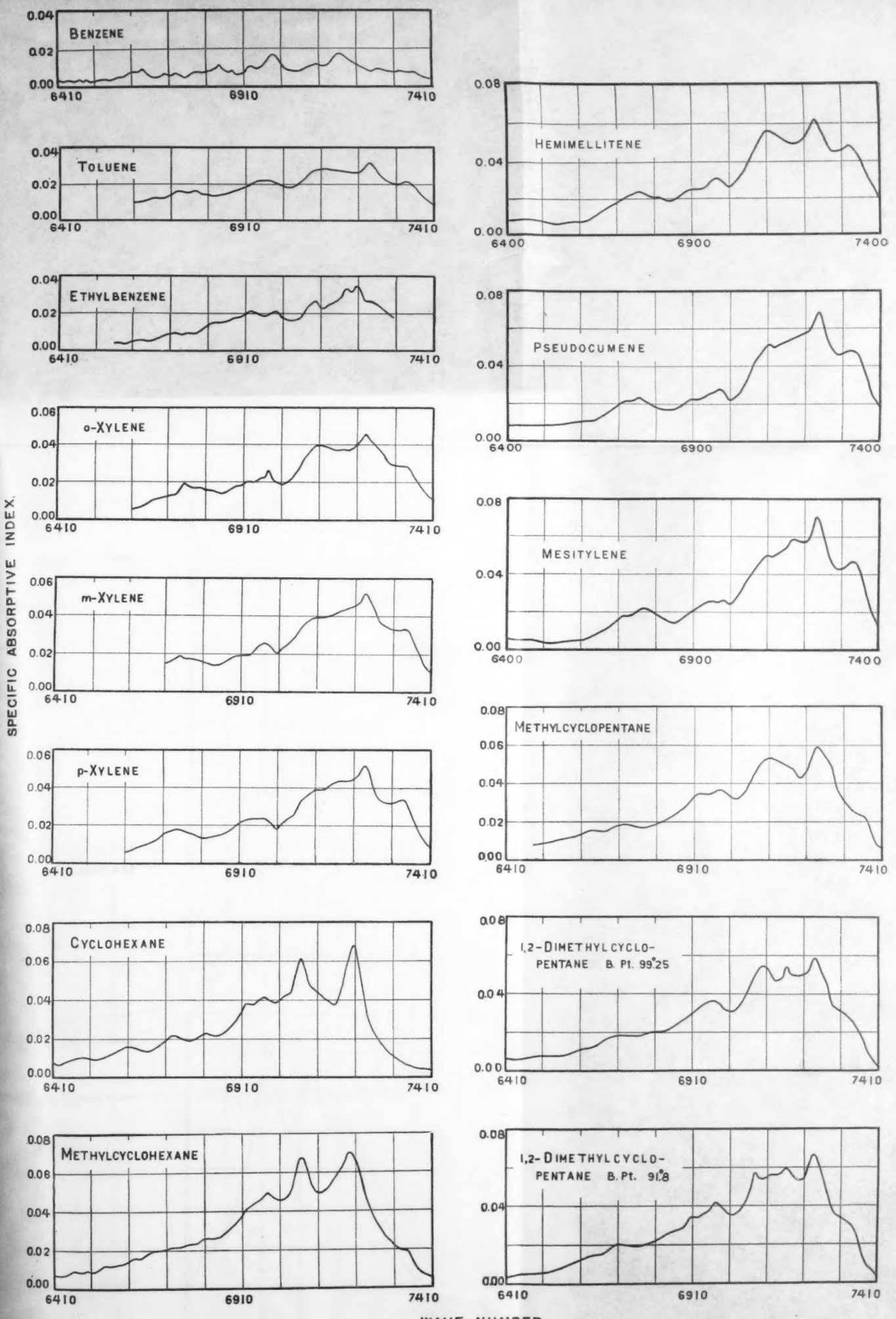

FIGURE 11.

12317—33 (Face p. 610.) No. 1.

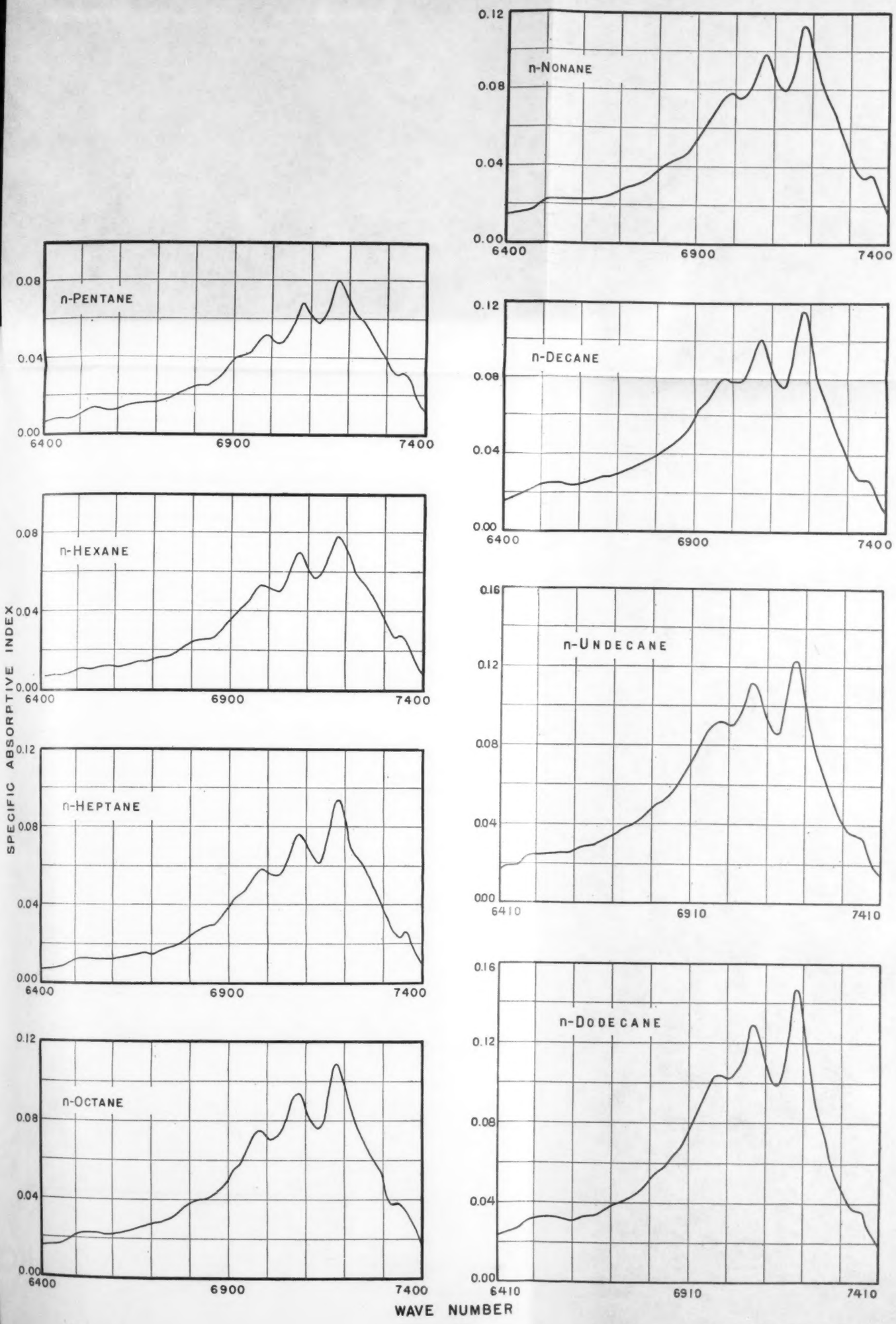
n-NONANE
n-PENTANE
n-DECANE
n-HEXANE
n-UNDECANE
n-HEPTANE
n-DODECANE
n-OCTANE
SPECIFIC ABSORPTIVE INDEX
WAVE NUMBER
0.12
0.08
0.04
0.00
0.16
6400
6900
7400
6410
6910
7410

FIGURE 12.

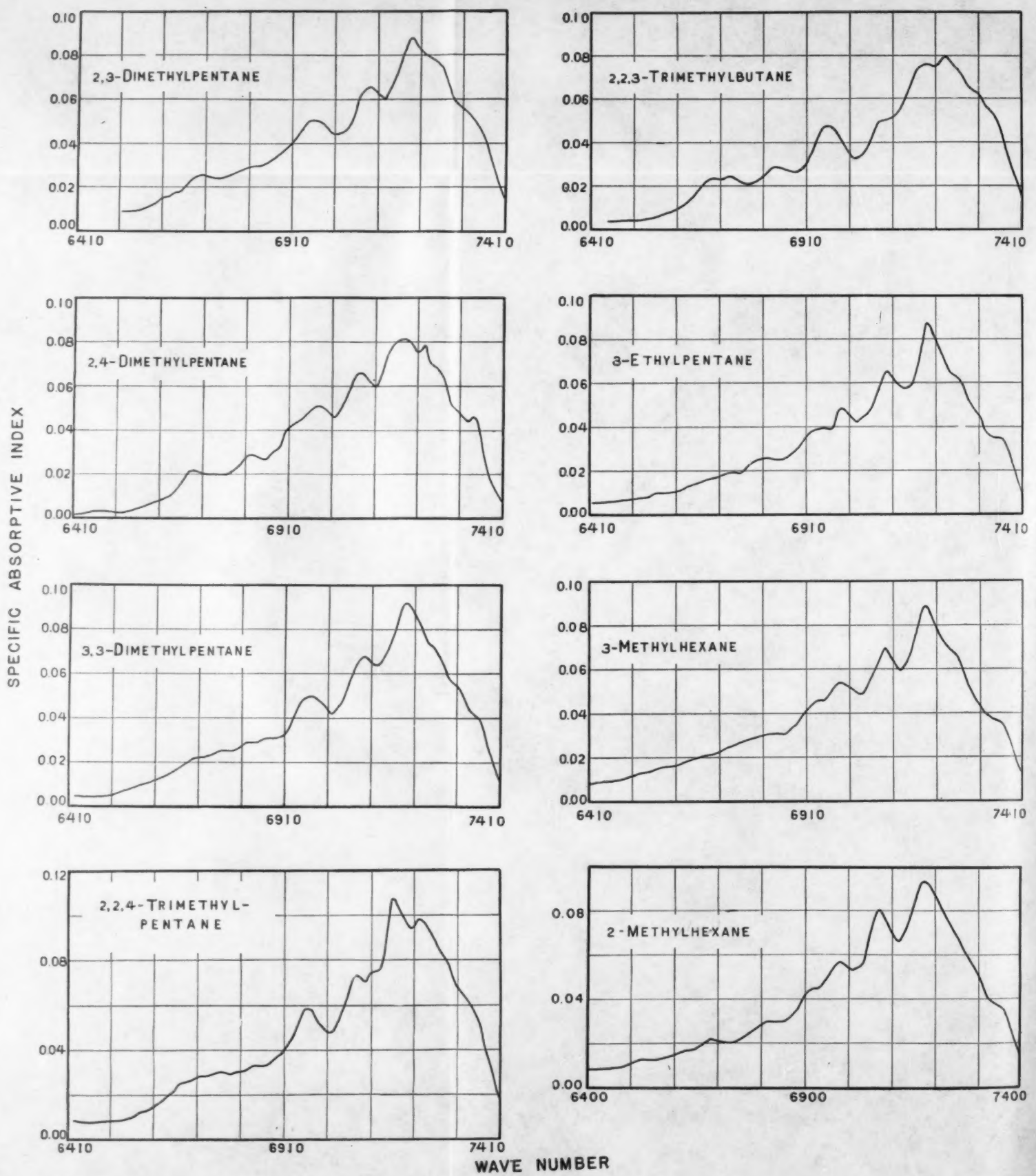

13317—33. (Face p. 611.)

FIGURE 15.

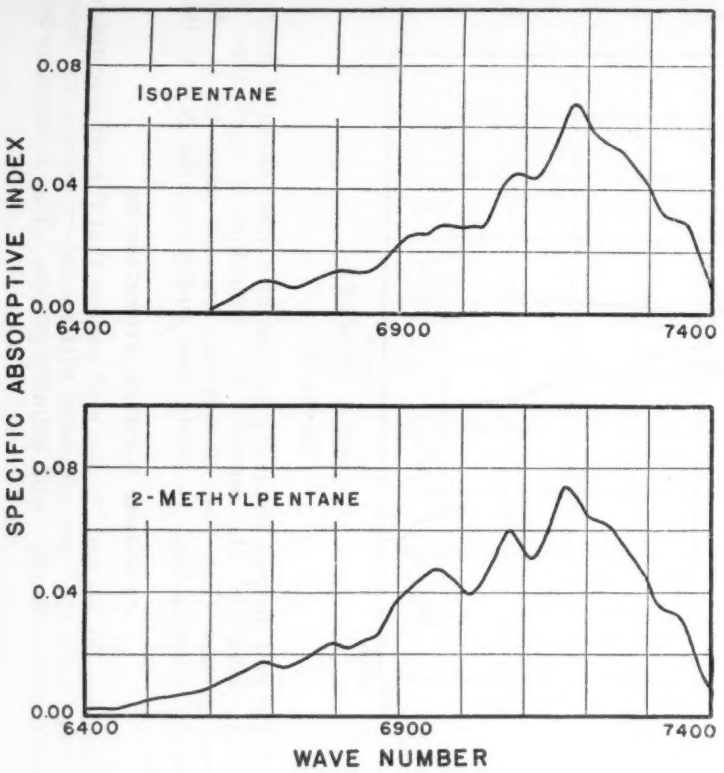

FIGURE 13.

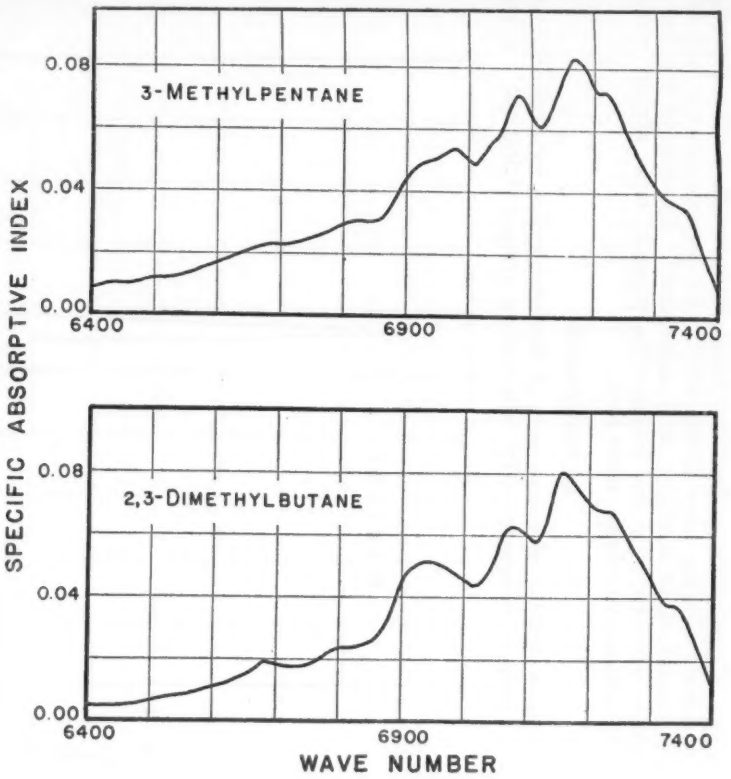

FIGURE 14.

molecule. There seem to be three main components in the absorption of hemimellitene near 5,900 cm^{-1}. In pseudocumene, one of these is considerably stronger, with appreciable decrease of another. Mesitylene exhibits only one intense sharp peak, with almost complete subordination of the other two.

(b) NAPHTHENES

The quite striking characteristic of the absorption by cyclohexane (fig. 19) here as compared with absorption around 8,300 cm^{-1} is its

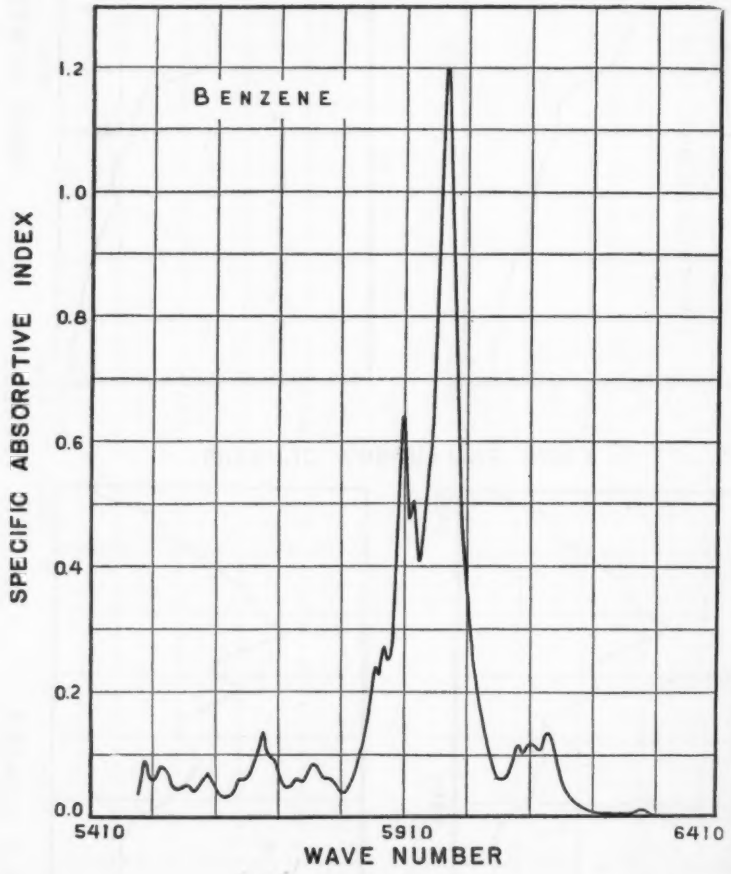

FIGURE 16.

simplicity and distinct similarity to that of normal aliphatic hydrocarbons. However, the intensity of absorption is more than 50 percent greater than that of *n*-hexane in this same region. No pertinent remarks may be made now concerning the rest of this group.

(c) NORMAL ALIPHATIC HYDROCARBONS

Here (figs. 20, 21, and 22) one may suggest that the two maxima at 5,670 and 5,790 cm^{-1} are associated with secondary groups, and those at 5,860 and 5,900 cm^{-1} with primary groups. This is based on the

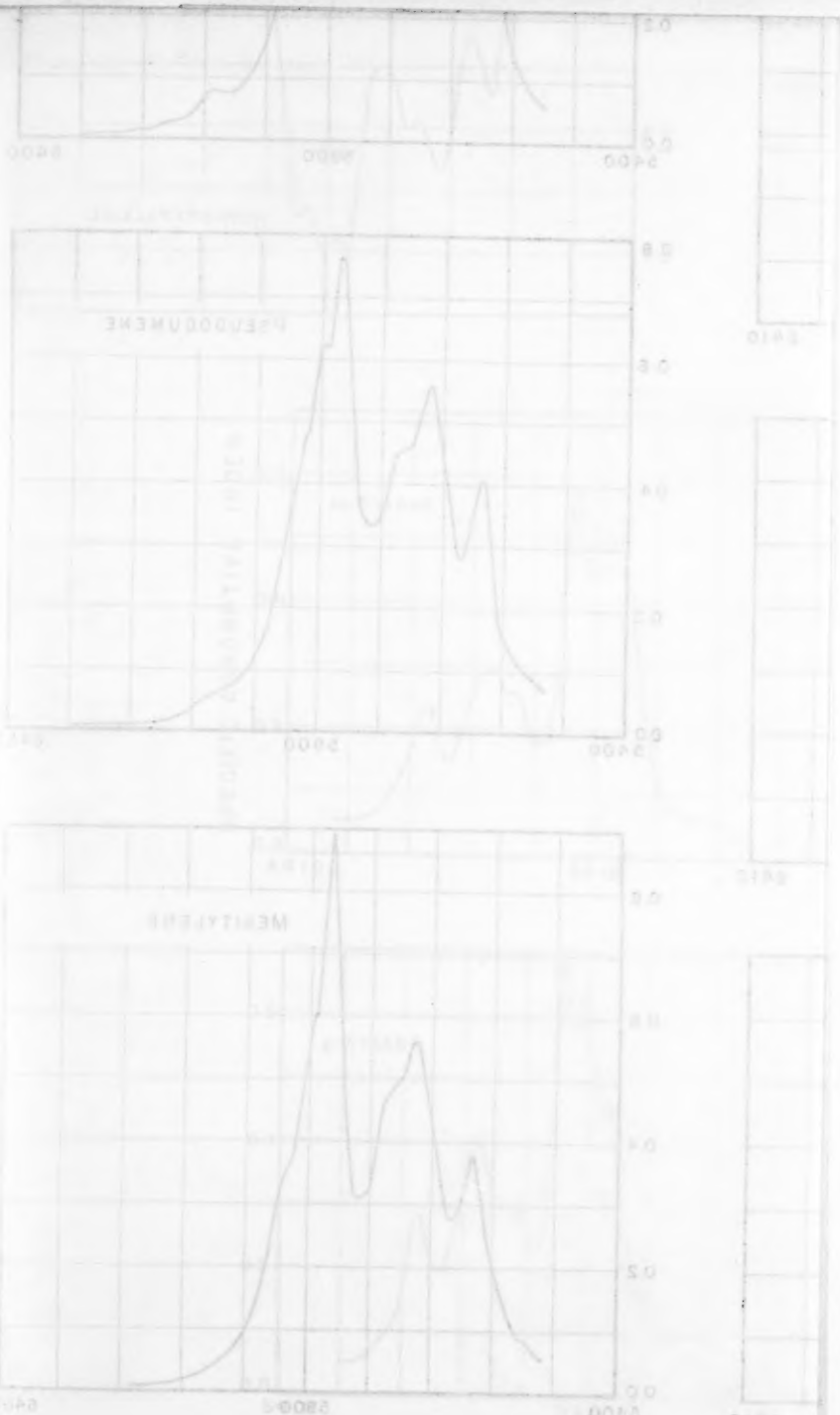

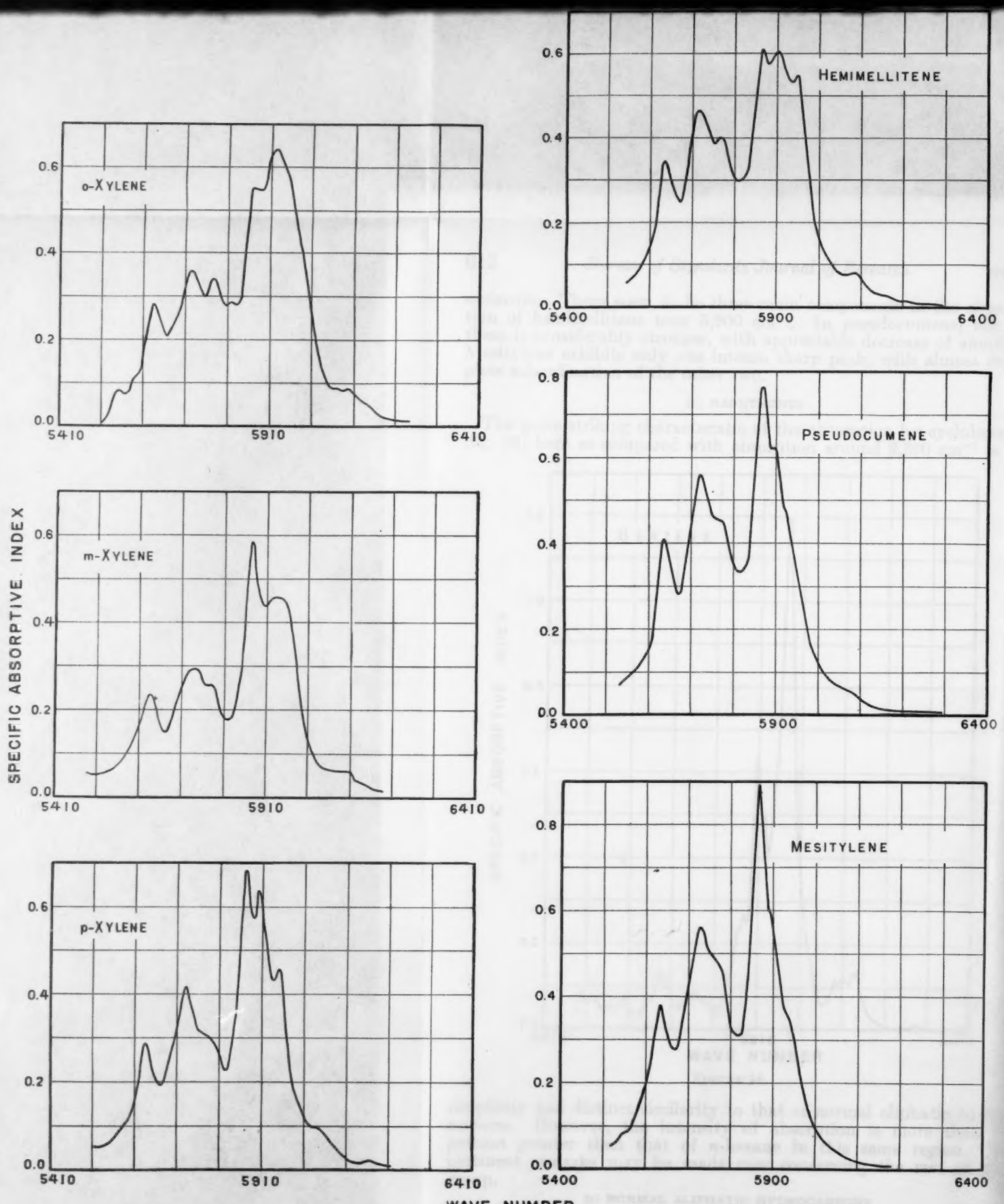

13317—33. (Face p. 613.) No. 1.

Figure 18.

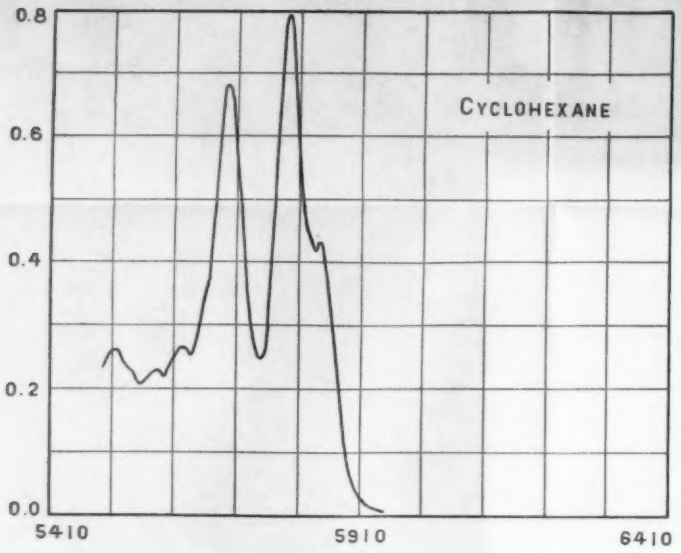

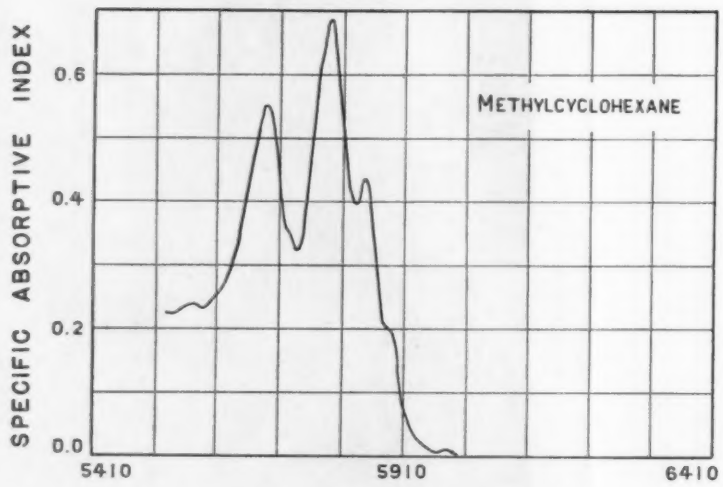

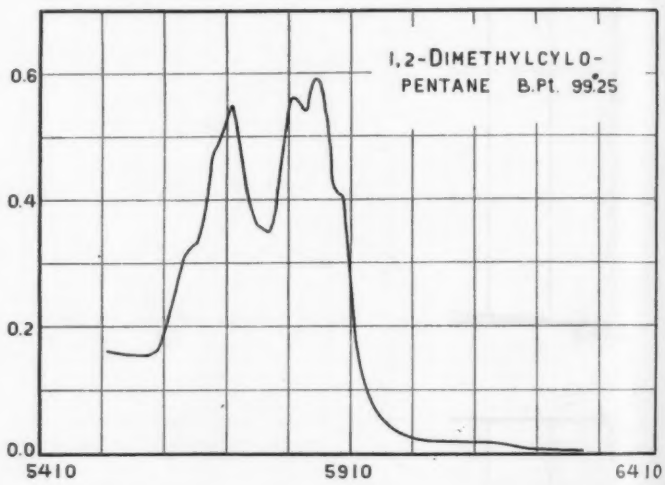

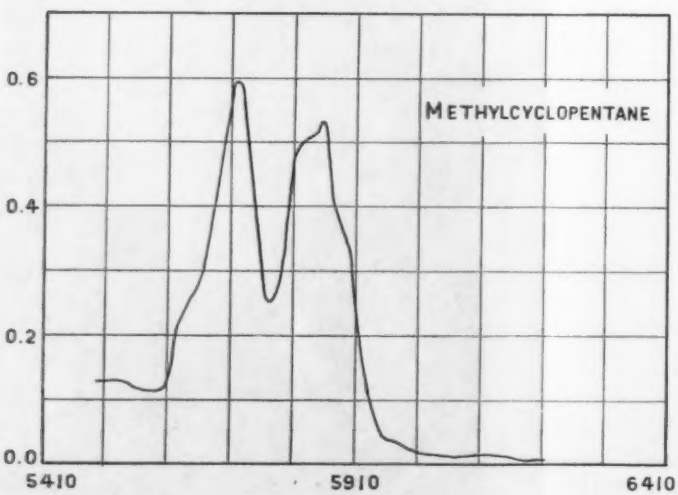

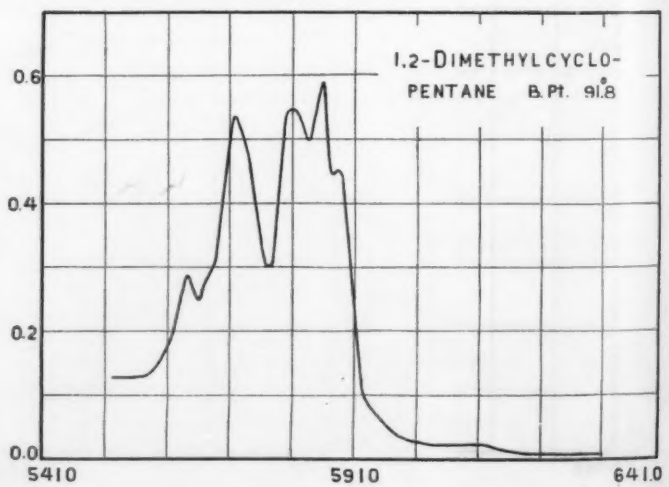

WAVE NUMBER

13317—33. (Face p. 613.) No. 2.

Figure 19.

observation that the first two increase with increasing length of chain and the last do not. In character these bands are almost identical

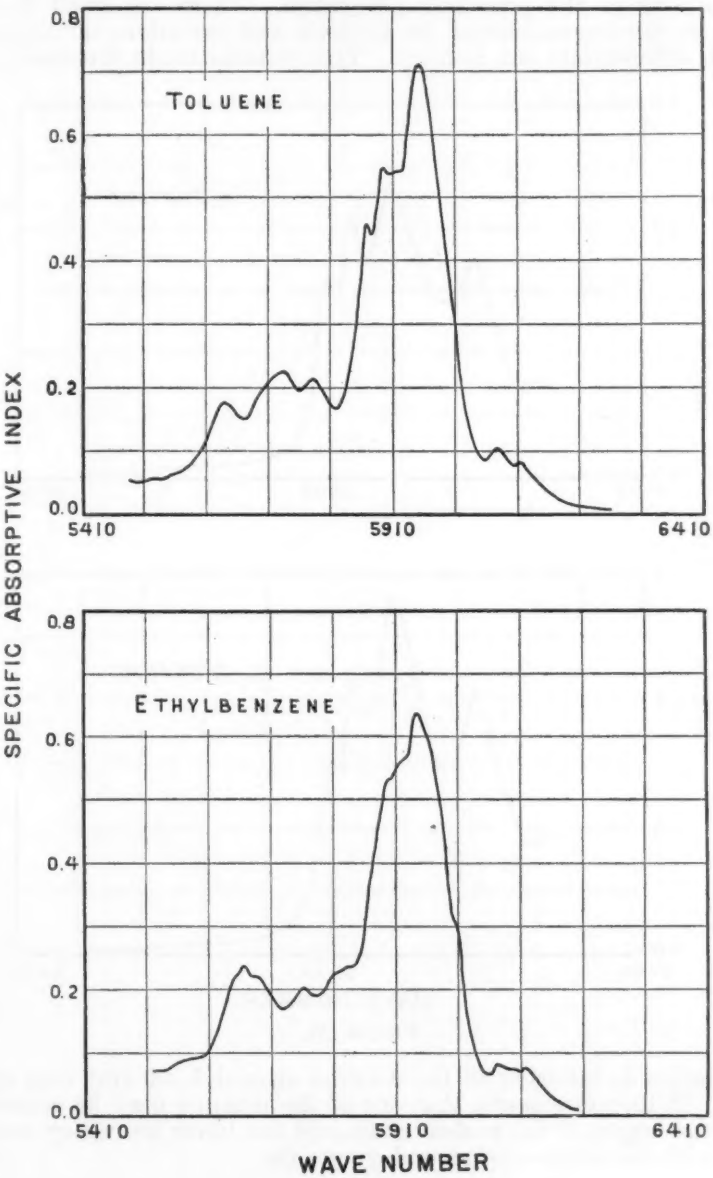

FIGURE 17.

with those around 7,100 cm^{-1} but are several times as intense, as would be expected.

(d) ISOMERIC ALIPHATIC HYDROCARBONS

In a general manner these curves (figs. 23, 24, 25) bear out the suggestions in the preceding paragraph. There are small fluctuations in the frequencies of the maxima and variations in intensities which differentiate the isomers. The remarks made concerning the

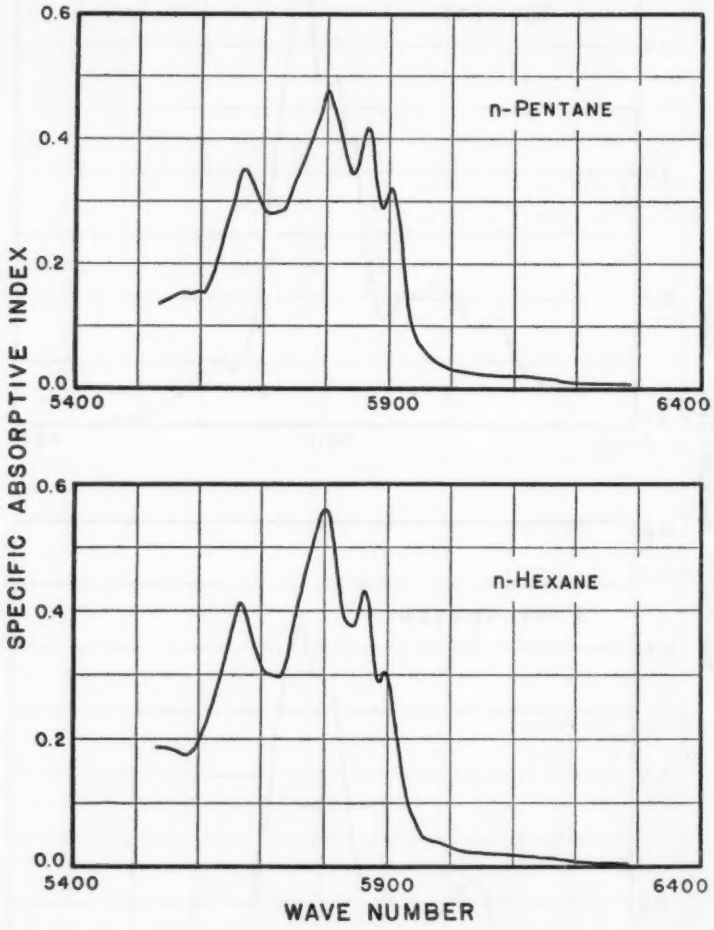

FIGURE 20.

alternation in intensity of the maxima around 7,100 cm^{-1} also apply here. It therefore seems that one of the maxima may be connected with the length of the carbon chain and the lower frequency component with the number of secondary groups.

IV. DISCUSSION OF RESULTS

For many years it has been considered that the complete infrared absorption spectrum of any compound is a unique characteristic of that compound, even among isomers. Experimental technique required, however, makes it rather difficult to obtain the spectrum of

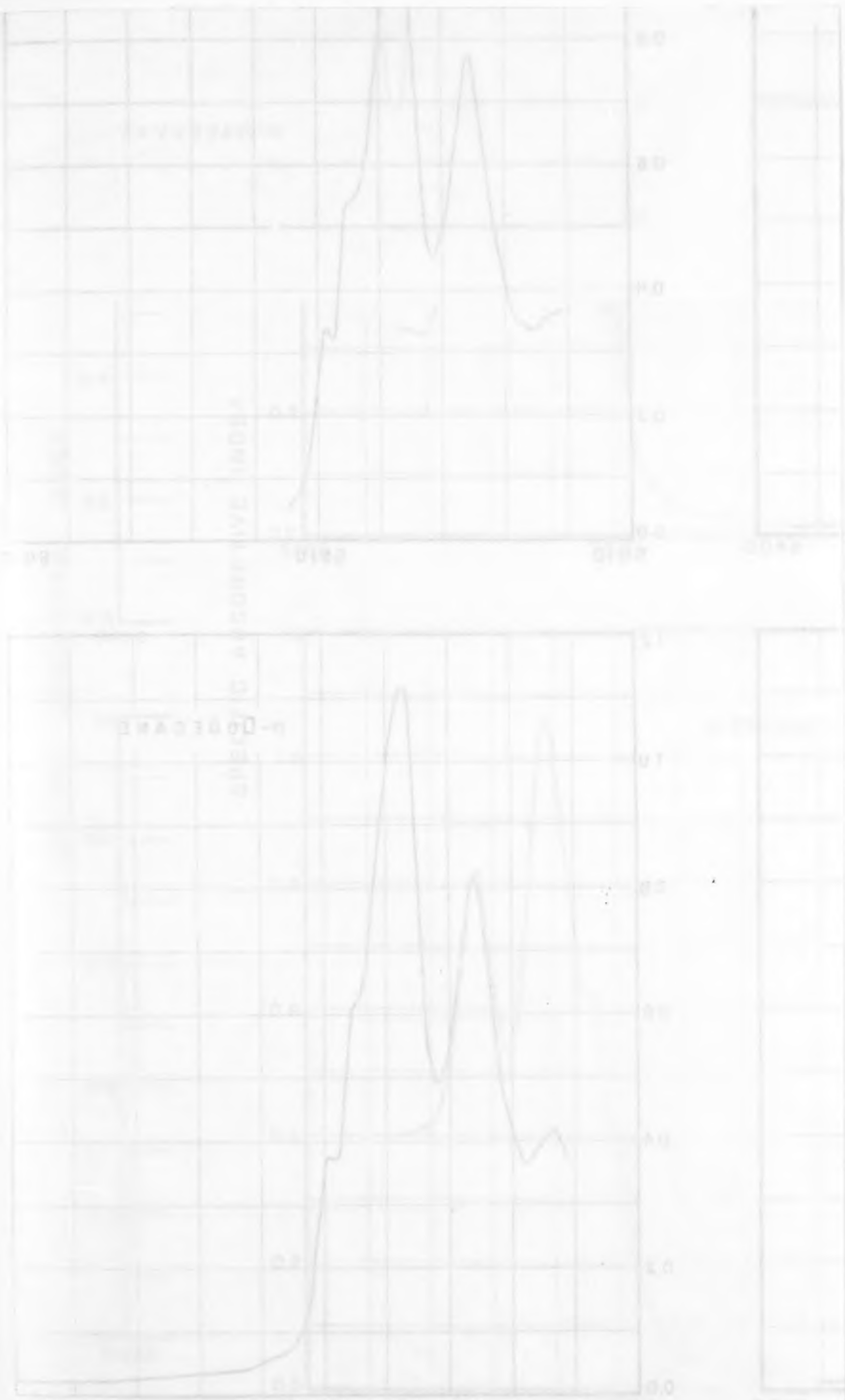

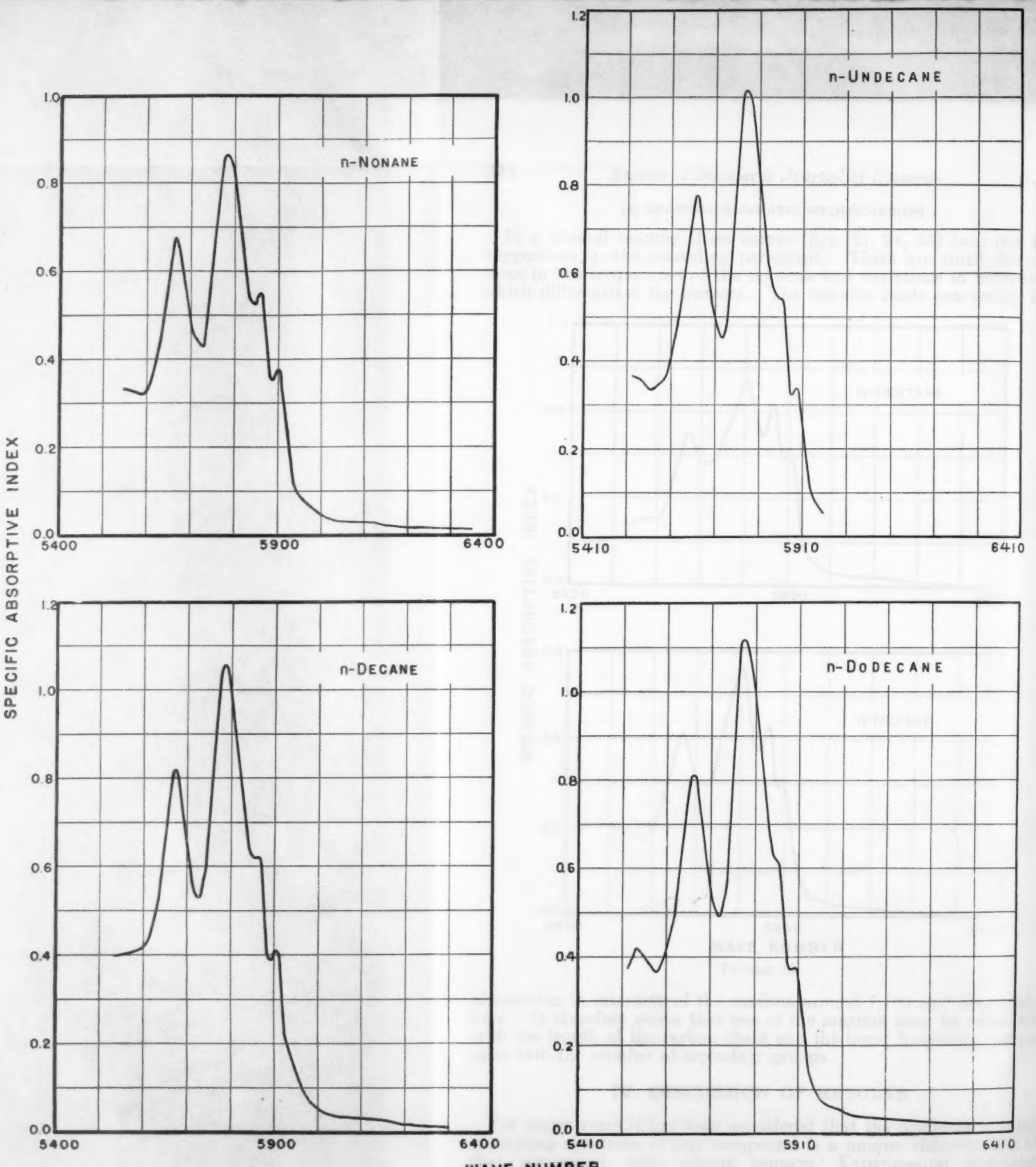

13317—33. (Face p. 615.)

FIGURE 22.

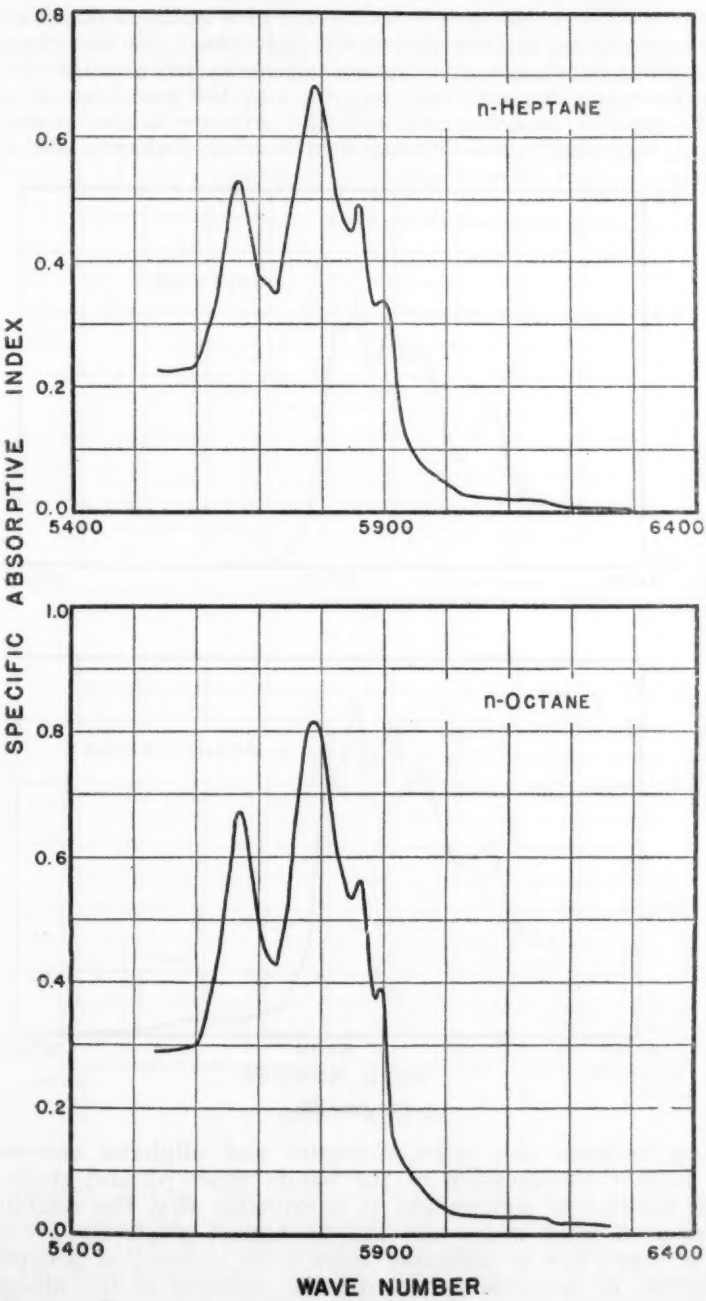
n-HEPTANE
n-OCTANE
SPECIFIC ABSORPTIVE INDEX
0.0
0.2
0.4
0.6
0.8
1.0
5400
5900
6400
WAVE NUMBER

FIGURE 21.

the whole region. In this study using high resolution, further evidence is given that the fine structure of certain bands in the near infrared, obtainable with rather simple technique, give quite as definite information concerning the identity of the molecules. Certain characteristics of these bands seem to be intimately connected with the structure of the molecule, as previously stated; i.e., the positions of certain maxima seem to be connected with the presence in the molecule of primary, secondary, and tertiary hydrocarbon linkages, also distin-

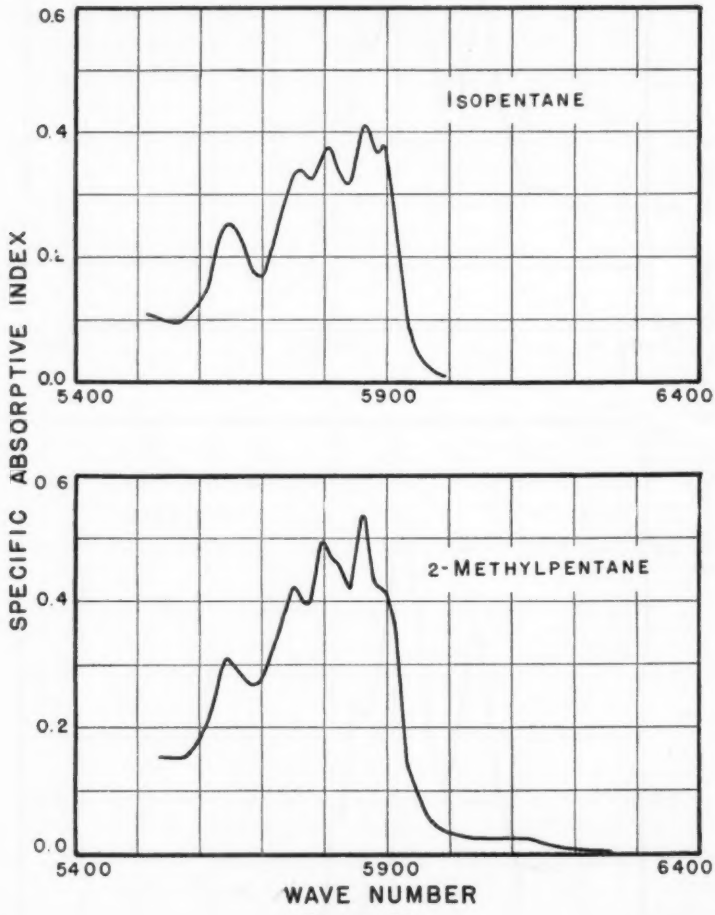

FIGURE 23.

guishing between the types aromatic and aliphatic compounds. With further classification of the bands observed and study of a greater number of compounds, it is probable that the structure of an unknown pure compound can be almost positively predicted. Also, if Beer's law is valid and there is no interaction between the compounds in solution, a quantitative estimate of the amount of each component present in a mixture can be made. No results are given herein in support of this last statement, but two experiments have been made in which it proved valid. Further work not possible

at the present time is necessary. However, analysis of a mixture of three similar components is very difficult, and of a greater number practically impossible.

In the high frequency region, it is seen that the absorptions of aromatic and aliphatic linkages are widely separated, and that variations of the type of absorption indicate the manner in which the groups are bound together. Confirmation of this indication comes from a study of the other two regions. These last two regions might well be used for first considerations except that they are considerably

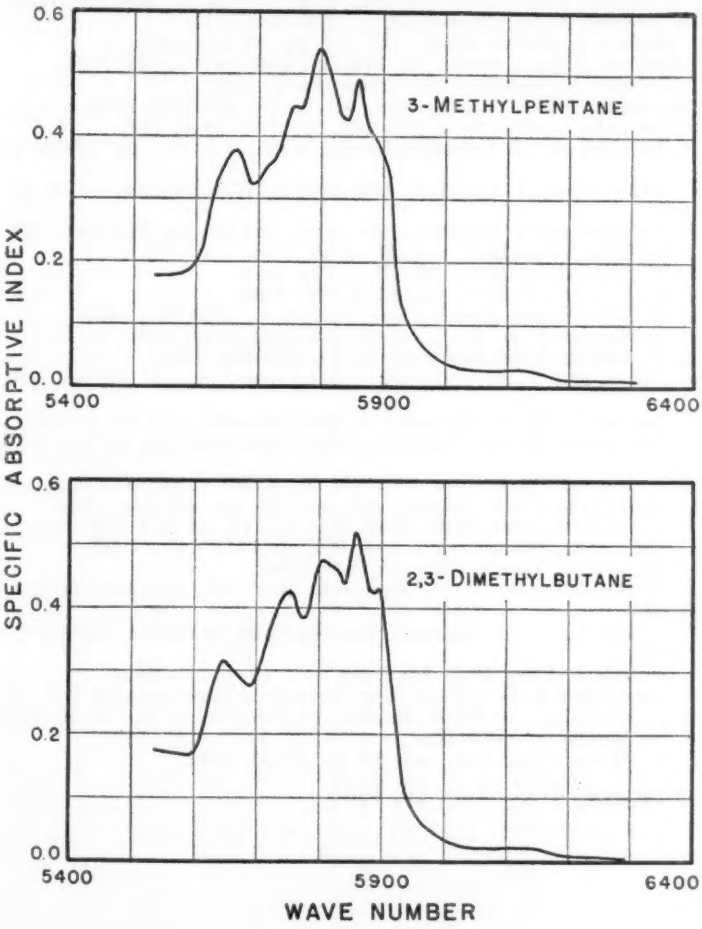

FIGURE 24.

more complex, arising from different transitions in the energy levels of the molecules and being contaminated with transitions of weaker intensity other than the main series under consideration.

It is not to be understood that this method will ever find universal application in analytical organic chemistry. There undoubtedly are specific examples the study of which would be impossible. It is merely offered as an additional aid to other forms of technique and as such should prove very valuable.

This work was initiated at the suggestion of Dr. E. W. Washburn, whose assistance and cooperation has made it possible. F. W. Rose, Jr., has aided materially in preparing the illustrations of this paper.

V. BIBLIOGRAPHY

1. W. Abney and B. Festing, Phil. Trans., vol. 172, p. 887, 1881; Proc. Roy. Soc. (London) (A), vol. 31, p. 416, 1881.
2. H. Julius, Verhandel Akad. Wetenschappen Amsterdam, Deel i, no. 1, 1892.
3. W. W. Coblentz, Investigations of Infrared Spectra, Pub. No. 35, Carnegie Inst., Washington, 1905.
4. J. E. Purvis, Proc. Cambridge Phil. Soc., vol. 21, pp. 556–565, 1923.
5. Th. Dreisch, Z. Physik, vol. 30, pp. 200–216, 1924.
6. L. Marton, Z. physik. chem., vol. 117, pp. 97–128, 1925.
7. J. Lecomte, Compt. rend., vol. 178, pp. 1530, 1698, 2073, 1924.
8. J. Lecomte, Le Spectre Infra Rouge, Paris, 1928.
9. J. Lecomte, Trans. Faraday Soc., vol. 25, pp. 864–876, 1929.
10. J. Lecomte, Compt. rend., vol. 194, pp. 2037–2040; 1932.
11. P. Lambert and J. Lecomte, Compt. rend., vol. 194, pp. 77–79, 960–962, 1932.
12. P. Lambert and J. Lecomte, Ann. combustibles liquides, vol. 6, pp. 1001–1083, 1931.
13. P. Lambert and J. Lecomte, Ann. phys., vol. 18, pp. 329–390, 1932.
14. J. W. Ellis, Phys. Rev., vol. 23, p. 48, 1924.
15. J. W. Ellis, Phys. Rev., vol. 27, p. 298, 1926.
16. J. W. Ellis, Phys. Rev., vol. 32, p. 906, 1928.
17. J. W. Ellis, Trans. Faraday Soc., vol. 25, pp. 888–898, 1929.
18. R. B. Barnes, Phys. Rev., vol. 35, pp. 1524–1532, 1930.
19. R. B. Barnes, Phys. Rev., vol. 36, pp. 296–304, 1930.
20. J. Barnes and W. H. Fulweiler, J.Am.Chem.Soc., vol. 49, pp. 2034–2037, 1927.
21. J. Barnes and W. H. Fulweiler, J. Am.Chem.Soc., vol. 50, p. 1033, 1928.
22. J. Barnes and W. H. Fulweiler, J.Am.Chem.Soc., vol. 51, pp. 1750–1752, 1929.
23. G. B. Bonino, Gazz. chim. ital., vol. 53, p. 267 et seq. 576 et seq., 1923.
24. G. B. Bonino, Trans. Faraday Soc., vol. 25, pp. 876–888, 1929.
25. F. S. Brackett, Proc. Natl. Acad. Sci., vol. 14, pp. 857–864, 1928.
26. R. Freymann, Compt. rend., vol. 194, pp. 1471–1474, 1932.
27. R. Freymann, Thesis, Univ. of Paris, 1933.
28. F. S. Brackett and E. D. McAlister, Rev. Sci. Instruments, vol. 1, pp. 181–193, 1930.
29. C. Schaefer and F. Matossi, Das Ultrarot Spektrum, Springer & Co., Berlin, 1931.
30. E. O. Salant, Proc. Natl. Acad. Sci., vol. 12, p. 370, 1926.
31. R. Davis and K. S. Gibson, Bur. Standards Miscellaneous Pub. No. 114.
32. C. F. Kettering and W. W. Sleator, Physics., vol. 4, pp. 39–49, 1933.
33. E. D. McAlister, Phys. Rev., vol. 34, pp. 1142–1147, 1929.
34. E. K. Plyler, Phys. Rev., vol. 39, pp. 77–82, 1932.

WASHINGTON, D.C., July 19, 1933.

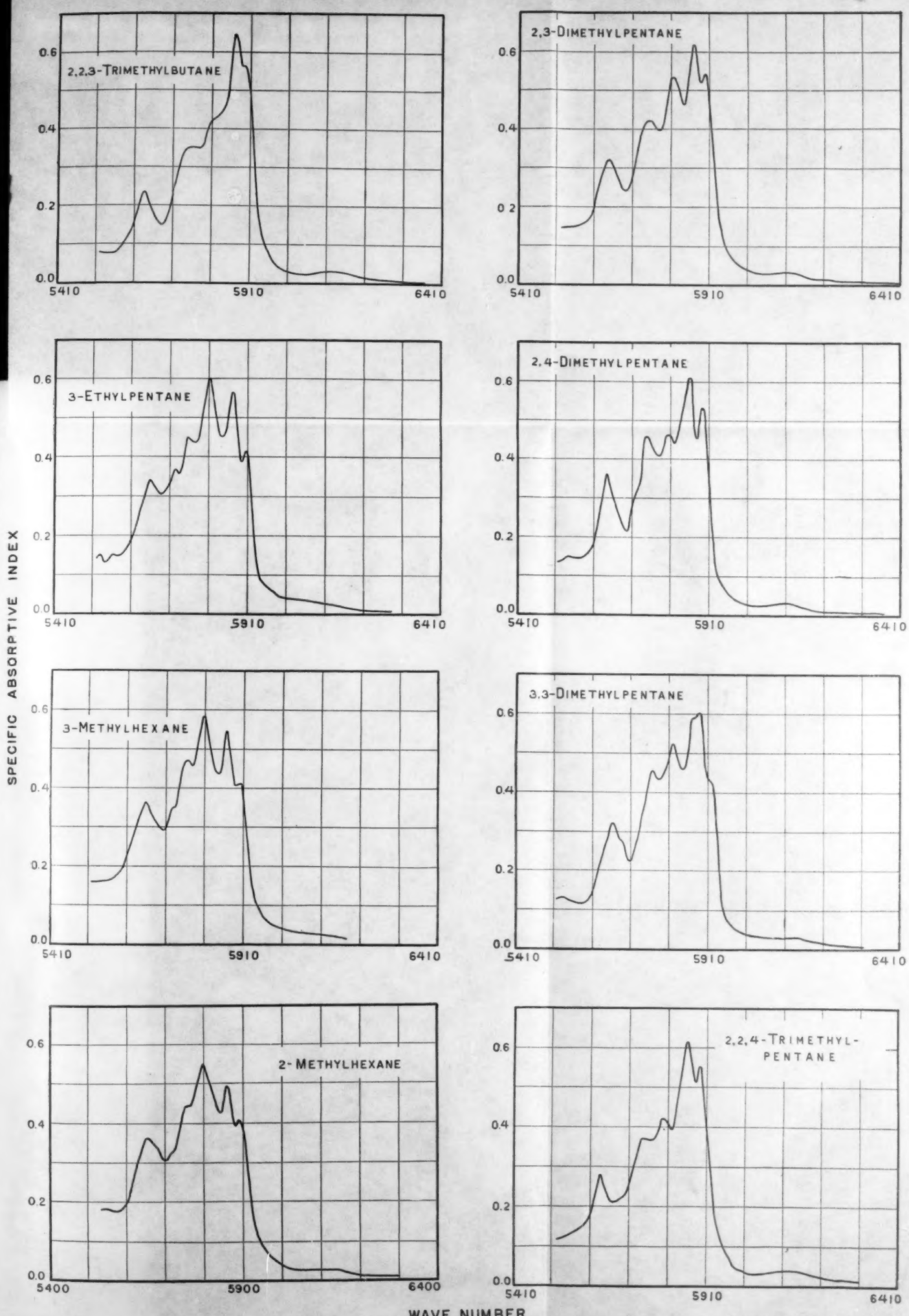

13317—33. (Face p. 618.)

FIGURE 25.

SPECIFIC ABSORPTIVITY INDEX
WAVE NUMBER

U.S. Department of Commerce, Bureau of Standards

RESEARCH PAPER RP611

Part of Bureau of Standards Journal of Research, Vol. 11, November 1933

THE STABILITY OF LEVULOSE IN AQUEOUS SOLUTIONS OF VARYING pH

By Joseph A. Mathews and Richard F. Jackson

ABSTRACT

Levulose was subjected at five temperatures to the action of buffer solutions whose pH varied from −2.6 to 14.2. In its earlier stages the decomposition reaction is unimolecular and approaches an equilibrium which cannot be realized but by a new method can be calculated. The equilibrium values are a function of pH and give evidence of the nature of the reaction. In acid solutions levulose is dehydrated to form levulosans of negative rotation, in alkaline solutions the familiar Lobry de Bruyn-van Ekenstein transformation occurs, and in intermediate reactions both transformations occur. Velocity constants of the early stages of the decomposition were measured in 50 experiments. Polariscopic, total reducing sugar, and selective levulose analyses gave approximately the same velocity constants. A plot of these velocity constants against pH showed that the stability of levulose passed through a maximum at pH 3.3. Neutral solutions are alkaline with respect to this maximum. The temperature coefficient of the reaction at constant pH is shown to be relatively high. The periods of time required for a 1 percent decomposition of levulose are tabulated as a function of pH and temperature.

CONTENTS

		Page
I.	Introduction	619
II.	Methods	620
III.	Typical reaction curves and the determination of the equilibrium	622
IV.	The variation of equilibrium values with pH	625
V.	The stability of levulose	629
VI.	The temperature coefficients	631
VII.	Summary	632

I. INTRODUCTION

Levulose is one of the more reactive sugars and in aqueous solution is particularly unstable at the extreme ranges of pH. In the process of its preparation from the juices of the Jerusalem artichoke or other natural sources by the method described by Jackson, Silsbee, and Proffitt [1] the sugar is necessarily subjected to relatively high acidity during the hydrolysis of the polysaccharides, to high alkalinity during the calcium levulate precipitation, and to intermediate reactions after the pure substance has been isolated in aqueous solution. It therefore becomes important to determine the degree of stability of levulose under the conditions to which it is subjected in order to evaluate and as far as possible minimize the losses. It is expected, moreover, that the data secured in the present investigation will have a more general applicability since levulose is a constituent of practically all fruit juices and occurs in a great variety of commercial sirups and other products.

[1] B. S. Sci. Papers No. 519, vol. 20, p. 519, 1926.

Nef [2] has shown that the prolonged action of relatively strong alkali leads to a complete disintegration of the levulose molecule with the possible formation of about 116 products. Lobry de Bruyn and van Ekenstein [3] showed that action of mild alkali leads to formation of an equilibrium between levulose, dextrose, and mannose, established by rearrangement of the common dienol.

Strong acid solutions have been shown by Pictet and Chavan [4] to yield by dehydration heterolevulosan as a primary product. This substance in the same series of reactions condenses in part to the dimer, diheterolevulosan. More prolonged action of acid solutions results in the formation of levulinic and formic acids, oxymethyl furfural, and humus substances of high carbon content.[5] In none of the work cited has the reaction velocity been measured.

In the present investigation we have sought to measure the velocities of the respective reactions in their initial stages as functions of pH and temperature and, by computing the time required for decomposition of the first 1 percent of levulose, to state in quantitative terms the stability of the sugar under the specified conditions.

We emphasize the fact that the reactions here studied are not susceptible to exact measurement since they are in many cases accompanied by competitive, consecutive, and secondary reactions. We have based our conclusions upon statistics drawn from a large number of observations, none of which has been rejected. That the conclusions are fundamentally correct is attested by the regularity with which the experimental data, all acquired independently, fit into a system of curves.

II. METHODS

Pure crystalline levulose or levulose sirups of about 99 percent purity were mixed with buffer solutions of systematically varying pH and subjected to the influence of carefully controlled temperatures for such periods of time as permitted measurements of the rates of decomposition. The concentration of levulose in the reaction mixture was varied between 2 and 10 grams per 100 ml.

The change in the reaction mixture was followed in every instance polariscopically, and in selected cases by change in reducing sugar, and in levulose determined selectively.

Polariscopic measurements were made with a Bates type quartz-wedge saccharimeter in water-jacketed polariscope tubes. Total reducing sugars were determined by Lane and Eynon's volumetric method [6] and levulose selectively by Jackson and Mathews' [7] modification of Nyns' method. The copper reduction methods were carried out in duplicate and were controlled by analyses of standard solutions of pure levulose.

The buffering substances were those recommended by Clark and by Sørensen. The concentrations of buffer in the buffer-sugar mixtures were, however, made double those given by Clark [8] in order that the decomposition products of levulose should alter the pH as slightly as possible. Borate buffers were found unsuitable because

[2] Ann., vol. 335, p. 191, 1904; vol. 357, p. 214, 1907; vol. 376, p. 1, 1910; vol. 403, p. 204, 1914.
[3] Rec. trav. Chim., vol. 14, p. 156 and 203, 1895; vol. 16, p. 256, 1897.
[4] Helv. Chim. Acta, vol. 9, p. 809, 1926.
[5] v. Lippmann, Die Chemie der Zuckerarten, vol. I, p. 837, 1904. Vieweg und Sohn, Braunschweig.
[6] J.Soc.Chem.Ind., vol. 42, p. 32, 1923.
[7] B. S. Jour. Research, vol. 8 (RP426), p. 422, 1932; J. Assoc. Off. Agri. Chemists, vol. 15, p. 198, 1932.
[8] The Determination of Hydrogen Ions. Williams and Wilkins, Baltimore, Md.

the reaction between the sugar and the borate ion caused a change in the pH of the buffer mixture. Phosphate, phthalate, and glycine buffers showed no change in pH upon addition of levulose.

The pH of the buffer-sugar mixture was determined at intervals during the course of the reaction either by the colorimetric method or with the quinhydrone electrode at the temperature of the room, and the pH found was corrected to the temperature of the reaction by temperature coefficients accompanying the buffer tables. In some experiments a slight but progressive change of pH occurred as a result of acid formation. In such cases a weighted average was accepted for tabulation.

Sodium hydroxide solutions were used to obtain reaction mixtures of hydroxyl ion concentration greater than that represented by pH 13.5, the upper limit of the glycine buffers. For such a reaction mixture the pH was not determined by direct measurement, but was calculated on the assumption that the activity of the hydroxyl ion in the levulose solution was the same as that in the pure aqueous sodium hydroxide solution. Such an assumption is not strictly correct, for levulose acts as a very weak acid [9] (dissociation constant is 9×10^{-13}) and unites with 1 molecule of the hydroxide. However, the change in the pH of the solution on the addition of sugar was assumed to be negligible, especially when the molar concentration of the hydroxide was greater than that of the sugar.

Hydrochloric and sulphuric acids of the proper normality were used to maintain hydrogen ion concentrations greater than that represented by pH 1.2. Here again the pH was calculated on the assumption that the sugar was without effect on the activity of the acid.

The method of calculating pH from the activities is as follows:

For acids

$$\mathrm{pH}=\log 1/\gamma N$$

where γ is the activity coefficient of the hydrogen ions in an N normal solution of the acid.

For alkalis

$$\mathrm{pH}=\log 1/K_w-\log 1/\gamma N$$

in which K_w is the dissociation constant of water, and γ the activity coefficient of hydroxyl ion in an N normal solution of the alkali.

The activity coefficients are given by Lewis and Randall.[10] It should be noted that pH as used in the present paper is a measure of activity and not of concentration.

The types of buffers and the ranges for which they were used were as follows:

Type of buffer	pH
Hydrochloric or sulphuric acids	−2.6 to 1.2
Glycine-hydrochloric acid	1.4 to 2.0
Phthalate-hydrochloric acid	3.0
Phthalate-sodium hydroxide	4.0 to 6.0
Phosphate-sodium hydroxide	6.0 to 8.0
Glycine-sodium hydroxide	8.0 to 13.4
Sodium hydroxide	13.7 to 14.4

[9] Michaelis and Rona, Biochem. Zeit., vol. 49, p. 232, 1913.

[10] Thermodynamics and the Free Energy of Chemical Substances. McGraw-Hill Book Co., Inc., New York, 1923.

The reaction mixtures were kept at constant temperature during the course of the reaction, samples being withdrawn for analysis at proper intervals of time. In a few instances the reaction was followed by direct observation in a water-jacketed polariscope tube. When the rate of reaction was high the reaction was stopped by adding to a measured sample a definite quantity of acid or alkali which would give a pH near neutrality. The whole was then made to a definite volume with water and analyzed. All the polarizations for any one run were made under identical conditions, where possible, to eliminate

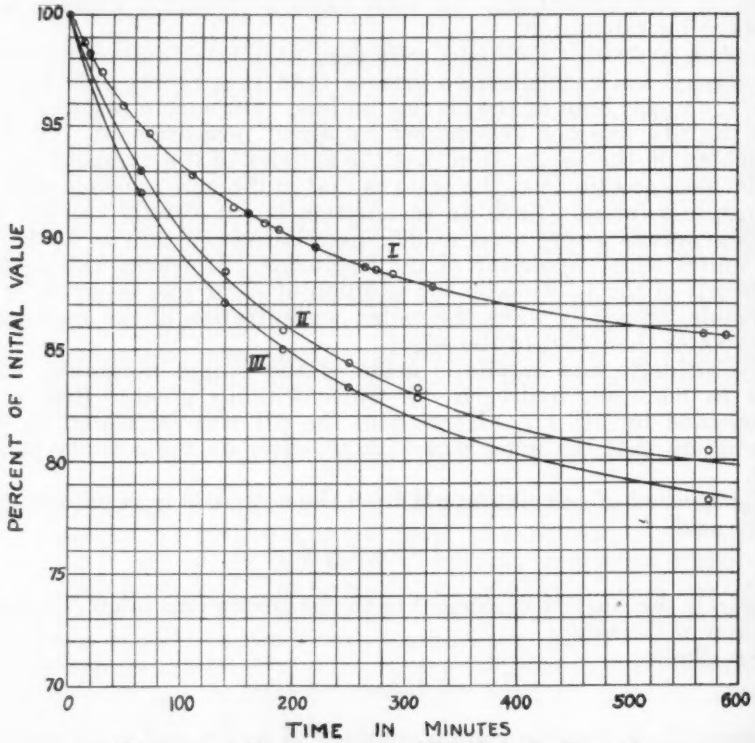

FIGURE 1.—*Reaction curves at 20° C. and pH −2.0.*

(5 g levulose per 100 ml; buffer, 8.31 *N* HCl. Curve I shows change in polarization; II, reducing sugar; III, levulose.)

errors that might have been introduced by correcting the readings for temperature and dilution. Rapid reactions were followed to the point where the development of color or turbidity made polarization difficult. This point was reached when the polarization had fallen from 10 to 30 percent, which change was sufficient for the calculation of the velocity constants. Slower reactions were followed until the polarization had changed enough to give velocity constants of sufficient accuracy.

III. TYPICAL REACTION CURVES AND THE DETERMINATION OF THE EQUILIBRIUM

By the methods described above, 50 experiments were made to determine the rates of decomposition of levulose under widely varying conditions of pH and temperature.

The courses of two typical reactions are given in figures 1 and 2, the former showing the decomposition in strongly acid solution, the latter in alkaline solution. The experimental observations are given in tables 1 and 2.

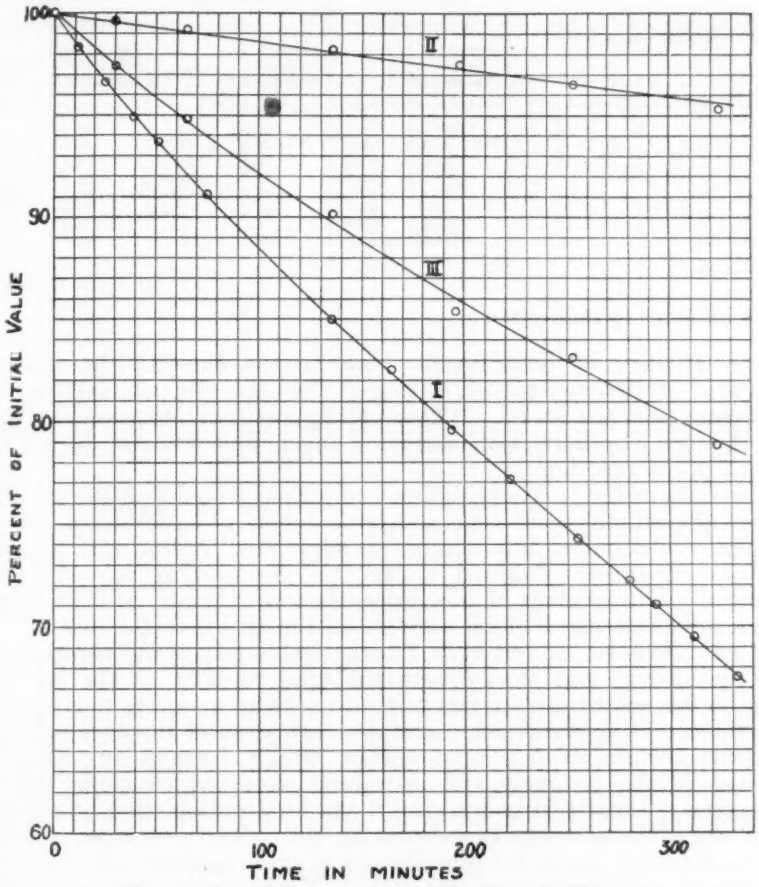

FIGURE 2.—*Reaction curves at 20° C. and pH 13.4.*
(5 g levulose per 100 ml; buffer, glycine-sodium hydroxide. Curve I shows change in polarization; II, reducing sugar; III, levulose.)

TABLE 1.—*Decomposition of levulose at 20° C. in 8.3 N HCl, pH—2.0*
(5 g levulose per 100 ml)

Time (in minutes)	Polarization		Reducing sugar		Levulose	
	Percent of initial reading	*K*	Percent of initial concentration	*K*	Percent of initial concentration	*K*
0	100.0		100.0		100.0	
64	94.9	0.0028	93.0	0.0022	92.0	0.0026
140	91.6	.0026	88.5	.0024	87.1	.0022
192	90.3	.0024	85.9	.0025	84.8	.0021
251	89.1	.0023	84.3	.0025	83.2	.0019
313	88.0	.0023	83.3	.0024	82.9	.0016
573	85.7	.0022	80.5	.0016	78.2	.0019
∞	[1] (85.1)		[1] (75.5)		[1] (74.8)	
Average		0.0024		0.0023		0.0021

[1] Values in parentheses are calculated.

TABLE 2.—*Decomposition of levulose at 20° C. in a glycine-sodium hydroxide buffer, pH 13.4*

(5 g levulose per 100 ml)

Time (in minutes)	Polarization		Reducing sugar		Levulose	
	Percent of initial reading	K	Percent of initial concentration	K	Percent of initial concentration	K
0	100.0		100.0		100.0	
30	95.8	0.00081	99.6	0.00074	97.4	0.00069
65	92.0	.00073	99.2	.00071	94.8	.00063
136	85.0	.00069	98.2	.00068	90.1	.00059
198	79.2	.00074	97.5	.00097	86.4	.00058
253	74.4	.00071	96.5	.00081	83.0	.00059
323	68.3	.00071			78.8	.00061
∞	[1] (23.0)		(91.9)		(41.6)	
Average		0.00073		0.00078		0.00062

[1] Values in parentheses are calculated.

The number of polarimetric observations exceeds the number indicated in these two tables, but all of the observed polarizations are plotted in figures 1 and 2. These two figures show diagrammatically the changes in polarization, reducing sugar, and levulose during the course of the reaction.

The form of the curves in figures 1 and 2 suggested that the reaction was of the unimolecular type and approached an equilibrium. That the reaction is indeed unimolecular is supported by that fact that the velocity constants obtained under this assumption proved to be essentially independent of the concentration of sugar, at least in the dilute solutions which alone were studied in this investigation.

It was, however, found to be impracticable to run the reactions to the equilibrium and thus obtain the final rotation of the solution because the coloring materials formed made an accurate polarization impossible. The clarification and decolorization of the dark solution by lead acetate or activated carbon would remove an unknown amount of the products and introduce errors which could not be evaluated. Indeed, it is doubtful if the final polarization at equilibrium would be of value in calculating the velocity constant for the initial reaction, since the equilibrium is undoubtedly influenced by secondary and consecutive reactions. Under such circumstances a calculated value for the equilibrium is more significant, inasmuch as it shows the equilibrium which the initial reaction would approach if it could be entirely separated from the secondary reactions. It is impossible to separate the various reactions in practice, but if only the initial reaction is considered, that is, only the disappearance of levulose during the initial period of reaction, the influence of the secondary reactions will be small, and the resulting velocity constant should approximate that which would be found if the initial reaction could be isolated.

Calculations of equilibrium values were made by application of the formula for unimolecular reactions. The method of calculation is illustrated by its application to polarization changes, but is equally applicable to the reducing sugar and levulose data.

Polarizations are observed or read from a curve at exactly equal intervals of time. If a, b, c, d, etc., are the polarizations at the times,

t_1, t_2, t_3, t_4, etc., the time intervals between observations being equal, we can set up a series of equations of the form,

$$K=\frac{1}{t_2-t_1}\log\frac{a-x}{b-x} \tag{1}$$

in which K is the unknown velocity constant and x the polarization at equilibrium.

Elimination of K between two of these equations gives

$$\frac{1}{t_2-t_1}\log\frac{a-x}{b-x}=\frac{1}{t_4-t_3}\log\frac{c-x}{d-x}$$

But as $t_2-t_1=t_4-t_3$,

$$\frac{a-x}{b-x}=\frac{c-x}{d-x}$$

Solving for x,

$$x=\frac{ad-bc}{a+d-b-c} \tag{2}$$

Equation (2) was used in the calculation of equilibrium polarizations. It was found that the polarizations from the initial portions of the velocity curves gave constant values for the equilibrium polarizations, but extension of the calculations to the polarizations made at later periods of the reaction, when much color had developed, gave values for the equilibrium polarization that were progressively smaller, indicating that secondary reactions had begun to interfere. The average value from the initial portion of the reaction curve was used in the calculation of the velocity constant.

IV. THE VARIATION OF EQUILIBRIUM VALUES WITH pH

Eight experiments in which the reaction products were determined by three methods of analysis were carried out at such a distribution of pH as permitted plotting continuous curves of the equilibrium values throughout the whole range. Since it proved true that the equilibria were dependent solely upon the pH and were independent of temperature, such curves enabled us to determine by interpolation the equilibrium values for the large number of experiments which were required to cover the whole range of pH and temperature.

The equilibrium values expressed in terms of percent of initial concentration or polarization, together with the velocity constants calculated from the three independent series of analyses, are shown in table 3. The three velocity constants are, with some exceptions, in satisfactory agreement, showing that the rates of change indicated by the three methods of analysis are essentially the same. The general agreement of the three sets of measurements is shown by the close agreement of the averaged values. These averages of course have no other significance.

Since the polariscopic method furnished a reliable measure of reaction rate, it alone was used for the remaining measurements.

TABLE 3.—*Decompositions for which the equilibrium values of polarization, reducing sugar, and levulose were determined*

(Equilibrium values expressed as percent of initial value, velocity constants in terms of minutes and common logs)

Run no.	Temperature	pH	Type of buffer	Polarization		Reducing sugar		Levulose	
				Equilibrium value	*K*	Equilibrium value	*K*	Equilibrium value	*K*
	°C.			*Percent*		*Percent*		*Percent*	
1	20	−2.0	8.3 *N* HCl	85.1	0.00254	75.5	0.00232	74.8	0.00213
2	45	−1.2	5.45 *N* HCl	80.5	.0084	75.5	.0120		
3	100	1.4	HCl-glycine	55.3	.00127	81.2	.00183	73.2	.00190
4	100	4.0	NaOH-phthalate	46.5	.000059	86.9	.000068	72.7	.000057
5	100	7.3	NaOH-KH_2PO_4	43.5	.00564	93.1	.00484	65.3	.00517
6	45	10.2	NaOH-glycine	36.7	.00110	93.4	.00109	55.3	.00108
7	45	10.4	do	37.1	.00148	94.4	.00120	55.0	.00145
8	20	13.4	do	23.0	.00078	91.9	.00076	41.6	.00062
Average (excluding run no. 2)					.00184		.00173		.00184

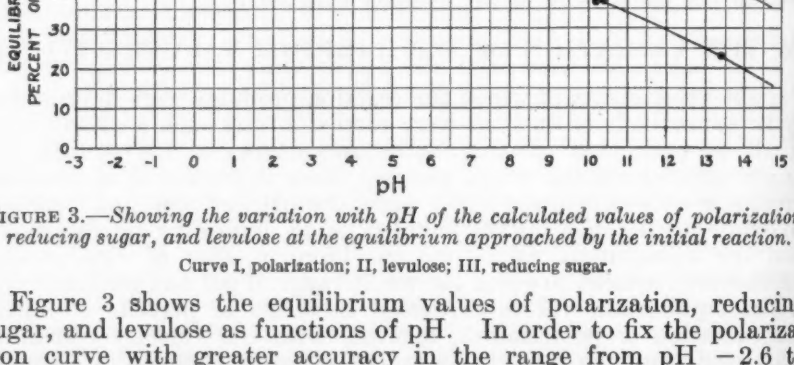

FIGURE 3.—*Showing the variation with pH of the calculated values of polarization, reducing sugar, and levulose at the equilibrium approached by the initial reaction.*

Curve I, polarization; II, levulose; III, reducing sugar.

Figure 3 shows the equilibrium values of polarization, reducing sugar, and levulose as functions of pH. In order to fix the polarization curve with greater accuracy in the range from pH −2.6 to pH 2.0, several additional points were calculated from the data of experiments in which the course of the reaction was followed by polarization only.

In general these curves indicate the type of the reaction which takes place at the various concentrations of hydrogen and hydroxyl ions. At high acidities the polarization falls by a comparatively small amount, while the loss in reducing sugar and levulose is greater. At the equilibrium the concentrations of levulose and of reducing sugar are the same, indicating that levulose is the sole reducing sugar occurring in the equilibrium mixture. The predominant reaction is, then, the formation of nonreducing substances, whose rotations are negative, but less negative than that of levulose. The average specific

rotation, $[\alpha]_D$, of the products in experiment 1 can be roughly estimated to be -42. Pictet and Chavan [11] found the rotation of heterolevulosan to be -45 and its dimer -65. Thus the predominant reaction is dehydration to heterolevulosan and its dimer both of which are nonreducing. Side reactions show their effects, for the rotation is slightly lower than would be expected if the two anhydro sugars were the sole products.

Thus it appears that these fructosans, which Pictet and Chavan designated heterolevulosan and diheterolevulosan, play an important role in the chemistry of levulose. Not only are they formed under the conditions of high acidity which Pictet and Chavan employed in their preparation, but they are formed in mild acidities whose pH is as high as 2. They are probably introduced in all operations in which levulose is subjected to treatment by strong or even mild acidities. Indeed it is even doubtful if cane sugar can be hydrolyzed by acid without introducing small quantities of these fructosans. Jackson and Gillis [12] determined by stop-watch experiments the minimum conditions of time and temperature for the inversion of sucrose at varying concentrations of hydrochloric acid and extrapolated their curve to zero concentration of acid. They found that twice the rotation of the half normal weight of sucrose after inversion was $-32.0°$ S. at 20° C., whereas Paine and Balch [13] found the value $-32.1°$ S. by use of invertase. The more drastic methods of acid inversion which are in common use yield still lower values. Zerban [14] found that commercial invert sugar which had been prepared by acid inversion contained reversion products which were hydrolyzable by acid and not by invertase. It is probable that these reversion products are these same fructosans.

We have repeated Pictet and Chavan's preparation, following their procedure in detail, and have isolated the crystalline fructosans having essentially the properties which they describe.

In highly alkaline solutions of levulose the predominant reaction is the Lobry de Bruyn and van Ekenstein transformation. A rough estimation of the products obtained in experiment 8 (pH 13.4) can be made. The equilibrium rotation is 23 percent of the initial rotation of levulose, hence $[\alpha]_D = -21$.

Assuming that glucose and mannose are in the ratio 5 to 1 [15] and combining the rotation of such a mixture with the rotation of the levulose remaining in the equilibrium, that is, $\frac{41.6}{91.9}$ or 45 percent of the reducing sugar, we should observe a specific rotation of -17 for the products of decomposition, in rough agreement with the -21 found. The results are sufficiently in agreement to indicate that we are dealing with the familiar Lobry de Bruyn-van Ekenstein transformation.

In the range between high hydrogen and high hydroxyl ion concentrations this transformation is favored above pH 3, while below this pH, dehydration is predominant. There is no clear-cut division point between the two types of reactions, since both can apparently take place together, the preference for the one or the other being dependent upon the pH of the solution.

[11] See footnote 4.
[12] B.S. Sci. Papers No. 375, vol. 16, p. 166, 1920.
[13] Ind. Eng. Chem., vol. 17, p. 240, 1925.
[14] J. Assoc. Off. Agri. Chemists, vol. 8, p. 396, 1925; vol. 9, p. 171, 1926; vol. 12, p. 162, 1929.
[15] Nef, Ann., vol. 357, p. 214, 1907.

In acid reactions an agreement among the three velocity constants determined by the three methods of analysis is to be expected since the changes in polarization, reducing sugar, and levulose are all

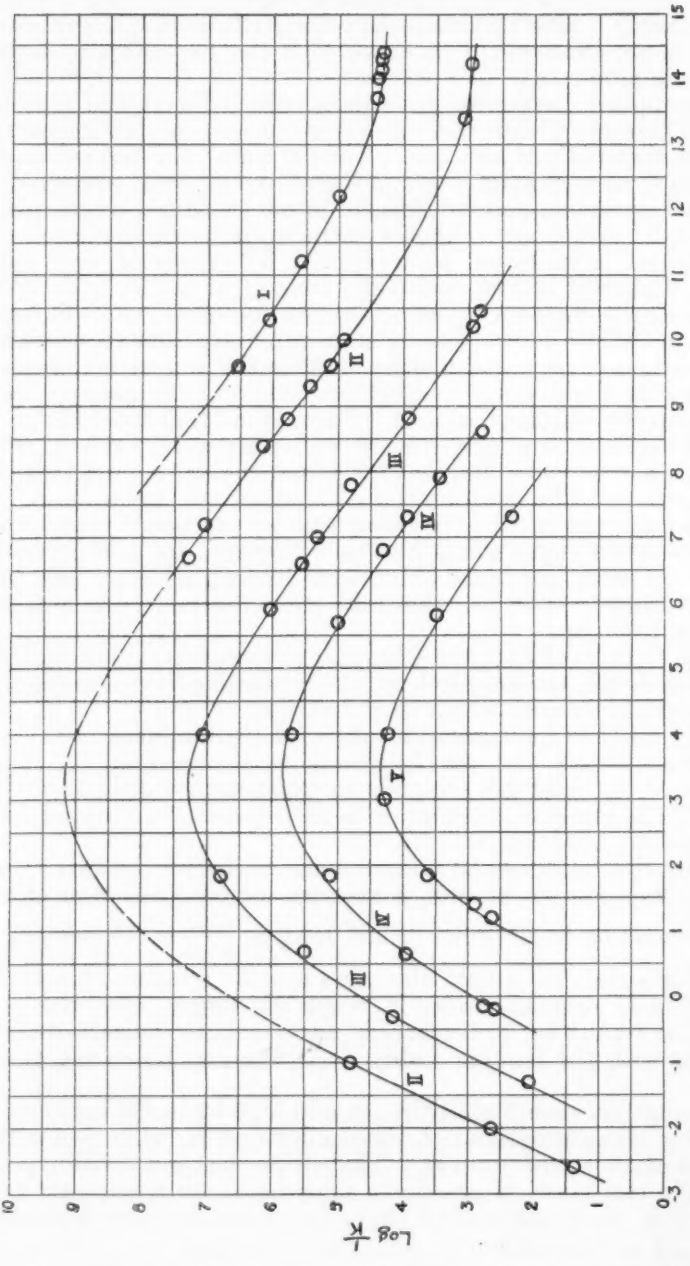

FIGURE 4.—*Variation of log 1/K with pH at I, 4° C.; II, 20° C.; III, 45° C.; IV, 70° C.; V, 100° C.*

(Levulose is most stable in solutions of pH 3.3; in more acid solutions it is transformed to levulosans; in alkaline solutions it undergoes the Lobry de Bruyn-van Ekenstein rearrangement to dextrose and mannose.)

largely measures of the same reaction, that is, the conversion of levulose into heterolevulosan. In alkaline reactions an agreement among the three constants cannot be predicted, for while the change in polar-

ization and the decrease in levulose are largely measures of the rate of conversion of levulose into glucose and mannose, the loss of reducing power is largely a measure of the rate of side reactions. The rates of change of polarization and levulose should then be approximately equal, but it does not follow a priori that loss in reducing power must proceed at the same rate. Actually, however, the rates of change of the three independent measurements are approximately equal.

V. THE STABILITY OF LEVULOSE

In table 4 are given the results obtained in 50 experimental determinations of the rates for the decomposition of levulose in the early stages. The fifth column gives the velocity constants calculated from the observed changes in polarization. In making the calculations of these constants, the equilibrium values of the polarization were read directly from the interpolation curve in figure 3 plotted from data obtained in this series of experiments.

TABLE 4.—*Velocity constants*

Temperature, °C.	pH	Type of buffer	Concentrations of levulose	K (minutes and common logs)	Time for loss of first 1 percent of total levulose
			g/100 ml		*Minutes*
4	9.6	NaOH-glycine	2	2.90×10^{-7}	37,000
4	10.3	do	2	8.6×10^{-7}	11,500
4	11.2	do	2	2.71×10^{-6}	3,310
4	12.2	do	2	1.01×10^{-5}	850
4	13.7	0.1 *N* NaOH	2	3.70×10^{-5}	190
4	14.0	0.2 *N* NaOH	2	3.93×10^{-5}	174
4	14.1	0.3 *N* NaOH	2	4.40×10^{-5}	158
4	14.3	0.4 *N* NaOH	2	4.43×10^{-5}	151
4	14.4	0.5 *N* NaOH	2	4.80×10^{-5}	138
20	−2.6	12 *N* HCl	10	4.15×10^{-2}	0.42
20 [1]	−2.0	8.3 *N* HCl	5	2.54×10^{-3}	6.9
20	−1.0	4.0 *N* HCl	10	1.55×10^{-4}	1,000
20	6.7	NaOH-KH_2PO_4	10	5.35×10^{-5}	248,000
20	7.2	do	10	9.0×10^{-5}	141,000
20	8.4	NaOH-glycine	10	7.3×10^{-7}	15,900
20	9.3	do	10	3.60×10^{-6}	3,050
20 [1]	13.4	do	5	7.37×10^{-4}	10.0
20	14.2	2 *N* NaOH	4	1.04×10^{-3}	6.6
25	8.8	NaOH-glycine	5	3.13×10^{-6}	3,600
25	9.6	do	5	1.24×10^{-5}	870
25	10.0	do	5	2.11×10^{-5}	468
45 [1]	−1.2	5.45 *N* HCl	2	8.4×10^{-3}	2.05
45	−0.3	2.0 *N* HCl	8	7.0×10^{-5}	245
45	0.7	0.3 *N* HCl	4	3.30×10^{-6}	5,200
45	1.85	HCl-glycine	10	1.64×10^{-7}	102,000
45	4.0	NaOH-phthalate	10	8.7×10^{-8}	186,000
45	5.9	do	10	9.3×10^{-7}	15,500
45	6.6	NaOH-KH_2PO_4	10	2.91×10^{-6}	4,780
45	7.0	do	10	4.81×10^{-6}	2,750
45	7.8	NaOH-glycine	10	1.55×10^{-5}	790
45	8.8	do	10	1.16×10^{-4}	100
45 [1]	10.2	do	7	1.10×10^{-3}	9.1
45 [1]	10.4	do	3.5	1.48×10^{-3}	6.6
70	−0.2	5.4 *N* H_2SO_4	2	2.57×10^{-3}	6.7
70	−0.15	1.5 *N* HCl	5	1.75×10^{-3}	10.0
70	0.65	0.4 *N* HCl	5	1.09×10^{-4}	158
70	1.85	HCl-glycine	10	8.0×10^{-6}	2,130
70	4.0	NaOH-phthalate	10	2.05×10^{-6}	7,900
70	5.7	NaOH-KH_2PO_4	10	1.01×10^{-5}	1,480
70	6.8	do	10	4.89×10^{-5}	275
70	7.3	do	10	1.16×10^{-4}	112
70	7.9	NaOH-glycine	10	3.60×10^{-3}	33
70	8.6	do	10	1.67×10^{-3}	6.9
100	1.2	0.2 *N* HCl	4.5	2.41×10^{-3}	7.2
100 [1]	1.4	HCl-glycine	5	1.27×10^{-3}	13.5
100	1.85	do	5	2.40×10^{-4}	71
100	3.0	HCl-phthalate	5	5.37×10^{-5}	309
100 [1]	4.0	NaOH-phthalate	5	5.90×10^{-5}	275
100	5.8	do	5	3.20×10^{-4}	45.5
100 [1]	7.3	NaOH-KH_2PO_4	10	4.67×10^{-3}	2.75

[1] These reactions were followed by determinations of reducing sugar and levulose as well as by polarizations.

Figure 4 shows diagrammatically the variation of log $1/K$ with the pH at five temperatures. The 4° isotherm was determined only in the range of high alkalinities, and the 20° curve was not determined in the middle range, because the time required at these temperatures for a measurable decomposition is extremely long. Some of the slower reactions at both 4° and 20° gave such small decompositions, even after 10 weeks, that the calculated velocity constants may be in error by large percentages.

All the isotherms pass through a maximum at approximately pH 3.3 at which point the stability of levulose is at its maximum. It follows that pH 7 is highly alkaline with respect to the maximum stability point of levulose and considerable decomposition of the sugar may be expected in neutral solutions at the higher temperatures or over extended periods of time. In harmony with the results of the present investigation, Lobry de Bruyn found that levulose in pure aqueous solution suffered decomposition at elevated temperatures. It is of interest to note that the pH of honeys and fruits which contain large percentages of levulose lies between 3 and 4.

In the cane sugar refining industry the juices which always contain invert sugar are kept approximately neutral during the refining process. Blake [16] has shown that in these products there is a progressive destruction of levulose.

On the acid side of the maximum point the slope of the curve changes rapidly until in strong acids it becomes 2, indicating that the rate of the purely acid decomposition of the sugar is proportional to the square of the hydrogen ion activity. In the range between the neutral point and mild alkalinities the rate of decomposition is a little less than proportional to the concentration of the hydroxyl ions. The slope of the curve is here about 0.75, an indication that the rate is proportional to the 0.75 power of the hydroxyl ion activity. In the high alkalinities, the rate tends to become constant as is shown by the flattening of the curve. This is in agreement with the observations of Powell [17] who found that the rate of volume change accompanying decomposition of levulose in normal sodium hydroxide was only four times the rate in tenth normal.

In the last column of table 4 is given the time in minutes required for the loss of the first 1 percent of the total levulose in the solution at the given temperature and pH. The time required for the loss of the first 1 percent of total levulose is different from that required for the reaction to proceed 1 percent of the way toward equilibrium, since at equilibrium a large fraction of the levulose remains unchanged. The latter time is given by the equation

$$t = \frac{1}{K} \log \frac{100}{100-1} \tag{3}$$

while the time required for loss of 1 percent of the total levulose is

$$t = \frac{1}{K} \log \frac{100-L}{99-L} \tag{4}$$

in which L is the percent of the initial amount of levulose remaining in the reaction mixture at equilibrium. L can be read directly from

[16] Ind. Eng. Chem., vol. 12, p. 1104, 1920.
[17] Powell, J.Chem.Soc., vol. 107, p. 1335, 1915.

the interpolation curve of figure 3. The distinction between the equations is important since the two times may differ by several hundred percent. For practical purposes the time given by equation (4) is the more significant and is given in the sixth column of table 4.

VI. THE TEMPERATURE COEFFICIENTS

Temperature coefficients of the decomposition reactions were determined directly from the curves in figure 4 at either the experimentally determined points or points near them. By substituting in the Arrhenius equation

$$A=\frac{2.303T_1T_2}{T_2-T_1}\left(\log\frac{1}{K_{T_1}}-\log\frac{1}{K_{T_2}}\right)$$

in which K_{T_1} and K_{T_2} are the velocity constants at a fixed pH and at the absolute temperatures, T_1 and T_2, a series of nineteen values of A was obtained between the various experimental temperatures and at different pH's. A was found essentially independent of the temperature and varied only with the pH. The experimentally calculated values of A were plotted against the pH and a curve constructed from which adjusted values of A were read. The numerical values of this constant are given in table 5.

TABLE 5.—*The variation with pH of the values of A in the Arrhenius equation*

pH	A	pH	A	pH	A
−2	19, 200	4	14, 400	10	15, 400
−1	18, 200	5	14, 300	11	15, 600
0	17, 200	6	14, 500	12	15, 800
1	16, 200	7	14, 700	13	16, 000
2	15, 300	8	14, 900	14	16, 200
3	14, 700	9	15, 100	15	16, 400

By means of the adjusted values of A, all experimental values of $\log 1/K$ at other than 20° were corrected to 20° C. These corrected values, together with those actually determined at 20°, were plotted against the pH. All points were in satisfactory agreement with a smooth curve, the 20° C isotherm of figure 4.

From this composite curve were read the values of $\log 1/K_{20}$ from which the corresponding values of $\log t_{20}$ were calculated (t being the time for decomposition of the first 1 percent of the total levulose). Values of $\log t$ at other temperatures were then calculated from the Arrhenius equation in the form,

$$\log t_T=\log t_{20}-\frac{A(T-293)}{2.303\times 293T}$$

in which A must correspond to the pH for which the calculation is made.

The temperature coefficients of both the alkaline and acid decompositions are greater than those ordinarily encountered. In general, rates are doubled or trebled for a 10° increase in temperature, and A has a value of 10,000 to 12,000. For decomposition of levulose, rates are increased from 5 to 10 times for a 10° rise in temperature, and the value of A varies from 14,000 to 19,000.

The great variations in the stability of levulose under the different conditions which may be encountered are emphasized in table 6.

TABLE 6.—*Time required for the decomposition of the first 1 percent of the total levulose in aqueous solutions at integral units of pH and 10° intervals of temperature*

pH	Temperature °C.										
	0°	10°	20°	30°	40°	50°	60°	70°	80°	90°	100°
−2	17 h	87 m	8.7 m	1 m							
−1	75 d	165 h	19 h	145 m	21 m	3.5 m	0.6 m				
0	8 y	310 d	40 d	135 h	22 h	240 m	49 m	11 m	2.6 m		
1		13 y	2 y	110 d	20 d	98 h	21 h	310 m	80 m	22 m	6.8 m
2			11 y	2.5 y	140 d	32 d	127 h	47 h	13 h	240 m	78 m
3			24 y	4.7 y	365 d	85 d	520 h	141 h	43 h	810 m	275 m
4			20 y	4.0 y	320 d	76 d	480 h	138 h	42 h	810 m	280 m
5			8 y	1.6 y	130 d	31 d	200 h	56 h	17 h	245 m	108 m
6		11 y	1.9 y	135 d	30 d	165 h	44 h	12 h	225 m	71 m	25 m
7	14 y	2.1 y	132 d	25 d	130 h	30 h	7.6 h	126 m	38 m	12 m	4.1 m
8	2.5 y	129 d	21 d	95 h	20 h	4.6 h	69 m	18.5 m	5.5 m	1.7 m	.6 m
9	190 d	21 d	83 h	15 h	3.1 h	42 m	10 m	2.7 m	.8 m	.2 m	
10	29 d	95 h	15 h	2.6 h	30 m	6.9 m	1.7 m	.4 m			
11	185 h	20 h	3.0 h	32 m	6.0 m	1.3 m	.3m				
12	40 h	5.2 h	47 m	8 m	1.5 m	.4m					
13	13 h	102 m	15 m	2.5 m	.5 m						
14	6 h	45 m	6.3 m	1.0 m							
15	4 h	29 m	4.0 m								

m=minutes; h=hours; d=days; y=years.

The time required for the loss of the first 1 percent of the total levulose is given at unit intervals of pH and 10° intervals of temperature. This table is serviceable for the estimation of small losses of levulose under specified conditions. The result will be accurate when the decomposition is small, that is, not more than 1 or 2 percent of the total sugar, and although accuracy decreases when larger decompositions are involved, the results will be significant for decompositions as great as 5 percent. If very large decompositions are to be estimated, a special calculation must be made using the velocity constant and the equilibrium value of levulose at the pH of the reaction.

VII. SUMMARY

1. The rates of the decomposition of levulose in the early stages of the reaction have been determined over a range of temperature from 4° to 100° C., and of pH from −2.6 to 14.2, that is, from 12 *N* hydrochloric acid to 2 *N* sodium hydroxide.

2. The decomposition rate is independent of the concentration of levulose within the limits used in the experiments, and in the early stages of the reaction the decomposition curves follow closely those for unimolecular reactions.

3. A method for calculating the equilibrium of a reaction, when the equilibrium cannot be reached in practice because of interfering secondary reactions, is described.

4. The calculated equilibrium values indicate that in acid solution the primary decomposition of levulose results in the formation of heterolevulosan and its dimer, and that in alkaline solution the Lobry de Bruyn and van Ekenstein transformation to glucose and mannose is the predominant reaction.

5. The stability of levulose is maximum in solutions of pH 3.3. The point of maximum stability is independent of the temperature.

6. The temperature coefficients of decomposition are higher than those ordinarily encountered and depend upon the pH, being greatest in strong acid solutions.

7. In order to facilitate practical application of the results, the times required for 1 percent decomposition are tabulated for integral pH's at 10-degree intervals of temperature.

WASHINGTON, August 5, 1933.

U.S. Department of Commerce, Bureau of Standards

RESEARCH PAPER RP612

Part of Bureau of Standards Journal of Research, Vol. 11, November 1933

WEAR RESISTANCE OF NATURAL STONE FLOORING

By D. W. Kessler

ABSTRACT

Since the hardness testing devices in general use are not well adapted to floor surfacing materials, an apparatus for this purpose was designed. In order to determine if the results of tests with this device bear a definite ratio to wear in service, a comparison was made with 22 materials which had been on stair treads under service conditions and which represented about 10 percent of the total number received for tests. The degree of correlation between the tests and actual wear was found to be high and, hence, the test values should enable one to predict service wear with a fair degree of accuracy. Subsequently samples representing the marbles, limestones, slates, etc., commonly used in floor surfaces were tested, and the approximate values for the different types range as follows: Marbles, from 7 to 42; limestones, 2 to 24; sandstones, 2 to 26; slates, 6 to 12; granites, 44 to 66; serpentines, 15 to 111; travertines, 5 to 17. On this scale the most resistant material (quartz) showed a value of 180. Materials used for general flooring purposes in this country show values between 15 and 20.

CONTENTS

	Page
I. Introduction	635
II. Development of Apparatus and Test Methods	637
1. Laboratory test	637
(a) Design of apparatus	637
(b) Test procedure	637
2. Service tests	638
3. Correlation of preliminary laboratory values with service values	639
III. Results of Laboratory Tests	640
1. Marble	640
2. Limestone	642
3. Sandstone	643
4. Slate	643
5. Granite	644
6. Serpentine	645
7. Travertine	645
8. Miscellaneous materials	646
IV. Discussion of Results	646
V. Conclusions	648

I. INTRODUCTION

The purpose of this investigation was to determine the comparative resistance to wear of the natural stones commonly used in floor surfaces and other parts of buildings exposed to the abrasive action of traffic. For several years there has been a growing demand for information on this subject which could not be adequately supplied from published data on hardness tests. The United States Bureau of Public Roads [1] has published a large amount of valuable data on

[1] Bureau of Public Roads, Bulletins Nos. 44, 370, 1132; Dept. of Agriculture, Washington, D.C., Goldbeck, Jackson, Hubbard.

tests with the Dorry and Deval machines, but the materials referred to usually do not correspond with those used in floors. The rate of wear on heavy duty floors is of considerable importance and due consideration to wearing qualities in the selection of materials may often prevent annoyance or replacement. When floors are made a decorative feature of the building the design often requires the selection of materials for color effect. In the absence of comparative data on the wearing qualities of the different materials one may select an unfortunate combination that will soon result in an uneven surface.

The subject of accidents in public buildings has been a matter of some concern. While the question of slipperiness is not within the scope of this study, it seems probable that irregular surfaces, especially on stair treads, are a contributing factor to accidents. Some varieties of stone which have high decorative values due to their veined or mottled appearance may wear unevenly. Where a considerable range in wear resistance is shown for different specimens of a sample the material may be expected to wear unevenly in service.

An examination of the methods and apparatus employed for hardness determinations shows various conceptions of this property. These methods may be roughly classified as follows: the determination of the resistance of the material to (1) penetration of a spherical surface or conical point (Brinell [2] and Rockwell [2] tests); (2) scratching with materials of standard hardness (Moh's hardness scale [3]); (3) abrasion with loose, granular materials of standard hardness (Dorry [4] and Amsler [5] tests); (4) the cutting action of a hard granular substance of standard hardness under impact (sandblast); (5) a combination of impact and abrasion between broken fragments of the sample (Deval test [6]); (6) cutting with a tool of standard hardness (Bauer drill test [7] for metals and Jagger's boring test [8] for minerals).

The test for flooring materials should simulate closely the conditions to which a floor is exposed. Although the surface of a floor is evidently subjected to a mild form of impact, the greatest amount of wear is probably due to cutting or scratching of hard particles forced into or rolled over the surface under pressure. While the Deval test combines the two factors assumed to be largely concerned in the wear on floors, the impact action is much greater than the abrasive action. Besides, the type of floor samples usually received for test purposes are not well adapted to this apparatus. The Dorry and Amsler machines produce an abrasive action similar to that occurring on floors, but some modifications would be necessary to adapt them to the test samples. It was considered more feasible to design an apparatus of compact form and determine experimentally whether it produced results comparable to the wear on floors.

The results given in tables 1 to 8 inclusive were determined at low humidity (below 35) to afford a more definite comparison. Since the abrasive resistance of some materials decreases appreciably as the humidity increases, the test values may not properly rate all materials as to service wear when used under various conditions of humidity.

[2] B. S. Jour. Research (RP185), vol. 5, p. 19, 1930, S. N. Petrenko.
[3] Textbooks on mineralogy such as Dana's and Idding's, Moses and Parsons, etc.
[4] U.S.Dept.Agri., Bu. of Public Roads Bull. No. 44, Albert T. Goldbeck & Frank H. Jackson.
[5] Herschwald's Handbuch der bautechnischen Gesteinprüfung Gebrüder Borntraeger, Berlin.
[6] See footnote 4.
[7] B. S. Tech. Paper No. 11, Ralph P. Devries.
[8] Am. Jour. Sci., vol. 4, p. 399, 1897, T. A. Jagger, Jr.

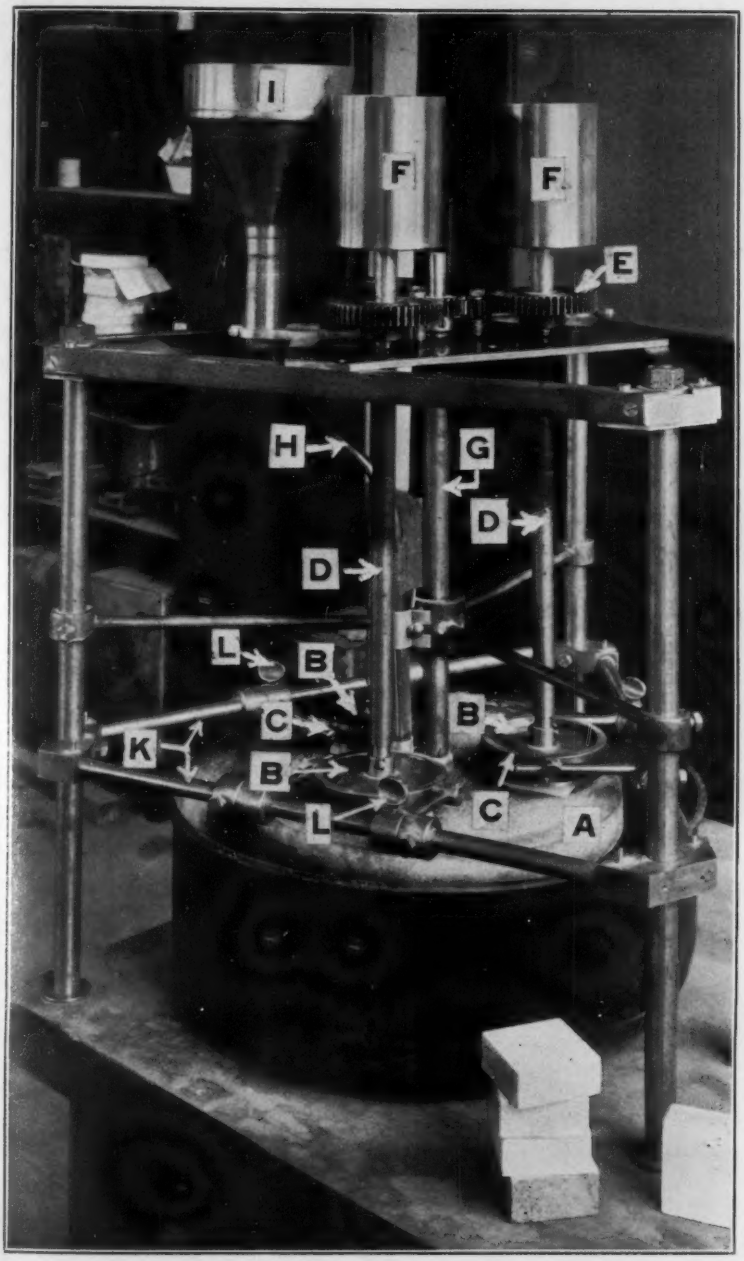

FIGURE 1.—*Photograph of apparatus with specimens in position for testing.*

A, Grinding lap; B, specimen holder; C, specimen holder guide rings; D, spinning rods; E, spinning gear; F, weight hoppers; G, spinning drive; H, abrasive conduit; I, abrasive hopper; K, guide ring support; L, guide ring clamp.

The samples tested were supplied by the producers as being representative of the various quarries or grades. Variations occur in all quarries and hence the test results can be only as representative as the samples were.

II. DEVELOPMENT OF APPARATUS AND TEST METHODS

1. LABORATORY TEST

(a) DESIGN OF APPARATUS

The original design of the testing apparatus was modified in some respects after the service tests (part II, 2) were made in order to secure a satisfactory agreement between the test values and service values. The final form is shown in figure 1.[9] It consists essentially of (1) a grinding disk 10 inches in diameter which is revolved in a horizontal plane at 45 r.p.m.; (2) a hopper for the abrasive and a conduit for feeding the abrasive to the disk; (3) a means of holding the specimens on the disk at a constant pressure; (4) a means of distributing fresh abrasive over the disk as the grinding proceeds. Three disk-shaped specimen holders having recesses 2 by 2 by ⅜ inch for the specimens are spaced at 120° angles around the disk. Guide rings hinged to the frame support the specimen holders near the grinding disk. The holders are weighted and revolved by means of vertical rods. The lower ends of the rods fit loosely in sockets in the tops of the specimen holders, the upper ends pass through bearings and are geared to the main drive shaft which extends upward through the grinding disk. On the upper end of each rod is a receptable for weights. The weight on each specimen includes the weight of the holder, the rod, one spur gear, the receptacle, and enough added weight to make 2,000 grams.[10] The usual size of specimens is 2 by 2 by 1 inch, but any thickness from ½ to 2 inches can be used. The abrasive (no. 60 artificial corundum) flows in the dry condition from an orifice 0.1 inch in diameter, which is ⅜ inch above the grinding disk and 1¼ inches from the center. A device is attached to each specimen holder for distributing fresh abrasive over the disk and moving the worn material outward over the edge as the test proceeds.

(b) TEST PROCEDURE

The specimens are weighed in the dry condition, placed in the apparatus, and subjected to abrasion for 5 minutes (225 revolutions of the grinding disk), after which they are weighed again. Before each succeeding test the disk is brushed free of the used grit and stone dust, after which a fresh layer of grit is distributed over the surface.

The difference between the original and final weights of the specimens is inversely proportional to their wear resistances. However, the most satisfactory means of comparing the resistance of materials of variable density is to use the volume losses rather than the weights.

[9] A detail drawing of this apparatus may be found in vol. 28, 1928, part II, p. 855, Proc.A.S.T.M., D. W. Kessler.

[10] It was found to be more convenient to keep the superimposed weight constant and apply a correction for the specimen weight. The rate of abrasion was found to be proportional to the pressure; for example, with 4,000 grams load the abrasion was twice that for 2,000 grams load. The correction factor is

$$\frac{2{,}000}{W_s+2{,}000}$$

where W_s is the average weight of the specimen.

The volume is obtained by dividing the weight-loss [11] by the bulk density of the material. The bulk density, G is easily obtained by dividing the weight of the dry specimen, W_1, by $W_2 - W_3$ where W_2 equals the weight of the specimen after soaking in water for an hour or more and surface dried with a towel, and W_3 equals the weight of the saturated specimen suspended in water.

The abrasive resistance is expressed as $H_a = 10/V$ where V is the volume of abraded material and equals weight-loss/G. Incorporating the correction factor $\frac{W_s + 2{,}000}{2{,}000}$ for the weight of specimen, the formula becomes:

$$H_a = \frac{10(W_s + 2{,}000)G}{2{,}000 W_a} \tag{1}$$

where W_a is the weight in grams of material abraded in the test, and W_s is the mean of the original and final weights of the specimen. This form of equation has an advantage over the linear equation used for computing the results in the Dorry test because the hyperbolic form above gives positive values in all cases while the Dorry formula may give negative values for very soft materials. The H_a values stand in direct relation to the abrasive resistance and hence afford a simple means of comparison.

It was found by preliminary tests that variations in humidity affected the results quite appreciably for some materials. Tests on such materials at high humidities generally gave lower H_a values than when tested at low humidity. For this reason all of the tests were made when the relative humidity was 35 or lower.

2. SERVICE TESTS

Service values were obtained by subjecting a number of tiles to the action of foot traffic on a staircase. The tiles used in these experiments were 4 by 4 by ⅞ inches and 12 tiles were used on each step. A form was made for each tread, the form having wood sides, a composition-board bottom and a metal strip for the lip. These forms were held rigidly in place on the treads by means of bolts and the tiles were laid into the recess. In order to prevent abrasion of the tiles against each other or against the metal lip the recess was made about ⅛ inch oversize and thin strips of cardboard inserted between the tiles and also around the sides.

The 22 materials used in this experiment are listed in figure 2. Preliminary experiments showed that the wear was not uniform over the surface of one tread, the greatest amount being at the middle portion and near the front. There were 2 rows of tiles on each tread, 1 row of 6 occupying the portion next to the riser and the other row the portion to the front. In order to compare the amounts of wear on different materials it was necessary to have a standard of reference in all of the 12 positions, hence the middle step in the flight was covered entirely with marble no. 7. In order to check the assumption that the wear at any given position on different steps was uniform, two tiles of marble no. 7 were placed on each of the other treads.

[11] All weighings to the nearest 0.01 g.

After 6 weeks of exposure to service conditions the tiles were removed, cleaned, dried, and weighed for comparison with the original weights. The weight losses were reduced to volume losses as in the laboratory tests. The results indicated that the wear was fairly uniform for the same positions on different steps.

The wear ratios were computed between the standard marble and the other materials, only identical positions on each tread being compared. For instance, if the wear of the standard marble for one position was 0.25 cc, this figure and those obtained for all other materials in the same relative position on other steps were divided by 0.25. Thus the wear of the reference material was expressed as unity and the others in their appropriate ratios. Since the H_a values are reciprocals of wear, the service wear ratios also are expressed as reciprocals to afford a direct comparison.

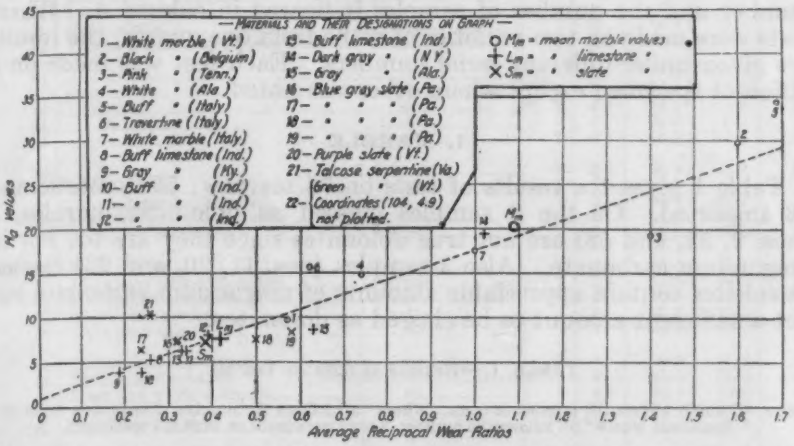

FIGURE 2.—*Relation between H_a values and average reciprocal wear ratios for 21 materials.*

3. CORRELATION OF PRELIMINARY LABORATORY VALUES WITH SERVICE WEAR

In figure 2 the H_a values are plotted against the wear ratio reciprocals for all materials subjected to the service test except the serpentine. The deviations from a linear relation are probably within the precision of the tests.

The correlation coefficient (r) was computed for the values of the two variables given in figure 2 by the formula

$$r=\frac{\Sigma(xy)-\dfrac{\Sigma(x)\Sigma(y)}{N}}{\sqrt{\left(\Sigma x^2-\dfrac{(\Sigma x)^2}{N}\right)\left(\Sigma(y)^2-\dfrac{(\Sigma y)^2}{N}\right)}} \tag{2}$$

where x and y are the variables and N is the number of determinations. This gave the value $r=0.990$ indicating a high degree of correlation. The coefficient of alienation, $K=\sqrt{1-r^2}$, gives a value of $K=0.14$ which indicates that the error in estimating service values from H_a values will ordinarily be about one seventh of the error made by a

random selection. Expressing the individual deviations from the linear relation as percentages of the measured service values it appears that the probable error of rating materials from their H_s values is 16.6 percent. These computations are based on the 22 samples used in the service tests and, since the samples cover practically the entire range in abrasive hardness of stone flooring, the correlation is assumed to apply to all the 215 materials tested.

III. RESULTS OF LABORATORY TESTS

The data obtained are given in tables nos. 1 to 8, inclusive. The samples are designated by serial numbers, grouped according to producing districts and briefly described as to class and color. Where more than one sample was tested from a given quarry in which the product was fairly uniform, the results are included under one serial number and the number of samples indicated in column 4. Where tests were made on two varieties of stone from one quarry, the results are given under different serial numbers. Each test was made on a different specimen except where otherwise noted.

1. MARBLE

Table 1 gives the results of tests on 78 marbles; 50 domestic and 28 imported. Of the 8 samples classed as dolomitic marbles, 3 (nos. 9, 52, and 58) are not true dolomites since they are too low in magnesium carbonate. Also 3 samples (nos. 11, 20, and 23) classed as calcites contain appreciable amounts of magnesium carbonate but not a sufficient amount to be classed as dolomites.

TABLE 1.—*Results of tests on marble*

[NOTE.—Column 5 gives the number of tests. Where "a" follows the number, 2 tests were made on 1 specimen; where "b" follows the number, 2 tests were made on each of 2 specimens]

Serial numbers of samples	Variety	Source	Number of samples	Number of tests	Abrasive hardness H_s		
					Maximum	Minimum	Average
1	Light bluish gray calcite	Vermont	1	4 b	14.6	13.3	13.8
2	Dark bluish gray calcite	do	1	4 b	12.8	11.7	12.3
3	Dark veined white calcite	do	2	7	14.3	9.5	10.8
4	Light-gray calcite	do	1	4 b	10.8	10.4	10.5
5	Dark bluish gray calcite	do	1	4 b	15.4	15.3	15.4
6	Bluish gray calcite	do	1	4 b	13.0	12.0	12.4
7	Light-gray calcite	do	1	4 b	14.2	13.6	13.9
8	White and green calcite	do	1	2	6.7	6.7	6.7
9	Red and white (dolomitic)	do	1	4 b	33.9	24.6	30.9
10	White calcite	do	2	9	9.1	7.6	8.4
11	Black calcite (fossiliferous)	do	1	4 b	26.0	22.9	24.8
12	Dark veined white calcite	do	1	1			12.0
13	do	do	1	5	12.1	10.5	11.2
14	do	do	1	3	14.8	9.0	13.5
15	Light bluish gray calcite	do	1	3	15.6	14.0	14.9
16	Green veined white calcite	do	1	3	10.8	10.0	10.3
17	White dolomite	New York	1	4 b	13.6	11.6	12.5
18	Pink fossiliferous calcite	do	1	4 b	17.1	15.3	16.6
19	Gray fossiliferous calcite	do	1	3	18.6	18.2	18.3
20	Gray calcite	do	1	4 b	15.4	13.5	14.6
21	White dolomite	Massachusetts	1	4 b	13.2	12.8	13.0
22	Buff dolomite	Maryland	1	3	13.4	12.1	12.9
23	Black calcite	Virginia	1	7	43.5	38.9	41.7
24	Pink calcite	Tennessee	1	4 b	21.9	18.9	20.2
25	Chocolate colored calcite	do	1	4 b	18.8	17.8	18.4

TABLE 1.—*Results of tests on marble*—Continued

Serial numbers of samples	Variety	Source	Number of samples	Number of tests	Abrasive hardness H_a		
					Maximum	Minimum	Average
26	Gray calcite	Tennessee	1	4 b	19.0	17.8	18.4
27	Pink calcite	do	1	4 b	19.5	18.7	19.2
28	Gray calcite	do	1	3	21.3	21.0	21.2
29	Pink calcite	do	1	2 a	20.3	19.2	19.8
30	Blue calcite	North Carolina	1	3	17.4	16.8	17.0
31	Blue and gray calcite	do	1	4 b	25.7	24.0	24.7
32	White dolomite	do	1	3	18.5	17.5	18.0
33	White and black calcite	Georgia	1	5	15.4	12.3	13.7
34	Light-gray calcite	do	1	3	12.6	11.5	12.2
35	Dark veined white calcite	do	1	3	11.7	10.9	11.3
36	Pink calcite	do	1	4 b	17.5	15.6	16.4
37	Dark veined white calcite	Alabama	1	4 b	17.3	12.5	15.0
38	Light-buff calcite	do	1	3	8.9	8.3	8.7
39	Gray calcite	do	1	3	16.2	14.4	15.4
40	Yellow veined gray calcite	Missouri	1	4 b	18.8	17.2	18.0
41	Pink calcite	do	1	4	19.3	16.9	18.0
42	Gray calcite	do	1	3	14.3	13.5	13.8
43	do	do	2	6	14.3	13.8	14.0
44	do	do	1	3	20.2	19.1	19.7
45	do	do	2	6	14.9	12.1	13.8
46	do	Arkansas	3	10	21.0	12.1	16.0
47	White calcite	Colorado	1	4 b	7.8	7.5	7.6
48	Gray calcite (fossiliferous)	Utah	1	6	33.4	28.7	31.1
49	Dark-veined white dolomite	California	1	3	15.5	14.0	14.9
50	Black and white calcite	Alaska	1	3	14.9	13.3	14.1
51	Black calcite	Belgium	1	4 b	33.5	27.7	30.9
52	White and pink (dolomitic)	Norway	1	3	15.3	10.2	13.3
53	Buff fossiliferous calcite	France	1	4	16.2	13.5	14.6
54	Violet pink calcite	do	1	4	28.2	20.7	24.2
55	Light pink calcite	do	1	4	35.2	29.0	32.6
56	Dark-veined red calcite	do	1	4	25.9	25.4	25.6
57	Pinkish buff calcite	do	1	4	35.6	33.8	35.0
58	Black and white dolomite	do	1	4 b	33.1	29.0	30.6
59	Buff calcite	do	1	3	31.2	30.8	31.0
60	Light buff calcite	do	1	3	15.2	14.9	15.0
61	do	do	1	4	30.9	29.6	30.3
62	Dark-veined white calcite	Italy	2	6	14.1	11.0	12.6
63	Buff calcite (fossiliferous)	do	1	3	34.4	32.9	33.7
64	Pink calcite (fossiliferous)	do	1	3	33.4	27.1	31.2
65	Gray calcite (fossiliferous)	do	1	3	34.0	33.7	33.8
66	White calcite	do	1	2	12.7	12.2	12.4
67	Dark-veined white calcite	do	2	6	16.5	13.4	14.8
68	do	do	1	4 b	14.5	13.8	14.2
69	Yellow-veined black calcite	do	1	4 b	25.7	23.5	24.5
70	Brown calcite	do	1	4	11.4	9.4	10.6
71	Light buff calcite	do	1	4	28.8	25.0	26.7
72	Black and yellow breccia (calcite)	do	1	4	27.0	23.8	25.8
73	Dark gray calcite (fossiliferous)	do	1	3	27.0	24.3	25.5
74	Light buff calcite	do	1	4 b	31.5	29.5	30.1
75	Violet gray calcite (fossiliferous)	Germany	1	4	26.4	25.0	25.6
76	Red calcite (fossiliferous)	do	1	3	22.5	20.4	21.4
77	Red and pink calcite	do	1	3	26.7	24.2	25.7
78	Yellow calcite	Algeria	1	6	25.6	17.3	21.2

The results do not indicate that the dolomites are more resistant to abrasion than the calcites, although mineralogists assign a higher hardness value to dolomite than calcite. It appears from the tests that the abrasive resistance is influenced more by the compactness of the material than by differences in hardness of constituent minerals. The highest H_a value obtained on dolomitic marble was 30.9 (no. 9) and the lowest 12.5 (no. 17). The highest value for any calcitic marble was 41.7 (no. 23) and the lowest 6.7 (no. 8).

2. LIMESTONE

Table 2 gives the results for 39 limestones, 34 domestic and 5 imported. The range in H_a values for the samples was from 24.1 to 1.3, with a weighted average of 8.4. This group consists of limestones used mainly for ashlar purposes although many of them are used in floors and steps.

TABLE 2.—*Results of tests on limestone*

Serial numbers of samples	Variety	Source	Number of samples	Number of tests	Abrasive hardness H_a		
					Maximum	Minimum	Average
1	Dark gray (crystalline)	New York	1	3	19.6	18.5	19.2
2	Statuary buff (oolitic)	Indiana	1	3	6.8	6.4	6.6
3	Select buff (oolitic)	do	1	5	6.7	5.0	6.1
4	do	do	1	3	7.1	6.6	6.9
5	Select gray (oolitic)	do	1	6	11.6	7.3	9.6
6	Hard buff (oolitic)	do	1	3	6.3	6.1	6.2
7	Rustic buff (oolitic)	do	1	3	5.7	5.0	5.4
8	Standard buff (oolitic)	do	1	3	6.6	6.4	6.5
9	do	do	1	2	5.1	5.1	5.1
10	Rustic buff (oolitic)	do	1	3	4.7	4.6	4.6
11	do	do	1	3	5.7	4.1	4.8
12	Select gray (oolitic)	do	1	3	8.4	7.9	8.1
13	Hard gray (oolitic)	do	1	3	18.3	14.8	16.9
14	do	do	1	3	6.4	6.2	6.3
15	Select buff (oolitic)	do	1	2	6.2	6.2	6.2
16	Standard buff (oolitic)	do	1	2	6.7	6.3	6.5
17	Gray (crystalline)	do	1	3	24.9	22.9	24.1
18	Gray (dolomitic)	Illinois	1	3	15.5	13.9	14.9
19	Gray (oolitic)	Kentucky	2	9	5.6	4.5	4.9
20	do	Alabama	4	14	9.7	4.9	6.9
21	Light buff (earthy)	Florida	3	9	3.1	1.5	2.1
22	Pink (dolomitic)	Minnesota	2	6	12.0	10.2	11.0
23	Yellow (dolomitic)	do	2	6	13.1	10.0	11.2
24	Buff (dolomitic)	do	2	6	12.2	8.3	10.0
25	Gray (dolomitic)	do	1	3	10.2	9.8	9.9
26	Bluish gray (dolomitic)	do	1	3	9.2	7.7	8.6
27	Buff (dolomitic)	do	1	3	11.2	9.2	10.3
28	Light gray (dolomitic)	do	1	3	7.6	7.1	7.3
29	Veined buff (dolomitic)	do	1	3	8.5	7.7	8.2
30	Buff (oolitic)	Kansas	1	3	3.7	3.5	3.6
31	Gray (oolitic)	Oklahoma	1	6	8.0	7.2	7.6
32	Buff (semicrystalline)	Texas	1	3	7.8	6.6	7.1
33	Gray (semicrystalline)	do	1	6	5.1	4.6	4.8
34	Light gray (oolitic)	do	1	3	1.8	1.0	1.3
35	Light buff	France	1	4	17.6	12.3	14.6
36	Buff	do	1	4	16.0	11.4	14.0
37	Light buff (semicrystalline)	do	1	4	7.3	4.5	7.1
38	Buff (oolitic)	do	1	4	6.4	4.2	5.2
39	Pink (fossiliferous)	Italy	1	5	9.0	7.6	8.4

3. SANDSTONE

Results for 22 sandstones are given in table 3. The range is about the same as for the limestones. Those used mainly for ashlar purposes (nos. 13, 14, and 15) generally show rather low H_a values. This brings out clearly the fact that abrasive resistance depends to a large extent on the cohesiveness of the stone. A test on a specimen cut from a quartz crystal gave an H_a value of 180. No doubt the individual sand grains in sandstone are as hard as the value given for quartz, but abrasion of the sandstone results in loosening and removing the grains. Modulus of rupture determinations were made on several of these sandstones in connection with other investigations, and the relation between this property and abrasive hardness is discussed in part IV.

TABLE 3.—*Results of tests on sandstone*

Serial numbers of samples	Variety	Source	Number of samples	Number of tests	Abrasive hardness H_a		
					Maximum	Minimum	Average
1	Brownstone	Massachusetts	1	2	10.8	10.8	10.8
2	Bluestone	New York	5	21	18.9	10.4	13.5
3	Purple flagstone	New Jersey	1	4	20.1	9.7	14.3
4	Blue flagstone	do	1	5	20.7	15.1	18.8
5	Gray flagstone	do	1	5	18.5	11.7	14.7
6	Brown flagstone	do	1	5	17.6	12.6	15.5
7	Gray sandstone	Pennsylvania	1	5	11.3	8.9	10.1
8	Buff flagstone	do	1	5	25.5	19.0	23.3
9	Blue flagstone	do	1	4	29.8	19.2	26.4
10	Red flagstone	do	1	5	17.2	13.8	15.6
11	Blue flagstone	do	1	3	15.0	12.2	14.0
12	Bluestone	do	1	3	23.2	13.1	18.2
13	Gray sandstone	Ohio	1	3	5.2	4.9	5.1
14	Buff sandstone	do	1	3	4.3	4.0	4.2
15	do	do	1	3	1.8	1.4	1.6
16	Bluish gray (fine grained)	do	5	19	8.8	5.2	6.3
17	Buff (fine grained)	do	1	5	4.5	3.7	4.0
18	Bluish gray (fine grained)	do	4	22	9.2	6.0	7.3
19	Free stone (fine grained)	Kentucky	2	13	12.0	7.2	9.0
20	Buff flagstone	Tennessee	6	24	46.0	9.6	29.0
21	Gray (fine grained)	do	1	3	20.4	14.7	17.7
22	Buff (coarse grained)	California	1	3	15.5	11.0	12.9

4. SLATE

Table 4 gives results for 32 domestic slates. The greatest use of slate is for roofing purposes where abrasive qualitites are not important, but some of the Pennsylvania and Vermont slates are used in stair treads and flooring. The tests of different slates show considerable uniformity in the abrasive resistance. The highest mean H_a value for any sample was 11.7 (no. 13) and the lowest 5.6 (nos. 27 and 29) with a weighted average for all of 7.7.

TABLE 4.—*Results of tests on slate*

[NOTE.—Column 5 gives the number of tests. Where "a" follows the number, 2 tests were made on each of 3 specimens; where "b" follows the number, tests were repeated on 2 of the 3 specimens; where "c" follows the number, 3 tests were made on each of 3 specimens]

Serial numbers of samples	Variety	Source	Number of samples	Number of tests	Abrasive hardness H_a		
					Maximum	Minimum	Average
1	Purple	Vermont	1	5 b	9.0	6.9	8.2
2	Unfading green	do	1	6 a	8.1	7.0	7.6
3	Green and purple	do	1	5 b	8.5	7.6	8.0
4	Weathering gray	do	1	5 b	7.9	7.5	7.7
5	Unfading purple	do	1	5 b	7.3	6.7	7.1
6	do	do	1	6 a	9.2	8.8	9.0
7	Unfading green	do	3	14	12.0	8.1	9.6
8	Green and purple	do	1	4	8.9	7.4	7.9
9	Dark gray	Maine	2	6	9.8	8.8	9.4
10	Red	New York	1	6 a	12.2	10.7	11.4
11	Silver gray	do	1	5 b	7.8	7.3	7.5
12	Gray and black	do	1	5 b	7.2	7.0	7.1
13	Purple and green	do	1	6 a	15.2	7.4	11.7
14	Weathering green	do	1	5 b	8.0	7.6	7.7
15	Unfading green	do	1	6 a	7.6	7.2	7.5
16	Blue-gray, clear	Pennsylvania	2	6	7.0	5.8	6.3
17	do	do	1	3	7.7	7.5	7.6
18	do	do	1	3	6.6	6.3	6.5
19	do	do	1	5 b	7.2	6.3	6.5
20	do	do	5	15	7.2	6.2	6.9
21	Blue-gray, ribbon	do	1	3	7.8	7.4	7.5
22	Blue-gray, clear	do	1	3	7.7	7.0	7.4
23	do	do	7	29	7.7	5.8	6.5
24	Blue-gray, ribbon	do	2	15	7.2	6.2	6.6
25	Blue-gray, clear	do	4	12	6.4	5.6	6.0
26	Blue-gray, ribbon	do	2	6	7.2	6.5	6.9
27	Blue-gray, clear	do	2	6	5.8	5.5	5.6
28	Hard vein	do	1	9 c	9.3	6.8	8.3
29	Dark gray	Maryland	1	3	5.7	5.5	5.6
30	do	Virginia	1	5 b	12.2	9.9	10.9
31	Green	Georgia	1	5 b	8.9	7.9	8.5
32	do	Tennessee	1	6 a	7.0	6.5	6.8

5. GRANITE

Table 5 gives results of tests on 11 domestic granites. All show high values and a lower percentage variation from the mean than any of the other types of stone. The minerals in these granites are mainly quartz and feldspar. The H_a values obtained are usually between those obtained by testing specimens cut from crystals of the two minerals but are much nearer the feldspar values. Granites usually possess a high cohesive strength but apparently the wear test produces a slight crumbling effect as noted for the sandstones. Repeated tests on samples of polished granite showed higher H_a values as the depth of abrasion was increased. This seems to substantiate the theory that hard stones are injured to some extent near the surface by the finishing process.

TABLE 5.—*Results of tests on granite*

[Note.—Column 5 gives the number of tests. Where "a" follows the number, 2 tests were made on each of 3 specimens; where "b" follows the number, 3 tests were made on each of 3 specimens]

Serial numbers of samples	Variety	Source	Number of samples	Number of tests	Abrasive hardness H_a		
					Maximum	Minimum	Average
1	Pink biotite granite	Maine	1	3	69.2	60.2	63.2
2	Light gray muscovite—biotite	do	1	3	48.5	40.8	45.9
3	Bluish-gray muscovite—biotite	New Hampshire	1	3	72.5	56.6	64.0
4	Pink biotite granite	do	1	3	72.9	60.2	66.4
5	Green biotite—hornblend	do	1	3	75.1	60.6	66.3
6	Light gray quartz—monzonite	Vermont	1	3	55.0	37.0	43.9
7	Gray biotite granite	do	1	3	55.7	50.0	53.2
8	Gray hornblend granite	Massachusetts	1	3	76.0	59.0	67.7
9	Green hornblend granite	do	1	6 a	98.4	77.3	87.9
10	Gray biotite granite	North Carolina	1	3	53.9	44.6	50.5
11	Dark gray hornblend	Colorado	1	9 b	65.2	42.9	59.5

6. SERPENTINES

The results in table 6 for 5 domestic and 6 imported serpentines show a large variation and some values higher than any obtained for granite.

TABLE 6.—*Results of tests on serpentine*

[NOTE.—Column 5 gives the number of tests. Where "a" follows the number 2 tests were made on each of 2 specimens]

Serial numbers of samples	Variety	Source	Number of samples	Number of tests	Abrasive hardness H_a		
					Maximum	Minimum	Average
1	Green, pale green veins	Vermont	1	3	97.6	86.1	92.6
2	Dark green, pale green clouds	Massachusetts	1	5	16.7	12.9	15.0
3	Pale green	New Jersey	1	4	40.6	30.2	35.3
4	Dark green, pale green veins	Maryland	1	6	158.0	75.0	111.4
5	Green to grayish-green	Georgia	1	4 a	26.9	23.0	24.9
6	Pale green and gray	Sweden	1	6	22.7	15.6	18.8
7	Emerald-green	Italy	1	4	37.6	31.7	34.8
8	Green, white veins	do	1	3	81.0	65.0	74.2
9	Red, white, and green	do	1	4 a	21.0	16.0	17.8
10	Dark green, white veins	France	1	4	15.3	10.2	13.3
11	Green, white veins	Greece	1	4 a	80.0	74.3	77.2

Textbooks on mineralogy give the hardness (Moh's scale) of the mineral serpentine as ranging from 2.5 to 4.0 while the principal granite minerals, quartz, and feldspar, are 6 and 7, respectively. The high values obtained for some of the serpentines would be surprising but for the fact that this type of material is seldom if ever pure serpentine. Such hard minerals as pyrite, hornblend, olivine, and pyroxene are usually present in variable amounts.

7. TRAVERTINES

Table 7 gives the results of tests on 7 domestic and 4 imported products. Some of these are travertines in a commercial sense only. This is especially true of the black travertine (no. 11) which is an

igneous rock. Also the fossiliferous and sedimentary limestones (nos. 1, 2, 3, and 9) are not travertines according to a strict interpretation of the term, but are known in the trade as such on account of their cellular structure.

TABLE 7.—*Results of tests on travertine*

[NOTE.—Column 5 gives the number of tests. Where "a" follows the number, 2 tests were made on each of 2 specimens]

Serial numbers of samples	Variety	Source	Number of samples	Number of tests	Abrasive hardness H_a		
					Maximum	Minimum	Average
1	Buff (sedimentary)	Florida	5	20	17.6	5.6	12.4
2	Buff (fossiliferous)	Georgia	1	4 a	13.4	11.7	12.6
3	Buff (sedimentary)	Minnesota	1	3	12.5	10.0	11.2
4	Buff	Montana	1	3	14.4	14.1	14.3
5	Pink	do	1	3	13.3	8.8	11.4
6	Gray	do	1	3	5.8	5.0	5.4
7	Pinkish-buff	Colorado	1	3	8.8	8.3	8.6
8	Buff	Italy	1	3	16.7	15.2	15.7
9	Light buff (sedimentary)	France	1	2	.6	.6	.6
10	Buff	Germany	1	4	18.4	15.3	16.5
11	Black (vesicular basalt)	do	1	4	50.7	35.6	40.6

8. MISCELLANEOUS MATERIALS

Certain grades of the secondary rocks classed as talcose serpentine and chloritic amphibole (nos. 1, 2, 6, 7, and 8) are used to a considerable extent in floors and stair treads. The results on these are given in table 8 with results on 3 common minerals for comparative purposes. The large variations in the secondary rocks from different quarries (nos. 1 to 6, inclusive) or different ledges (nos. 7 and 8) are due evidently to the amount of alteration from the original igneous rock. In general, the softer varieties of these materials are used in tanks, tubs, table tops, etc., where the abrasive factor is not important.

TABLE 8.—*Results of tests on miscellaneous materials*

[NOTE.—Column 5 gives the number of tests. Where "a" follows the number, 5 tests were made on 2 specimens; where "b" follows the number, 3 tests were made on 1 specimen]

Serial numbers of samples	Variety	Source	Number of samples	Number of tests	Abrasive hardness H_a		
					Maximum	Minimum	Average
1	Talcose serpentine	Virginia	1	2	23.2	22.0	22.6
2	do	do	1	2	10.0	9.6	9.8
3	do	do	1	2	5.6	5.4	5.5
4	do	do	1	2	4.9	4.2	4.6
5	do	do	1	2	4.4	4.2	4.3
6	do	do	7	14	21.6	11.7	16.3
7	Chloritic amphibole	do	1	3	16.2	15.7	16.0
8	do	do	3	11	9.9	5.6	7.2
9	Feldspar (orthoclase)	New York	1	3	55.0	50.5	52.7
10	Feldspar (albite)	?	1	5 a	89.8	75.0	80.9
11	Quartz	Brazil	1	3 b	187.0	176.0	179.7

IV. DISCUSSION OF RESULTS

The wear resistance values obtained by this test procedure and the commonly accepted Moh's scale values for some materials are apparently not in accord. This may be due to the different forms

in which minerals occur. The mineralogist deals usually with individual crystals of the substance while rocks are mainly aggregations of small crystals. Loosely bonded aggregations of hard minerals in this test invariably show low resistance to wear. This is illustrated by the tests on some of the sandstones which were almost entirely quartz but gave lower H_a values than most of the limestones. The abrasive resistance of sandstone seems to depend mainly on its cohesive strength. The correlation coefficient (r) between the H_a values and modulus of rupture values for 21 sandstones, computed by formula (2), was 0.81.

Accuracy and dependability of test methods are essential considerations. There is no standard process for determining the accuracy of an abrasive hardness test. If it were possible to secure an absolutely homogeneous material, repeated tests would show the variations in the test itself. However, the selection of a material to be used for a standard must depend on some measurement of uniformity in abrasive resistance which again involves the errors of the test employed. A considerable number of the materials tested in this investigation gave quite uniform results for the different determinations made on them. Probably the best way of studying the accuracy of the test is to consider the variations obtained from a large number of determinations on materials which appear to be homogeneous. The range in values obtained for any particular material may represent either the sums or differences of variations in the material and inaccuracies of the test, but the mean variation for a large series of tests will tend to balance these variable effects.

A study was made of the variations obtained on 85 samples of the 78 marbles by expressing the difference between the highest and lowest values obtained on each sample as a percentage of the mean of all determinations on that sample. The mean of all the percentage variations for the 85 samples was found to be 11.3 percent. For 66 of these samples, which appeared to be fairly uniform in composition and texture, the mean percentage variation was 9.2 percent. Forty-two samples of slate gave a percentage variation of nearly 11 percent, but when those which were obviously nonhomogeneous were eliminated from the computations, the mean percentage variation was found to be less than 8 percent. Such considerations seem to indicate that the precision of the test is within ± 5 percent.

Experience with various floor-surfacing materials has shown the need for adapting the wearing surface to traffic conditions. Entrance ways to public buildings usually require paving materials of high wear resistance. Hallways, stair treads, and other places of concentrated traffic also need some degree of care in the selection of the surfacing materials, while for spaces having a good distribution of traffic the selection is not so important.

A comparison of the actual service wear of widely used stones with their H_a values gives fairly definite information as to what test values should be specified for any particular case where the traffic conditions can be estimated. An interesting comparison between two marbles used in the floor of an important railroad station may be cited. A red marble giving an H_a value of approximately 31 was used with a white marble giving a test value of about 10. After nearly 30 years of service this floor has worn to a very uneven surface in which the red tile surfaces are standing quite perceptibly higher than those

of the white tiles. This particular case has brought forth considerable comment and was, to some extent, instrumental in bringing about this investigation. Observations on several of the more important flooring marbles under various conditions of service seem to justify the following statements: Surfacing materials showing H_a values of 30 or higher are very resistant to wear and should prove reasonably satisfactory under severe traffic conditions. For railroad stations, hotel lobbies, department stores, etc., the surfacing materials should test as high as 15 or, in some cases, 20. For a large percentage of floor areas where the traffic conditions are not especially severe good service may be obtained from surfacing materials testing as low as 6.

V. CONCLUSIONS

1. The correlation existing between the results obtained with the testing apparatus and the results of service tests seems to be such as to enable one to satisfactorily predict service wear from the abrasive resistance (expressed as H_a) values.

2. The abrasive resistance of stone depends on its cohesive strength and the hardness of the minerals of which it is composed.

3. Determinations on 78 marbles including both calcites and dolomites show that some varieties are five or six times as resistant to abrasion as others. The results do not indicate that dolomitic marbles are more resistant than calcitic marbles.

4. As a class the limestones are shown to be considerably less resistant to abrasion than the marbles although those limestones which approach marble in density and strength usually show resistance values comparable to those of marble.

5. The abrasive resistance of sandstone depends on the cohesion between the sand grains. The varieties used for flagging gave values similar to those of the marbles, while those used mainly for ashlar purposes gave low resistance values.

6. The slates studied gave quite uniform test results with an average somewhat lower than the average for limestone.

7. The granites give relatively high test results in a rather narrow range for the 11 samples tested. Duplicate tests on polished specimens showed higher values with increasing depth which seems to indicate that this material is injured appreciably near the surface by the finishing process.

8. The materials grouped under the trade classification of travertines gave variable results. Those samples which could be classed as real travertine gave values somewhat below the average for marble.

9. The average value for the serpentines was somewhat below the average for granite but the range of values for the serpentines was very large and two samples gave values much higher than any of the granites.

10. Materials which are formed from igneous rocks by surface weathering, such as serpentines and chloritic amphiboles, show wide variations in resistance to abrasion, depending on the degree of weathering.

11. Since the values for most of the types of stone tested overlap in many instances, it is not possible to evaluate the relative wear resistance of materials by type alone.

WASHINGTON, August 30, 1933.

U.S. DEPARTMENT OF COMMERCE, BUREAU OF STANDARDS

RESEARCH PAPER RP613

Part of Bureau of Standards Journal of Research, Vol. 11, November 1933

PREPARATION AND PROPERTIES OF ALDONIC ACIDS AND THEIR LACTONES AND BASIC CALCIUM SALTS

By Horace S. Isbell and Harriet L. Frush

ABSTRACT

Directions are given for the preparation of the crystalline acids and lactones derived from gluconic, mannonic, galactonic, xylonic, arabonic, and rhamnonic acids. The compositions of the basic calcium salts of mannonic, galactonic, xylonic, arabonic, rhamnonic, lactobionic, and maltobionic acids are reported and their use for the purification of sugar acids is described. The utility of dioxane as a solvent in preparing the free sugar acids and their lactones is emphasized. The method for preparing gluconic acid by crystallization from water is suitable for the manufacture of that substance in large quantity.

CONTENTS

	Page
I. Introduction	649
II. Gluconic acid and its derivatives	651
1. Dioxane method for preparing crystalline gluconic acid	653
2. Crystallization of gluconic acid from aqueous alcohol	653
3. Crystallization of gluconic acid from water	653
4. Preparation of gluconic δ-lactone	654
5. Preparation of gluconic γ-lactone from gluconic δ-lactone	655
III. Xylonic acid and its derivatives	655
1. Preparation of calcium xylonate from xylose	656
2. Preparation of xylonic γ-lactone	657
3. Preparation of basic calcium salts for analysis	657
IV. Mannonic acid and its derivatives	658
1. Calcium mannonate	658
2. Mannonic δ-lactone	659
3. Mannonic γ-lactone	659
V. Galactonic acid and its derivatives	660
1. Galactonic acid	660
2. Galactonic γ-lactone	661
VI. Arabonic acid and its derivatives	661
1. Arabonic acid	662
2. Arabonic γ-lactone	662
VII. Rhamnonic acid and its derivatives	663
1. Rhamnonic δ-lactone	663
2. Rhamnonic γ-lactone	663
VIII. Summary	664

I. INTRODUCTION

The electrolytic method [1] for the oxidation of aldoses has simplified the production of aldonic acids so that the acids derived from the more abundant naturally-occurring sugars are available in large quantities

[1] Isbell and Frush, B.S. Jour. Research, vol. 6 (RP328), p. 1145, 1931; and Isbell, Frush, and Bates, B.S. Jour. Research, vol. 8 (RP436), p. 571, 1932.

for investigation. Although many of the sugar acids have been known for a long time and some of the methods for separating the crystalline products are satisfactory, other methods are too difficult to follow and are of little practical importance. Consequently, one desiring to prepare the substances is required to do considerable experimental work in order to select a suitable procedure. The purpose of this publication is to report methods which have been found most satisfactory for preparing the sugar acids and for obtaining the crystalline lactones, with the object of making the lactones and acids more readily available so as to stimulate their industrial application. Since there are large undeveloped sources of dextrose, mannose, galactose, xylose, arabinose, and rhamnose, the acids and lactones derived from these sugars are of particular interest, even though the commercial application of the sugar acids, other than gluconic, must await cheaper methods for the preparation of the parent sugars or their solutions.

In aqueous solution the aldonic acids form γ- and δ- lactones spontaneously and reversibly.[2] This is illustrated in the case of gluconic acid by the following formulas:

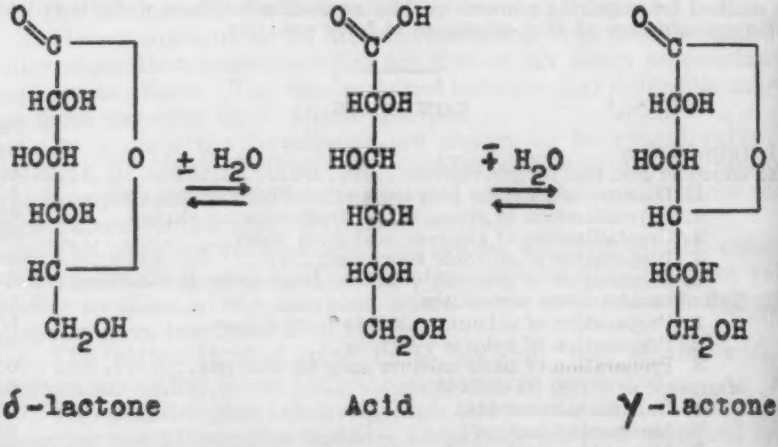

Equilibrium solutions of certain acids such as gluconic and lactobionic give relatively strongly acid reactions, showing the presence of considerable free acid; others, as for example, gulonic and α-glucoheptonic, give nearly neutral solutions. The relative amounts of the γ- and δ-lactones in the equilibrium solutions are also subject to wide variation. The pH of the solution, the availability of the acid and the ease of separation of the products are dependent on the position of the equilibrium.

The acids are ordinarily obtained by evaporating at a low temperature freshly prepared aqueous solutions, such as may be derived by treating the calcium salts with oxalic acid. Since the δ-lactones are formed rapidly they are obtained in like manner by dehydrating the acid solution at a low temperature, in the absence of mineral acid and with proper seeding. The γ-lactones are prepared by dehydration of the acids at higher temperatures and in the presence of mineral acids. Because of the equilibrium existing between the free acid and its lactones, a solution will sometimes yield nearly quantitatively

[2] Levene and Simms, J. Biol. Chem., vol. 65, p. 31, 1925. Charlton, Haworth, and Peat. J. Chem. Soc. p. 89, 1926. Haworth and Nicholson, J. Chem. Soc., p. 1899, 1926.

either the free acid or the lactone, depending upon the substance which happens to crystallize first. For example, an 80 percent aqueous solution of gluconic acid, on seeding with gluconic δ-lactone, gives exclusively crystalline gluconic δ-lactone. On the other hand, we have found that in the absence of δ-lactone seed and in the presence of gluconic acid seed, it gives exclusively crystalline gluconic acid. It is emphasized that concentrated aqueous solutions of the sugar acids are frequently supersaturated with respect to more than one constituent and may yield more than one product. It is frequently difficult to obtain the crystalline acid or lactone for the first time, particularly when the equilibrium is not favorable for its separation, but after crystals are available for seeding no further difficulty is experienced.[3]

In this paper emphasis is placed on the use of several solvents which have recently become commercially available. The use of dioxane in particular is noteworthy. Since this solvent boils at 100° C. and does not combine chemically with either the free acids or their lactones, it may be used to advantage in dehydrating aqueous solutions by distillation. The water and dioxane distill simultaneously, leaving a solution from which either the δ-lactone or acid crystallizes readily. The use of dioxane in separating the sugar acids on a large scale is limited by the cost, but since it can be recovered this solvent may find some application in working up products which are not sufficiently pure to crystallize from water alone.

If the electrolytic process is employed for converting the sugar into the acid, the crude sirups obtained by the hydrolysis of polysaccharides may be used. Thus, many of the sugar acids or their salts can be prepared as cheaply and readily as the corresponding crystalline sugars. In the event that the lactone of the sugar acid crystallizes easily it may be prepared directly from the electrolyzed solution. In such case the calcium or barium is removed by precipitation as oxalate or sulphate; on evaporating the resulting solution the crystalline lactone is obtained. This method is particularly useful for preparing rhamnonic lactone, but it is not suitable for preparing lactones which are difficult to crystallize.

A new method for preparing aldonic acids and their δ-lactones from their sodium salts was recently reported by Brackenbury and Upson.[4] The sodium salt is treated with glacial acetic acid and the δ-lactone or acid is crystallized from the mixture of acetic acid and sodium acetate.

II. GLUCONIC ACID AND ITS DERIVATIVES

In 1884 Kiliani and Kleemann [5] showed that the residue obtained by evaporating an aqueous gluconic acid solution contained a large quantity of lactone. Somewhat later Fischer [6] succeeded in isolating pure crystalline gluconic γ-lactone. In 1914 Nef [7] reported a second lactone now called gluconic δ-lactone, while in 1928 Rehorst [8] prepared crystalline gluconic acid. The equilibrium between gluconic

[3] The polarimetry section of the Bureau of Standards will furnish seed of any of the products described in this paper upon request as long as the present supply is available.
[4] Brackenbury and Upson, J. Amer. Chem. Soc., vol. 55, p. 2512, 1933.
[5] Kiliani and Kleemann, Ber., vol. 17, p. 17, 1884.
[6] Fischer, Ber., vol. 23, pp. 804 and 2625, 1890.
[7] Nef, Ann., vol. 403, p. 323, 1914. This substance was reported as gluconic β-lactone.
[8] Rehorst, Ber., vol. 61, p. 163, 1928.

acid and its lactones in aqueous solution was investigated first by Nef, who found that the δ-lactone is formed more rapidly than the γ-lactone and that if one evaporated a gluconic acid solution at a low temperature the δ-lactone was obtained in predominating amount, but if the solution were dehydrated at a high temperature in the presence of mineral acids the γ-lactone predominated. Until recently the γ-lactone was obtained by evaporation of aqueous gluconic acid to dryness, extraction of the residue with alcohol, and crystallization from the alcoholic extract. This method is not satisfactory because the alcohol used as a solvent esterifies a part of the sugar acid, forming ethyl gluconate, which interferes with the crystallization of the desired product. Condensation products are also formed which are troublesome to remove and reduce the yield of lactone.

As pointed out by Nef, these amorphous condensation products probably contain glucono-gluconic acid and similar substances, which have not been studied extensively. A better method for the preparation of gluconic γ-lactone was devised by Pasternack and Cragwall.[9] It consists in dehydrating aqueous gluconic acid by distillation in the presence of butyl alcohol. Although the γ-lactone crystallizes readily from the butyl alcoholic solution, considerable difficulty is usually encountered in eliminating the butyl gluconate formed during the dehydration. This objectionable feature is overcome by the new method reported on page 655, which consists in heating gluconic δ-lactone in glacial acetic acid. Inasmuch as the δ-lactone is commercially available at low cost, this simple process makes the γ-lactone available for instruction and research in carbohydrate chemistry.

Gluconic δ-lactone is prepared commercially by the method of Pasternack and Giles,[10] which consists in crystallizing the lactone from concentrated aqueous solutions containing gluconic δ-lactone seed. Small amounts of the lactone can be made without seed by the dioxane method reported in this paper. Gluconic δ-lactone crystallizes in large compact crystals which are easily separated from even thick sirups.

As reported by Rehorst,[11] an aqueous gluconic acid solution on evaporation at 100° C. gives a thick sirup which solidifies under appropriate conditions yielding crystalline gluconic acid. In our experience the acid is obtained only in the absence of δ-lactone seed and by seeding with crystalline gluconic acid. The product obtained by this method is a hard solid which contains all the impurities of the original material. We have found that crystalline gluconic acid can be prepared in nearly pure filterable crystals by evaporating a solution of gluconic acid to about 65 percent, seeding and continuing the evaporation while crystallization of the free acid takes place. It is noted that gluconic acid will crystallize from an aqueous solution in equilibrium with its lactones. Consequently one can prepare the acid easily from gluconic γ- or δ-lactone. In the event that the γ-lactone is used as a raw material it is advantageous to add some acetic acid, as this aids in establishing the equilibrium and also decreases the solubility of the acid. Although crystallization of gluconic acid from aqueous solution is probably the cheapest method, the others are suitable for preparing small quantities and for instruction of students in carbohydrate chemistry.

[9] Pasternack and Cragwall, U.S. Patent No. 1830618, Nov. 3, 1931.
[10] Pasternack and Giles, U.S. Patent No. 1862511, June 7, 1932.
[11] Rehorst, Ber., vol. 63B, p. 2279, 1930.

1. DIOXANE METHOD FOR PREPARING CRYSTALLINE GLUCONIC ACID

One hundred grams of dry calcium gluconate and 27 g of crystalline oxalic acid are mixed with 100 ml of water in a 300 ml Erlenmeyer flask. The flask is shaken vigorously for 5 minutes; the precipitated calcium oxalate is removed by passing the solution through a Büchner funnel fitted with a filter paper covered with a thin layer of kieselguhr. The filtrate is cooled in an ice bath. After the residue on the filter has been washed successively with 10 ml of water and 10 ml of dioxane, the filtrate is transferred to a 2-liter distillation flask and 200 ml of dioxane added. The resulting solution is concentrated rapidly under reduced pressure at about 30° C. Although crystallization of the acid frequently occurs spontaneously as evaporation takes place, it is desirable to seed the product because otherwise the δ-lactone may crystallize first. Crystals of the acid for seeding can be obtained by evaporating a few ml of the freshly prepared solution containing dioxane on a watch crystal. When the material becomes thick with the crystalline product, distillation is stopped and the crystals are transferred to a filter with about 25 ml of dioxane. The first crop of crystals is usually nearly pure gluconic acid and weighs about 30 g. If the temperature of the distillation is too high the product may be contaminated with δ-lactone. By evaporating the mother liquor additional crystals are obtained but these usually contain more or less δ-lactone.

2. CRYSTALLIZATION OF GLUCONIC ACID FROM AQUEOUS ALCOHOL

A dry mixture containing equimolecular proportions of finely powdered crystalline calcium gluconate (50 g) and oxalic acid (13.5 g) is added in small portions with vigorous mechanical stirring to a small quantity of ice water (25 ml). When stirred several minutes all the calcium gluconate is converted into gluconic acid and calcium oxalate. The mixture is diluted with 50 ml of isopropyl alcohol and poured on a 4-inch Büchner funnel fitted with a filter paper covered with kieselguhr. The residue is washed with a few ml of water and the filtrate is diluted with isopropyl alcohol until the volume is about 250 ml. Crystallization of gluconic acid may be induced by seeding or scratching the walls of the flask. After standing 18 hours in the refrigerator the resulting crystalline gluconic acid is separated, washed with isopropyl alcohol, and dried. About 7 g is obtained. Absolute ethyl alcohol may be used in place of the isopropyl alcohol, in which case the yield is slightly lower. This is the simplest method for preparing small quantities of gluconic acid.

3. CRYSTALLIZATION OF GLUCONIC ACID FROM WATER

About 500 ml of a 40-percent solution of aqueous gluconic acid, which may be prepared from calcium gluconate and oxalic acid, is placed in a 2-liter Claissen distillation flask containing an inlet tube for introducing additional liquid. The solution is evaporated rapidly under reduced pressure at about 40° C. When the material in the flask becomes sirupy (about 65 percent dry substance), gluconic acid seed is added and evaporation is continued while simultaneously freshly prepared gluconic acid solution is introduced dropwise into

the flask at such a rate that the crop of crystals continues to increase. The freshly prepared gluconic acid solution is made from time to time during the distillation from 100 g of calcium gluconate, 27 g of oxalic acid and 200 ml of water, or from crude crystalline gluconic acid which it is desired to purify. Addition of gluconic acid and simultaneous evaporation are continued until the desired quantity of crystals is present in the flask. The material is transferred to a filter and the crystals are separated from the mother liquor. In small-scale preparations, a small amount of acetic acid or ethyl alcohol may be used in removing the crystals from the flask. The product is washed with ethyl alcohol followed by dry ether or dioxane. Nearly quantitative yields may be obtained by reworking the mother liquors. The product may be purified by repeating the process, or if desired it may be recrystallized by dissolving it in cold water and adding glacial acetic acid according to the method of Brackenbury and Upson (footnote 4).

Crystalline gluconic acid may also be made from gluconic δ- or γ-lactone. One part of δ-lactone is dissolved in one part of boiling water; after filtration the solution is cooled in ice water and seeded with crystalline gluconic acid. After standing several hours at 0° C. a crop of crystalline acid may be separated. The mother liquors can be concentrated and additional acid obtained. Use of an organic solvent such as acetic acid or dioxane is advantageous in washing the crystals and working up the mother liquors. Crystalline gluconic acid melts at 120°–131° C., the temperature varying with the rate of heating. In 5 percent aqueous solution $[\alpha]_D^{20} = -6.9°$, 2 minutes after solution, +7.3° after 24 hours. Rehorst (footnote 11) reports the melting point as 130°–132° C. (not sharp, sintering at 112°) and the specific rotation as −6.7°, initially, +7° after 24 hours.

4. PREPARATION OF GLUCONIC δ-LACTONE

A dry mixture of 150 g of calcium gluconate and 40.6 g of crystalline oxalic acid is added in portions, with shaking, to 150 ml of warm water in a 500 ml Erlenmeyer flask. After the calcium gluconate is decomposed, 150 ml of dioxane is added, and the resulting solution is passed through a Büchner funnel fitted with a filter paper covered with kieselguhr. The filtrate is cooled to room temperature and evaporated rapidly at about 35° C. in vacuo by using a good water pump. When the volume of the solution is reduced to about 100 ml, 150 ml of dioxane and some crystalline gluconic δ-lactone are added. Distillation at 30° to 35° C. is continued until the mixture becomes thick with the crystalline product. The crystals are separated by filtration, washed with dioxane, and dried. The mother liquor is returned to the distillation flask and concentrated until additional crystals are obtained. In a typical experiment the first crop weighed 69 g and gave $[\alpha]_D^{20} = +64.9°$ initially, +10° after 24 hours; the second crop weighed 32 g and gave $[\alpha]_D^{20} = +63.5°$ initially, +17.0° after 24 hours; the third crop weighed 11.5 g and gave $[\alpha]_D^{20} = +58.2°$ initially, +13.5° after 24 hours. If the solution is heated too long or at too high a temperature, the last fractions will contain gluconic γ-lactone, while if the solution of gluconic acid is evaporated too rapidly at a low temperature gluconic acid will crystallize rather than the lactone. Any fraction which contains crystalline gluconic acid and the δ-lactone may be converted into δ-lactone by digesting a short time with

dioxane. The presence of the acid in the lactone can be detected by its sour taste or by its appearance. It crystallizes in small irregularly shaped clusters of slender pointed crystals, while the δ-lactone separates in large chunky prisms. The lactone melts at 150° to 152° C. In 5 percent aqueous solution, $[\alpha]_D^{20} = +66.2°$ initially, +8.8° after 24 hours. These rotations are in approximate agreement with those recently reported by Brackenbury and Upson (footnote 4).

5. PREPARATION OF GLUCONIC γ-LACTONE FROM GLUCONIC δ-LACTONE

About 100 ml of glacial acetic acid and 50 g of gluconic δ-lactone are placed in a round-bottomed pyrex flask fitted with a reflux condenser. The mixture in the flask is heated to boiling and refluxed about 1 hour. On cooling the resulting solution and seeding with γ-lactone, crystalline gluconic γ-lactone separates slowly. After standing overnight in the refrigerator the product is collected on a filter, washed successively with glacial acetic acid, alcohol, and ether. About 23 g of crude γ-lactone of about 90 percent purity is obtained. If desired, additional δ-lactone may be added to the acetic acid mother liquor to replace that converted to γ-lactone and the process repeated. The crude γ-lactone can be recrystallized by dissolving it in 3 parts of hot acetic acid or about 12 parts of hot dioxane. The lactone separates on cooling the solution. The mother liquors may be used for recrystallizing additional material.

The γ-lactone melts at 133° to 135° C. In 5 percent aqueous solution, $[\alpha]_D^{20} = +68.0°$ initially, +67.2° after 24 hours. Fischer (footnote 6) previously reported the melting point as 130° to 135° C., and $[\alpha]_D^{20} = +68.2°$.

Gluconic γ-lactone seed may be made in the following manner: An aqueous gluconic acid solution is evaporated in vacuo to a thick sirup. After being heated for several hours in order to convert the acid to the lactone the residue is extracted with hot normal butyl alcohol. Upon cooling the alcoholic extract, crystallization occurs spontaneously, particularly when the solution is allowed to evaporate in an open dish.

III. XYLONIC ACID AND ITS DERIVATIVES

Xylonic acid and strontium xylonate were prepared first by Allen and Tollens [12] by the oxidation of xylose with bromine water. Subsequently characteristic cadmium-cadmium bromide [13] and cadmium chloride salts have been reported. These salts are useful for identification purposes but they are not suitable for preparing xylonic acid and its derivatives. The free acid can be prepared from calcium xylonate [14] or from lead xylonate.[15] We have previously reported (RP328) a simple method for preparing amorphous calcium xylonate by the electrolytic oxidation of xylose, and separation of the product as a basic calcium xylonate. Although crystalline xylonic acid is at present unknown, the γ-lactone crystallizes fairly readily. Heretofore this lactone has been prepared only in small quantities, but with

[12] Allen and Tollens, Ann., vol. 260, p. 306, 1890.
[13] Bertrand, Bull. soc. chim. (3), vol. 5, p. 556, 1891.
[14] Nef, Ann., vol. 403, p. 252, 1914.
[15] Hasenfratz, Compt. rend., vol. 196, p. 350, 1933.

the development of cheaper methods for the production of xylose [16] and calcium xylonate it is now possible to prepare it in any desired quantity. Previous investigators usually crystallized the lactone from acetone.[17] This solvent is not satisfactory for preparing the crude lactone because a large part of the material is left in the form of an amorphous residue. We have found that this difficulty may be overcome by crystallization from a concentrated aqueous solution without the use of solvents other than water. Since the lactone is very soluble in water it is difficult to obtain high yields in small-scale preparations, but in large quantities the heavy massecuite may be treated more economically. In small-scale laboratory preparations crystallization from dioxane is advantageous. Xylonic γ-lactone is miscible with dioxane at the boiling point (760 mm), while at 20° C. 100 g of dioxane dissolves about 7 g of lactone.

1. PREPARATION OF CALCIUM XYLONATE FROM XYLOSE

A solution containing 300 g of xylose and 30 g of potassium bromide in 1 liter of water is placed with 100 g of calcium carbonate in a 2-liter three-necked flask cooled by running water, and equipped with a mechanical stirrer and two graphite electrodes about 2.2 cm in diameter and immersed to a depth of 6.7 cm. A current of 1 ampere at 15 volts is passed through the solution. Under these conditions the current density is about 2 amperes per dm^2 of anode surface. After 110 ampere-hours about 98 percent of the sugar is oxidized with an anode efficiency of about 95 percent. When a Fehling's test on the electrolyte is nearly negative, electrolysis is stopped. The electrolyzed solution is filtered and the xylonic acid is precipitated as basic calcium xylonate by the addition of 200 g of hydrated lime in 2 liters of water (150 g theoretically required). In order to obtain a product which filters readily it is necessary to precipitate the basic salt slowly. This is done by allowing the hot milk of lime and hot calcium xylonate solution to flow slowly and simultaneously, with stirring, into a precipitating jar. After the solutions are mixed, the product is heated to about 80° C. in order to complete the precipitation.

The basic salt is collected on a large Büchner funnel and washed with lime water until free from bromide. It is then suspended in water and carbon dioxide introduced with agitation until the solution gives a neutral reaction to phenolphthalein. An excess of CO_2 should be avoided as it results in a residue which is difficult to separate. The insoluble calcium carbonate is removed by filtration and the filtrate concentrated to 650 ml. The resulting solution usually contains about 225 g of calcium xylonate which corresponds to a 60 percent yield. The mother liquor from the basic salt may be used in a subsequent oxidation in order to reclaim the calcium xylonate and potassium bromide contained therein. Or if desired a second crop of basic salt may be obtained by concentrating the solution and adding more lime, followed by heating.

[16] Schreiber, Geib, Wingfield, and Acree, Ind. Eng. Chem., vol. 22, p. 497, 1930.
[17] Clowes and Tollens, Ann., vol. 310, p. 175, 1899.

2. PREPARATION OF XYLONIC γ-LACTONE

A hot solution containing 215 g of calcium xylonate in 650 ml of water is mixed with 73.25 g of crystalline oxalic acid. The precipitated calcium oxalate is separated and after the addition of a few ml of concentrated hydrochloric acid the solution is evaporated in vacuo. When the sirup becomes thick it is cooled to 30° C. and seeded with crystalline xylonic γ-lactone, after which boiling is continued. The lactone crystallizes slowly from the solution and the material finally becomes solid. It is necessary to conduct the evaporation slowly and to heat the residue in vacuo for several hours in order to convert the acid into the lactone. The residue is extracted with about 150 ml of hot dioxane. Most of the material goes into solution, leaving a small quantity of residue (8 g). The composition of this residue and the conditions under which it is formed are not known. The amount varies in an unknown manner, possibly depending on the method of dehydration. In order to obtain the crystalline lactone without seed it is usually necessary to extract the thick aqueous sirup containing the crude lactone with acetone. The acetone extract on evaporation in an open dish gives crystalline xylonic lactone.

The dioxane solution is concentrated in a distillation flask under reduced pressure to about 100 ml. The resulting sirup is seeded with xylonic γ-lactone crystals and benzene is added until the solution becomes slightly turbid. On standing, about 110 g of lactone crystallizes from the solution. After separation of the crystals the mother liquor is concentrated and additional lactone obtained. The total yield of crude lactone is about 160 g or approximately 90 percent.

The crude xylonic lactone may be recrystallized by dissolving it in boiling dioxane, using 2 ml of dioxane for each gram of lactone. A small quantity of amorphous residue remains which is separated by filtration. On cooling, nearly pure xylonic γ-lactone crystallizes from the resulting solution. When in fairly pure state, xylonic lactone may be recrystallized easily from numerous solvents, such as acetone, isopropyl, butyl, isoamyl alcohol, or glacial acetic acid. The lactone melts at 98° to 101° C. In 5 percent aqueous solution, $[\alpha]_D^{20} = +91.8°$ 2 minutes after solution, +86.7° after 24 hours. The melting point agrees with that of other investigators but the initial rotation is slightly higher than the values of Nef, +89.56° (footnote 14) or Hasenfratz, +85.5° (footnote 15).

3. PREPARATION OF BASIC CALCIUM SALTS FOR ANALYSIS

A solution containing 20 g of calcium xylonate in 600 ml of ice water is mixed with 400 ml of cold milk of lime containing 7 g of calcium oxide. The solution is filtered quickly and the clear filtrate evaporated in vacuo to about 100 ml. The mixture is then warmed on the steam bath in order to complete the precipitation of the basic salt, which is subsequently collected on a filter, washed with lime water, and dried at 60° C. in vacuo. All operations are conducted rapidly in order to avoid contamination with carbon dioxide. The calcium content, reported in table 2, was determined by precipitation as calcium oxalate. The CaO content was determined by dissolving in 0.5 *N* HCl, followed by the addition of an excess of standard alkali and back titration with 0.1 *N* HCl by using phenolphthalein as an indicator.

IV. MANNONIC ACID AND ITS DERIVATIVES

Mannose occurs in many vegetable products in the form of polysaccharides which give the sugar by hydrolysis. A convenient source is shavings from ivory nuts, which can be purchased from button factories. The liquors obtained from the hydrolysis of ivory nuts can be used directly for preparing calcium mannonate.[18]

The methods for separating calcium mannonate from the by-products of the older bromine or chlorine oxidation of mannose required considerable work, and the use of expensive chemicals. Our electrolytic process of oxidation, (RP328), eliminates these expensive steps because the desired product crystallizes from the electrolyte without prior purification. The salt separates in well defined crystals provided that the solution is not too concentrated, is seeded and kept in motion during crystallization; if these precautions are not observed a gelatinous product results.

Bernhauer and Irgang,[19] in applying the electrolytic method to crude mannose derived from the hydrolysis of ivory nuts observed a lower efficiency than we did with pure mannose. It has been our experience that crude glucose, mannose, xylose, and arabinose solutions frequently give low and variable current efficiencies, while high current efficiencies are nearly always obtained with fairly pure materials. The lower efficiencies are probably due to reactions brought about by the impurities. This subject requires further investigation.

As shown by Nef,[20] mannonic δ-lactone is obtained by evaporating a freshly prepared solution of mannonic acid. The equilibrium solution of mannonic acid contains a large quantity of γ-lactone and very little δ-lactone and free acid. Hence it is necessary to work rapidly and to take precaution to avoid the formation of γ-lactone. Mannonic δ-lactone crystallizes very readily but it will not crystallize from an equilibrium mannonic acid solution, in which respect it differs from gluconic δ-lactone. Crystalline mannonic acid is at present unknown.

1. CALCIUM MANNONATE

A 300 g sample of 20-mesh ivory nut meal is treated according to the method of Nelson and Cretcher (footnote 18) with 3 liters of boiling 1 percent sodium hydroxide and the mixture allowed to stand 30 minutes, with occasional stirring. It is then filtered through muslin, washed thoroughly, and dried in air. The purified meal (207 g) is mixed with an equal weight of 75 percent sulphuric acid and allowed to stand 22 hours at room temperature. Then the thick mass is mixed with 2.3 liters of water and heated to boiling. After 6 hours at about 100° C. the mixture is filtered and the hot filtrate neutralized with calcium carbonate.

The solution containing calcium sulphate in suspension is decolorized by the addition of about 10 g of activated carbon followed by filtration. If sufficient decolorizing carbon is not used the solution foams during distillation and must be treated again with carbon. It is then concentrated by distillation under reduced pressure to about 1.5 liters and the amount of sugar in solution is determined by

[18] Nelson and Cretcher, J.Amer.Chem.Soc., vol. 52, p. 404, 1930.
[19] Bernhauer and Irgang, Biochem.Z., vol. 249, p. 216, 1932.
[20] Nef, Ann., vol. 403, p. 306, 1914; also Hedenberg, J.Am.Chem.Soc., vol. 37, p. 345, 1915. This substance was originally called a "β"-lactone. See Goodyear and Haworth, J.Chem.Soc., p. 3136, 3144, 1927; also Haworth and Nicholson, J.Chem.Soc., p. 1899, 1926.

Fehling's method. The solution usually contains about 150 g of sugar calculated as mannose. After the addition of about 45 g of calcium carbonate and 20 g of calcium bromide the solution is electrolyzed, using an anode current density of 2 amperes/dm.^{2} When nearly all of the sugar has been oxidized electrolysis is stopped. The oxidation of crude mannose solution usually requires about 1.5 times the theoretical amount of current. Theoretically 1 mole of sugar requires 53.6 ampere hours. The electrolyzed solution is filtered, concentrated to about 400 ml, and refiltered hot. The resulting solution, seeded with calcium mannonate, and stirred during crystallization, will yield about 100 g. The crystalline salt, $Ca(C_6H_{11}O_7)_2 \cdot 2H_2O$ is separated by filtration. The calcium mannonate which remains in solution is precipitated as the basic salt by adding an excess of hydrated lime (60 g) to the mother liquor, essentially as described on page 656. After carbonation of the resulting basic salt additional calcium mannonate is obtained. The total yield is usually about 65 percent of that theoretically possible from the mannose in the solution.

2. MANNONIC δ-LACTONE

A dry mixture of 250 g of calcium mannonate and 67.6 g of crystalline oxalic acid is added in portions, with mechanical mixing, to 250 ml of water; the resulting solution is filtered and quickly cooled in an ice bath. An equal volume of dioxane is added and the solution is evaporated rapidly at 35° C. in vacuo. Crystalline mannonic δ-lactone separates as the solution is concentrated. It is advisable to separate the product in several fractions, as the first crystals are pure δ-lactone, while the later fractions are largely γ-lactone. The crystals are separated and washed with dioxane. About 115 g of pure δ-lactone (m.p. 158° to 160° C.) and 55 g of γ-lactone are usually obtained from the amounts stated. The δ-lactone can be obtained without the use of dioxane but the yield is less. The lactone can be recrystallized by dissolving it in the smallest possible amount of water at room temperature, filtering the resulting solution, adding an equal volume of dioxane, and evaporating rapidly in vacuo until a crop of crystals is obtained. The δ-lactone is difficult to purify as it is easily converted into γ-lactone. It is necessary to work rapidly and to avoid high temperatures. In 5 percent aqueous solution $[\alpha]_D^{20} = 114.8°$, 2 minutes after solution, +30.3° after 24 hours. These values agree approximately with the results obtained by Goodyear and Haworth (footnote 20).

3. MANNONIC γ-LACTONE

The calcium is removed from 100 g of calcium mannonate in 100 ml of hot water by treatment with 27 g of oxalic acid. After filtration the aqueous mannonic acid is evaporated in vacuo in the presence of a few drops of hydrochloric acid. When the solution becomes concentrated, crystallization occurs. Evaporation is continued, however, until the residue is nearly solid and the hydrogen chloride is largely evaporated. The resulting crude lactone is recrystallized from water. By carefully working up the mother liquors a nearly quantitative yield is obtained. The product melts at 151° to 152° C. and gives $[\alpha]_D^{20} = +51.5°$, 2 minutes after solution. Fischer and Hirschberger[21] originally reported the melting point as 149°–153° and $[\alpha]_D^{20} = +53.81°$, while Nef (footnote 20) found $[\alpha]_D^{20} = +51.8°$.

[21] Fischer and Hirschberger, Ber., vol. 22, p. 3218, 1889.

V. GALACTONIC ACID AND ITS DERIVATIVES

As early as 1862 Barth and Hlasiwetz [22] prepared galactonic acid and its γ-lactone. The constitution of these substances was uncertain until studied by Schnelle and Tollens [23] and by Nef.[24]

Galactonic acid differs from the other sugar acids in that it is easily crystallized from water. It then contains 2 molecules of water for each molecule of acid,[25] but if crystallized from hot aqueous alcohol the product contains only 1 molecule of water for each 2 molecules of acid. Nef designated the latter product ortho-bis-galaconic acid. The more highly hydrated product gives up water easily and is difficult to prepare in pure state. The ortho-bis-galactonic acid is more stable but even this on treatment with dehydrating agents yields the anhydrous form. The γ-lactone also forms a hydrate which on careful drying becomes anhydrous.

Galactonic δ-lactone has not been prepared in the crystalline state although a solution of it may be obtained by the oxidation of galactose with bromine water in the presence of a buffer.[26] The δ-lactone exhibits a dextro rotation and is hydrolyzed fairly rapidly. In this respect it differs widely from the γ-lactone which is hydrolyzed very slowly and only to a small degree.

The most convenient source of galactonic acid is calcium galactonate prepared by the electrolytic oxidation of galactose in the presence of a bromide and calcium carbonate (RP328). Calcium galactonate is more difficultly soluble than most salts of the sugar acids and crystallizes very easily. Hence it may be prepared by the electrolytic method from the hydrolytic products derived from lactose,[27] or better, from galactan-bearing plants such as agar-agar or the Western larch.[28]

1. GALACTONIC ACID

Equivalent quantities of finely powdered oxalic acid and calcium galactonate are added, with stirring, to 1 g of hot water for each g of calcium galactonate. The mixture is shaken about 3 minutes and the resulting aqueous galactonic acid is filtered and cooled. Crystalline galactonic acid hydrate separates at once. A second crop may be obtained by the addition of about four volumes of absolute ethyl alcohol. One experiment, using 100 g of calcium galactonate, yielded a first crop of 16 g (m.p. 120° to 124° C.), and a second crop (from alcohol) of 21 g (m.p. 125° to 127° C.). The dihydrate first described by Kiliani gives up water easily even by air-drying at room temperature, thereby forming the hydrate $(C_6H_{12}O_7)_2 \cdot H_2O$, termed ortho-bis-galactonic acid by Nef (footnote 24). The crude product is usually a mixture of the two forms melting at any point between 120° and 140° C. The dihydrate melts at 118° to 120° C., and the ortho-bis acid at 140° to 142° C. The latter may be conveniently prepared by crystallization from aqueous alcohol as described by Nef.

The anhydrous acid has recently been obtained by Brackenbery and Upson (footnote 4) by treating sodium galactonate with acetic acid.

[22] Barth and Hlasiwetz, Ann., vol. 122, p. 96, 1862.
[23] Schnelle and Tollens, Ann., vol. 271, p. 81, 1892.
[24] Nef, Ann., vol. 403, p. 273, 1914.
[25] Kiliani, Ber., vol 55, p. 95, 1922.
[26] Isbell and Hudson, B.S.Jour. Research, vol. 8, (RP418), p. 332, 1932.
[27] Kiliani, Ber., vol. 65B, p. 1269, 1932.
[28] A process for preparing a galactose solution from Western larch is described by Acree in U.S. Patent No. 1816136, dated July 28, 1931.

We have found that the anhydrous form may be prepared by digesting the crude hydrate for 5 or 10 minutes with boiling dioxane. The product so obtained melts at 148° C. $[\alpha]_D^{20} = -13.6°$ (2 minutes).

2. GALACTONIC γ-LACTONE

An aqueous solution of galactonic acid is prepared from equivalent quantities of calcium galactonate (100 g) and oxalic acid (24.2 g) by using about 2 parts of hot water for each part of calcium galactonate. After filtration a few drops of concentrated hydrochloric acid are added and the solution concentrated to about 100 ml, after which an equal volume of secondary amyl alcohol is added and the mixture concentrated to a thick sirup. A second addition of secondary amyl alcohol and further boiling in vacuo results in a sirup which on seeding or scratching gives crystalline anhydrous galactonic γ-lactone. After being cooled and allowed to stand for about 1 hour the crystals are separated by filtration and washed with a 50 percent mixture of absolute ethyl and secondary amyl alcohols. A second crop of crude anhydrous γ-lactone crystals is obtained by evaporating the mother liquors. The total yield is nearly quantitative.

The crude anhydrous galactonic γ-lactone may be purified by recrystallization from hot absolute ethyl alcohol.

Galactonic γ-lactone melts at 110° to 112° C. and gives $[\alpha]_D^{20} = -77.4°$.

These values agree with the results of Nef (footnote 24). The anhydrous lactone is easily converted into the hydrated form, which melts at 66° C. A 100 g sample of galactonic γ-lactone is dissolved in 35 ml of boiling water. After the addition of 150 ml of isopropyl alcohol, cooling, and seeding, crystallization occurs. About 85 g of nearly pure galactonic γ-lactone hydrate (m.p. 66° C.) is obtained. Additional product may be reclaimed from the mother liquors. The lactone hydrate may be prepared also by crystallization from aqueous acetic acid as described by Levene and Meyer.[29]

VI. ARABONIC ACID AND ITS DERIVATIVES

Arabinose occurs in many gums and other plant products, frequently in combination with galactose and other sugars. The best sources are mesquite and cherry gums. The gum is hydrolyzed with acid, the excess acid neutralized with calcium carbonate, the solution concentrated, and the arabinose extracted with methyl alcohol. After evaporating the alcohol the resulting crude arabinose may be used directly for preparing calcium arabonate by means of the electrolytic method (RP328). The acid is easily separated from the impurities as the crystalline calcium salt [30] or the basic calcium salt reported in table 2.

Crystalline arabonic acid was prepared first by Hauers and Tollens [31] and again by Böddener and Tollens,[32] but it was not correctly identified until recently.[33] It crystallizes well, resembling galactonic acid in many respects. The crystalline acid can be separated easily from

[29] Levene and Meyer, J.Biol.Chem., vol. 46, p. 307, 1921.
[30] Kiliani, Ber., vol. 19, p. 3029, 1886.
[31] Hauers and Tollens, Ber., vol. 36, p. 3321, 1903.
[32] Böddener and Tollens, Ber., vol. 43, p. 1645, 1910.
[33] Rehorst, Ber., vol. 63B, p. 2279, 1930.

a concentrated aqueous solution, particularly by using dioxane as outlined below. Arabonic δ-lactone is unknown at present, but as shown by Isbell and Hudson (footnote [26]), it is dextrorotatory and is hydrolyzed comparatively rapidly. Arabonic γ-lactone [34 35] was prepared first by evaporation of aqueous arabonic acid. This method requires considerable time and is not as satisfactory as dehydration of the aqueous acid by distillation with butyl alcohol in a manner analogous to the preparation of gluconic γ-lactone (footnote 9).

1. ARABONIC ACID

Equivalent quantities of calcium arabonate (75 g of $Ca(C_5H_9O_6)_2.5H_2O$) and oxalic acid (20.6 g), are mixed dry and added in portions to a small volume of water (100 ml). The resulting mixture is shaken continuously for 5 minutes and passed through a filter paper covered with kieselguhr into a flask kept in ice water. The residue is washed, first with a little water and then with dioxane. After addition of 125 ml of dioxane the solution is evaporated in vacuo at about 35° C. to approximately 50 ml, when 50 ml of dioxane is added and evaporation continued. Crystalline arabonic acid forms as the solution becomes quite concentrated. When the material in the flask has largely crystallized, evaporation is interrupted and 100 ml of dioxane is added. After standing for several hours the crystalline arabonic acid is separated, washed with dioxane, and air-dried at room temperature. The mother liquors on concentration at a low temperature yield a second crop of arabonic acid. The total yield is about 40 g or nearly 75 percent. The residues may be reclaimed as γ-lactone. The crude arabonic acid is recrystallized by dissolving it in an equal weight of water and repeating the above process. The product melts at 111° to 116° C. and gives $[\alpha]_D^{20} = -9.8°$, 2 minutes after solution.

2. ARABONIC γ-LACTONE

Equivalent amounts of oxalic acid (34 g) and calcium arabonate (124 g of $Ca(C_5H_9O_6)_2.5H_2O$) are mixed in 500 ml of hot water. The mixture is filtered and after the addition of a few drops of hydrochloric acid the solution is concentrated in vacuo to about 100 ml, when 150 ml of normal butanol is added. The solution is boiled down again to about 100 ml and 100 ml of butanol added. After a third concentration the solution is removed from the flask with the aid of 50 ml of butanol, and seeded. Crystallization begins at once, and a large crop of crystals forms in the course of half an hour. The crystalline product (46 g) is collected on a filter, washed with butanol, and dried at 30° C. in vacuo.

The mother liquors give additional lactone by concentrating in a current of air. The crude product can be purified by recrystallization from hot dioxane.

The lactone melts at 95° to 98° C. and gives $[\alpha]_D^{20} = -71.6°$, 2 minutes after solution.

Fischer and Piloty reported $[\alpha]_D^{20} = -73.9°$ and Böddener and Tollens −70.8°.

[34] Bauer, J. prakt. Chem., vol. 30, p. 380, 1884.
[35] Fischer and Piloty, Ber., vol. 24, p. 4218, 1891.

VII. RHAMNONIC ACID AND ITS DERIVATIVES

Rhamnonic acid forms two crystalline lactones[36 37 38] which crystallize readily and are easily prepared from an aqueous solution of rhamnonic acid. The crystalline acid is not known but aqueous solutions may be prepared from calcium or barium rhamnonate. The latter substances are obtained readily by the electrolytic oxidation of rhamnose in the presence of a bromide and calcium or barium carbonate (RP328). Calcium rhamnonate crystallizes in slender needles, which occlude the mother liquor, forming gelatinous masses from which it is difficult to separate the pure salt. A solution of calcium rhamnonate suitable for preparing the lactones can be easily obtained by means of the basic calcium salt reported in table 2. The method of preparation is analogous to that described for the preparation of calcium xylonate on page 656.

1. RHAMNONIC δ-LACTONE

A solution of 75 g of anhydrous calcium rhamnonate in 300 ml of water is treated at 60° C. with 23.7 g crystalline oxalic acid. After filtration the solution is evaporated at about 35° C. in vacuo and brought to crystallization. The product (45 g) is collected on a filter, washed with ethyl alcohol, and dried in vacuo.

A small second crop of δ-lactone is obtained by concentrating the mother liquor in vacuo. The residue, on evaporation in air, gives rhamnonic γ-lactone. Virtually all the product crystallizes. Rhamnonic δ-lactone melts at 172° to 182° C. and gives $[\alpha]_D^{20} = -100.4°$, 2 minutes after solution. Jackson and Hudson found the same melting point and $[\alpha]_D^{20} = -98.4°$, 7 minutes after solution.

2. RHAMNONIC γ-LACTONE

A solution containing 45.5 g of rhamnose, 15 g of barium bromide ($BaBr_2.2H_2O$), and 1 liter of water is placed with 25 g of barium carbonate in an electrolytic cell, and a current of 0.5 ampere is passed through the solution. After 15.5 ampere-hours about 96 percent of the sugar is oxidized with an anode efficiency of about 80 percent. When a Fehling's test is nearly negative electrolysis is stopped and the electrolyzed solution filtered.

The barium is removed by the addition of the required amount of sulphuric acid. The bromide ion is precipitated by the addition of the equivalent amount of silver carbonate after which a few drops of concentrated hydrochloric acid are added to make the solution strongly acid. The barium sulphate and silver bromide are separated by filtration and the aqueous rhamnonic acid is evaporated in vacuo to a thick sirup from which crystalline rhamnonic γ-lactone separates. The crystals are collected on a filter, washed with ethyl alcohol, and dried. The mother liquor gives additional material on evaporation, and the total yield is about 80 percent of the theoretical. The lactone is easily recrystallized from ethyl alcohol. It melts at 149° to 151° C. and gives $[\alpha]_D^{20} = -39.2°$, 2 minutes after solution. These values agree with those reported by other investigators.

[36] Will and Peters, Ber., vol. 21, p. 1813, 1888.
[37] Jackson and Hudson, J.Am.Chem.Soc., vol. 52, p. 1270, 1930.
[38] Votoček and Beneš, Bull. Soc. chim., vol. 43, p. 1330, 1928.

VIII. SUMMARY

Directions are given for the preparation of the more common aldonic acids and their lactones. The melting points and specific rotations of the acids and lactones are given in table 1.

The composition of the basic calcium salts reported in the paper are given in table 2. The samples were prepared by the method outlined in detail for the basic salt of xylonic acid (p. 657). Small variations in composition are inherent in the method of preparation, and since the products cannot be recrystallized because of hydrolysis, the analyses are on relatively crude salts.

TABLE 1.—*Specific rotations and melting points*

Substance	Formula	Melting point	Specific rotation [1]			
			2 minutes	5 minutes	10 minutes	24 hours
		°C.				
Gluconic acid	$C_6H_{12}O_7$	120–131	−6.9	−5.2	−4.2	+7.3
Gluconic γ-lactone	$C_6H_{10}O_6$	133–135	+68.0	+68.0	+68.0	+62.7
Gluconic δ-lactone	$C_6H_{10}O_6$	150–152	+66.2	+65.6	+63.9	+8.8
Galactonic acid	$C_6H_{12}O_7$	148	−13.6	−13.2	−13.0	−17.0
Galactonic γ-lactone hydrate	$C_6H_{10}O_6.H_2O$	65–66	−71.0	−71.0	−71.0	−70.6
Galactonic γ-lactone anhydrous	$C_6H_{10}O_6$	110–112	−77.4	−77.4	−77.4	−76.4
Mannonic γ-lactone	$C_6H_{10}O_6$	151–152	+51.5	+51.5	+51.5	+51.5
Mannonic δ-lactone	$C_6H_{10}O_6$	158–160	+114.8	+114.5	+114.2	+30.8
Rhamnonic γ-lactone	$C_6H_{10}O_5$	149–151	−39.2	−39.2	−39.2	−39.1
Rhamnonic δ-lactone	$C_6H_{10}O_5$	172–182	−100.4	−100.1	−99.6	−35.1
Xylonic γ-lactone	$C_5H_8O_5$	98–101	+91.8	+91.8	+91.8	+86.7
Arabonic acid	$C_5H_{10}O_6$	111–116	−9.8	−9.5	−9.3	−11.8
Arabonic γ-lactone	$C_5H_8O_5$	95–98	−71.6	−71.6	−71.6	−71.6

[1] Aqueous solutions containing 1.25 g of substance dissolved in 25 ml read at 20° C. in a 2 dm tube on a Bates saccharimeter. The factor 0.3462 was used to convert the ° S. to angular degrees.

TABLE 2.—*Basic calcium salts of aldonic acids*

Basic calcium salt of	Formula	Analysis			
		Found		Calculated	
		Total Ca	CaO	Total Ca	CaO
d-Gluconic [1]	$Ca(C_6H_{11}O_7)_2.2CaO$	22.10	20.30	22.12	21.65
d-Mannonic	$Ca(C_6H_{11}O_7)_2.2CaO$	23.51	22.45	22.12	21.65
d-Galactonic	$Ca(C_6H_{11}O_7)_2.2CaO$	24.06	23.02	22.12	21.65
d-Xylonic	$Ca(C_5H_9O_6)_2.2CaO$	25.05	22.74	24.90	23.24
l-Arabonic	$Ca(C_5H_9O_6)_2.2CaO$	24.85	22.89	24.90	23.24
l-Rhamnonic	$CaC_6H_{11}O_5)_2.2CaO$	24.32	22.05	23.50	21.93
Maltobionic	$Ca(C_{12}H_{21}O_{12})_2.4CaO$	20.52	22.93	20.45	22.90
Lactobionic [2]	$Ca(C_{12}H_{21}O_{12})_2.4CaO$	20.65	23.00	20.45	22.90

[1] Fischer, Ber., vol. 23, p. 2615, 1890.
[2] Hudson and Isbell, B.S.Jour. Research, vol. 3 (RP82), p. 60, 1929.

WASHINGTON, August 30, 1933.

U.S. Department of Commerce, Bureau of Standards

RESEARCH PAPER RP614

Part of Bureau of Standards Journal of Research, Vol. 11, November 1933

THE ISOLATION OF MESITYLENE, PSEUDOCUMENE, AND HEMIMELLITENE FROM AN OKLAHOMA PETROLEUM [1]

By Beveridge J. Mair [2] and Sylvester T. Schicktanz [2]

ABSTRACT

Mesitylene, pseudocumene, and hemimellitene have been isolated in very pure condition from a midcontinent petroleum. This has been accomplished by extracting with liquid sulphur dioxide the fraction distilling from 118° to 132° C. at 215 mm and fractionally distilling and crystallizing the extract. Selective sulphonation and crystallization of the sulphonic acids and their hydrolysis have also been employed. The boiling points, freezing points, refractive indices, densities, and infrared absorption spectra of these hydrocarbons have been measured. Mesitylene was found to have two crystalline modifications melting at −44.78° and −51.74° C., respectively.

The content of pseudocumene and hemimellitene in the crude petroleum was about 0.2 and 0.06 percent, respectively. The amount of mesitylene in the fraction extracted was about 0.02 percent of the crude. More mesitylene, however, may be expected in the lower boiling fractions.

CONTENTS

		Page
I.	Introduction	665
II.	Description of the fraction containing the trimethylbenzenes	666
III.	Extraction with sulphur dioxide and description of the sulphur-dioxide extract	666
IV.	Isolation of pseudocumene by physical methods	669
V.	Separation of pseudocumene and mesitylene	671
VI.	Pseudocumene from the pseudocumene mother liquor	671
VII.	Physical constants of pseudocumene	672
VIII.	Purification of mesitylene	673
IX.	Physical constants of mesitylene	673
X.	Crystalline modifications of mesitylene	674
XI.	Isolation of hemimellitene	674
XII.	Physical constants of hemimellitene	677
XIII.	Infrared absorption of the trimethylbenzenes	678
XIV.	Content of the trimethylbenzenes in the crude oil	679
XV.	Bibliography	679

INTRODUCTION

The occurrence of mesitylene (1, 3, 5-trimethylbenzene) and pseudocumene (1, 2, 4-trimethylbenzene) in petroleums of widely different origin has long been well established. LaRue and Müller (1)[3] in 1856 prepared the "sulphocumolate of barium" (probably the barium salt of pseudocumenesulphonic acid) from a Burma

[1] Financial assistance has been received from the research fund of the American Petroleum Institute. This work is part of Project No. 6: The Separation, Identification, and Determination of the Constituents of Petroleum.

[2] Research associate representing the American Petroleum Institute.

[3] Arabic numerals in parentheses here and throughout the text relate to the bibliography at the end of this paper.

petroleum. Engler (2) succeeded in separating the trinitro derivatives of mesitylene and pseudocumene by crystallization from hot alcohol, and by using this method on petroleums of different origin established the almost universal occurrence of these hydrocarbons. Markownikoff (3) established the presence of pseudocumene in a Caucasian petroleum by purifying the sulphonic acid, converting it into the corresponding acid chloride and amide, and determining the melting points of these derivatives. He also established the presence of mesitylene by crystallizing the nitro derivative from hot alcohol. Many other investigators (4) have established the presence of mesitylene and pseudocumene. All, however, used similar methods for proving the identity of the hydrocarbon, namely, isolation of a small quantity of one or more solid derivatives and measurement of its melting point.

The presence of hemimellitene (1, 2, 3-trimethylbenzene) in petroleum appears to have escaped detection until now.

Although rough estimates of the total quantity of mesitylene and pseudocumene in certain fractions of petroleum are available (2), based on the total nitro compounds isolated, no one appears to have separated the three trimethylbenzenes from each other and estimated their amounts in a particular petroleum.

This paper contains a description of the isolation of these hydrocarbons in a pure state by physical and chemical methods and an estimation of the amounts present in an Oklahoma petroleum (5).

II. DESCRIPTION OF THE FRACTION CONTAINING THE TRIMETHYLBENZENES

The petroleum, after a preliminary distillation in an oil refinery, was further fractionated with the aid of efficient rectifying columns (6), the final distillations being performed at a pressure of 215 mm. At this pressure, the fraction containing the trimethylbenzenes distilled from 118° to 130° C., which corresponds approximately to 162° to 174° C. at 760 mm. The distribution by volume of this fraction with respect to boiling range is shown in figure 1. The total volume of this fraction was 35,120 ml. This was combined with 5,050 ml of mother liquors of the fraction from which *n*-decane had been removed by equilibrium melting (7). Before the removal of *n*-decane this fraction distilled between 169.5° and 175° C. The volume and approximate boiling range at 215 mm of this fraction are shown by the shaded block in the lower right corner of figure 1. The high refractive indices of the *n*-decane mother liquors ($n_D^{20}=1.45$–1.46) indicated the presence of aromatics. The refractive indices of the rest of the fraction (a maximum of $n_D^{20}=1.452$ at 125° to 126° C. and minima $n_D^{20}=1.439$ at 118° to 119° C. and $n_D^{20}=1.436$ at 129° to 130° C.) were also higher than could be accounted for by the paraffins and naphthenes boiling in this region and suggested the presence of aromatics.

III. EXTRACTION WITH SULPHUR DIOXIDE AND DESCRIPTION OF THE SULPHUR-DIOXIDE EXTRACT

The 40-liter combined fraction described above was extracted with liquid sulphur dioxide at −35° to −50° C., in an extractor previously used for the isolation of the xylenes (8). Both the miscible

and immiscible portions were left standing over night in open vessels to allow a considerable portion of the sulphur dioxide to evaporate. The fractions were washed with a solution of sodium carbonate, then with water, and finally dried with anhydrous calcium chloride. The immiscible fraction was again fractionally distilled and the portions with high refractive indices again extracted.

The miscible portion was finally distilled once in the very efficient columns packed with jeweler's locket chain (9). The distribution by

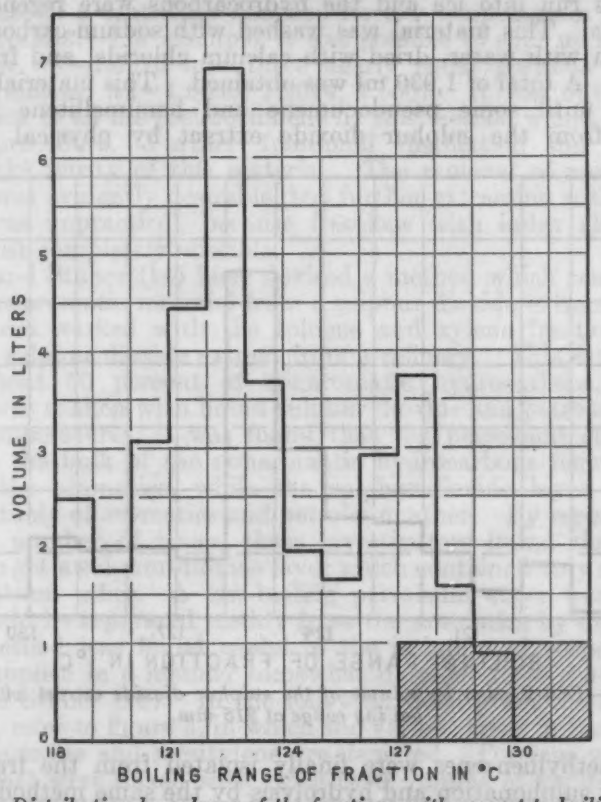

FIGURE 1.—*Distribution by volume of the fractions with respect to boiling range at 215 mm.*

volume of the miscible portion with respect to boiling range is shown in figure 2. The total volume of this distillate was 9,537 ml.

The refractive indices of these fractions ranged from the low value $n_D^{20}=1.456$ for the fractions distilling around 119° C. to the value $n_D^{20}=1.502$ for the fractions distilling between 125° and 126° C. The indices then decreased to $n_D^{20}=1.486$ at 127.5° C. and rose again to a maximum of $n_D^{20}=1.5116$ around 130° C. Crystals could be obtained only with difficulty from the fractions distilling below 123° C. because these became very viscous or glassy on cooling. In other fractions crystals appeared at from −90° to −120° C. The temperature at which crystals appeared rose from −73° C. for the fraction distilling at 123° C. to −50° C. for that distilling at 126° C. In the distillation range 126.5° to 127.5° C. the fractions became glassy.

Crystals again appeared in the distillates from 128° to 132° C., the maximum freezing point, −33° C., coinciding with the high refractive index $n_D^{20}=1.5116$ for the fraction distilling at 130° C.

In addition to the sulphur-dioxide extract just described, a further aromatic fraction was obtained by treating the immiscible portions with concentrated sulphuric acid. The fractions were stirred vigorously at room temperature for 22 hours with one fourth of their volume of 100 percent sulphuric acid. The sulphuric acid layer was run into ice and the hydrocarbons were regenerated by hydrolysis. This material was washed with sodium-carbonate solution, then with water, dried with calcium chloride, and fractionally distilled. A total of 1,030 ml was obtained. This material was kept separate until some pseudocumene and hemimellitene had been isolated from the sulphur dioxide extract by physical methods.[4]

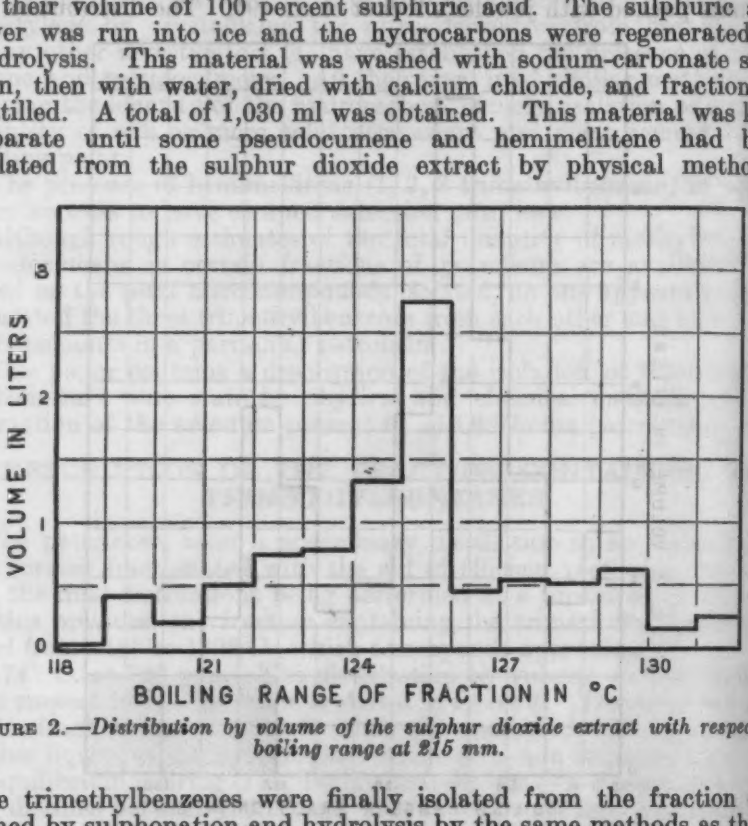

FIGURE 2.—*Distribution by volume of the sulphur dioxide extract with respect to boiling range at 215 mm.*

The trimethylbenzenes were finally isolated from the fraction obtained by sulphonation and hydrolysis by the same methods as those applied to the extract.

Some of the immiscible fractions were treated a second time with sulphuric acid. Since these showed no change in refractive index on this treatment, it was concluded that the aromatics had been completely removed and the fractions were reserved for the isolation of their other constituents.

[4] Baeyer (10) has shown that some of the hydrogenated aromatics on treatment with a nitric-sulphuric acid mixture yield nitro compounds of the atomatics. The extra hydrogen atoms apparently are oxidized. White and Rose (11) at this Bureau have confirmed this by obtaining nitromesitylene from 1, 3, 5-trimethylcyclohexane. The objection might consequently be raised that the isolation of the nitro compound, or any derivative where a strong oxidizing agent has been used, does not necessarily prove the existence of the aromatic itself. This objection is not valid for the trimethylbenzenes in the case of a petroleum which has been effectively fractionated by distillation and in which a narrow fraction 160° to 175° C. is used, since the trimethylcyclohexanes boil 15° to 20° C. lower. Another possible objection concerns the Jacobsen rearrangement. Jacobsen (12) has shown that durene and the pentamethylbenzenes undergo a rearrangement on treatment with concentrated sulphuric acid and that trimethylbenzenesulphonic acids are produced from durene. Since durene boils at 195° C., it is not likely to be present in the 160° to 175° C. region of a carefully fractionated petroleum.

IV. ISOLATION OF PSEUDOCUMENE BY PHYSICAL METHODS

From a consideration of the properties of the distilled extract described in the preceding paragraph, it was obvious that at least two aromatic hydrocarbons were present. The presence of pseudocumene was suspected in the region from 123° to 126° C. and of hemimellitene in that from 128° to 132° C. The isolation of pseudocumene was attempted first. Purification by equilibrium melting with the use of a centrifuge designed for low temperatures (13) gave only fair results. For example, it was possible to split up a fraction with index $n_D^{20}=1.5016$ into three nearly equal portions with the following indices: $n_D^{20}=1.5030$, 1.5014, 1.5007. It was obvious that the isolation of all the pseudocumene by this method would be a very tedious procedure. Further fractional distillation did little to improve the purity of this material. The removal of nonaromatic material was evidently desirable, but further extraction with sulphur dioxide was impractical, because fractions with index above 1.46 were almost completely miscible.

Tausz and Stüber (14) have devised a method which removes the bulk of nonaromatic material from a sulphur dioxide extract. These investigators worked with the toluene and xylene fractions of an Edeleanu sulphur dioxide extract from a refinery. This extract contained about 50 percent of nonaromatic hydrocarbons. If this material was shaken with liquid sulphur dioxide and petroleum ether at low temperatures, it was found that the petroleum ether layer contained the bulk of the nonaromatic hydrocarbons together with some of the atomatics, while the sulphur-dioxide layer consisted almost entirely of aromatics and petroleum ether. By repeating this process a number of times, these investigators found that it was possible to get a sulphur-dioxide layer which contained only aromatics and petroleum ether. A low-boiling petroleum ether was used so that it could be separated readily from the aromatics by distillation.

This method was found useful in the isolation of pseudocumene but was applied in a manner somewhat different from that used by Tausz and Stüber (14). In the following description the letters *A*, *B*, *C*, etc., refer to figure 3, in which the various steps in the isolation of pseudocumene and mesitylene are depicted. Portions of the distilled extract were mixed with twice their volume of low-boiling petroleum ether and run through the extractor at −40° C. (*A*). The petroleum ether was removed from the immiscible portion by distillation. The aromatic hydrocarbons in this portion had now decreased sufficiently so that it could be run through the extractor without the admixture of petroleum ether (*B*). The miscible portion thus obtained was then extracted after admixture with petroleum ether (*C*). The combined extracts were treated as before to remove sulphur dioxide and dried (*D*). They were then fractionally distilled (*E*). It was evident from the rise in the refractive indices that the greater part of the nonaromatics had been removed by this treatment.

Equilibrium melting and centrifuging were again applied to the fractions with indices above 1.50, which distilled between 124° and 126° C. (*F*). The fractions were, however, viscous at their freezing point and, as previously mentioned, only a fair separation was obtained. By mixing the fraction with 30 to 40 percent of dimethyl

ether,[5] the viscosity of the liquid was considerably diminished, and the texture of the crystals was improved. White, dry crystals were obtained on centrifuging. These crystals were wetted with a small quantity of dimethyl ether and again centrifuged. This method was about three times as effective as crystallization without a solvent.

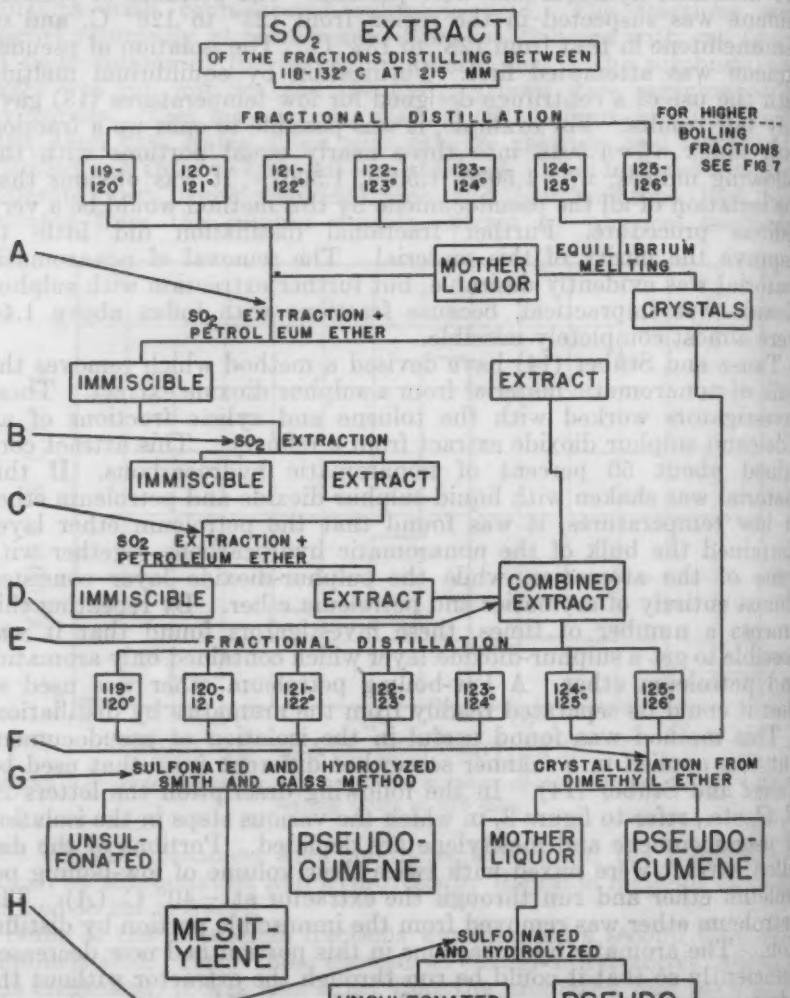

FIGURE 3.—*Chart showing the steps in the isolation of pseudocumene and mesitylene.*

The dimethyl ether was removed from the mother liquor by distillation and used over again. Before determining the physical constants of the crystal fraction, the last traces of dimethyl ether were removed by refluxing the sample for a few minutes in a long-necked flask. The pseudocumene thus obtained is listed in table 1 as "pseudocumene by physical methods."

[5] The dimethyl ether was furnished through the courtesy of E. I. duPont de Nemours and Co.

TABLE 1.—*Pseudocumene isolated from petroleum*

Method of isolation	Volume	Refractive index N_D^{25}	Freezing point in air	Purity
	ml		*°C.*	*mole, per-cent*[1]
Physical method	90	1.5025	−44.09	99.90
Do	610	1.5023	−44.6	98.56
Do	540	1.5015	−45.8	95.46
Do	340	1.5013	−46.6	93.44
By hydrolysis from mixtures with mesitylene	675	1.5022	−45.6	95.97
From mother liquors by hydrolysis	1,035	1.5025	−46.95	92.56

[1] The purity of the pseudocumene was calculated from equation (47), p. 203, E. W. Washburn, Principles of Physical Chemistry, McGraw-Hill Book Co., 1921. For the heat of fusion of pseudocumene the value 2,750 g-cal is/mole determined by Rossini (15) was used. It was assumed that the freezing point of pure pseudocumene was 0.04° higher than that of the best sample recorded above.

V. SEPARATION OF PSEUDOCUMENE AND MESITYLENE

Two aromatic hydrocarbons are reported in the literature with boiling points immediately below that of pseudocumene. These hydrocarbons and some of their constants are recorded below:

	B.P.$_{760}$	M.P.	n_D^{20}
	°C.	*°C.*	
Tertiary butylbenzene	168.7	−58.1	1.4969
Mesitylene	164.6	−51.7	1.4992

The presence of one or both of these hydrocarbons together with pseudocumene was suspected in the fractions distilling between 119° and 124° C. The low refractive indices of these fractions, $n_D^{20} = 1.491$ to 1.499, were in accord with this suspicion. Since these fractions became very viscous and froze at very low temperatures, −80° to −120° C., it was decided to attempt their separation by sulphonation and hydrolysis rather than by fractional crystallization.

An excellent method for the separation of mesitylene and pseudocumene, depending on the hydrolysis of mesitylenesulphonic acid from constant-boiling hydrochloric acid at 80° C. and subsequent hydrolysis of pseudocumenesulphonic acid from sulphuric acid at 130° to 140° C., has been developed by Smith and Cass (16). This method was applied to the fractions distilling between 119° and 124° C. (*G*, fig. 3), yielding only mesitylene, pseudocumene, and nonaromatic material. The recovery was about 90 percent. The presence of tertiary butylbenzene was not detected.

VI. PSEUDOCUMENE FROM THE PSEUDOCUMENE MOTHER LIQUORS

The mother liquors from the fractional crystallization of pseudocumene previously described (*F*, fig. 3), with refractive indices n_D^{20} from 1.497 to 1.500, contained nonaromatic material as their principal impurity.

These mother liquors were sulphonated, and steam was passed through the solution of the sulphonic acids at 105° to 110° C. to

remove the unsulphonated material. After this had been removed, more sulphuric acid was added and the pseudocumene hydrolyzed at 130° to 140° C. (*H*, fig. 3). The amount of pseudocumene thus obtained is listed in table 1.

VII. PHYSICAL CONSTANTS OF PSEUDOCUMENE

Values of certain physical constants for the best pseudocumene isolated from petroleum are compared in table 2 with values for synthetic material recorded in the literature. The agreement, although not perfect, establishes the identity of the hydrocarbon isolated from petroleum as pseudocumene. The density was determined by the Capacity and Density Section of this Bureau. The refractive index was measured with a calibrated Abbé refractometer (Valentine design) at 25.0 ± 0.1° C.

The freezing and boiling points were determined with a platinum-resistance thermometer and accessory apparatus described elsewhere (17). The first few attempts to determine the freezing point were not satisfactory. Fluctuations in temperature readings as great as

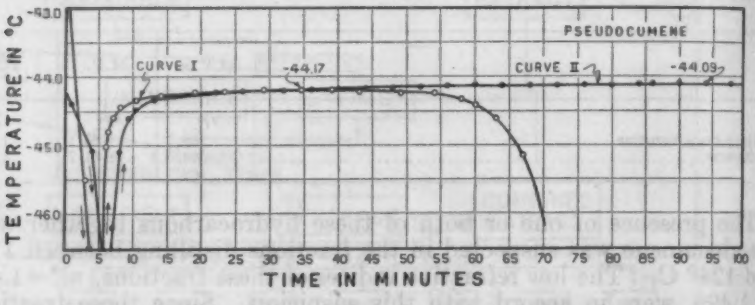

FIGURE 4.—*Time-temperature cooling curves for pseudocumene.*

0.2° C. were obtained in an individual experiment. The pseudocumene supercooled 6° or 7° C. and was very viscous at its freezing temperature. Presumably, equilibrium between the crystals and liquid was not readily attained. The fluctuations in temperature were found to depend on the rate of stirring; by stirring rapidly and uniformly the fluctuations were very much reduced and satisfactory freezing curves obtained. Curve *I*, figure 4, shows the freezing behavior when the vacuum-jacketed tube was immersed in carbon dioxide slush at −78° C. Crystallization of the pseudocumene was induced 4° C. below the freezing point by insertion of a brass rod cooled with liquid air. The maximum temperature attained, −44.17° C., occurred 32 minutes after the initiation of crystallization. At this time the pseudocumene was so nearly solid that stirring was difficult and was stopped about 4 minutes later. It seems probable that the true freezing point was not attained. Curve *II* shows the freezing behavior when the tube was immersed in *n*-nonane slush at −55° C. The maximum temperature attained in this instance was −44.09° C. The temperature was constant within 0.02° C. from the 54th to the 100th minute. In determining the boiling point two thirds of the sample was found to distil over within 0.03° C.

TABLE 2.—*Physical constants of pseudocumene*

Reference	Density at 20° C.	Refractive index n_D^{25}	Boiling point 760 mm	Freezing point in air
	g/ml		° *C.*	° *C.*
Mair and Schicktanz from petroleum	0.8762	1.5025	169.18	−44.00
Smith and Lund (18)		[1] 1.5027	169.1	−45.00
Smith and Cass (16)		[1] 1.5024		
Richards and Barry (19)			169.27	
von Auwers (20)	.876	[1] 1.5021	168.7—169.2	

[1] Corrected to 25° C., assuming $\frac{dn_D}{dt} = 0.0005$.

VIII. PURIFICATION OF MESITYLENE

The mesitylene separated by hydrolysis (*G*, fig. 3) was purified first by the method of Smith and Cass (16), that is, by crystallization of the sulphonic acid from cold 20 percent hydrochloric acid, followed by hydrolysis of the sulphonic acid with constant-boiling hydrochloric acid at 80° C. The mesitylene was then washed, dried, and distilled from sodium. In this manner 308 ml with $n_D^{25} = 1.4962$ was obtained. The freezing behavior showed that this material was not quite pure. After two crystallizations from a 50 percent solution in dimethyl ether a very pure sample was obtained. The dimethyl ether was removed by refluxing the mesitylene in a long-necked flask for a few minutes.

IX. PHYSICAL CONSTANTS OF MESITYLENE

Values of certain physical constants of mesitylene isolated from petroleum, determined in the same manner as those of pseudocumene, are compared in table 3 with values for synthetic material obtained by different observers. The material prepared by White and Rose (11) of this Bureau was obtained by condensation of acetone with sulphuric acid, and purified by fractional distillation in an efficient fractionating column and by fractional crystallization from dichlorodifluoromethane. The agreement between the values for the synthetic sample of White and Rose (11) and that from petroleum is excellent and leaves no question as to the identity of the hydrocarbon from petroleum. The slightly lower freezing point indicates that the synthetic sample was somewhat less pure than that from petroleum.

TABLE 3.—*Physical constants of mesitylene*

Reference	Density at 20° C.	Refractive index n_D^{25}	Boiling point 760 mm	Freezing point in air
	g/ml		° *C.*	° *C.*
Mair and Schicktanz from petroleum	0.8653	1.4967	164.64	(α) −44.78 (δ) −51.74
White and Rose (11)	.8654	1.4967	164.65	(α) −44.83 (δ) −51.83
Richards and Barry (19)			164.72	
Richards and Shipley (21)	.8634			
Mass and Russell (22)			164.5	−53.5
von Auwers (20)	.862	[1] 1.4942	165—166	
Smith and Cass (16)		[1] 1.4949		

[1] Corrected to 25° C., assuming $\frac{dn_D}{dt} = 0.0005$.

X. CRYSTALLINE MODIFICATIONS OF MESITYLENE

It was found that mesitylene had two crystalline modifications, as shown by the time-temperature cooling curves in figures 5 and 6. When the sample was cooled while stirring in the ordinary manner, the lower-freezing (δ) modification was obtained. When, however, a brass rod cooled with liquid air was inserted in the freezing tube be-

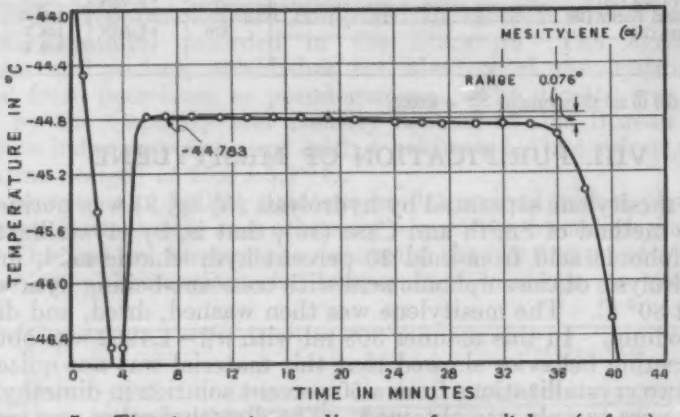

FIGURE 5.—*Time-temperature cooling curve for mesitylene (α form).*

tween −44.78° and −51.74° C. the higher freezing (α) modification resulted.

The purity of the mesitylene was calculated on the assumption that the freezing point of pure mesitylene was higher than the initial freezing point of this sample by an amount equal to the difference between the initial freezing temperature and the temperature when half the sample was frozen. For the latent heat of fusion of the α

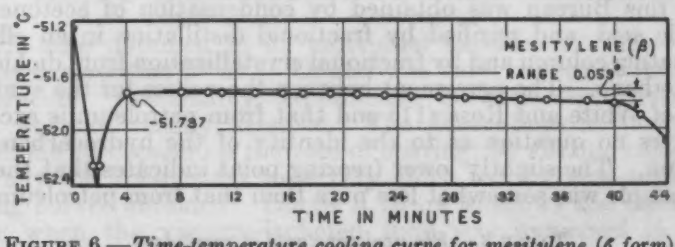

FIGURE 6.—*Time-temperature cooling curve for mesitylene (δ form).*

modification the value 2,280 g-cal.$_{15}$ per mole, obtained by Rossini (15) was used. The purity of the mesitylene calculated in this manner was 99.95 mole percent.

XI. ISOLATION OF HEMIMELLITENE

The letters *A*, *B*, *C*, etc., throughout the following description refer to figure 7 which shows diagrammatically the isolation of hemimellitene. The fractions which distilled between 128° and 132° C. crystallized readily (*A*). These fractions were combined in two portions according to refractive indices (*B*). One portion with refractive index above 1.50 was crystallized from a solution containing 30 to 40 percent of dimethyl ether (*C*) and yielded pure hemimellitene. The

other portion with refractive index below 1.50 was extracted again after admixture of petroleum ether (*D*) in a manner similar to that described for pseudocumene. The extract was fractionally distilled and the distillates combined according to whether their refractive indices were above or below 1.50 (*E*). The portion with refractive index

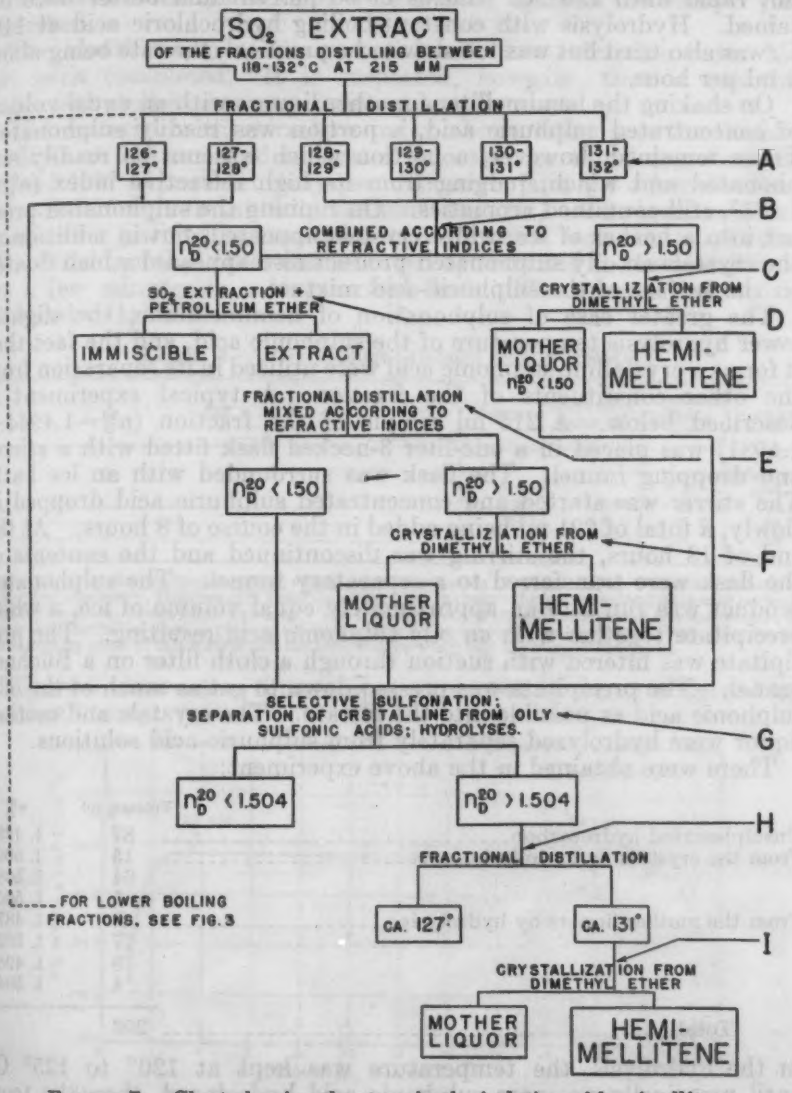

FIGURE 7.—*Chart showing the steps in the isolation of hemimellitene.*

above 1.50 yielded a further sample of hemimellitene on crystallization from dimethyl ether (*F*). When the freezing points of the mother liquors became so low that the use of a centrifuge at the temperatures of solid carbon dioxide was no longer feasible, it was decided to continue the separation by sulphonation and hydrolysis.[6]

[6] Although only solid carbon-dioxide slush was used in the centrifuge jacket, liquid air was used to crystallize the fraction. The effective range of the centrifuge was thus increased somewhat.

Preliminary experiments showed that hemimellitene sulphonates about as readily as pseudocumene. White crystals were obtained when the sulphonated product was run into ice. The hydrolysis of the sulphonic acid from a sulphuric-acid solution was just detectable at 110° C. and progressed with fair speed at 120° to 125° C. It was not rapid until 130° C. Yields of 90 percent and better were obtained. Hydrolysis with constant-boiling hydrochloric acid at 110° C. was also tried but was too slow to be practical, the rate being about 1 ml per hour.

On shaking the hemimellitene mother liquors with an equal volume of concentrated sulphuric acid, a portion was readily sulphonated. There remained, however, a portion which was not so readily sulphonated and which, judging from its high refractive index (n_D^{20}= 1.475), still contained aromatics. On running the sulphonated product into a beaker of ice, white crystals appeared, but in addition to the crystals an oily sulphonated product also appeared which floated on the surface of the sulphuric-acid mixture.

The greater ease of sulphonation of hemimellitene, the slightly lower hydrolysis temperature of the sulphonic acid, and the fact that it forms a crystalline sulphonic acid were utilized in its separation from the other constituents of the fraction. A typical experiment is described below. A 215 ml sample of the fraction (n_D^{20}=1.4944–1.4981) was placed in a one-liter 3-necked flask fitted with a stirrer and dropping funnel. The flask was surrounded with an ice bath. The stirrer was started and concentrated sulphuric acid dropped in slowly, a total of 221 ml being added in the course of 8 hours. At the end of 13 hours, the stirring was discontinued and the contents of the flask were transferred to a separatory funnel. The sulphonated product was run into an approximately equal volume of ice, a white precipitate together with an oily sulphonic acid resulting. The precipitate was filtered with suction through a cloth filter on a Büchner funnel. The precipitate was pressed down to get as much of the oily sulphonic acid as possible into the filtrate. The crystals and mother liquor were hydrolyzed separately from sulphuric-acid solutions.

There were obtained in the above experiment:

	Volume, ml	n_D^{20}
Unsulphonated hydrocarbon	87	1.4888
From the crystals by hydrolysis	15	1.5097
	64	1.5081
	5	1.5068
From the mother liquors by hydrolysis	3	[1] 1.4871
	17	1.5021
	8	1.4964
	4	1.5045
Total	203	

In the hydrolysis, the temperature was kept at 120° to 125° C. until practically no more sulphonic acid hydrolyzed, then the temperature was slowly raised to 180° C. In every case, a very small amount of highly refractive material came over at a high temperature. A possible explanation for this is that a second hemimellitenesulphonic acid, hydrolizing at a higher temperature than the first, is formed in small quantities. The entire fraction distilling from 126°

[1] Unsulphonated.

to 132° C. was treated in this manner (*G*). This included the hemimellitene mother liquors and some material in the region from 127° to 128° C. which it had not been possible to crystallize. The lower fractions around 126° C. contained some pseudocumene also. The fractions were collected according to refractive index and those with a refractive index below 1.504 were treated again in the manner just described.

The identification of the material with low refractive index has not been completed. It is suspected, however, that it contains either isobutylbenzene or secondary butylbenzene.

The material with refractive index above 1.504 was fractionally distilled at 215 mm and separated into two fractions, one distilling around 127° C., substantially pseudocumene, and the other distilling around 131° C., substantially hemimellitene (*H*). The hemimellitene was further purified by fractional crystallization from dimethyl ether (*I*). The dimethyl ether was removed by refluxing the hemimellitene for a few minutes in a long-necked flask. The amount isolated is recorded in table 4.

TABLE 4.—*Hemimellitene isolated from petroleum*

Lot	Volume	Refractive index n_D^{25}	Freezing point in air	Purity [1]
	ml		*° C.*	*Mole per cent*
I	280	1.5116	−25.47	99.95
II	510	1.5115	−26.21	98.75
III	80	1.5062	−51	62

[1] The purity of the hemimellitene was calculated from equation 47, p. 203, E. W. Washburn, Principles of Physical Chemistry, McGraw-Hill Book Co., 1921. For the heat of fusion the value 2,000 g-cal[15] per mole obtained by F. D. Rossini (15) was used. The freezing point of pure hemimellitene was assumed to be higher than the initial freezing point of the best sample by an amount equal to the difference between the initial freezing point of this sample and the temperature when half the sample was frozen.

Figure 8 shows the time-temperature cooling curve obtained on hemimellitene.

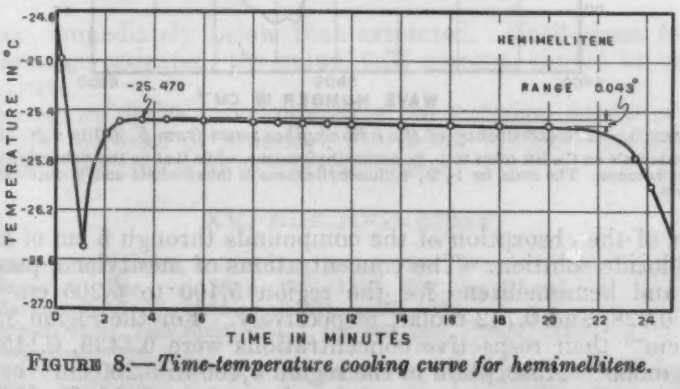

FIGURE 8.—*Time-temperature cooling curve for hemimellitene.*

XII. PHYSICAL CONSTANTS OF HEMIMELLITENE

The physical constants of hemimellitene were determined in a manner similar to that employed with mesitylene and pseudocumene. These constants are recorded in table 5 together with values reported by von Auwers (20). Judging from the boiling range, the sample of

von Auwers was not pure and the agreement consequently is as good as could be expected. At least there is no question as to the identity of the hydrocarbon from petroleum, since all the other aromatic hydrocarbons boiling near 176° C. have much lower densities and refractive indices.

TABLE 5.—*Physical constants of hemimellitene*

Reference	Density at 20° C.	Refractive index n_D^{25}	Boiling point 760 mm	Freezing point in air
	g/ml		*° C.*	*° C.*
Mair and Schicktanz from petroleum	0.8951	1.5116	176.10	−25.47
von Auwers (20)	.895	[1] 1.5107	175.8–176.8	

[1] Corrected to 25° C., assuming $\frac{dn_D}{dt}$=0.0005.

XIII. INFRARED ABSORPTION SPECTRA OF THE TRIMETHYLBENZENES

Transmission curves of the three trimethylbenzenes at the wave numbers indicated on the graphs (figs. 9 and 10) were obtained from

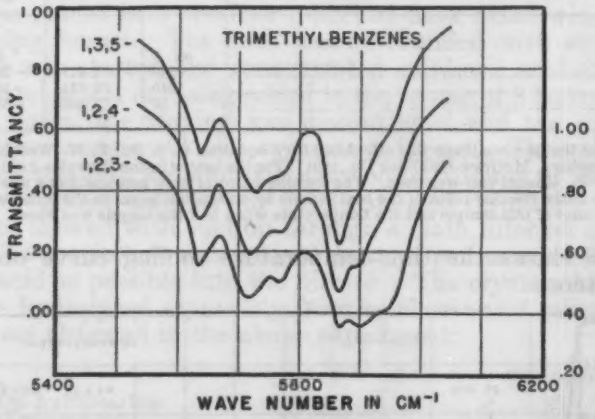

FIGURE 9.—*Transmittancy of the trimethylbenzenes from 5,400 to 6,200 cm⁻¹.*

The ordinate scale on the left refers to 1-, 3-, 5-trimethylbenzene, while that on the right refers to 1-, 2-, 3-trimethylbenzene. The scale for 1-, 2-, 4-trimethylbenzene is intermediate and is displaced 0.2 from the others.

records of the absorption of the compounds through 5 cm of carbon tetrachloride solution. The concentrations of mesitylene, pseudocumene and hemimellitene for the region 5,400 to 6,200 cm^{-1} were 0.718, 0.728, and 0.742 molar, respectively. For the region 8,100 to 8,900 cm^{-1} their respective concentrations were 0.1436, 0.1456, and 0.1484 molar. Absorption in the region 5,400 to 6,200 cm^{-1} has been assigned as the first overtone of the absorption of the *C—H* linkage around 2,900 cm^{-1}, and that between 8,100 and 8,900 cm^{-1} as the second overtone of the same band. The band near 8,700 cm^{-1} is to be attributed to the nuclear *C—H* linkages and that around 8,400 cm^{-1} to the side chains. These curves were obtained by U. Liddel, of the Bureau of Chemistry and Soils, and Charles Kasper, of the

Bureau of Standards. A further discussion of these bands and correlations with other hydrocarbons will appear shortly in a paper by Liddel and Kasper.

XIV. CONTENT OF THE TRIMETHYLBENZENES IN THE CRUDE PETROLEUM

Based upon the total amount of the crude petroleum used (600 gallons of specific gravity 0.9) and making reasonable allowances for losses during fractionation, it is estimated that the amounts of pseudocumene and hemimellitene in the crude petroleum are about 0.2 and 0.06 percent, respectively.

The amount of mesitylene in the fraction extracted was about 0.02 percent of the crude petroleum. Since the extraction was carried only as far as the fractions distilling 2° C. below the boiling point of mesitylene, it is possible that more mesitylene will be found in the

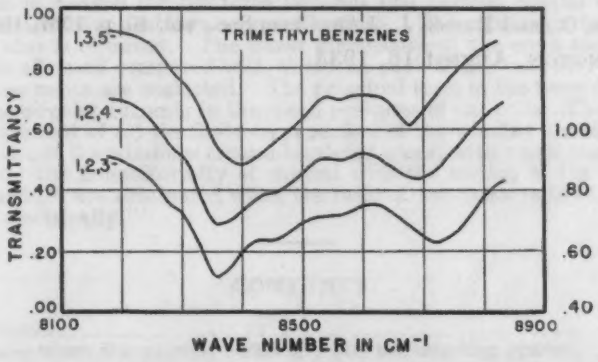

FIGURE 10.—*Transmittancy of the trimethylbenzenes from 8,100 to 8,900 cm⁻¹.*

The ordinate scale on the left refers to 1-, 3-, 5-trimethylbenzene, while that on the right refers to 1-, 2-, 3-trimethylbenzene. The scale for 1-, 2-, 4-trimethylbenzene is intermediate and is displaced 0.2 from the others.

fractions immediately below that extracted. Until these fractions have been investigated, the value, 0.02 percent, should be regarded as tentative.

The authors desire to acknowledge the technical advice of E. W. Washburn, Director of American Petroleum Institute project no. 6, throughout the course of this investigation.

XV. BIBLIOGRAPHY

1. de La Rue, Warren, and Müller, Hugo, Proc. Roy. Soc., vol. 8, p. 221, 1856.
2. Engler, C., Ber., vol. 18, p. 2234, 1885; Ber., vol. 12, p. 2187, 1879.
3. Markownikoff, W., Ann., vol. 234, p. 97, 1886.
4. Engler-Höfer, Das Erdöl, vol. 1, pp. 362, 363, Hirzel, Leipzig, 1913, and the references cited there.
5. Washburn, E. W., Bruun, J. H., and Hicks, M. M., B.S. Jour. Research, vol. 2, p. 469; table 1, 1929.
6. (*a*) Washburn, E. W., Bruun, J. H., and Hicks, M. M., B.S. Jour. Research, vol. 2, p. 470, 1929; (*b*) Leslie, R. T., and Schicktanz, S. T., B.S. Jour. Research, vol. 6, p. 378, 1931; (*c*) Bruun, J. H., and Schicktanz, S. T., B.S. Jour. Research, vol. 7, p. 851, 1931.

7. Bruun, J. H., and Hicks-Bruun, M. M., B.S. Jour. Research, vol. 8, p. 584, 1932.
8. (*a*) Leslie, R. T., B.S. Jour. Research, vol. 8, p. 591, 1932; (*b*) White, J. D., and Rose, F. W., Jr., B.S. Jour. Research, vol. 9, p. 711, 1932.
9. Schicktanz, S. T., B.S. Jour. Research, vol. 11, p. 89, 1933.
10. Baeyer, A., Ann., vol. 155, p. 275, 1870.
11. White, J. D., and Rose, F. W., Jr., B.S. Jour. Research (unpublished).
12. Jacobsen, O., Ber., vol. 19, p. 1209, 1886. See also Smith, L. I., and Lund, A. P., J.Am.Chem.Soc., vol. 51, p. 2994, 1929.
13. Hicks-Bruun, M. M., and Bruun, J. H., B.S. Jour. Research, vol. 8, p. 528, 1932.
14. Tausz, Jeno, and Stüber, A., Z.angew.Chem., vol. 32, I, pp. 175–6, 1919.
15. Rossini, F. D., B.S. Jour. Research, vol. 11, pp. 553–9, 1933.
16. Smith, Lee I., and Cass, Oliver W., J.Am.Chem.Soc., vol. 54, p. 1603, 1932.
17. Mair, B. J., B.S. Jour. Research, vol. 9, p. 457, 1932.
18. Smith, Lee I., and Lund, A. P., J.Am.Chem.Soc., vol. 52, pp. 4144 to 4150, 1930.
19. Richards, T. W., and Barry, F., J.Am.Chem.Soc., vol. 37, p. 999, 1915.
20. Auwers, K. v., Ann., vol. 419, p. 117–118, 1919.
21. Richards, T. W., and Shipley, J. W., J.Am.Chem.Soc., vol. 41, p. 2008, 1919.
22. Maas, O., and Russel, J., J.Am.Chem.Soc., vol. 40, p. 1567, 1918.

WASHINGTON, August 16, 1933.

U.S. DEPARTMENT OF COMMERCE, BUREAU OF STANDARDS

RESEARCH PAPER RP615

Part of Bureau of Standards Journal of Research, Vol. 11, November 1933

THE ATTRACTION BETWEEN COILS IN THE RAYLEIGH CURRENT BALANCE

By Chester Snow

ABSTRACT

A formula is derived for the force between two parallel coaxial coils whose winding channels have rectangular cross sections. The expression for the maximum force also is obtained. The linear dimensions of the cross section of the windings are all small compared with the mean radii of the coils and sixth-order terms in these ratios are neglected. The principal term in the force corresponds to two linear circular currents in the mean positions of the coils. The remaining terms take account of (*a*) the finite cross section of the winding channels, (*b*) the discrete nature of the windings (round insulated wires) with waste space between them, and (*c*) the nonuniformity of current over the section of the wire. The effects (*b*) and (*c*) are eliminated when the ratio of the mean radii of the coils is determined electrically.

CONTENTS

	Page
I. Introduction	681
II. The force when the current uniformly fills the winding spaces	682
III. The maximum force	684
IV. The fractional error in the maximum force	685
V. Correction for current distribution	686
VI. Conclusion	689

I. INTRODUCTION

The absolute measurement of an electric current by the use of a certain type of current balance requires the computation of the force $\mathfrak{F}$ between two coaxial coils in which electric currents I_1 and I_2 are circulating, and when the coils are so spaced as to make this force a maximum, which is then indicated by $\mathfrak{F}_m$.

If the distance between their mean planes is in the general case z (and z_m when the force is a maximum), and if their mean radii are a_1 and a_2, and if the axial breadth $2b_i$ and radial depth $2c_i$ (for $i=1,2$) of the rectangular cross sections of the winding channel are such that the quantities b_i and c_i are small compared to either of the three finite quantities a_1, a_2, or z, then the principal part of this force is n_1, n_2, I_1 I_2 F where n_i is the number of turns and F is the force between two circular, coaxial, unit-current filaments having the mean radii and lying in the mean planes z_1 and z_2 of the coils. This force F is a function of two dimensionless variables x and α.

$$\alpha \equiv \frac{a_2}{a_1} < 1,\ x \equiv \frac{z}{A},\ A^2 \equiv a_1^2 + a_2^2 \qquad (1)$$

where $z=z_1-z_2$. When x and α are known, $F(x, \alpha)$ may be computed with great precision by Maxwell's formula in terms of the complete elliptic integrals K and E with modulus k where

$$k^2=\frac{4a_1a_2}{(a_1+a_2)^2+z^2}=\frac{2\sqrt{1-\beta^2}}{1+x^2+\sqrt{1-\beta^2}} \text{ and } \beta\equiv\frac{1-\alpha^2}{1+\alpha^2} \tag{2}$$

$$F(x,\alpha)=\frac{\pi zk}{\sqrt{a_1a_2}}\left[\frac{2-k^2}{1-k^2}E-2K\right]=2\sqrt{2}\pi^2x(1-\beta^2)^{-\frac{1}{2}}k^4\phi'(k^2) \tag{3}$$

where $\phi'(k^2)$ denotes $d\phi/dk^2$ and

$$\phi=\frac{2}{\pi k}(K-E)-\frac{kK}{\pi} \tag{4}$$

The function ϕ satisfies the differential equation

$$k^4(1-k^2)\phi''=k^4\phi'+\frac{3}{4}\phi \tag{5}$$

The force $\mathfrak{F}$ between the actual coils obtained by integration over their cross sections will be expressible in the form

$$\mathfrak{F}(x,\alpha)=n_1n_2I_1I_2F(x,\alpha)[1+\Delta_2(x,\alpha)+\Delta_4(x,\alpha)\ \ldots] \tag{6}$$

where the functions of x and α designated by Δ_2 and Δ_4 are correction terms of the second and fourth order in the small constant ratios b_1/a_1, c_1/a_1, etc., and are to be found.

II. THE FORCE WHEN THE CURRENT UNIFORMLY FILLS THE WINDING SPACES

The force between two current filaments of radii r_1 and r_2 planes z_1' and z_2' may be expanded by Taylor's theorem in terms of the small quantities $z_1'-z_1$, $z_2'-z_2$, r_1-a_1, r_2-a_2. Integrating this over the two cross sections gives on neglecting terms of higher order than the fourth,

$$\frac{\mathfrak{F}}{n_1n_2I_1I_2}=F+\frac{1}{6}\left\{(b_1^2+b_2^2)D_z^2F+c_1^2D_{a_1}^2F+c_2^2D_{a_1}^2F\right\}$$

$$+\frac{1}{360}\Big\{[3(b_1^4+b_2^4)+10b_1^2b_2^2]D_z^4F+3(c_1^4D_{a_1}^4F+c_2^4D_{a_2}^4F) \tag{7}$$

$$+10c_1^2c_2^2D_{a_1}^2D_{a_2}^2F+10(b_1^2+b_2^2)(c_1^2D_{a_1}^2D_z^2F+c_2^2D_{a_2}^2D_z^2F)\Big\}$$

where the partial derivatives of F imply it is a function of three variables z, a_1, and a_2.

A first step in reducing this to a workable formula is to express all the partial derivatives in terms of z-derivatives and then these in terms of x-derivatives. Let F^{I}, F^{II}, etc., denote D_zF, D_z^2F, etc., so

that $D_s^n F = F^{(n)}/A^n$. Then it is found by the use of equations (1) to (5) that

$$\left.\begin{aligned} D_{a_1}^2 F &= -\frac{F^{II}}{A^2} - \frac{1}{2a_1^2}\left[\left(x - \frac{\beta}{x}\right)F^I + \frac{\beta}{x^2}F\right] \\ D_{a_2}^2 F &= -\frac{F^{II}}{A^2} - \frac{1}{2a_2^2}\left[\left(x + \frac{\beta}{x}\right)F^I - \frac{\beta}{x^2}F\right] \end{aligned}\right\} \tag{8}$$

By use of these, all the terms of second order in (7) may be expressed in terms of F, F^I, and F^{II}.

For the partial derivatives of fourth order which appear in (7), one finds.

$$\left.\begin{aligned} D_{a_1}^2 D_s^2 F &= -\frac{F^{IV}}{A^4} - \frac{1}{2A^2a_1^2}\left[\left(x - \frac{\beta}{x}\right)F^{III} + \left(2 + \frac{3\beta}{x^2}\right)F^{II} - \frac{6\beta}{x^3}F^I + \frac{6\beta}{x^4}F\right] \\ D_{a_2}^2 D_s^2 F &= -\frac{F^{IV}}{A^4} - \frac{1}{2A^2a_2^2}\left[\left(x + \frac{\beta}{x}\right)F^{III} + \left(2 - \frac{3\beta}{x^2}\right)F^{II} + \frac{6\beta}{x^3}F^I - \frac{6\beta}{x^4}F\right] \end{aligned}\right\} \tag{9}$$

It is also found that

$$\left.\begin{aligned} D_{a_1}^4 F &= -\frac{F^{IV}}{A^4} + \frac{F^{II}}{A^2a_1^2} - 2D_{a_1}^2 D_s^2 F \\ D_{a_2}^4 F &= -\frac{F^{IV}}{A^4} + \frac{F^{II}}{A^2a_2^2} - 2D_{a_2}^2 D_s^2 F \end{aligned}\right\} \tag{10}$$

and

$$D_{a_1}^2 D_{a_2}^2 F = -\frac{F^{IV}}{A^4} - D_{a_1}^2 D_s^2 F - D_{a_2}^2 D_s^2 E + \frac{1}{2a^2a^2}[(1+x^2)F^{II} + 3xF^I] \tag{11}$$

By use of (9) to (11) the term of fourth order in (7) is expressible in terms of F, F^I, $F^{II} \ldots F^{IV}$. It is then possible to express F^{II}, F^{III}, and F^{IV} in terms of F and F^I, for it is found from (1) to (5) that if a_1 and a_2 are constant the force F satisfies the ordinary differential equation in x.

$$(x^4 + 2x^2 + \beta^2)x^2F^{II} + (5x^4 + 2x^2 - 3\beta^2)xF^I - (2x^2 - 3\beta^2)F = 0 \tag{11}'$$

From this and the equation found by differentiating it successively, all derivatives of higher order than the first may be expressed in terms of F and F^I. However, for the purpose of computation, it is simpler not to make this elimination but to compute in succession the functions of x and α, λ_1, $\lambda_2 \ldots \lambda_4$, which are defined by

$$\left.\begin{aligned} \lambda_1 &\equiv \frac{xF^I}{F} \\ \lambda^2 &\equiv -\frac{x^2F^{II}}{F} = \frac{3\beta^2 - 2x^2 + (5x^4 + 2x^2 - 3\beta^2)\lambda_1}{x^4 + 2x^2 + \beta^2} \\ \lambda_3 &\equiv \frac{x^3F^{III}}{F} = \frac{4x^2 - (25x^4 + 4x^2)\lambda_1 + (11x^4 + 10x^2 - \beta^2)\lambda_2}{x^4 + 2x^2 + \beta^2} \\ \lambda_4 &\equiv -\frac{x^4F^{IV}}{F} = \frac{x^2[75x^2\lambda_1 - 3(23x^2 + 8)\lambda_2 + 16(x^2+1)\lambda_3]}{x^4 + 2x^2 + \beta^2} \end{aligned}\right\} \tag{12}$$

In this way the expression (7) leads to the form (6) where

$$\Delta_2(x,\alpha)=\frac{1}{12x^2}\left\{-\left[\frac{c_1^2}{a_1^2}-\frac{c_2^2}{a_2^2}\right]\beta-\left[(x^2-\beta)\frac{c_1^2}{a_1^2}+(x^2+\beta)\frac{c_2^2}{a_2^2}\right]\lambda_1 - \frac{2[b_1^2-c_1^2+b_2^2-c_2^2]}{A^2}\lambda_2\right\} \quad (13)$$

$$\Delta_4(x,\alpha)=\frac{1}{360A^2x^4}\left\{B_4\lambda_4-(B_3x^2-\beta B_1)\lambda_3-\left[5\left(\frac{c_1c_2A}{a_1a_2}\right)^2x^4+B_2x^2-3\beta B_1\right]\lambda_2 + 3\left[5\left(\frac{c_1c_2A}{a_1a_2}\right)^2x^4+2\beta B_1\right]\lambda_1-6\beta B_1\right\} \quad (14)$$

where

$$\begin{aligned}
B_1&=\frac{c_1^2}{a_1^2}[5(b_1^2+b_2^2-c_2^2)-3c_1^2]-\frac{c_2^2}{a_2^2}[5(b_1^2+b_2^2-c_1^2)-3c_2^2]\\
B_2&=\frac{c_1^2}{a_1^2}[5(b_1^2+b_2^2-c_2^2)-3c_1^2]+\frac{c_2^2}{a_2^2}[5b_1^2+b_2^2-c_1^2)-3c_2^2]\\
B_3&=\frac{c_1^2}{a_1^2}[9c_1^2+15c_2^2-10(b_1^2+b_2^2)]+\frac{c_2^2}{a_2^2}[9c_2^2+15c_1^2-10(b_1^2+b_2^2)]\\
B_4&=\frac{1}{A^2}[-3(b_1^4+c_1^4+b_2^4+c_2^4)+10(b_1^2c_1^2+b_2^2c_2^2)-10(b_1^2-c_1^2)(b_2^2-c_2^2)]
\end{aligned} \quad (15)$$

III. THE MAXIMUM FORCE

In the absolute measurement of current, the distance between the mean planes of the coils is adjusted by trial to a value z_m which makes $\mathfrak{F}$ a maximum. The corresponding value of x is x_m. The value z_0 (and x_0 corresponding) which makes $\mathfrak{F}$ a maximum is slightly different on account of the correction terms Δ_2 and Δ_4. If primes denote x-derivatives as before, the equation to determine x_m is

$$\frac{\mathfrak{F}^1(x_m,\alpha)}{\mathfrak{F}(x_m,\alpha)}=\frac{\mathfrak{F}^1(x_m,\alpha)}{\mathfrak{F}(x_m,\alpha)}+\frac{\Delta_2{}^1(x_m,\alpha)+\Delta_4{}^1(x_m,\alpha)}{1+\Delta_2(x_m,\alpha)}=0 \quad (16)$$

whereas the corresponding equation determining x_0 is

$$\frac{F^1(x_0,\alpha)}{F(x_0\alpha)}=0 \quad (16)'$$

Writing $x_m=x_o+\delta x_o$ in (16) and expanding the functions on the right in ascending powers of δx_o, and taking account of (16)′, shows that δx_o is a second-order quantity whose principal part is

$$\delta x_0=\frac{x_0^2\Delta'_2(x_0,\alpha)}{\lambda_2(x_0,\alpha)} \quad (17)$$

Consequently the maximum force $\mathfrak{F}_m=\mathfrak{F}(x_m,\alpha)$ is given to the fourth order inclusive by

$$\mathfrak{F}_m=n_1n_2I_1I_2F(x_0,\alpha)\left[1+\Delta_2(x_0,\alpha)+\Delta_4(x_0,\alpha)+\frac{(x_0\Delta'_2(x_0,\alpha))^2}{2\lambda_2(x_0,\alpha)}\right] \quad (18)$$

where

$$x_0\Delta_2'(x_0,\alpha)=\frac{1}{12x_0^2}\left\{2\beta\left(\frac{c_1^2}{a_1^2}-\frac{c_2^2}{a_2^2}\right)+\left[(x_0^2-\beta)\frac{c_1^2}{a_1^2}+(x_0^2+\beta)\frac{c_2^2}{a_2^2}\right]\lambda_2(x_0,\alpha)\right.$$

$$+2\frac{(b_1^2-c_1^2+b_2^2-c_2^2)}{A^2}\lambda_3(x_0,\alpha)\Big\} \tag{19}$$

$$\Delta_2(x_0,\alpha)=\frac{1}{12x_0^2}\left\{-\left(\frac{c_1^2}{a_1^2}-\frac{c_2^2}{a_2^2}\right)\beta-2\frac{(b_1^2-c_1^2+b_2^2-c_2^2)}{A^2}\lambda_2(x_0,\alpha)\right\} \tag{20}$$

The term $\Delta_4(x_0,\alpha)$ is computed from (14) and (15) for the value $x=x_0$ which makes $\lambda_1=0$ so that by (12) the functions λ_2, λ_3, and λ_4 become rational fractions in x_0^2 and β^2.

IV. THE FRACTIONAL ERROR IN THE MAXIMUM FORCE

In evaluating the small terms Δ_2, etc., the axial width $2b_1$ and radial depth $2c_1$ of the winding section must be measured. The mean radii of the coils (a_1 and a_2) may also be obtained from measurements with sufficient precision for this part of the computation. For the principal term $F(x_0)$ these enter only through their ratio $\alpha=a_2/a_1$ and this must be known with the highest precision although x_0 need be known only with moderate exactness since its error makes an uncertainty of second order in the force. The fractional error in $\mathfrak{F}_m$ due to this source is

$$\left(\frac{\delta\mathfrak{F}_m}{\mathfrak{F}}\right)_{x_0}=-\frac{3}{2}\cdot\frac{\beta^2-\frac{2}{3}x_0^2}{\beta^2+2x_0^2+x_0^4}\left(\frac{\delta x_0}{x_0}\right)^2\approx-.694\left(\frac{\delta x_0}{x_0}\right)^2 \text{ if } \alpha=.5 \tag{21}$$

approximately so that an error of 0.1 percent in x_0 would only make an error of 1.5 parts in a million in the force $\mathfrak{F}_m$. It is evident, therefore, that when α is known, x_0 may be obtained with ample precision by interpolation in the table 4 given by Dr. Grover.[1] This table gives $y_m\equiv z_0/a_1$ so that by (1)

$$x_0=\frac{y_m}{\sqrt{1+\alpha^2}} \tag{22}$$

An estimate of the fractional error introduced into the force (equation (18)) by all errors in measurement of the dimensions of the coils is found by taking the first-order variation of this equation. In doing this the δx_0 is omitted since by (21) it produces no variation of first order. Also the terms of fourth order in (18) may obviously be unvaried (since they are almost negligible themselves). Furthermore, in the term Δ_2 the errors δb_1 and δc_1 in the measurement of the cross-sectional dimensions of the coils will be dominant, while those caused by uncertainty in a_1, a_2, and x_0 will be here of no practical importance.

With this understanding, the first-order variation in $\mathfrak{F}_m$ is

$$\frac{\delta\mathfrak{F}_m}{\mathfrak{F}_m}=\frac{1}{2x_0^2}\left\{\beta\frac{\delta\alpha}{\alpha}+\frac{1}{3}\frac{c_1^2}{a_1^2}[(1+\beta)\lambda_2-\beta]\frac{\delta c_1}{c_1}+\frac{1}{3}\frac{c_2^2}{a_2^2}[(1-\beta)\lambda_2+\beta]\frac{\delta c_2}{c_2}\right.$$
$$\left.-\frac{(1+\beta)\lambda_2}{3}\frac{b_1^2}{a_1^2}\frac{\delta b_1}{b_1}-\frac{(1-\beta)\lambda_2}{3}\frac{b_2^2}{a_2^2}\frac{\delta b_2}{b_2}\right\} \tag{23}$$

[1] F. W. Grover: Bul. Bu. Stand. vol. 12, Sci. Paper No. 255, p. 372; 1915.

This is not final; it is necessary to express $\delta\alpha/\alpha$ in terms of quantities more directly measurable. The ratio α is obtained by measuring the current ratio I_2'/I_1' when the coils carrying these currents are made coplanar and produce equal axial components of magnetic field H at their common center.

If H be computed on the same assumption which has been made in deriving the formula for $\mathfrak{F}_m$, which is that the current uniformly fills the winding channels, it is found that

$$H_1=\frac{2\pi n_1 I_1'}{a_1}\left[1+\frac{J_1}{a_1^2}+\frac{G_1}{a_1^4}\right] \tag{24}$$

with a similar expression for H_2, where

$$J_i=\frac{c_i^2}{3}-\frac{b_i^2}{2} \text{ and } G_i=\frac{c_i^4}{5}-b_i^2c_i^2+\frac{3}{8}b_i^4 (i=1,2) \tag{24'}$$

When $H_1=H_2$ the ratio α is given (to the fourth order) by

$$\alpha=\tau\left\{1-\frac{1}{a_1^2}\left(J_1-\frac{J_2}{\tau^2}\right)+\frac{1}{a_1^4}\left[J_1^2-G_1+\frac{J_1J_2}{\tau^2}+\frac{G_2-2J_2^2}{\tau^4}\right]\right\} \tag{25}$$

where τ is the measured ratio n_2I_2'/n_1I_1'. The first variation of α is found from this (with the same assumptions as were used in getting (23)).

$$\frac{\delta\alpha}{\alpha}=\frac{\delta\tau}{\tau}-\frac{\delta J_1}{a_1^2}+\frac{\delta J_2}{a_2^2}=$$

$$=\frac{\delta\tau}{\tau}-\frac{1}{3}\left\{2\,\frac{c_1^2}{a_1^2}\frac{\delta c_1}{c_1}-2\,\frac{c_2^2}{a_2^2}\frac{\delta c_2}{c_2}-\frac{3b_1^2}{a_1^2}\frac{\delta b_1}{b_1}+\frac{3b_2^2}{a_2^2}\frac{\delta b_2}{b_2}\right\} \tag{26}$$

Introducing this value of $\delta\alpha/\alpha$ into (23) gives finally the fractional error in $\mathfrak{F}_m$

$$\frac{\delta\mathfrak{F}_m}{\mathfrak{F}_m}=\frac{1}{2x_0^2}\left\{\beta\frac{\delta\tau}{\tau}+\left[\frac{(1+\beta)\lambda_2}{3}-\beta\right]\left[\frac{c_1^2}{a_1^2}\frac{\delta c_1}{c_1}-\frac{b_1^2}{a_1^2}\frac{\delta b_1}{b_1}\right]+\left[\frac{(1-\beta)\lambda_2}{3}+\beta\right]\right.$$

$$\left.\left[\frac{c_2^2}{a_2^2}\frac{\delta c_2}{c_2}-\frac{b_2^2}{a_2^2}\frac{\delta b_2}{b_2}\right]\right\} \tag{27}$$

This expression is symmetric with respect to the two coils. This may be seen by noting that β and $\delta\tau/\tau$ are antisymmetric, while x_0^2 and λ_2 are symmetric with respect to the subscripts 1 and 2.

V. CORRECTION FOR CURRENT DISTRIBUTION

In this section are found corrections to $\mathfrak{F}_m$ and also to α (in both cases of fourth order), which are made necessary by the facts that (a) the wires are round, leaving some waste space in the winding channels, and (b) the current density may not be uniformly distributed over the section of each wire, as is generally assumed for steady currents. It is in fact possible that a theoretical examination might lend more probability to the so-called natural distribution in which the current density at any point in the wire is inversely proportional to its distance from the axis of the turn.

It will presently be seen that the correction due to current distribution which must be made in $\mathfrak{F}_m$ is compensated for by the correction which must be made in α when it is determined electrically—the resultant of the two corrections is of higher order than the fourth.

To obtain the correction (a) imagine each coil to consist of n_t turns of square wire all in contact, each having a uniform current distribution. Let $\mathfrak{F}_s$ denote the force between two such turns, one in coil no. 1, the other in no. 2. Since there is no waste space, the force $\mathfrak{F}$, equation (6), is $\Sigma\mathfrak{F}_s$, the summation being extended to all possible pairs of turns, one of which is in no. 1, the other in no. 2.

The force $\mathfrak{F}+\delta\mathfrak{F}^1$ between the actual coils which consist of discrete windings with wire of radius ρ_t will be the corresponding sum

$$\mathfrak{F}+\delta\mathfrak{F}^1=\Sigma\mathfrak{F}_c$$

where $\mathfrak{F}_c$ is the force between the two turns of circular wire which have the same mean plane and same mean radius as the pair of turns of square wire to which $\mathfrak{F}_s$ refers, the current being assumed to be uniform in both cases. If their mean planes are z_1 and z_2 and mean radii are r_1 and r_2, it is found by an expansion similar to (7) that $\mathfrak{F}_c-\mathfrak{F}_s=$

$$\frac{-I_1I_2F(x_1\alpha)}{12x^2}\left\{\left(\frac{c_1^2}{a_1^2}\epsilon_1'-\frac{c_2^2}{a_2^2}\epsilon_2'\right)\beta+\lambda_1\left[(x^2-\beta)\frac{c_1^2}{a_1^2}\epsilon_1'+(x^2+\beta)\frac{c_2^2}{a_2^2}\epsilon_2'\right]\right\} \quad (28)$$

+ terms of higher order than the fourth $\left(\text{where } x=\frac{z_1-z_2}{A}=\frac{z}{A}\right)$.

The term retained is in fact of the fourth order since the small quanties ϵ_t' are of the second order, defined by

$$\epsilon_t'=-\frac{a_t^2}{r_t^2}\cdot\frac{b_t}{nc_t}\left(1-\frac{3\rho_t^2n_t}{4b_tc_t}\right) \quad (28')$$

where $2\sqrt{\frac{b_tc_t}{n_t}}$ is the side of the square wire section and $2\rho_t$ the diameter of the circular wire. Since $\pi\rho_t^2n_t$ is the total metallic cross section, the fraction $1-\frac{3\rho_t^2n_t}{4b_tc_2}$ is approximately the fraction of cross section which is waste space. For ordinarily close windings, this will be of the order of magnitude (but never less than) $1-\frac{\pi}{4}=0.21$. Hence if the ratio of the diameter of the wire to a side of the cross section of the winding channel is of the same order as b_1/a_1, i.e., of the first order, then $1/n_1$ and ϵ' will be of the second order and the terms above representing $\mathfrak{F}_c-\mathfrak{F}_s$ are of the fourth order, and we may place $a_i^2/r_i^2=1$, $x=x_o$, which gives

$$\epsilon_i'=\frac{3}{4}\frac{\rho_i^2}{c_i^2}-\frac{b_i}{n_ic_i} \quad (i=1,2) \quad (29)$$

and

$$\mathfrak{F}_c=\mathfrak{F}_s-\frac{I_1I_2F(x_o,\,\alpha)}{12x_o^2}\,\beta\left(\frac{c_1^2}{a_1^2}\epsilon_1^1-\frac{c_2^2}{a_2^2}\epsilon_2^1\right) \text{ (since } \lambda_1(x_o,\,\alpha)=0).$$

Summing the $n_1 n_2$ elementary forces between pairs of turns of this type gives

$$\Sigma \mathfrak{F}_c = \mathfrak{F}_m + \delta \mathfrak{F}_m{}^1 = \Sigma \mathfrak{F}_s - \frac{n_1 n_2 I_1 I_2 F(x_0, \alpha)}{12 x_0^2} \beta \left(\frac{c_1^2}{a_1^2} \epsilon_1^1 - \frac{c_2^2}{a_2^2} \epsilon_2^1 \right)$$

Hence, since $\Sigma \mathfrak{F}_s = \mathfrak{F}_m$, we find for this fourth-order correction

$$\frac{\delta \mathfrak{F}_m^1}{\mathfrak{F}_m} = -\frac{\beta}{12 x_0^2} \left(\frac{c_1^2}{a_1^2} \epsilon_1^1 - \frac{c_2^2}{a_2^2} \epsilon_2^1 \right) \tag{30}$$

This takes account of the fact that the coils are wound with wire of circular section having a certain amount of waste space between them. This $\delta \mathfrak{F}_m'$ must be added to the second member of (18) to get the maximum force between the actual coils.

For the correction (b), consider the current density i_1 in a round wire in coil no. 1 to be a function of the distance r_1' of a point in this turn from the axis of the turn. Then expanding to the second order we find

$$i_1 = \frac{I_1}{\pi \rho_1^2} \left[1 + C_1 \left(\frac{r_1^1 - r_1}{r_1} \right) + \frac{C_1^1 \frac{\rho_1^2}{4} - (r^1 - r_1^2)}{r_1^2} \right]. \tag{31}$$

For uniform distribution $C_1 = C'_1 = 0$; for the natural distribution $C_1 = C_1' = -1$. If F_s' is the force between two circular turns when the current distribution is given by (31) and F_s as defined above, the force between them when their current is uniformly distributed, we find with an expansion similar to (7) by integrating over their sections that $F_s' - F_s$ is a small quantity of the fourth order which is obtained by replacing the ϵ_i' in the second member of (28) by ϵ_i'' where

$$\epsilon_i'' = \frac{3}{2} C_i \frac{\rho_i^2}{c_i^2} \tag{32}$$

Hence by a similar argument the correction to the force F_m due to this cause is given by

$$\frac{\delta F_m''}{F_m} = -\frac{\beta}{12 x_0^2} \left(\frac{c_1^2}{a_1^2} \epsilon_1'' - \frac{c_2^2}{a_2^2} \epsilon_2'' \right) \tag{33}$$

The correction $\delta^* \mathfrak{F}_m = \delta \mathfrak{F}_m' + \delta \mathfrak{F}_m''$ due to waste space and to non-uniformity of current in each wire is given by

$$\frac{\delta^* \mathfrak{F}_m}{\mathfrak{F}_m} = -\frac{\beta}{12 x_0^2} \left(\frac{c_1^2}{a_1^2} \epsilon_1 - \frac{c_2^1}{a_2^2} \epsilon_2 \right) \text{ where } \epsilon_i = \epsilon_i' + \epsilon_i''. \tag{34}$$

The details in computing these two effects on the magnetic field H produced by the coils are so similar to those just sketched that they need not be given. The final result is that (24) is only altered by a change in J_i so that $(24)^a$ has to be replaced by

$$J_i = \frac{c_i^2}{3} \left(1 - \frac{\epsilon_i}{2} \right) - \frac{b_i^2}{2} \tag{35}$$

The result of this change is to add a term $\delta^*\alpha/\alpha$ to the second member of (26) where

$$\frac{\delta^*\alpha}{\alpha}=\frac{1}{6}\left(\frac{c_1^2}{a_1^2}\epsilon_1-\frac{c_2^2}{a_2^2}\epsilon_2\right) \tag{36}$$

The contribution of $\delta^*\alpha/\alpha$ to the second member of (23) is

$$\frac{\beta}{12x_c^2}\left[\left(\frac{c_1}{a_1}\right)^2\epsilon_1-\left(\frac{c_2}{a_2}\right)^2\epsilon_2\right],$$

which is exactly canceled by the correction (34) to $\mathfrak{F}_m$ which must be made at the same time. Thus, after taking account of these two distribution effects (to the fourth order), we come back to precisely the earlier equation (27) for the fractional error in the force. But this equation (27) was derived from the expression (18) for the maximum force. Moreover (18) was derived by assuming that the current uniformly filled the winding channels, that is, by neglecting both of these distribution effects. We arrive then at the following conclusion.

VI. CONCLUSION

If the ratio α of the mean radii of the coils of the current balance is determined electrically and this value is used in the computation of the maximum force between the coils using equation (18), the force thus computed will differ from the maximum force between the *actual* coils by an amount which, compared to this force, is a small quantity of order higher than the fourth in the small quantities $\frac{b_1}{a_1}$, $\frac{c_1}{a_1}$, $\frac{b_2}{a_2}$, and $\frac{c_2}{a_2}$, where $2\,b_i$ and $2\,c_i$ are the axial breadth and radial depth respectively of the rectangular cross sections of the winding channels—provided also that the number of turns n_i in each coil is so large that $1/n_i$ is in each case $i=1$ and $i=2$ a small quantity of the order of $(b_i/a_i)^2$ or smaller. These conditions are met in practice. The effects of errors in measurement of cross sectional dimensions may be computed by equation (27). This conclusion rests upon the derivation of equation (18) and also upon the investigation of section V, where account is taken of the facts that the actual coils consist of many turns of round wire with waste space between them, and that the current may not be uniformly distributed over the section of the wires (although the distribution is assumed to be of the same nature in all wires). This section appears, therefore, to give a greater validity to the force equation (18) than was to be expected from the mode of its derivation for it was derived on the assumption that the current uniformly filled the winding channels. The crux of the matter is the electrical determination of the ratio of the radii. If this ratio α were determinable with the desired precision by geometrical measurements of the coils, the conclusion stated above would not be true. In that case, the computation of the force would require a knowledge of the correction term δ^*F_m of (34), which would then be added to the second member of (18).

WASHINGTON, August 8, 1933.

U.S. Department of Commerce, Bureau of Standards

RESEARCH PAPER RP616

Part of Bureau of Standards Journal of Research, Vol. 11, November 1933

FORMULA FOR SPECIFIC VOLUMES OF SATURATED VAPORS

By Cyril H. Meyers

ABSTRACT

A formula for calculating the specific volume of saturated vapors is given. This formula expresses the specific volume of the vapor in terms of the vapor pressure, the specific volume of the liquid, and two empirical constants, one of which was the same for all the substances tried. The liquid volume need be known only approximately. For pressures up to one fourth the critical pressure, the formula represents the data on 23 substances within the experimental error. Graphs are given showing the application of the formula to 15 substances.

An equation of state applicable over a limited range, to superheated vapors, is developed from an approximation to this formula and an assumption in regard to the form of the isotherms.

In previous work on CO_2[1] it was desired to obtain from the available data the best possible value for the specific volume of carbon dioxide vapor at the triple point. With the aim of finding some relation which would make possible a reliable extrapolation to the triple point of the volumetric data at other temperatures, various functions of the vapor pressure, the orthobaric volumes, and the absolute temperature were examined. One formula was found to be particularly useful on account of its simplicity and close representation of the observed data at lower pressures. This formula employs a function of the deviation of the saturated fluid from the behavior of an ideal gas. An ideal gas is defined by the relation $\pi V/R\theta = 1$, where π is the pressure, V the specific volume, and θ is the temperature on thermodynamic scale, and R is the universal gas content divided by the molecular weight. The deviation in behavior of an actual fluid at the saturation limit from that of an ideal gas is therefore $\left(1 - \frac{\pi V}{R\theta}\right)$.

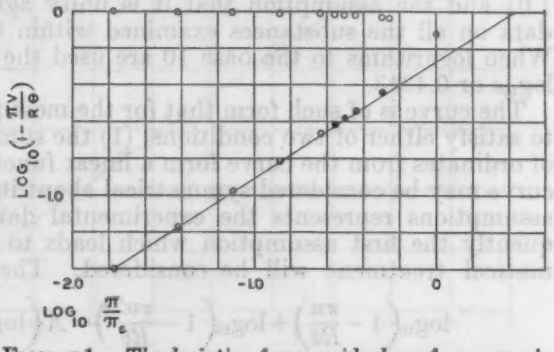

FIGURE 1.—*The deviation from an ideal gas for ammonia in the vapor and the liquid phases.*

Pressures for all points were taken from B.S.Sci. Papers, vol. 16, p. 1 (SP369), 1920.

○ Liquid volumes from B.S.Sci. Papers, vol. 17, p. 287 (SP420), 1921; vapor volumes from B.S.Sci. Papers, vol. 18, p. 707 (SP467), 1922.

● Volumes from Beattie and Lawrence, J.Am.Chem.Soc., vol. 52, p. 1264, 1929.

The logarithm of this expression bears a simple relation to the logarithm of the vapor pressure. The application of this relation to ammonia is illustrated in figure 1. The ordinate is the logarithm of

[1] B.S.Jour. Research (RP538), vol. 10, p. 381, 1933.

the deviation from an ideal gas or $\log_{10}\left(1-\frac{\pi V}{R\theta}\right)$ and the abscissa is $\log_{10}\frac{\pi}{\pi_c}$ where π_c is the critical pressure. The points shown represent experimental data for ammonia from $-20°$ C. up to the critical temperature. They lie along a smooth curve with the abscissa of the critical point equal to zero and with the liquid line approaching the axis $\log_{10}\left(1-\frac{\pi V}{R\theta}\right)=0$ at low pressures. Although very similar to a hyperbola the curve approaches its asymptotes more rapidly. In fact at one tenth the critical pressure the approach has been so close that the lower asymptote represents the observed value for the volume of the vapor within about 1 part in 1,000.

Similar curves were obtained for all substances tried and for most of them the abscissa of the intersection of the asymptotes is between 0.4 and 0.5. For ammonia and water on which accurate data are available the abscissa is between 0.43 and 0.44. This numerical value depends upon the number used for the base of the logarithms which has been chosen arbitarily for convenient use with our decimal system of numbers. If the Naperian system of logarithms is used the value of the abscissa for ammonia or water is between 0.99 and 1.01 and the assumption that it is unity agrees with the observed data on all the substances examined within the experimental error. When logarithms to the base 10 are used the corresponding value is $\log_{10}e$ or 0.4343.

The curve is of such form that for the most part is may be assumed to satisfy either of two conditions, (1) the sum of corresponding pairs of ordinates from the curve form a linear function of $\log\ \pi$, or (2) the curve may be considered symmetrical about its axis. Either of these assumptions represents the experimental data equally well, consequently the first assumption which leads to a more simple mathematical treatment will be considered. The resulting equation is

$$\log_{10}\left(1-\frac{\pi u}{R\theta}\right)+\log_{10}\left(1-\frac{\pi u''}{R\theta}\right)=A\left(\log_{10}\frac{\pi}{\pi_c}\right)-0.4343$$
$$=A\left(\log_{10}\frac{\pi}{2.718\pi_c}\right) \qquad (1)$$

where u is the specific volume of the liquid u' is the specific volume of the vapor, and A is a characteristic empirical constant.

The number 2.718 appearing in the right-hand term was obtained empirically. Although it was used in all calculations and the method of attacking the problem led to the Naperian number e, a number could have been used with equally good results which was 1 percent greater for ammonia or 1 percent less for water while the tolerance permitted by the data on most of the substances was several percent. If u and π are known functions of the temperature then only the constant A need be determined for the calculation of u' in the region where the equation is applicable. The linear relation fails to represent the experimental data as the critical pressure is approached, a fact which will be considered later and discussed more in detail. The relation expressed in equation (1) is illustrated by plotting $\log_{10}\left(1-\frac{\pi u}{R\theta}\right)\left(1-\frac{\pi u'}{R\theta}\right)$ as ordinate, and $\log_{10}\frac{\pi}{2.718\pi_c}$ as abscissa. Such

a diagram is shown for normal pentane in figure 2, where Young's data are represented by circles.

A considerable magnification of the scale used in figure 2 may be obtained by plotting as ordinate the differences between

$$\log_{10}\left(1-\frac{\pi u}{R\theta}\right)\left(1-\frac{\pi u'}{R\theta}\right)$$

and

$$A\log_{10}\frac{\pi}{2.718\pi_c}$$

instead of the actual values of

$$\log_{10}\left(1-\frac{\pi u}{R\theta}\right)\left(1-\frac{\pi u'}{R\theta}\right)$$

This has been done in figure 3 for ammonia, carbon dioxide, and water, the abscissa remaining unchanged. Supplementary abscissas in

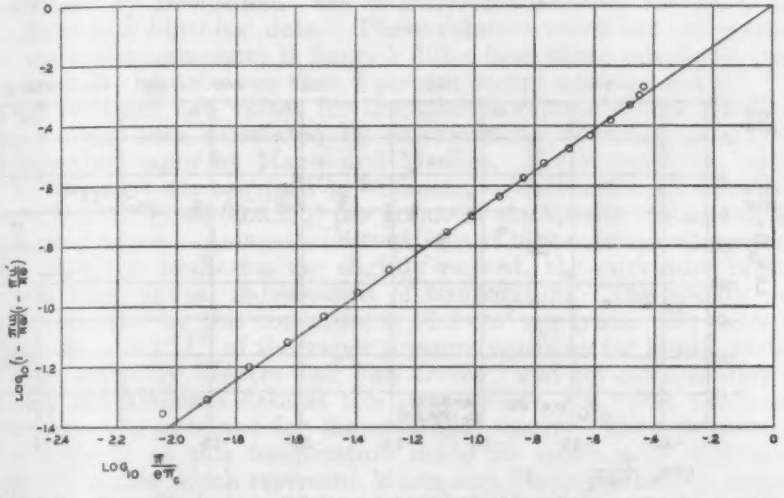

FIGURE 2.—*Logarithmic sum of the terms for the liquid and the vapor of n-pentane.*

degrees centigrade have been marked along the top of each part of figure 3. The dotted curves in the figures have been drawn to make possible a visual estimate of the differences between observed specific volumes of the vapor and those calculated from equation (1). The curves marked "*CC'*" are the loci of points for which these differences are 1 percent, those marked "*MM'*" are the loci for which the differences are 1 part in 1,000.

The critical pressure of ammonia, 111.5 atmospheres, corresponding to the temperature 132.4° C. was taken from International Critical Tables. Beattie and Lawrence [2] have observed vapor pressures which are 1 percent higher in the critical region than the values previously accepted. The use of the higher critical temperature 132.9° C. which was observed by Cardoso and Giltay [3] together with the vapor pressures observed by Beattie and Lawrence would lead to a critical

[2] J.Am.Chem.Soc., vol. 52, p. 1264, 1929.
[3] Arch. sci. phys. nat. Geneve, vol. 34, p. 20, 1912.

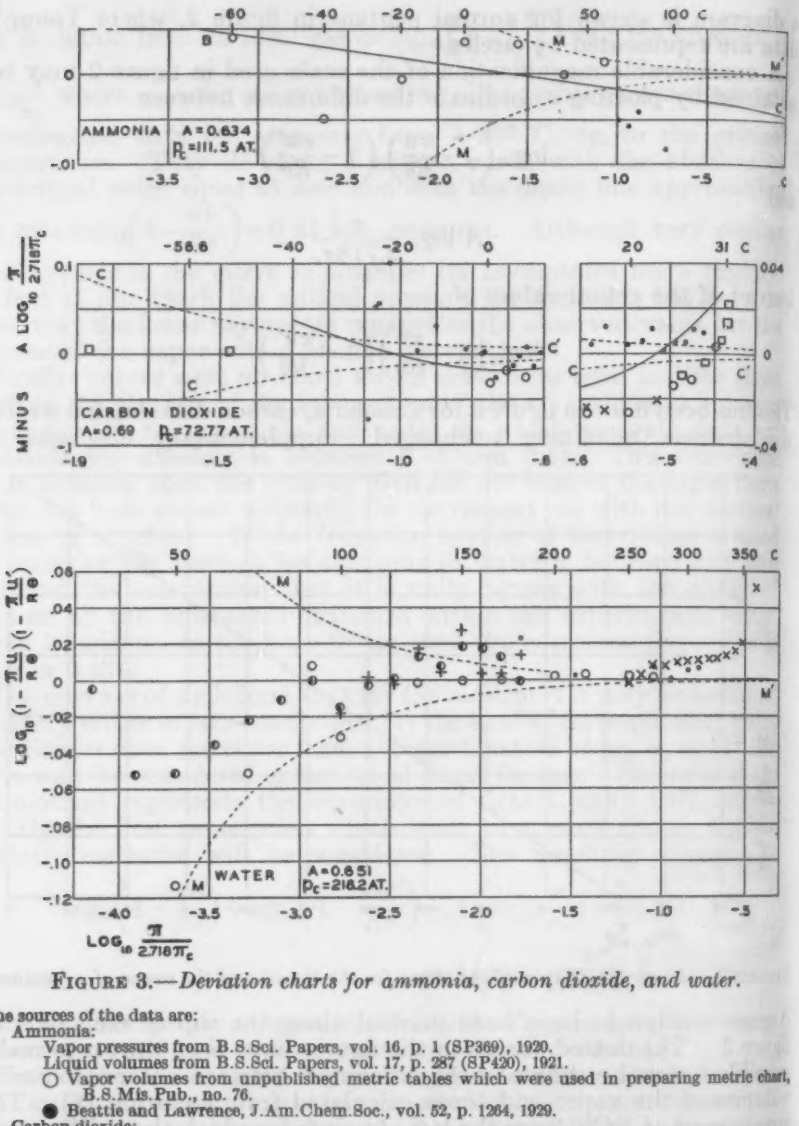

FIGURE 3.—*Deviation charts for ammonia, carbon dioxide, and water.*

The sources of the data are:

Ammonia:

Vapor pressures from B.S.Sci. Papers, vol. 16, p. 1 (SP369), 1920.

Liquid volumes from B.S.Sci. Papers, vol. 17, p. 287 (SP420), 1921.

○ Vapor volumes from unpublished metric tables which were used in preparing metric chart, B.S.Mis.Pub., no. 76.

● Beattie and Lawrence, J.Am.Chem.Soc., vol. 52, p. 1264, 1929.

Carbon dioxide:

Vapor pressures from B.S.Jour. Research (RP538), vol. 10, p. 381, 1933.

Liquid volumes from International Critical Tables, vol. 3, p. 236.

× Lowry and Erickson, J.Am.Chem.Soc., vol. 41, p. 2729, 1927.

○ Amagat Ann. chim. phys., vol. 29, p. 136, 1893. (Only a few of the published points are shown.)

● Cailletet and Mathias, J.de Phys. (Ser. 2), vol. 5, p. 549, 1886.

□ (Left-hand figure.) Maass and Mennie, Proc. Roy. Soc. London (Ser. A.), vol. 110, p. 198, 1926. (Extrapolated from superheat.)

□ (Right-hand figure.) Keesom. Comm. Phys. Lab. Leiden, no. 88, 1903.

— The continuous curve for carbon dioxide was calculated with the Clapeyron equation from data on latent heat as correlated by Bridgeman in International Critical Tables, vol. 5, p. 136.

Water:

Vapor pressures and $d\pi/d\theta$ at 100° C. and higher temperatures from Osborne, Stimson, Fiock, and Ginnings, B.S.Jour. Research (RP523) vol. 10, p. 155, 1933.

Vapor pressures and $d\pi/d\theta$ below 100° C. and liquid volumes from Keyes and Smith, Mech. Eng. vol. 53, p. 132, 1931.

○ $u'=\frac{\gamma}{\theta}d\pi/d\theta.\gamma$ from B.S.Jour. Research (RP209) vol. 6, p. 881, 1931; and B.S.Jour. Research (RP416), vol. 8, p. 321, 1932.

(Legend continued at bottom of page 695.)

pressure of about 113.4, and would necessitate the use of an origin in figure 3 for ammonia about 0.0045 lower, with a value of A about 0.004 smaller. The resulting equation would be represented by the straight line BC. Although this would improve the agreement with observed values somewhat, there would still be about 0.8 percent deviation from the specific volume at the highest pressure observed by Beattie and Lawrence. This illustrates how such a graph may be used to exhibit intercomparisons of various groups of experimental data and to adjust the value of A for the best representation of the data.

The observations on carbon dioxide by Cailletet and Mathias and by Amagat appear to be equally accurate, but there are differences in the observed vapor volumes of several percent. Although the more recent observations made by Keesom and by Lowry and Erickson are in agreement with those made by Amagat, the observations of Cailletet and Mathias follow better the trend of the formula. The volumes calculated with the Capeyron equation from the latent heats as correlated by Bridgeman [4] are intermediate between Amagat's and Cailletet and Mathias' data. These volumes which are represented by the continuous curve in figure 3 differ from those calculated from equation (1) by not more than 2 percent except near the critical. At lower pressures two values for the specific volume of the saturated vapor have been calculated by extrapolating observations on the superheated vapor by Maass and Mennie. If the isotherms on the PV, $1/V$ chart are assumed to be linear, extrapolation of their data at $-50.3°$ C. gives 56.0 cm³ per gram for the specific volume of the saturated vapor. Amagat's observations at higher temperatures indicate that the isotherms are slightly curved, the curvature in this region being almost independent of temperature. The specific volume corrected for this curvature is 56.2 cm³ per gram. By extrapolation to $-70.2°$ C. of the vapor pressure equation for liquid carbon dioxide given by Meyers and Van Dusen,[5] and by extrapolation of Maass and Mennie's data at this temperature, the value 189.2 cm³ per gram was obtained for the saturated vapor. The curvature of the isotherm at this temperature made no appreciable difference. The two points which represent Maass and Mennie's data in figure 3 correspond to the values 56.2 and 189.2 cm³, respectively.

The measurements on water, because of their accuracy and range, present a more exacting test for an equation than do the measurements on any other substance. Although there are consistent differences between the experimental data and values calculated from equation (1) as shown in figure 3 for water at 100° C. and at lower temperatures, these differences are probably no greater than the experimental error.

For part of the upper range of pressures the deviations in figure 3 become negative for carbon dioxide and ammonia, which corresponds to calculated values of u' smaller than those observed. For steam

[4] International Critical Tables, vol. 5, p. 138.
[5] See footnote no. 1.

● $u'=u+\frac{L}{\theta}\,d\pi/d\theta$. L observed by Jakob, Forsch. geb. Ingenieurw., no. 310, 1928.
+ Values of u' observed by Knoblauch, Linde, and Klebe, corrected by Jakob, same reference as preceding.
× Values of u' observed by Keyes and Smith, Mech. Eng., vol. 53, p. 132, 1931.
◑ $u'=u+\frac{L}{\theta}\,d\pi/d\theta$. L from Jakob's formulation of Henning's data, Forsch. geb. Ingenieurw. no. 310, 1928.

and several of the other substances to be considered later, however, there are no consistent deviations of this nature. Since these negative deviations in most cases are no greater than the experimental error, and since for carbon dioxide there are conflicting data, it is not certain whether these deviations are an indication of experimental error or of a defect of equation (1). There is no doubt, however, that the linear relation expressed in that equation fails in the critical region and gives values of u' which are too large. For steam and at least some other substances the range of the equation could be extended up to the critical point by making the quantity A a function of pressure or temperature increasing rapidly from an initial value at the critical and approaching asymptotically toward a constant limiting value at lower pressures, but the data available at present are not sufficient to determine a form of this function.

The values of A for 23 substances are given in table 1. Where the value of A is considered uncertain by more than 0.01 the mean value

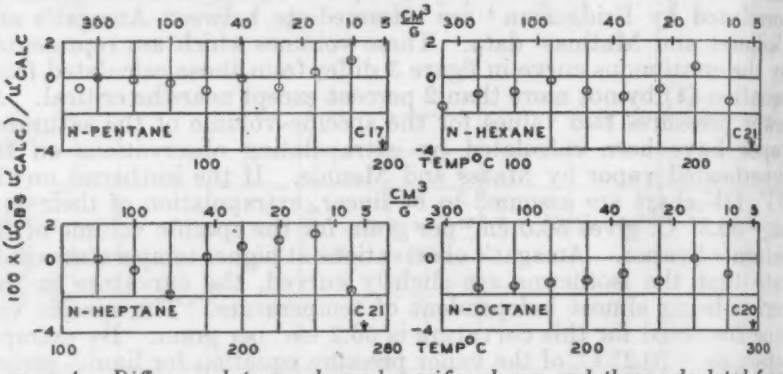

FIGURE 4.—*Difference between observed specific volumes and those calculated from equation (1) with $A=0.69$.*

is given together with the amount by which the value may be in error. Ammonia, water, and the alcohols which are not classed as normal substances have low values of A. The value 0.69 for methane is based on volumes calculated with the Clapeyron equation from unpublished data observed at the Bureau of Standards. The value of A for ethane was derived from data by Porter,[6] those for propane, normal and iso-butane from data by Dana, Jenkins, Burdick, and Timm,[7] and those for the remainder of the series from the data by Young.[8] The single value 0.69 appears to be applicable to the whole paraffin series within the experimental error of the data available. The deviations of Young's observed values for four substances of this series from those calculated with $A=0.69$ are represented in figure 4. The position of the critical point is marked by an arrow together with the letter C followed by a number which indicates the percent deviation.

[6] J.Am.Chem.Soc., vol. 48, p. 2051, 1926.
[7] Ref. Eng., vol. 12, p. 387, 1926.
[8] Proc. Roy. Dub. Soc., vol. 12, p. 374, 1909-10.

TABLE 1.—*Values of A for various liquids*

Substance	A	Substance	A
Ammonia	0.634	PARAFFIN SERIES	
Water	.651		
Carbon dioxide	.69	Methane	.69
Carbon tetrachloride	.69	Ethane	.69±.03
Benzene	.70±.02	Propane	.70±.05
Methanol	.61±.02	*n*-butane	.70±.05
Ethanol	.67±.03	iso-butane	.70±.05
Propyl alcohol	.64	*n*-pentane	.69
		iso-pentane	.69
RARE GASES		*n*-hexane	.69
		n-octane	.69
Helium	.72	di-iso-butyl	.67±.02
Neon	.72		
Argon	.72		
Xenon	.72		

A relatively large value of A (0.72) was obtained for the rare gases. Determinations of the orthobaric volumes of helium by Mathias, Crommelin, Onnes, and Swallow [9] and of the vapor pressure by Onnes, Weber, Keesom, Norgaard, and Schmidt [10] were used to determine A for helium. Since volumes and pressures were not in general measured at the same temperatures, the observed pressures were interpolated graphically.

Determinations of the orthobaric volumes of neon by Mathias, Crommelin, and Onnes [11] and of the vapor pressure by Crommelin and Gibson [12] were used. For interpolation between values of the vapor pressure, an equation of the form previously used for carbon dioxide [13] was found convenient. The equation is

$$\log_{10}\pi_{\text{atmos.}} = 3.5740 - \frac{1}{\theta}\{97.04 - 1.14(10)^{-9}(\theta^2 - 950)^3\} \qquad (2)$$

The average deviation from the observations is about 6 parts in 1,000 which corresponds to 0.02° C.

For interpolation of the values of the vapor pressure of argon the equation

$$\log_{10}\pi_{\text{atmos.}} = 3.9302 - \frac{1}{\theta}\{342.20 - 4.0(10)^{-12}(\theta^2 - 13200)^3\} \qquad (3)$$

was used. The average deviation from the data by Crommelin [14] and by Holst and Hamburger [15] is 1.7 parts in 1,000. The specfic volumes of argon were obtained from observations made by Mathias, Onnes, and Crommelin.[16]

For interpolation of the values of the vapor pressure of xenon the equation

$$\log_{10}\pi_{\text{atmos.}} = 3.9992 - \frac{1}{\theta}\{652.5 - 2.52(10)^{-13}(\theta^2 - 56000)^3\} \qquad (4)$$

was used. If it is assumed that an error of 1 meter of mercury was made in reporting the observation at −20° C by Patterson, Cripps,

[9] Leiden Comm., no. 172b.
[10] Leiden Comm., nos. 147b, 202b, and 202c.
[11] Leiden Comm., no. 162b.
[12] Leiden Comm., no. 185b.
[13] See footnote 1.
[14] Leiden Comm., no. 138c.
[15] Versl. Amst. vol. 24, p. 798, 1915; Zs. ph. Chem., vol. 91, p. 532, 1916.
[16] Leiden Comm., no. 131a.

and Gray,[17] the equation represents their data with an average deviation of 6 parts in 10,000. It represents the data at lower temperatures by Ramsay and Travers [18] and by Peters and Weil [19] within the precision of their data. The specific volumes of xenon were obtained from observations by Patterson, Cripps, and Gray.

The deviations of equation (1) from the observations on these rare gases are illustrated in figure 5. When the critical point is on the scale, it is labelled C, otherwise it is located in the same manner as in figure 4.

Methyl, ethyl, and propyl alcohol, and benzene are among the numerous substances observed by Young.[20] The latent heat of evaporation for methyl and ethyl alcohol, and benzene have been measured by Fiock, Ginnings, and Holton.[21] This gives two sets of values for these three substances, one entirely from Young's data, and the other from the latent heat data and Young's values of $d\pi/d\theta$. The first set is represented in figure 6 by circles and the second set

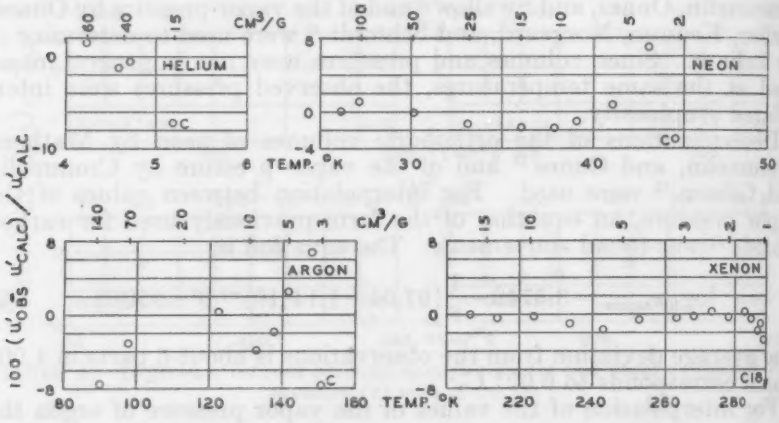

FIGURE 5.—*Difference between observed specific volumes and those calculated from equation (1) with $A=0.72$.*

by black dots. The zero line and the continuous curve for each substance represent volumes calculated from the values of A indicated.

Young's value for the density of methyl alcohol is higher by 0.00054 than that derived from the equation given on page 27 volume 3 of the International Critical Tables. This corresponds to a water content of about 0.3 percent. Young did not measure the density of the original sample of ethyl alcohol. It is probable that his samples of both of these alcohols contained water in sufficient quantities to render his values of both π and $d\pi/d\theta$ uncertain. The best average value of A for methanol and ethanol appears from figure 6 to be about 0.63 while the value for propyl alcohol is about 0.64. In view of the conclusions drawn for the paraffin series and the rare gases it is reasonable to assume that a single value of A applies to all the alcohols and that the best value obtainable from the data is 0.64.

[17] Proc. Roy. Soc. London, vol. 86, p. 579, 1912.
[18] Phil. Trans. Roy. Soc., vol. 197, p. 47, 1901.
[19] Zs. phys. Chemie, vol. A148, p. 27, 1930.
[20] See note no. 8.
[21] B. S. Jour. Research (RP312), vol. 6, p. 881, 1931.

Zmaczynski's [22] vapor pressure data for benzene differ consistently from Young's although the values of $d\pi/d\theta$ for the two are in good agreement up to 130° C.

In table 2 the values of specific volume of the vapor for ammonia, carbon dioxide, and water calculated from equation (1) using the values of A indicated in table 1, are presented and compared with the best available data.

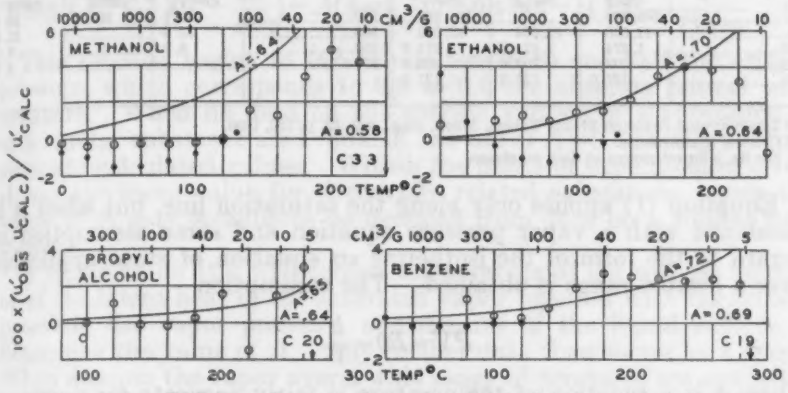

FIGURE 6.—*Difference between observed and calculated specific volumes.*

○ Pressures and volumes from Young. (See footnote 8.)
● Pressures and $d\pi/d\theta$ from Young.
γ from Fiock, Ginnings, and Holton. (See footnote 21.)

TABLE 2.—*Comparison of calculated specific volumes with observed values for the saturated vapors of ammonia, carbon dioxide, and water*

AMMONIA

Temperature, ° C.	Bureau [1] of Standards	Beattie [1] and Lawrence	Equation (1)	Temperature, ° C.	Bureau [1] of Standards	Beattie [1] and Lawrence	Equation (1)
	cm³/g	*cm³/g*	*cm³/g*		*cm³/g*	*cm³/g*	*cm³/g*
−77.7 [4]	15,685		15,688	40	83.26		83.25
−60	4,703		4,703	60	48.73		48.77
−40	1,552.1		1,551.6	67.90		40	39.85
−20	623.7		623.6	73.21		35	34.83
0	289.5		289.7	79.37		30	29.84
20	149.4		149.5	95.60		20	19.78

CARBON DIOXIDE

Temperature, ° C.	I.C.T. [2]	Plank [3] and Kuprianoff	Equation (1)	Temperature, ° C.	I.C.T. [2]	Plank [3] and Kuprianoff	Equation (1)
	cm³/g	*cm³/g*	*cm³/g*		*cm³/g*	*cm³/g*	*cm³/g*
−56.6 [4]		72.22	72.58	0	10.26	10.38	10.03
−50		55.41	55.59	10	7.57	7.52	7.19
−40		38.16	38.12	20	5.26	5.26	4.97
−30	27.19	27.00	26.80	30	3.00	2.99	2.97
−20	19.22	19.47	19.17	31 [4]	2.155	2.156	2.37
−10	13.83	14.19	13.86				

[1] See fig. 3 for references to data on ammonia.
[2] International Critical Tables, vol. 3, p. 236.
[3] Beiheft Zts. ges. Kalte-Ind., vol. 1, p. 9, 1929.
[4] Triple point temperature.

[22] J. chim. phys., vol. 27, p. 503, 1930.

TABLE 2.—*Comparison of calculated specific volumes with observed values for the saturated vapors of ammonia, carbon dioxide, and water*—Continued

WATER

Temperature, °C.	I.S.S.T.[4]	Calculated [7] from γ	Equation (1)	Temperature, °C.	I.S.S.T.[4]	Calculated [7] from γ	Equation (1)
	cm^3/g	cm^3/g	cm^3/g		cm^3/g	cm^3/g	cm^3/g
0	206, 400		206, 360	250	50. 1	50. 06	50. 10
50	12, 060	12, 054	12, 043	300	21. 8		21. 69
100	1, 674	1, 674. 7	1, 672. 9	350	8. 9		9. 02
150	393	392. 6	392. 6	374.1 [6]			4. 39
200	127. 0	127. 2	127. 3				

[4] International Skeleton Steam Tables, Mech. Eng., vol. 52, p. 120, 1930.
[6] Critical temperature.
[7] See fig. 3 for references to data on steam.

Equation (1) applies only along the saturation line, but when it is combined with a vapor pressure equation and some assumption in regard to the form of the isotherms an equation of state applicable over a limited range is obtained. The assumption

$$PV = R\theta - \frac{b}{V} \tag{5}$$

where b is a function of temperature is fairly accurate for pressures up to one tenth of the critical pressure. At the saturation line this equation becomes

$$\pi u' = R\theta - \frac{b}{u'} \tag{6}$$

Over the same pressure range the approximation to equation (1)

$$\log\left(1 - \frac{\pi u'}{R\theta}\right) = A \log \frac{\pi}{2.718\pi_c} \tag{7}$$

is sufficiently accurate. Solving for u' in equation (7) and substituting in (6) gives

$$b = \frac{(R\theta)^2}{\pi}\left(\frac{\pi}{2.718\pi_c}\right)^A\left[1 - \left(\frac{\pi}{2.718\pi_c}\right)^A\right] \tag{8}$$

When the vapor pressure is known equations (8) and (5) suffice for calculating (P, V, θ) data. If values of $d\pi/d\theta$ are also known, calorimetric quantities involving $db/d\theta$ can be calculated. The weight of a normal liter of ammonia calculated in this manner is only 3 parts in 10,000 greater than that observed by Dietrichson, Bircher, and O'Brien.[23] The calculated rate of change of enthalpy (H) with pressure at constant temperature of ammonia is about 7 percent greater at 0° C. and zero pressure and 9 percent less at 0° C. and saturation than the value indicated by the observations of Osborne, Stimson, Sligh, and Cragoe.[24] The calculated change in H at 0° C. between zero pressure and saturation is about 3 percent smaller than indicated by the results of those authors. For many substances this method of calculation would be useful for pressures up to one tenth the critical and for temperatures up to the corresponding saturation temperature, since the experimental data in the superheated region are not so accurate or else entirely lacking.

[23] J.Am.Chem.Soc., vol. 55, p. 1, 1933.
[24] B.S. Sci.Papers (no. 501), vol. 20, p. 65, 1925.

CONCLUSION

Provided the vapor pressure temperature relation for the saturated fluid, the critical pressure, and approximate values for liquid densities are known, the specific volume of the saturated vapor can be calculated, except near the critical temperature, with the determination of one empirical constant in the equation

$$\log_{10}\left(1-\frac{\pi u}{R\theta}\right)\left(1-\frac{\pi u'}{R\theta}\right)=A\left(\log_{10}\frac{\pi}{\pi c}\right)-0.4343=A\log_{10}\frac{\pi}{2.718\pi c} \quad (1)$$

This relation begins to fail at one fourth to one half the critical pressure, which corresponds to 0.8 to 0.9 the absolute critical temperature. When no data on the specific volume of a substance or of a similar substance are available, the use of $A=0.69$ will give fairly accurate calculated values. Within the limits of experimental error, A has the same value for chemically related substances, hence the value of A may sometimes be deduced from data on a similar substance.

A single value at a well-chosen temperature of the specific volume or of the latent heat of the saturated vapor together with the critical pressure, the vapor pressure, and density of the liquid suffices to determine the value of A. Any further data then serves as a check. When data on the vapor over a wide range of pressures are available, equation (1) affords an approximate method for estimating the critical pressure.

When equation (1) is combined with a vapor pressure equation and an appropriate assumption in regard to the form of the isotherms, an equation of state is obtained which is applicable with fair approximation over a limited range and which may be used in absence of more accurate experimental data in the superheated region.

WASHINGTON, June 24, 1933.

U.S. Department of Commerce, Bureau of Standards

RESEARCH PAPER RP617

Part of Bureau of Standards Journal of Research, Vol. 11, November 1933

INFRARED ABSORPTION SPECTRA OF SOME PLANT PIGMENTS

By R. Stair and W. W. Coblentz

ABSTRACT

An important study of the properties of matter is the effect of chemical constitution upon the spectral absorption of a substance.

The present contribution to this subject pertains to the infrared spectrum, extending to about 15μ.

A description is given of the absorption spectra, to about 15μ in the infrared, of the following plant pigments and derivatives: chlorophyll, carotin, xanthophyll, ethyl chlorophyllide, phytol, pheophytin, and copper pheophytin.

The data were obtained by means of a mirror spectrometer, vacuum thermopile and iron-clad Thomson galvanometer described in previous publications.

Changes in the absorption spectrum of carotin, accompanying oxidation, are described.

In general, the results are similar to those observed on the highly colored aniline dyes, in which there is an intense, wide absorption band in the short wave lengths, and the infrared absorption spectrum is composed of numerous small absorption bands, in contrast with substances having a simpler chemical structure, in which the absorption bands are less numerous, more intense, and more sharply defined.

CONTENTS

	Page
I. Introduction	703
II. Instruments and methods	704
III. Spectral transmission data	704
1. Chlorophyll	704
2. Carotin	705
3. Xanthophyll	706
4. Ethyl chlorophyllide	707
5. Phytol	708
6. Pheophytin	708
7. Copper pheophytin	709
IV. Discussion of the data	709
V. Bibliography	711

I. INTRODUCTION

An important study of the properties of matter is the effect of chemical constitution upon the spectral absorption of a substance. The present contribution to this subject pertains to the deep infrared spectrum, extending to about 15μ.

Through the generosity of Dr. F. M. Schertz of the Bureau of Chemistry and Soils, who presented us with samples of materials which he had prepared, we have been able to study the infrared absorption spectra of plant pigments (carotin, chlorophyll, and xanthophyll) and derivatives of these materials (1).[1]

[1] Figures in parentheses here and throughout the text indicate references given in the bibliography at the end of this paper.

Prior to this investigation but little had been done (2, 4) on the infrared absorption spectra of plant pigments, in which it is now found, as previously observed in some of the aniline dyes (5), that the absorption spectrum is composed of numerous small bands, in contrast with substances having a simpler chemical structure, in which the absorption bands are less numerous, more intense, and more sharply defined.

Data on the visible and ultraviolet absorption spectra of carotin and xanthophyll and the changes accompanying oxidation are given in a recent paper by McNicholas (11).

II. INSTRUMENTS AND METHODS

For a more detailed discussion of the experimental procedure, reference is made to previous publications (6, 7, 8, 9). The spectroradiometer consisted of a mirror spectrometer, with mirrors 50 cm in focal length. A fluorite prism was used in exploring the spectral region of 1μ to 8μ and a rock salt prism for the region to 15μ. For the fluorite prism the slit width decreased from 0.17μ at 2μ to 0.05μ at 6μ. For rock salt, the slit width decreased from 0.2μ at 6μ to 0.085μ at 14μ (see fig. 1).

The spectral radiation was measured with a vacuum thermopile and an iron-clad Thomson galvanometer. The source of radiation was a Nernst glower focused upon the entrance slit by means of a concave mirror.

The containers for the liquids were made of cleavage plates of rock salt, or polished plates of fluorite, placed at the entrance slit. The solid films were deposited by evaporation of liquid solutions or by melting some of the material on similar plates of rock salt, or fluorite. Variations from the standard procedure are noted in the text.

III. SPECTRAL TRANSMISSION DATA

Under this caption a brief description is given of the material examined, and the general properties of the absorption spectrum as compared with chemically related substances.

1. CHLOROPHYLL

The samples examined consisted of the two chlorophylls *a*, $C_{55}H_{72}O_5N_4Mg$ and *b*, $C_{55}H_{70}O_6N_4Mg$ unseparated as obtained (1) from wood nettles, in the ratio of about two parts of *a* to one of *b*.

The transmission curves (fig. 1) were obtained upon samples prepared by evaporation of an alcoholic solution of the pigment on cleavage plates of rock salt, leaving an almost (visually) opaque film, uniformly covering the plate. The curve for the shorter wave lengths was observed by using a fluorite prism. A rock salt prism was employed for the curve, extending from 5.88μ to 14μ.

According to Van Gulik (3) whose transmission measurements, using a quartz prism, extend to 3.6μ in the infrared, the *a*-component of chlorophyll has its maximum absorption at 0.65μ, with a weak absorption band at 0.8μ (4). The *b*-component has its maximum absorption at 0.63μ. According to his measurements, the strong absorption band at 3.43μ (fig. 1) is a complex of two bands at 3.4μ and 3.5μ. Using a rock salt prism, the writers have observed a similar

complexity, which is probably owing to errors resulting from the smaller dispersion of this kind of prism.

A conspicuous feature of the absorption spectrum of chlorophyll is its great opacity in the short wave lengths and its relatively high

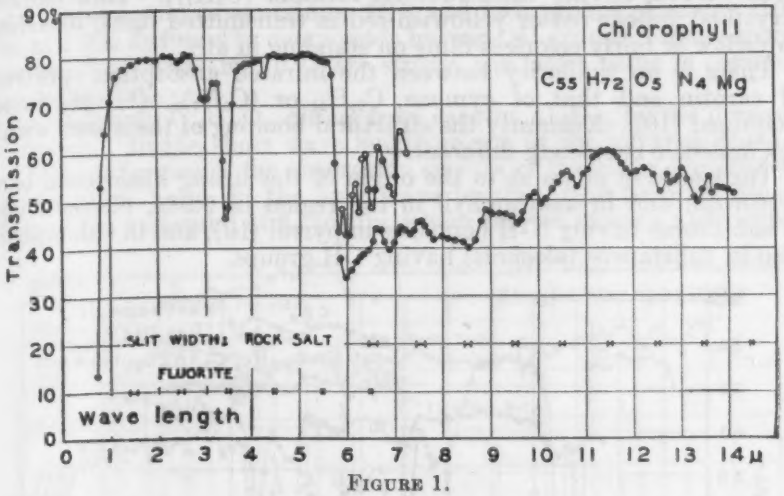

FIGURE 1.

transparency in the infrared, as previously observed in some of the aniline dyes (5).

2. CAROTIN

A film of carotin ($C_{40}H_{56}$) was prepared by gently heating the fine crystals on a cleavage plate of rock salt.

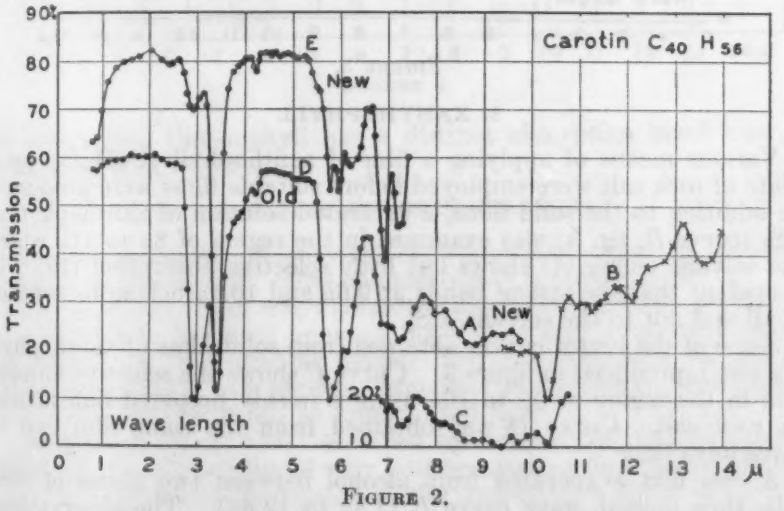

FIGURE 2.

In figure 2, curve *A* illustrates the spectral transmission of a freshly prepared film of carotin; curve *B* was obtained the next day, and curve *C* was obtained on the same sample 12 days later.

After the lapse of about two and one half years this sample was reexamined in the shorter wave lengths, using a fluorite prism, with

the result shown in curve *D* (marked "old"). A new sample, freshly prepared in the same manner as was the older one, gave the result shown in curve *E* (marked "new").

Chemically, this pigment is a strongly unsaturated auto-oxidizable hydrocarbon, having the structural formula $(C_5H_7)_x$. Thin laminae (crystals) appear red or yellowish-red in transmitted light; bleaching to yellow or fairly colorless films on standing in air.

There is no similarity between the infrared absorption spectrum of carotin and that of cymene, $C_{10}H_{14}$ or $(C_5H_7)_2$, (1), previously examined (10). Evidently the structural bonding of the atoms within the molecule is entirely different.

The question arises as to the origin of the strong absorption band in carotin and in xanthophyll in the region of 2.98μ, characteristic of substances having N-H bonds, as in pyrrol (10), and in chlorophyll; also in substances (alcohols) having OH groups.

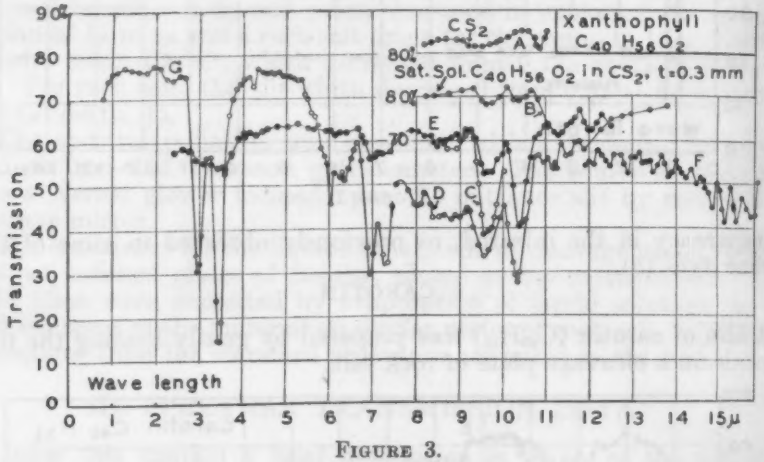

FIGURE 3.

3. XANTHOPHYLL

Various means of applying a film of xanthophyll ($C_{40}H_{56}O_2$) on a plate of rock salt were employed before suitable films were produced. In addition to the solid films, a saturated solution of xanthophyll in CS_2 (curve *B*, fig. 3) was examined in the region of 8μ to 11μ where the solvent (curve *A*) shows but little selective absorption (10). It is evident that the strong bands at 9.6μ and 10.4μ belong to xanthophyll and not to the solvent, CS_2.

Some of the better curves obtained from solid films of xanthophyll are also reproduced in figure 3. Curve *C* shows the selective absorption in the region of 9μ to 10μ using a freshly prepared film melted on rock salt. Curve *D* was obtained from the same film two to three days later.

A new film evaporated from alcohol between two plates of rock salt, then melted, gave curve *E* (2.3μ to 12.5μ). The observations 11.9μ to 16.1μ (curve *F*) were made on the same sample 12 days later.

A new sample melted on rock salt (curve *G*) gave some interesting absorption bands in the shorter wave lengths as observed with a fluorite prism.

A conspicuous feature of the infrared spectrum of xanthophyll is the sharply defined absorption bands at 3.43μ, 6.86μ, and 7.3μ, found in compounds containing CH_2 and CH_3 groups of atoms (10); also at 2.95μ as found in compounds having OH-groups. The absorption bands at 9.6μ and 10.3μ are strong, the latter being in common also in carotin.

Xanthophyll, $C_{40}H_{56}O_2$, differs from carotin, $C_{40}H_{56}$, by the presence of oxygen. In the short wave length region of the infrared, there is but little difference in the absorption spectra of these two compounds. On the other hand, in the long wave lengths, (the pure rotational effect of the molecule) at 8μ to 10μ, where carotin shows a wide region

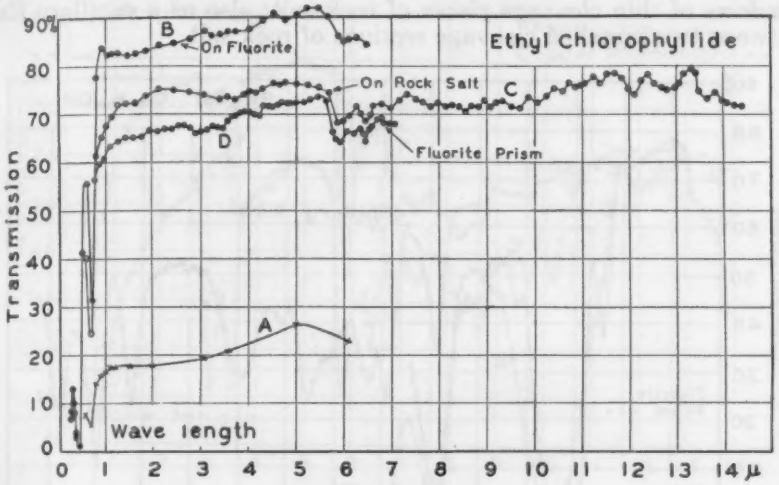

FIGURE 4.

of absorption, xanthophyll has a distinct absorption band with a maximum at 9.6μ.

4. ETHYL CHLOROPHYLLIDE

By the action of an enzyme, chlorophyllase, upon an alcoholic solution of chlorophyll, ethyl chlorophyllide is obtained (1).

The best samples of ethyl chlorophyllide were prepared by placing the crystalline material upon plates of rock salt (previously heated to remove the moisture) or fluorite, and dissolving it with alcohol. After evaporation, the pigment remained in a smooth, homogenous film that appeared green by transmitted light.

In figure 4, curve *A* was obtained by using a thin film on fluorite. Although the film appeared very homogenous, so that distant objects could be seen distinctly through it, the transmission is low in contrast with curve *B* which was obtained from a similarly prepared film. In addition to the infrared, the transmission bands in the green and in the ultraviolet spectrum (absorption maxima at 0.4μ and 0.7μ are shown for this sample (dots . . .).

Another film (curve *C*) was examined from 0.70μ to 14.36μ. About two and one half years later, this film was reexamined in the shorter wave lengths (curve *D*), using a fluorite prism) showing but little change in transmission.

A characteristic feature of the infrared absorption spectrum of ethyl chlorophyllide is the almost entire absence of strong bands of selective absorption, such as appear in the shorter wave lengths.

5. PHYTOL

Phytol ($C_{20}H_{39}OH$) is an unsaturated primary alcohol, with an open chain of carbon atoms (1). The sample examined was a transparent light yellow liquid obtained from crude chlorophyll. It is obtainable also in the preparation of ethyl chlorophyllide (1).

The samples were examined in a cell 0.3 mm in thickness, having windows of thin cleavage pieces of rock salt; also as a capillary film between two matched cleavage sections of rock salt.

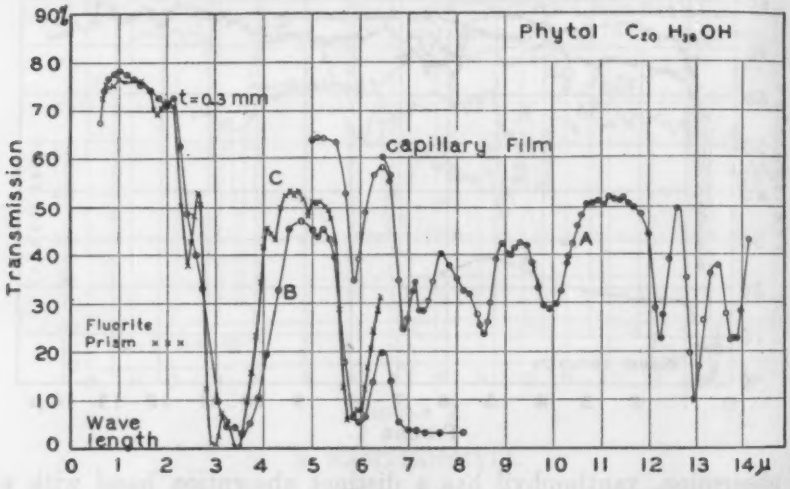

FIGURE 5.

The capillary film of liquid was obtained by splitting a crystal of rock salt (size 5 by 3 by 1 cm) into two parts, each about 5 mm in thickness, reassembling it accurately and placing a drop of the liquid in a conical or V-shaped depression, cut into one side, along the line of cleavage of the crystal. By capillary action, the film of liquid spreads uniformly, without interruptions by air bubbles, between the two plates.

A conspicuous feature of the infrared absorption spectrum is the intense absorption bands, particularly the approximately harmonic bands (10) at 3.43μ, 6.86μ, and 13.8μ; also the bands at 2.95μ and 5.9μ characteristic of (alcohols) substances containing OH- and NH-bonding.

6. PHEOPHYTIN

The compound, pheophytin (chemical formula not given) is a dark-colored, waxy substance formed by the action of oxalic acid upon chlorophyll (1). The transmission spectrum is shown by the

circles (o o o) in figure 6. For the region 6.6μ to 14μ a film of the wax was melted on a plate of rock salt. From 0.8μ to 7μ, where the fluorite prism was used, the film was prepared by dissolving the pheophytin in xylol, which was allowed to evaporate.

7. COPPER PHEOPHYTIN

Copper pheophytin (14.97 percent copper) is a dark substance having a greenish yellow color by transmitted light and a faint purplish color by reflected light.

The transmission curve is shown (dots . . .) in figure 6. The film examined in the spectral region from 7μ to 14μ was obtained by evaporation of a benzol solution of the material on rock salt. For the region of 0.8μ to 7μ the film was prepared by evaporation of a solution of copper pheophytin dissolved in xylol.

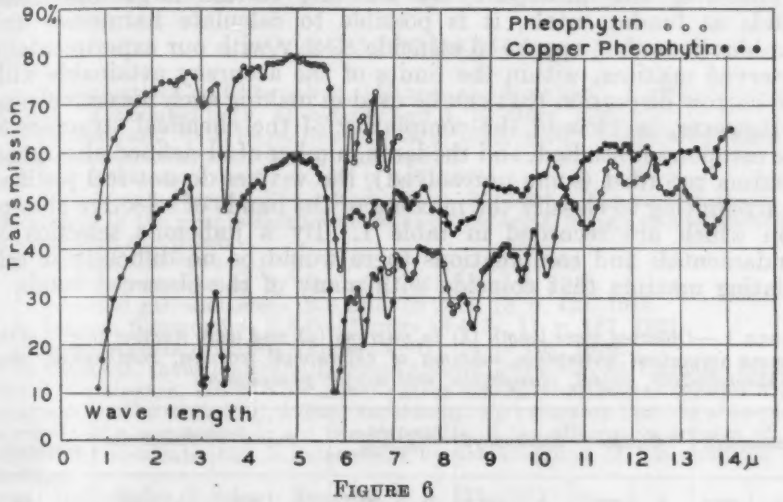

FIGURE 6

A conspicuous feature of the absorption spectra of pheophytin and copper pheophytin is the numerous absorption bands, some of which are in close coincidence with those of other chlorophyll derivatives described in this paper.

IV. DISCUSSION OF THE DATA

Present conceptions of the mechanism of absorption (some of which are now accepted as axiomatic) are built upon evidence, gathered slowly and laboriously, step by step, during the past 3 to 4 decades, showing: (*a*) that the absorption is intra-molecular; (*b*) that the absorption spectrum of a compound is not the composite of the absorption bands of the constituent elements; (*c*) that the grouping or bonding of the atoms determines the character of the absorption spectrum; and (*d*) that the arrangement of the groups within the molecule (e.g., the CH_3 group in the ortho-, meta-, and para-position in the benzene ring), as well as the atomic weight of the basic element (e.g., Mg, Pb, in the carbonates, sulphates, and nitrates) affect the position of the maximum absorption (10), (14).

The first observations (10) of closely harmonic absorption bands (e.g., the hydrocarbon absorption bands at 0.86μ, 1.71μ, 3.43μ, 6.86μ, and 13.8μ to 14μ; and the OH- or NH-bonding with maximum at 2.95μ, 5.9μ, and 11.8μ to 12μ, which in those days were considered as erroneous or accidental) have found a place in present-day speculations of the mechanism of absorption which now assumes each absorption band to be a fundamental, a harmonic, or a combination, involving vibrational and rotational states of the molecule.

In fact, the correlation of theory with experimental data has progressed to such a stage that, in a recent contribution on this subject, Cross and Daniels (12) have reconstructed the whole observed infrared absorption spectrum of certain ethyl halides by a judicious selection of fundamentals with their first harmonics, and combinations of these absorption bands.

Following this procedure, by selecting certain large absorption bands as fundamentals, it is possible to calculate harmonics and combinations that appear to coincide closely with our experimentally observed maxima, within the limits of the accuracy attainable with the narrow dispersion that can be used in making such measurements.

However, in view of the complexity of the chemical structure of the compounds studied, and the large number of ill-defined absorption maxima recorded (some unresolved), the writers do not feel justified in attempting to classify the maxima of the bands of selective absorption which are recorded in table 1. By a judicious selection of fundamentals and combinations there would be no difficulty in calculating maxima that coincide with many of the observed bands.

TABLE 1.—*Observed wave length* (λ) *in microns* (μ) *and wave number* (cm^{-1}) *of the more important absorption maxima of chlorophyll, carotin, xanthophyll, ethyl chlorophyllide, phytol, pheophytin, and copper pheophytin*

Chlorophyll		Carotin		Xanthophyll		Ethyl chlorophyllide		Phytol		Pheophytin		Copper pheophytin	
λ	cm^{-1}	λ	cm^{-1}	λ	cm^{-1}	λ	cm^{-1}	λ	cm^{-1}	λ	cm^{-1}	λ	cm^{-1}
						0.40	25,000						
						.68	14,700						
				1.80	5,555			1.78	5,260				
2.35	4,255			2.35	4,255			2.38	4,200	2.40	4,165		
2.97	3,365	2.92	3,425	2.95	3,390	2.90	3,445	2.96	3,380	2.98	3,355	2.98	3,355
3.43	2,915	3.43	2,915	3.43	2,915	3.40	2,940	3.43	2,915	3.43	2,915	3.44	2,905
4.24	2,360	4.24	2,360	4.24	2,360			4.24	2,360	4.24	2,360	4.24	2,360
								4.91	2,035				
5.79	1,730	5.79	1,730					5.73	1,745	5.80	1,725	5.75	1,740
5.97	1,675	5.97	1,675	6.01	1,665	5.90	1,695	5.97	1,675				
6.20	1,610	6.25	1,600	6.25	1,600					6.15	1,625	6.15	1,625
6.48	1,545					6.45	1,550			6.48	1,545	6.35	1,575
6.90	1,450	6.90	1,450	6.89	1,450	6.90	1,450	6.91	1,445	6.86	1,460	6.87	1,455
7.30	1,370	7.25	1,380	7.30	1,370			7.28	1,375	7.37	1,355	7.32	1,365
7.90	1,265	8.00	1,250	8.06	1,240							7.90	1,265
								8.20	1,220	8.24	1,215	8.24	1,215
8.60	1,160	8.70	1,150	8.50	1,175			8.57	1,165	8.72	1,145	8.60	1,160
								9.10	1,100				
9.58	1,045			9.62	1,040	9.60	1,040	9.95	1,005	9.70	1,030	9.70	1,030
10.06	995	10.38	965	10.38	965					10.23	975	10.58	945
10.84	920			10.87	920								
		11.25	890	11.25	890					11.12	900		
12.00	835	12.10	825	11.95	835	12.05	820	12.23	815	12.05	820	12.04	820
12.60	795			12.83	780	12.80	780	12.93	775	12.80	780	12.60	795
13.35	750	13.65	730			13.60	735	13.83	720	13.75	725	13.70	730

It will suffice to call attention to the conspicuous absorption maxima at 3.43μ, 4.3μ, 6.86μ, 7.3μ, 9.6μ, and 10.4μ previously recorded (10) in simpler compounds, particularly chain compounds of CH_2 and CH_3 groups; also absorption bands at 2.95μ, 5.9μ, and 8.6μ, in substances containing COC-, NH-, or OH-bonding. It is impressive to note that both types of absorption bands are present in the herein described compounds which have both types of atomic bonding.

The absorption band at 7.3μ occurs in common with the band at 6.86μ (10) and may perhaps be a fundamental as used by Cross and Daniels (12). The recent investigations by Kettering and Sleator (13) of hydrocarbon vapors, to 30μ in the infrared, show no strong absorption bands beyond about 15μ. From this, it appears highly improbable that the band at 7.3μ is the result of a combination of fundamentals, one of which is at a wave length longer than 15μ.

V. BIBLIOGRAPHY

1. Investigations on Chlorophyll, Methods and Results by R. Willstätter and A. Stoll. Translated by F. M. Schertz and A. R. Merz, 1927.

2. Coblentz and Stair, Phys. Rev. (2), 33, p. 1092, 1929. Preliminary report on carbon tetrachloride, chlorophyll, xanthophyll.

3. Van Gulik, Ann. der Phys., 46, p. 147, 1915.

4. Nichols and Merritt, Phys. Rev., 19, p. 26, 1904. The measurements on chlorophyll in the near infrared were made by Coblentz, using a mirror spectrometer and rock salt prism.

5. Johnson and Spence, Phys. Rev., (2), 5, p. 349, 1915.

6. Mirror spectrometer, B.S.Bull. (S. 204), 10, p. 1, 1913.

7. Iron-clad galvanometers, B.S.Bull. (S 282), 13, p. 423, 1916.

8. Vacuum thermopiles, B.S.Sci. Papers (S 413), 17, p. 187, 1921.

9. Prism material, B.S.Sci. Papers (S 401), 16, p. 701, 1920.

10. Coblentz, Investigation of Infrared Spectra, Publ. No. 35, Carnegie Institution of Washington, 1905. This memoir gives extensive references to, and a discussion of, earlier work (e.g., Julius, Aschkinass, etc.) showing that the absorption spectrum of a compound is not the composite of the absorption spectra of the constituent elements, but is determined by the grouping of the atoms in the molecule.

11. McNicholas, B.S.Jour. Research, 7, p. 171, 1931.

12. Cross and Daniels, Jour. Chemical Physics, 1, p. 48, 1933.

13. Kettering and Sleator, Physics, 4, p. 39, 1933.

14. The increase in wave length of the maximum of selective absorption and of selective reflection in carbonates, nitrates and sulphates, as a function of the atomic weight of the basic element, was first described by Coblentz in the Jahrbuch der Radioaktivität und Elektronik, 4, p. 132, 1907; see also Publications of the Carnegie Institution of Washington, No. 65, and No. 97, 1906 and 1908, respectively.

This phenomenon received favorable comment, at that time, by E. F. Nichols (Washington meeting, Amer. Phys. Soc., April 19, Phys. Rev., (2) 24, p. 522; 1907) who pointed out that he and Prof. H. Rubens had searched for such a shift in the longest residual rays—at 40μ to 60μ. According to Drude's theory (Ann. der Physik, 14, p. 677; 1904) the maximum absorption of the "ponderable atoms" should occur in the region of 12μ to 15μ. It is, therefore, of interest to note that Kettering and Sleator (13) find the hydrocarbons relatively transparent and free from bands of selective absorption, for wave lengths longer than 16μ to 20μ.

WASHINGTON, August 7, 1933.

U.S. Department of Commerce, Bureau of Standards

RESEARCH PAPER RP618

Part of Bureau of Standards Journal of Research, Vol. 11, November 1933

PREPARATION OF CALCIUM LACTOBIONATE AND LACTOBIONIC δ-LACTONE

By Horace S. Isbell

ABSTRACT

Crystalline lactobionic δ-lactone was obtained by dehydrating aqueous lactobionic acid by distillation with dioxane. This process is applicable for preparing lactones of other sugar acids. Lactobionic δ-lactone is a new substance of particular importance for investigations in the carbohydrate field. It is more soluble than gluconic δ-lactone, but it is not deliquescent and has a sweet taste. It melts at 195°–196° C.; in 5 percent water solution it gives $[\alpha]_D^{20}=+54°$ initially, decreasing in several hours to +22°. These values agree with the rotations of the product obtained by the oxidation of lactose with bromine water in the presence of barium carbonate.

Calcium lactobionate was prepared in the crystalline state. It separates in hairlike crystals which form gelatinous mixtures with the mother liquor from which it is difficult to separate the pure substance. Consequently the crystalline salt is not suitable for the purification of lactobionic acid.

CONTENTS

	Page
I. Calcium lactobionate	713
1. Preparation of calcium lactobionate-calcium chloride	714
2. Preparation of crystalline calcium lactobionate	715
II. Lactobionic δ-lactone	716
1. Preparation of crystalline lactobionic δ-lactone	717

I. CALCIUM LACTOBIONATE

$(Ca(C_{12}H_{21}O_{12})_2)$

The electrolytic method for the preparation of calcium lactobionate reported by Isbell and Frush,[1] is so satisfactory that this salt may be readily prepared in any desired amount. Attempts to obtain a crystalline product, however, have been unsuccessful, and consequently it has been necessary to separate the lactobionic acid as a basic calcium salt. The use of the basic salt is objectionable because the lime causes degradation of any unoxidized sugar and thus prevents the satisfactory operation of a continuous process such as that described by Isbell, Frush, and Bates [2] for calcium gluconate.

If a crystalline form of calcium lactobionate could be separated directly from the solution obtained by the oxidation of lactose its

[1] Isbell and Frush, B. S. Jour. Research, vol. 6 (RP328), p. 1151, 1931.
[2] Isbell, Frush and Bates, B. S. Jour. Research, vol. 8 (RP436), p. 571, 1932.

preparation would be simplified. This will be seen from the following equation:

$$\underset{\text{Lactose}}{C_{12}H_{22}O_{11}} + CaCO_3 + H_2O + \underset{\text{Catalyst}}{CaBr_2} \xrightarrow[\text{Electrolysis}]{} \underset{\text{Calcium lactobionate}}{Ca(C_{12}H_{21}O_{12})_2} + \underset{\text{Catalyst}}{CaBr_2} + CO_2 + 2H_2$$

Lactobionic acid was made first by Fischer and Meyer[3] by the oxidation of lactose with bromine. They prepared the amorphous calcium salt but were unable to bring it to crystallization. Subsequently Ruff and Ollendorff[4] reported a substance, which they believed to be crystalline, prepared by precipitating crude calcium lactobionate with alcohol. They did not describe the product in sufficient detail to reveal whether the substance was actually crystalline. By essentially the same procedure C. S. Hudson[5] and the writer obtained a granular precipitate in which no double refraction could be observed.

After many attempts the writer has now prepared crystalline calcium lactobionate. The first crystals were obtained from an aqueous solution of calcium lactobionate made from basic calcium lactobionate, which had been prepared from calcium lactobionate-calcium chloride.[6] Calcium lactobionate resembles calcium rhamnonate in that it separates in hairlike crystals which form in brushlike groups frequently oriented so that all the crystals in a given group affect polarized light in the same manner. Various procedures have been tried in vain to determine conditions for separating large and compact crystals. The crystalline salt apparently contains water of crystallization, but on account of the difficulty of separating it from the mother liquor it is not possible to distinguish between the occluded water and chemically bound water. The product when dried 8 hours at 60° C. in vacuo contains 4.74 percent calcium, which corresponds to a formula, $Ca(C_{12}H_{21}O_{12})_2.5H_2O$.

Unfortunately the salt is not easily separated in the electrolytic process, but its tendency to form gelatinous masses may prove of value in other fields.

1. PREPARATION OF CALCIUM LACTOBIONATE-CALCIUM CHLORIDE

Equimolecular proportions of calcium chloride and calcium lactobionate, prepared from lactose as described in Research Paper No. 328, were dissolved in water. The solution was evaporated in vacuo to a thin sirup from which crystalline calcium lactobionate-calcium chloride separated. The crude salt was recrystallized from water and dried in air at room temperature.

Analysis calculated for $Ca(C_{12}H_{21}O_{12})_2.CaCl_2.6H_2O$: Ca, 8.23; Cl, α7.29. Found: Ca, 8.25; Cl, 7.29. It gave $[\delta]_D^{20} = +20.0$. (1.3249 g dissolved in 25 ml of H_2O read 6.13° S. in a 2 dm tube.)

The mutarotation of lactobionic acid was determined from this salt in the following manner: A 6.0843 g sample of calcium lactobionate-calcium chloride was placed in a flask and 50.125 g 0.25 N

[3] Fischer and Meyer, Ber., vol. 22, p. 361, 1889.
[4] Ruff and Ollendorff, Ber., vol. 23, p. 1806, 1900.
[5] Hudson and Isbell, B. S. Jour. Research, vol. 3 (RP82), p. 57, 1929.
[6] Stoll and Kussmaul, U.S. Patent No. 1648368, dated Nov. 8, 1927.

HCl was added with a pipette. After 3, 5, 10, 15, 30, 60, and 120 minutes at 20° C. the solution read in a 2 dm tube +7.60°, +7.85°, +8.23°, +8.55°, +9.13°, +9.43°, and +9.55° S.

The specific rotations which are illustrated in figure 1 by the curve marked lactobionic acid are based on the weight of lactone ($C_{12}H_{20}O_{11}$) equivalent to the salt used. The conversion factor, 0.3462, was used for changing the degrees sugar to angular rotation. The density of the solution was 1.0493 g/ml.

2. PREPARATION OF CRYSTALLINE CALCIUM LACTOBIONATE

A 235 g sample of crystalline calcium lactobionate-calcium chloride was added in small portions, with stirring, to a suspension of 100 g of calcium oxide in 1 liter of hot water. After standing several

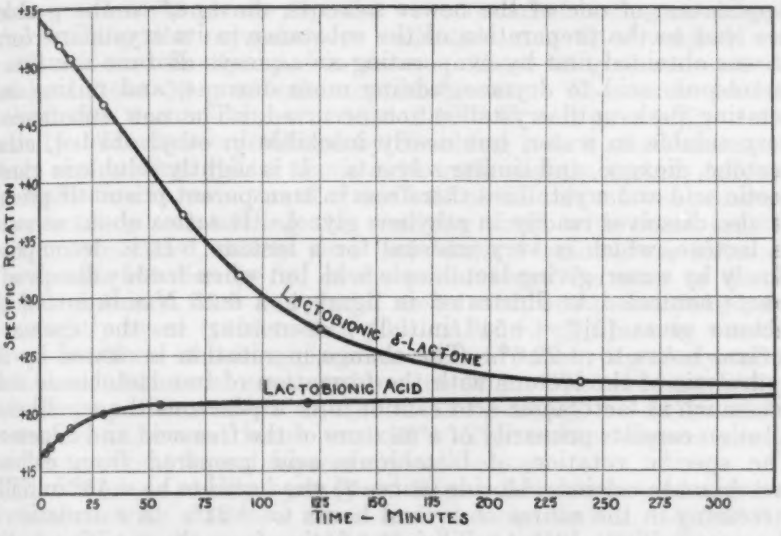

FIGURE 1.—*Change in specific rotation at 20° C. of 0.25 N aqueous lactobionic acid and 0.25 N lactobionic δ-lactone.*

hours the resulting basic calcium lactobionate was separated by filtration and washed with lime water until free from chloride. The basic salt (333 g air dried) was suspended in 2 liters of water and carbonated. The resulting solution of calcium lactobionate was filtered and evaporated to a thick sirup (refractive index = 1.4583 at 20° C.). After standing several weeks the product solidified. A microscopic examination showed double refractive slender needlelike crystals. The product was dried, without filtration, and pulverized. The crude product weighed 215 g and contained 4.43 percent calcium.

The crude calcium lactobionate was purified by dissolving 40 g in 60 ml of water, filtering, and adding methyl alcohol until the solution was nearly saturated. Care was taken not to add sufficient alcohol to cause a permanent precipitate of amorphous material. The resulting solution was seeded with crystalline calcium lactobionate and stirred for several hours. The final product contained long slender needle crystals which were separated by filter-pressing. The resulting

filter cake was dried 24 hours at 60° C in vacuo. The product in water solution gave $[\alpha]_D^{20} = +23.7°$. A 1.5745 g sample in 25 ml read 8.63° S. in a 2 dm tube. Analysis: Calculated for $Ca(C_{12}H_{21}O_{12})_2 \cdot 5H_2O$: Ca, 4.74. Found: Ca, 4.74.

II. LACTOBIONIC δ-LACTONE

$(C_{12}H_{20}O_{11})$

In a previous publication the writer and C. S. Hudson[7] showed that the lactone of lactobionic acid is formed by the oxidation of lactose prior to the formation of the free acid. The confirmation of this important observation required the preparation of the δ-lactone. Although a number of investigators have prepared aqueous lactobionic acid, heretofore the *crystalline* lactone has not been reported. Application of one of the newer solvents, dioxane,[8] to the problem has lead to the preparation of the substance in its crystalline form. It was obtained first by evaporating an aqueous dioxane solution of lactobionic acid to dryness, adding more dioxane, and mixing in a rotating flask until crystallization occurred. The new substance is very soluble in water, but nearly insoluble in ethyl alcohol, ether, acetone, dioxane, and similar solvents. It is slightly soluble in glacial acetic acid and crystallizes therefrom in transparent prismatic prisms. It also dissolves readily in ethylene glycol. It tastes about as sweet as lactose, which is very unusual for a lactone. It is decomposed slowly by water, giving lactobionic acid, but when freshly dissolved it reacts neutral. As illustrated in figure 1, a 0.25 *N* solution of the lactone gives $[\alpha]_D^{20} = +54°$ initially, decreasing in the course of several hours to +22.6°. The change in rotation is caused by the hydrolysis of the lactone with the formation of free lactobionic acid. Inasmuch as lactobionic acid cannot form a γ-lactone the equilibrium solution consists primarily of a mixture of the free acid and δ-lactone. The specific rotation of lactobionic acid prepared from calcium lactobionate-calcium chloride (curve 2) was found to be +16° initially, increasing in the course of several hours to +21°. A calculation of the composition of the equilibrium solution from the specific rotation of the lactone (+54) and the acid (+16) shows that an aqueous solution in equilibrium (+22) contains approximately 16 percent lactone and 84 percent acid. This is a relatively large proportion of free acid, and hence one might be able to crystallize the acid from aqueous solution provided crystals were available for nucleation.

The specific rotation of the product[9] obtained by the oxidation of β-lactose was +52.4° 10 minutes after the beginning of the reaction. This agrees with the rotation of lactobionic δ-lactone, +51.9° 10 minutes after solution. The subsequent changes in rotation are comparable, thus supporting the conclusion that lactobionic δ-lactone is formed by the oxidation of lactose by bromine water in slightly acid solution rather than lactobionic acid as previously believed.

[7] Hudson and Isbell, B.S.Jour. Research, vol. 8 (RP418), p. 327, 1932.

[8] The writer has found that dioxane can be used to advantage in the preparation of many lactones. Some examples are reported by Isbell and Frush, B.S.Jour. Research, vol. 11 (RP613), p. 649, 1933.

[9] The mutarotation of this product was given in Research Paper No. 441, p. 621, figure 3.

1. PREPARATION OF CRYSTALLINE LACTOBIONIC δ-LACTONE ($C_{12}H_{20}O_{11}$)

A solution of lactobionic acid was prepared by the addition of 7.6 g of oxalic acid to 50 g of $Ca(C_{12}H_{21}O_{12})_2.5H_2O$ dissolved in 100 ml of hot water. After filtration the solution was cooled to room temperature and evaporated in vacuo to a sirup. The aqueous sirup was dehydrated by the addition of 50 ml of dioxane, followed by distillation in vacuo until dry. The residue was mixed with 25 ml of dioxane and 25 ml of toluene and the process repeated. A friable material remained, which was titurated with 100 ml of dioxane and then allowed to stand with stirring until a portion of the product had crystallized. This required several weeks. The dioxane was removed by filtration and the residue dried at 60° C. in vacuo. The crude product (40 g) was digested with 500 ml of boiling acetic acid. After cooling, the crystals were collected on a filter washed with acetic acid and finally dried in vacuo. About 35 g of material was obtained from 50 g of calcium lactobionate. The crude product melted with decomposition at 185° to 190° C. and gave $[\alpha]_D^{20} = +49°$, initially. It was recrystallized by dissolving it in a small amount of water and adding glacial acetic acid until slightly turbid, followed by distillation in vacuo until about half of the solvent was removed. After cooling and seeding the resulting sirup with some crystals previously secured, nearly pure lactobionic δ-lactone was obtained. The specific rotation (+54) of the product was the same as that of crystals obtained from hot glacial acetic acid, but the melting point was slightly lower (185° to 195° C.). About 3 g of lactone was dissolved in 500 ml of boiling glacial acetic acid; about 1 g of crystalline lactobionic δ-lactone separated on cooling. The product melted with decomposition at 195° to 196° C. and gave $[\alpha]_D^{20} = +54°$, initially, decreasing in several hours to +22°. The mother liquors can be used as a solvent for subsequent crystallizations.

The lactone is readily hydrolyzed to give lactobionic acid and may be titrated with standard alkali and phenolphthalein. A 0.5861 g sample of the lactone required 17.31 ml of 0.1 *N* $Ba(OH)_2$ for saponification; the amount calculated for $C_{12}H_{20}O_{11}$ is 17.23 ml.

A 2.2355 g sample of the lactone ($C_{12}H_{20}O_{11}$) in 25 ml of water solution at 20° C. read on a Bates saccharimeter in a 2 dm tube +27.38°, +26.80°, +26.20° +24.10°, +19.18°, +16.50°, +14.07°, and +11.67° after 5, 10, 15, 30, 65, 90, 125, and 240 minutes. $[\alpha]_D^{20}$ = +53.0°, +51.9°, +50.7°, +46.7°, +37.1°, +31.9°, +27.2°, and +22.6°, respectively.[10]

A 1.2498 g sample of the lactone in 25 ml of water solution at 20° C. read in a 2 dm tube:

+15.43°, +15.21°, +14.87°, and +6.45° S after
2, 5, 10, and 1,440 minutes.

$[\alpha]_D^{20} = +53.4°$, +52.7°, +51.5°, and +22.3°, respectively

WASHINGTON, August 26, 1933.

[10] The conversion factor 0.3462 was used. International Critical Tables, vol. II, p. 336.

U.S. Department of Commerce, Bureau of Standards

RESEARCH PAPER RP619

Part of Bureau of Standards Journal of Research, Vol. 11, November 1933

PHASE EQUILIBRIA IN THE SYSTEMS TiO_2, TiO_2-SiO_2 AND TiO_2-Al_2O_3

By E. N. Bunting

ABSTRACT

The stable form of TiO_2 above 400° C. was found to be rutile with a melting point of 1,825° C. It forms no compounds with SiO_2, but gives a eutectic with 89.5 wt. percent SiO_2 at 1,540° C. With Al_2O_3, a compound $Ti\ O_2.Al_2O_3$ is formed, melting at 1,860° C. This compound forms a eutectic with TiO_2 at 15 wt. percent Al_2O_3 and 1,715° C., and a second eutectic with Al_2O_3 at 62 wt. percent Al_2O_3 and 1,850° C. Several low melting fluxes with nonvolatile acid radicals are described.

CONTENTS

	Page
I. Introduction	719
II. The system TiO_2	719
III. The system TiO_2-SiO_2	722
IV. The system TiO_2-Al_2O_3	724

I. INTRODUCTION

Titanium dioxide resembles silica in chemical behavior and has found use in the ceramic arts as an opacifying material in enamels and glass. Its high index of refraction might be of value in the preparation of special glasses, if clear titanate glasses can be made. The high melting point of titania makes it useful as a refractory, although it cannot compete at present with the cheaper refractories. However, complete information regarding its value to the ceramic industry can only be gained by a thorough investigation of its reactions with the ceramic materials. The present work deals with the forms of titanium dioxide and its reactions with silica and alumina.

II. THE SYSTEM TiO_2

Titania is found in nature in three crystalline forms, namely, anatase, brookite, and rutile. Anatase is formed whenever titanium hydroxide is dehydrated by heating to a temperature below about 900°.[1] It is reported in the literature [2] [3] that brookite was obtained by laboratory reactions at temperatures between 800° and 1,040°. However, the present work has shown that brookite changes to rutile below this temperature region in the presence of a suitable flux, or mineralizer, and that rutile is formed from anatase above 400°.

[1] All temperatures are given in degrees centigrade.

[2] P. Hautefeuille, Bull. soc. chim., vol. 5, p. 588, 1863; Compt. rend., vol. 57, p. 148, 1863; vol. 59, p. 188, 1864; vol. 90, p. 868, 1880; Ann. chim. phys. 4, vol. 4, p. 131, 1865.

[3] A. Daubree, Ann. mines, vol. 16, p. 129, 1849; Phil. Mag., vol. 9, p. 315, 1855; Edinburgh Phil. Jour., vol. 57, p. 307, 1854; Compt. rend., vol. 20, p. 227, 1849; vol. 30, p. 383, 1850; vol. 39, p. 153, 1853.

Conditions of stability for the natural minerals, without the presence of a mineralizer, have been studied by A. Schröder.[4] He found that anatase can exist in two forms, α and β, which are in equilibrium at 642°, while at 915° ± 15° the α-anatase changes irreversibly to

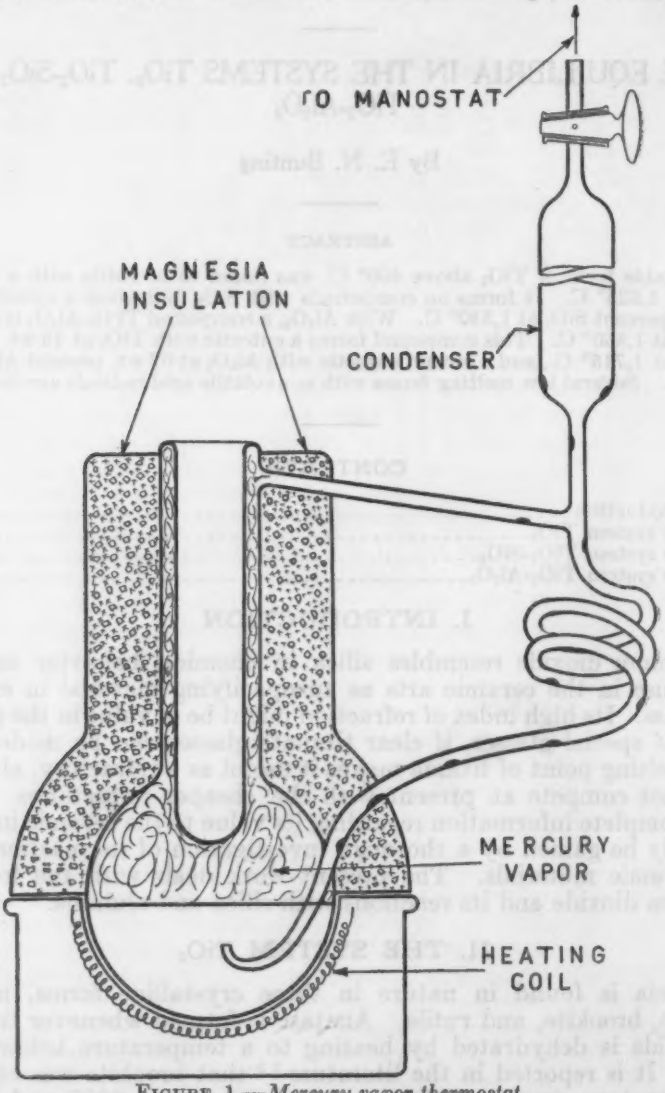

FIGURE 1.—*Mercury vapor thermostat.*

rutile. He also found that brookite changes to rutile with a velocity that is an exponential function of the temperature, the change not being measurable below about 650°. Rutile was not changed to the other forms at any temperature. His results were based on changes in prism angles and densities.

Anatase was prepared from $TiCl_4$[5] by hydrolysis with distilled water, the resulting hydroxide being dried at about 400°. On heating

[4] A. Schröder, Zeit. Krist., vol 66, p. 493, 1928, and vol. 67, p. 485, 1928.
[5] The $TiCl_4$ was prepared from commercial $TiCl_4$ by S. T. Schicktanz by fractional distillation through a 20-plate still, only the middle fractions being used.

above 1,000°, pure rutile was obtained. Analyses showed these preparations to contain 100.0 percent TiO_2. Brookite was used in the form of finely powdered natural mineral, purified somewhat by repeated extractions with hot hydrochloric acid.

For the experiments described below it was necessary to find suitable low melting fluxes in which TiO_2 would dissolve but with which not all of the sample would react. The vanadates and dichromates were found to be suitable, and the fusion temperatures of some mixtures were determined by the cooling and heating curve method, using about 50 g of stirred material. Melting points of commercial KVO_3, $NaVO_3$, and $LiVO_3$, each containing about 1 percent of carbonate, were found to be 527°, 588°, and 599°, respectively. The minimum melting temperature for KVO_3-$NaVO_3$ mixtures is 480°, at 85 wt. percent KVO_3, and for $NaVO_3$-$LiVO_3$ this temperature is 556°. A minimum melting temperature in KVO_3-$NaVO_3$-$LiVO_3$ is at 461°, with a composition close to 77.6 wt. percent KVO_3-13.4 percent $NaVO_3$-9.0 percent $LiVO_3$. The addition of 10 percent of V_2O_5 to this mixture gives one which is partially molten at 445°. The minimum melting temperature for $K_2Cr_2O_7$-$NaVO_3$ mixtures is 310°, in the neighborhood of 25 wt. percent $NaVO_3$.

A convenient mercury-vapor bath which was used for heating over long periods at temperatures between 300° and 380° is shown in figure 1. It is made of pyrex glass and is filled with nitrogen at a pressure determined by the temperature desired. With changes in room temperature of not more than 3°, the temperature of the bath will remain constant to within about 1°. A 200- to 300-watt heater serves to vaporize the mercury.

TABLE 1.—*Treatments given anatase seeded with brookite and rutile*

Mineralizer	Temperature	Duration	Result
	°C.	Hrs.	
Na_2WO_4	700	24	No change.
Do	725	24	Do.
Do	750	24	Do.
Do	775	24	Do.
Do	790	24	Do.
Do	800	24	All changed to rutile.
Do	840	24	Do.
$NaVO_3$	795	24	Do.
Do	725	24	Do.
$NaVO_3$+$LiVO_3$+$K_2Cr_2O_7$	575	24	Do.
$K_2Cr_2O_7$	425	168	No change.
$NaVO_3$+KVO_3+$LiVO_3$	465	125	Do.
Do	500	48	Do.
Do	515	24	Do.
Do	550	24	Anatase+rutile.
$NaVO_3$+$K_2Cr_2O_7$	550	24	Do.
Do	525	24	Do.
Do	400	600	Do.[1]
Do	350	700	No change.
$NaVO_3$+H_2O (in bomb)	350	90	Do.

[1] About 5 to 10 percent rutile. present.

In the presence of mineralizers anatase and brookite will change to rutile at much lower temperatures than those reported by Schröder, as shown in tables 1 and 2. The rate at which anatase is changed to rutile depends upon the flux present as well as upon the temperature. Table 3 shows the treatments given rutile, none of which resulted in changing it.

TABLE 2.—*Treatments given brookite seeded with anatase and rutile*

Mineralizer	Temperature	Duration	Result
	°C.	Hrs.	
$NaVO_3+H_2O$ (in bomb)	350	90	No change.
$K_2Cr_2O_7$	425	24	Do.
$NaVO_3+KVO_3+LiVO_3$	475	24	Do.
Do	525	24	All rutile.
$NaVO_3+K_2Cr_2O_7$	320	1,700	No change.

TABLE 3.—*Treatments given rutile seeded with anatase and brookite*

Mineralizer	Temperature	Duration	Result
	°C.	Hrs.	
Na_2WO_4	725	24	No change.
Do	840	24	Do.
Do	900	24	Do.
Do	950	24	Do.
Do	1,000	24	Do.
Do	1,100	24	Do.
Do	1,200	24	Do.
Do	1,400	24	Do.
$NaVO_3$	600	24	Do.
$NaVO_3+K_2Cr_2O_7$	500	168	Do.
$NaVO_3+KVO_3+LiVO_3$	475	168	Do.
$K_2Cr_2O_7$	425	24	Do.
$NaVO_3+H_2O$ (in bomb)	350	90	Do.
$NaVO_3+K_2Cr_2O_7$	350	700	Do.
Do	325	640	Do.

Identification of the crystal forms of the TiO_2 was made by X-ray spectrograms [6] of the powdered material after all the mineralizer had been thoroughly removed by repeated washings with water, dilute solutions of HCl, and aqueous ammonia. Samples of natural brookite and rutile obtained from the National Museum and anatase prepared artificially were used as identifying standards. All heatings were made in platinum crucibles in an electrically heated tube furnace controlled to $\pm 1°$.

The data indicate that if there is a temperature where rutile is in stable equilibrium with anatase or brookite, it must be below 400°.

The melting point of rutile [7] has been reported as 1,560° to 1,980°. Recent determinations by Wartenberg are 1,850° [8] and 1,825°.[9] The melting point, as determined in a hole in an iridium button heated by high-frequency induction [10] was found to be 1,825°. Although this determination can be duplicated within $\pm 5°$, a correction of 10° to 20° should be added, as the material would not be visible under exact black body conditions. The white color of anatase changes to a light tan when it changes to rutile, and the color darkens as the rutile is heated to higher temperatures, becoming blue-black on melting.

III. THE SYSTEM TiO_2-SiO_2

The only previous work on this system is that reported by Rieke,[11] who observed the fusion of cones of mixtures heated in a carbon resistance furnace. Considerable reduction of the TiO_2 must have occurred,

[6] The X-ray spectrograms were made by the metallurgical division of this Bureau.
[7] See J. W. Mellor, A Comprehensive Treatise on Inorganic and Theoretical Chemistry, vol. 7, Longmans Green, and Co., New York and London. 1927.
[8] Wartenberg and Gurr, Z. anorg. Allgem. Chem., vol. 196, p. 374, 1931.
[9] Wartenberg and Prophet, Z. anorg. allgem. Chem., vol. 208, p. 369, 1932.
[10] See Bunting, B. S. Jour. Research, vol. 4, p. 131, 1930.
[11] R. Rieke, Sprechsaal, vol. 41, p. 405, 1908.

or else he used impure TiO_2, as he found the melting point to be near cone 27, or about 1,600°. Under the reducing conditions in a carbon furnace it is not possible to obtain the correct temperatures for the fusion of binary mixtures containing reducible oxides.

Mixtures of ground quartz crystals (99.7 percent SiO_2) and rutile (100.0 percent TiO_2) were made by wet grinding in an agate mortar. Thorough mixing was further obtained by three fusions, in the oxy-hydrogen flame, and intermediate grindings. All mixtures containing not over 20 wt. percent of TiO_2 were heated in a platinum capsule in a rhodium wire resistance furnace for two hours or more before

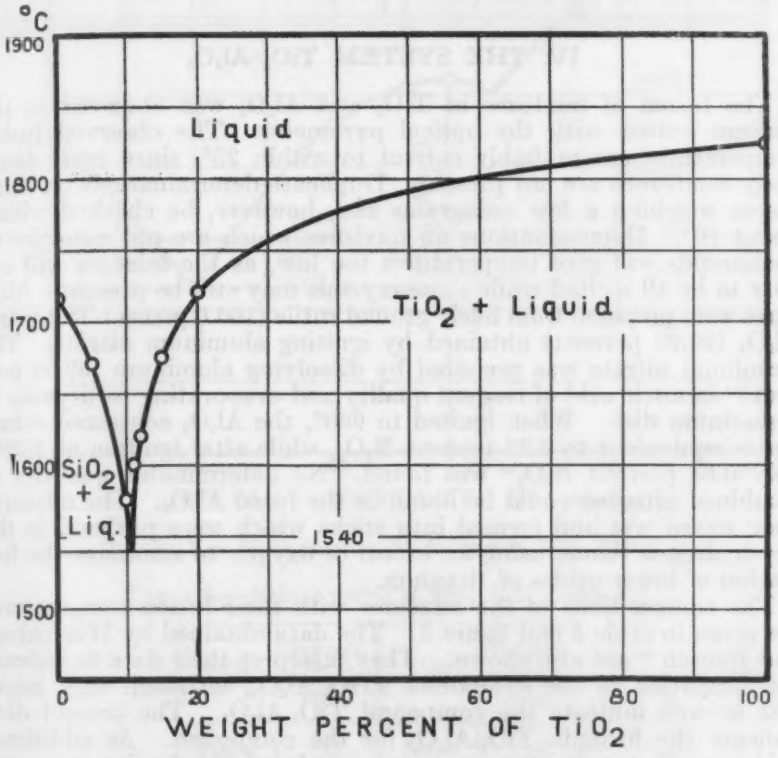

FIGURE 2.—*Phase diagram for the system TiO_2–SiO_2.*

quenching. The phases present in the quenched material were determined with a petrographic microscope. The fusion of mixtures containing over 20 percent TiO_2 was observed in the iridium button.[12] All temperatures were determined on a disappearing filament optical pyrometer [13] and are probably correct to within 10°. The results are shown in table 4 and figure 2. X-ray spectrograms of mixtures containing 40, 50, 57, 65, 70, and 80 wt. percent TiO_2, which were quenched from 1,720°, showed only the presence of rutile crystals. The data show that no compounds are formed and that the eutectic between rutile and cristobalite occurs at 10.5 wt. percent TiO_2 and 1,540° ± 10°.

[12] See footnote 10.
[13] Recently calibrated by the pyrometry section of this Bureau.

TABLE 4.—*Results with TiO_2–SiO_2 mixtures*

TiO_2 weight	Furnace temperature	Phases present	TiO_2 weight	Furnace temperature	Phases present
Percent			*Percent*		
5	1,670	All glass.	12	1,625	All glass.
	1,665	Glass + cristobalite.		1,620	Glass + rutile.
10	1,580	All glass.	15	1,680	All glass.
	1,575	Glass + cristobalite.		1,675	Glass + rutile.
	1,540	Cristobalite + rutile.	20	1,725	All glass.
11	1,605	All glass.		1,715	Glass + rutile.
	1,600	Glass + rutile.			
	1,540	Cristobalite + rutile.			

IV. THE SYSTEM TiO_2–Al_2O_3

The fusion of mixtures of TiO_2 and Al_2O_3 was observed in the iridium button with the optical pyrometer. The observed fusion temperatures are probably correct to within 25°, since exact black body conditions are not present. Duplicate determinations on small pieces weighing a few milligrams can, however, be checked within about 10°. Determinations on mixtures which are not eutectics or compounds will give temperatures too low, as the mixture will appear to be all melted while some crystals may still be present. Mixtures were prepared from finely ground rutile (100.0 percent TiO_2), and Al_2O_3 (99.95 percent) obtained by igniting aluminum nitrate. The aluminum nitrate was prepared by dissolving aluminum (99.95 percent)[14] in nitric acid of reagent quality and evaporating to dryness in a platinum dish. When ignited to 900°, the Al_2O_3 contained subnitrates equivalent to 0.22 percent N_2O_5, while after ignition at 1,200° only 0.04 percent N_2O_5[15] was found. No determinable quantity of combined nitrogen could be found in the fused Al_2O_3. The mixtures were mixed wet and formed into sticks which were prefused in the oxy-hydrogen flame, using an excess of oxygen to minimize the formation of lower oxides of titanium.

The compositions of the mixtures with their fusion temperatures are given in table 5 and figure 3. The data obtained by Wartenberg and Reusch [16] are also shown. They interpret their data to indicate the formation of the compound $2TiO_2.Al_2O_3$, although they might just as well indicate the compound $TiO_2.Al_2O_3$. The present data indicate the formula $TiO_2.Al_2O_3$ for the compound. As additional evidence, X-ray spectrograms were made of fused mixtures corresponding to these two formulas. The spectrograms showed that the compound is $TiO_2.Al_2O_3$, as no rutile lines were present in the fusion of this composition, while the spectrogram of the $2TiO_2.Al_2O_3$ mixture consisted only of the lines of the TiO_2-Al_2O_3 mixture plus those of rutile.[17] The melting point of $TiO_2.Al_2O_3$ is about 1,860°,

[14] Analysis by J. A. Scherrer of the Chemistry Division, Bureau of Standards.
[15] Analysis by H. A. Buchheit of the Chemistry Division, Bureau of Standards.
[16] Wartenberg and Reusch, Z. anorg. allgem. Chem., vol. 207, p. 10, 1932.
[17] A microscopic examination by Herbert Insley of the mixture with the composition $TiO_2.Al_2O_3$ which had been fired in the oxy-hydrogen flame showed it to be completely crystalline and to consist wholly of one phase. The crystals had the following optical properties: $\gamma_{Li}=2.015\pm0.01$, $\alpha_{Li}=1.975\pm0.01$, biaxial (−), medium 2V. Extinction parallel with a pronounced prismatic development and good cleavage parallel to α. Pleochroism is strong with α=nearly colorless, γ= deep bluish green. Thick crystals are so deeply colored in the γ direction as to be almost opaque.

and it forms a eutectic with TiO_2 at 15 wt. percent Al_2O_3 and 1,715° and a eutectic with Al_2O_3 at 62 wt. percent Al_2O_3 and 1,850°.

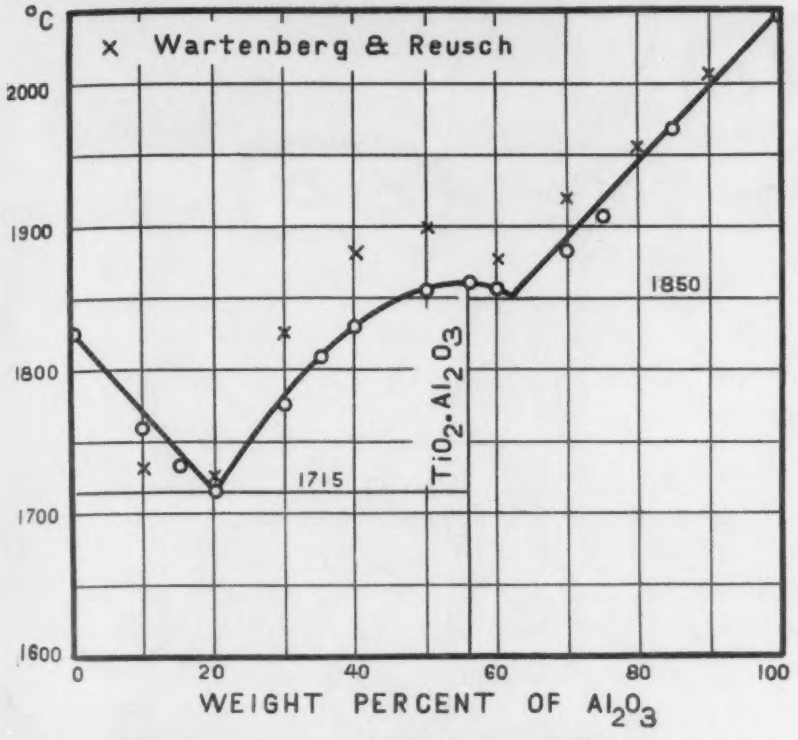

FIGURE 3.—*Phase diagram for the system TiO_2-Al_2O_3.*

TABLE 5.—*Melting points of TiO_2-Al_2O_3 mixtures*

Al_2O_3 weight	Temperature at complete fusion	Al_2O_3 weight	Temperature at complete fusion
Percent	*° C.*	*Percent*	*° C.*
10	1,760	56	1,860
15	1,730	60	1,855
20	1,715	70	1,880
30	1,775	75	1,905
35	1,810	85	1,965
40	1,830	100	2,045
50	1,855		

The writer is indebted to E. W. Washburn, Chief, Chemistry Division, under whose general direction the work was done.

WASHINGTON, August 12, 1933.

13317—33——11